5-9-2016

Transforming Dihydroxyacetone Phosphate-Dependent Aldolases Mediated Aldol Reactions From Flask Reaction Into Cell-Based Synthesis & Studying The Mechanism Of Chemical Desialylation In The Life Processes

Mohui Wei

TRANSFORMING DIHYDROXYACETONE PHOSPHATE-DEPENDENT ALDOLASES MEDIATED ALDOL REACTION FROM FLASK REACTION INTO CELL-BASED SYNTHESIS

&

STUDYING THE MECHANISM OF CHEMICAL DESIALYLATION IN THE LIFE PROCESSES

by

MOHUI WEI

Under the Direction of Peng George Wang, PhD

ABSTRACT

Dihydroxyacetone phosphate (DHAP)-dependent aldolases have been intensively studied and widely used in the synthesis of carbohydrates and complex polyhydroxylated molecules. However, the strict specificity toward donor substrate DHAP greatly hampers their synthetic utility. We transformed DHAP dependent aldolases mediated *in vitro* reactions into bioengineered *Escherichia coli* (*E. coli*). Such flask-to-cell transformation addressed several key issues plaguing *in vitro* enzymatic synthesis: 1) it solves the problem of DHAP availability by *in vivo* hijacking DHAP from glycolysis pathway of bacterial system, 2) it circumvents purification of recombinant aldolases and phosphatase, and 3) it dephosphorylates resultant aldol adducts *in vivo*, thus eliminating the additional step for phosphate removal and achieving *in vivo* phosphate recycling. The engineered *E. coli* strains tolerate a wide variety of aldehydes as acceptor, and provide a set of biologically relevant polyhydroxylated molecules in gram scale.

Sialic acids exist in abundance in glycan chains of glycoproteins and glycolipids on the surface of all eukaryotic cells and some prokaryotic cells. Their presence affects the molecular properties and structure of glycoconjugates, modifies their functions and interactions with other molecules. The sialylation status, referring to the expression levels and linkages of sialic acids on the cell surface, is determined by the dynamic balance between sialylation and desialylation (removal of sialic acids). Sialylation is mainly regulated through expression and activity of sialyltransferases. And the mainstream idea attributes desialylation to the sialidases. However, more and more emerging evidences support the existence of ROS/RNS mediated chemical desialylation process under some pathological conditions. We used electrochemical oxidation of sialic acid conjugates to mimic ROS mediated chemical desialylation. Such electrochemical

desialylation mimicry reveals that 1) β-linked sialic acid is much more difficult to de desialylated than α-linked sialic acid, 2) electron withdrawing residue and bulky underlying residue can facilitate the desialylation, 3) α-2,3-linked sialic acid is easier to be desialylated than α-2,6- and α-2,8-linked sialic acid. This information is highly valuable for identifying the ROS species participated in ROS mediated desialylation and unveiling corresponding mechanisms. The mechanism of ROS mediated desialylation was proposed to go through radical decarboxylation.

INDEX WORDS: DHAP-dependent aldolase, Metabolic engineering, *E. coli* synthetic machinery, Electrochemical desialylation, Desialylation mechanism.

TRANSFORMING DIHYDROXYACETONE PHOSPHATE-DEPENDENT ALDOLASES MEDIATED ALDOL REACTION FROM FLASK REACTION INTO CELL-BASED SYNTHESIS

&

STUDY THE MECHANISM OF CHEMICAL DESIALYLATION IN THE LIFE PROCESSES

by

MOHUI WEI

A Dissertation Submitted in Partial Fulfillment of the Requirements for the Degree of

Doctor of Philosophy

in the College of Arts and Sciences

Georgia State University

2016

RANSFORMING DIHYDROXYACETONE PHOSPHATE-DEPENDENT ALDOLASES MEDIATED ALDOL REACTIONS FROM FLASK REACTION INTO CELL-BASED SYNTHESIS

&

STUDY THE MECHANISM OF CHEMICAL DESIALYLATION IN THE LIFE PROCESSES

by

MOHUI WEI

Committee Chair: Peng George Wang

Committee: Jun Yin

Hao Xu

Electronic Version Approved:

Office of Graduate Studies

College of Arts and Sciences

Georgia State University

May 2016

DEDICATION

To my parents, brother, and sister for their love, understanding, and support.

ACKNOWLEDGEMENTS

The past five years of my life have been an incredible experience of growth, frustration, and joy. As I come to the end of this time, many thanks are owed to the people who help me through it.

First and foremost, I would like to express my sincere gratitude to my advisor Dr. Peng George Wang. I am especially thankful for his support at my most difficult times and his guidance at the times I got lost. Without his support and guidance, I couldn't go so far. I will cherish and remember the time spent in the Wang lab.

I also would like to thank Dr. Jun Yin and Dr. Hao Xu for their supportive guidance and opinion during my PhD study.

I especially want to thank my collaborators, Tiehai, Liuqing and Zijie. Without your support, the work in this dissertation couldn't be done.

I also want to thank Zhongying. We came to the Wang lab at the same time and we have been through so much together. Many thanks to Xuan and Angie for the support of daily life, to Dr. Junqiang Fang and Dr. Jing Li for suggestions about my future career. I also want to thank Yunpeng, Qing, Baolin, Garrett, Lei, Cheng, Jingyao, Wanyi, Zhigang, Yuxi, Jack, Megan, Hailiang, Chris, Kristina, Ebtesam, Shanshan, and all other lab members for their help in my research.

TABLE OF CONTENTS

LIST OF TABLES

LIST OF FIGURES

LIST OF SCHEMES

LIST OF EQUATIONS

1. CHAPTER 1 DIHYDROXYACETONE PHOSPHATE (DHAP)-DEPENDENT ALDOLASES: FROM FLASK REACTION TO CELL-BASED SYNTHESIS

1.1 Introduction

Aldolase (EC 4.1.2.x) is a subclass of lyase, which catalyzes the reversible addition of a ketone donor (nucleophile) onto an aldehyde acceptor (electrophile). While most aldolases are specific for their donors, they often tolerate different aldehydes as acceptors. Due to excellent control over stereochemistry and mild reaction conditions, aldolases exhibit unrivaled efficiency in the synthesis of carbohydrates and complex polyhydroxylated molecules, which are difficult to prepare and handle by conventional chemical synthesis. One elegant paradigm is the synthesis of statin (cholesterol-lowering drugs) side chain by deoxyribose-5-phosphate aldolase (DERA) catalyzed cascade aldol/aldol/hemiacetalization reaction between one molecule of α-substituted acetaldehyde and two molecules of acetaldehyde.[1, 2] For the high efficiency and excellent stereoselectivity, this method was developed into the industrial scale production of statin side chain and Pfizer developed the world top-selling drug Lipitor (atorvastatin)[3-7] with over $125 billion total sales since its approval in 1996. Among known aldolases, DHAP-dependent aldolases are most intensively studied and widely used so far, as configurations of two newly generated stereogenic centers can be chosen and controlled by an appropriate choice of four known DHAP-dependent aldolases.[8, 9] DHAP-dependent aldolases are comprised of Fructose-1,6-bisphosphate aldolase (FruA), Fuculose-1-phosphate aldolase (FucA), Tagatose-1,6-

bisphosphate aldolase (TagA) and Rhamnulose-1-phosphate aldolase (RhuA), which catalyze the reversible aldol addition reaction of DHAP to aldehyde acceptors. These four DHAP-dependent aldolases are stereocomplementary, thus a complete set of four stereoisomers could be accessed (**Scheme 1.1**).

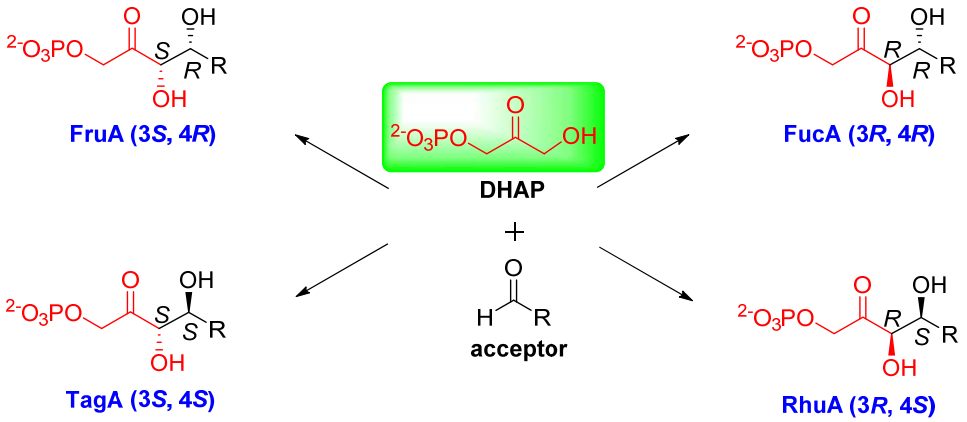

Scheme 1.1 *Stereochemical complementarity of DHAP-dependent aldolases.*

1.2 Synthetic Applications of DHAP Dependent Aldolases

With respect to synthetic application of DHAP-dependent aldolases, over 200 research papers have been published, ranging from synthesis of monosaccharides,[10-12] iminocyclitols,[13-16] higher carbon sugars,[17, 18] carbocycles[19-22] and natural products[23-25] to active pharmaceutical intermediates[26-28] (**Scheme 1.2**). More than 100 aldehydes have been used as acceptors for DHAP-dependent aldolases. These aldehydes can be unhindered aliphatic and aromatic aldehydes, α-heteroatom substituted aldehydes, azido aldehydes, protected amino aldehydes, monosaccharides, and their derivatives. The use of multienzyme systems and engineering of DHAP-dependent aldolases further broaden the substrate scope of aldehyde acceptors to unprecedented α, β-unsaturated aldehydes[29] and complex synthetic aldehydes.[30] Recent work on

combining DHAP-dependent aldolases mediated aldol reactions with other enzymatic transformations allows rapid construction of complex molecules with multiple stereogenic centers and diverse functionalities.[31] [32-34]

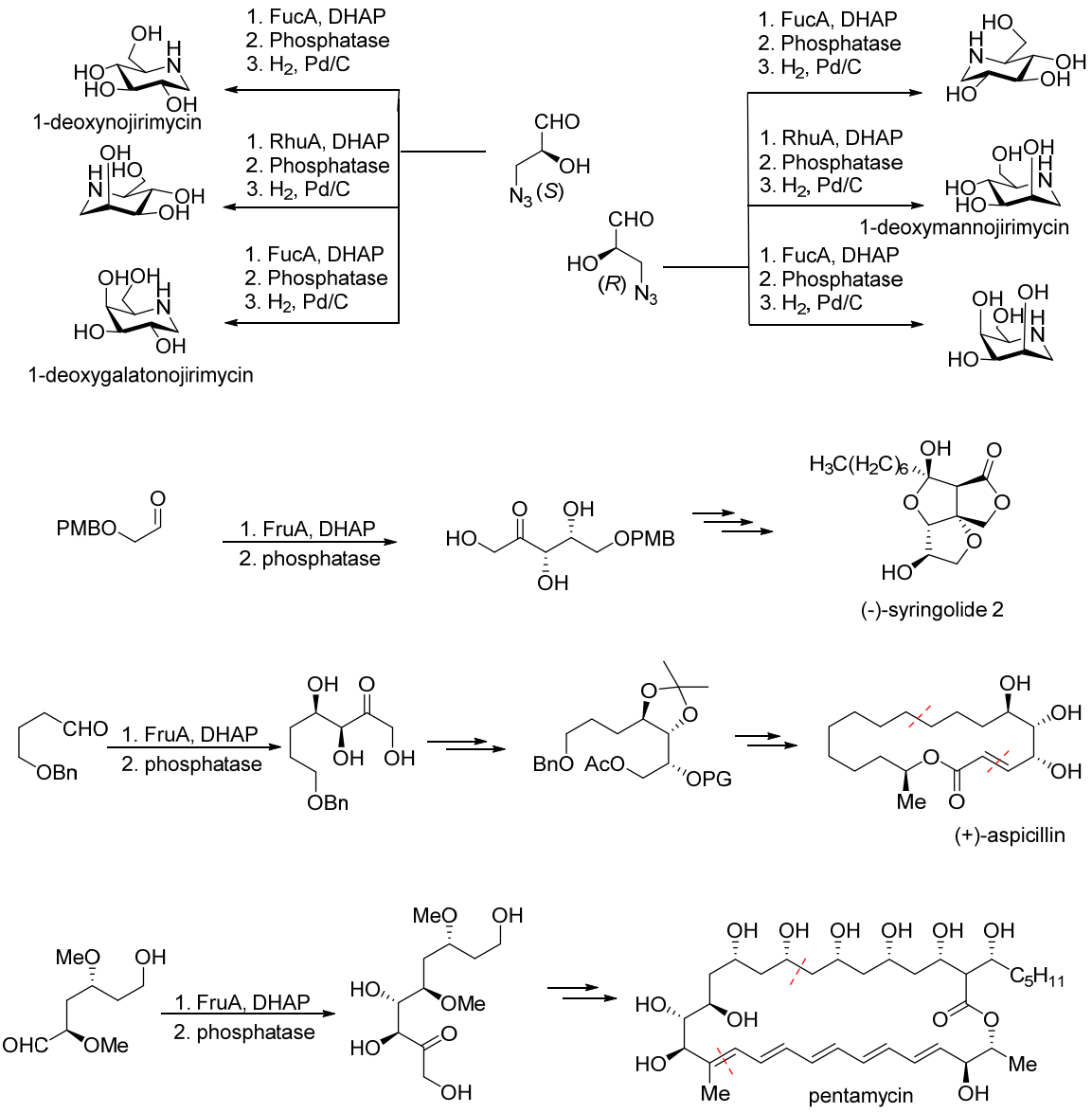

Scheme 1.2 *Synthetic applications of DHAP-dependent aldolases.*

1.3 DHAP Generation

However, the strict specificity toward donor substrate DHAP greatly hampers the large scale synthetic utility of DHAP-dependent aldolases, due to high cost and lability of DHAP.[32, 35] Therefore, effective production of DHAP is instrumental, and several chemical and enzymatic approaches have been developed for its synthesis. Chemical approaches focus on producing storable precursors that can be easily converted to DHAP immediately before its use (**Scheme 1.3**).[36-44] However, they suffer from either low yields, complicated work-up, or toxic reagents or catalysts.[45]

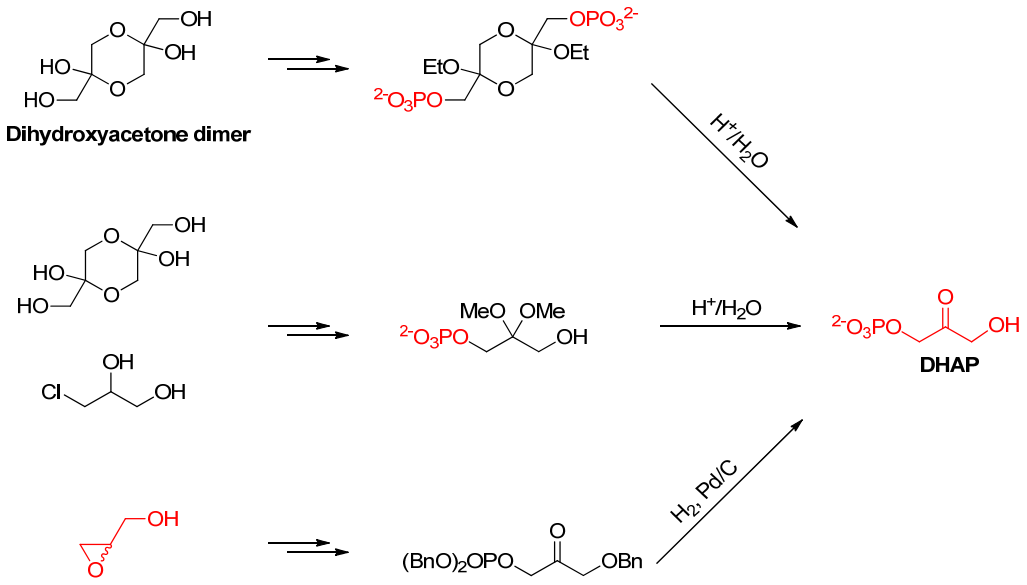

Scheme 1.3 *Chemical routes to DHAP.*

Enzymatic approaches generate DHAP *in situ* and follow three general routes: phosphorylation of dihydroxyacetone (DHA) (**Scheme 1.4 I**),[29, 46-50] oxidation of L-glycerol 3-phosphate (L-GP) (**Scheme 1.4 II**),[51-55] and mimicking glycolysis (**Scheme 1.4 III**).[36, 56] Though enzymatic approaches start from cheap non-phosphorylated precursors (DHA, glycerol, sucrose),

they employ multiple costly isolated enzymes. Both chemical and enzymatic approaches require further improvement to serve as a basis for scalable and cost-effective production of DHAP. Another issue associated with large scale synthetic utility of DHAP-dependent aldolases is that an additional step is required to remove phosphate group of aldol adducts, which necessitates the use of phosphatase and thus causes non-productive waste of phosphate component.

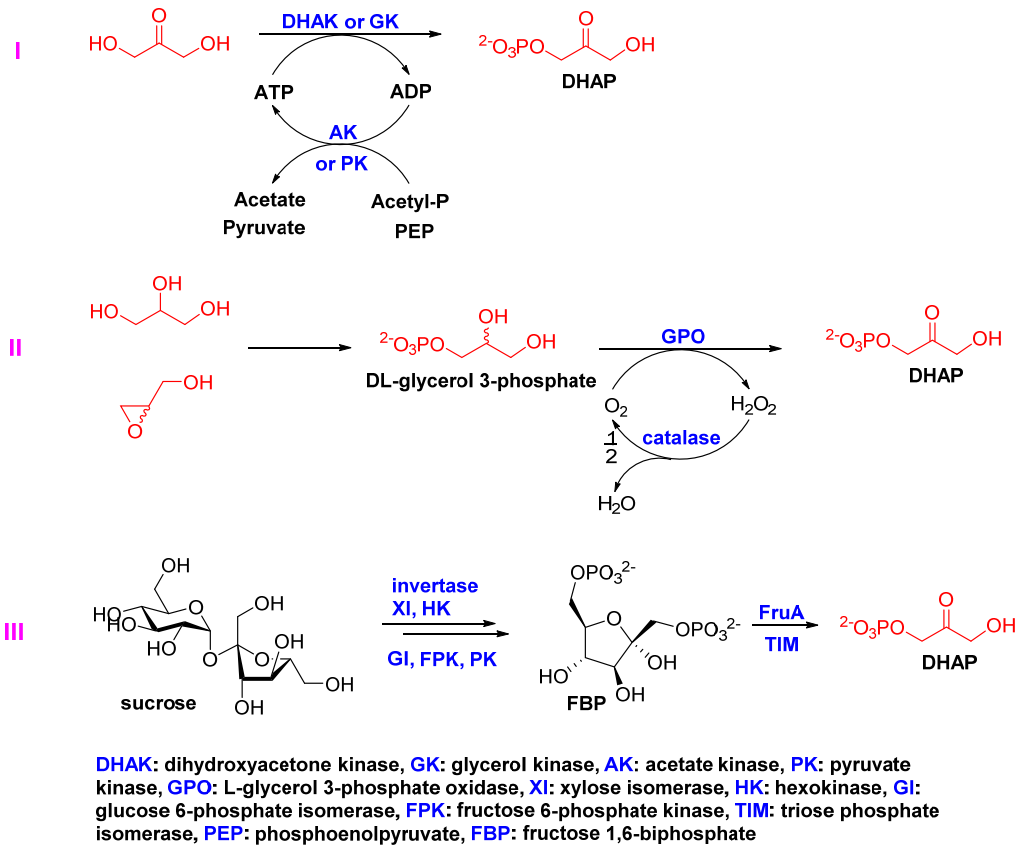

Scheme 1.4 *Enzymatic routes to DHAP.*

1.4 Overcoming DHAP Dependence

A desirable solution is to eliminate the requirement of DHAP and use readily available, inexpensive DHA. Recent efforts in overcoming DHAP-dependence by substrate/reaction

engineering, exploitation of newly discovered or designed enzymes, and directed evolution of aldolases have achieved great success.

1.4.1 Substrate/reaction engineering

Arsenate, vanadate, and borate can form esters with Dihydroxyacetone (DHA) *in situ* and reversibly. These esters act as phosphate ester (DHAP) mimics and can be accepted as donor by some DHAP-dependent aldolases (**Scheme 1.5**). Therefore, with the presence of these inorganic anions, DHAP-dependent aldolases can accept DHA as donor. In the presence of arsenate, FruA, FucA and RhuA can accept DHA as donor,[57, 58] but the required high concentration and the high toxicity of arsenate make this approach unsuitable to be used in preparative applications. For vanadate and borate, only RhuA can accept DHA as donor.[59-61] However, vanadate is susceptible of participating in secondary redox reactions and its expense limits its practical utility.

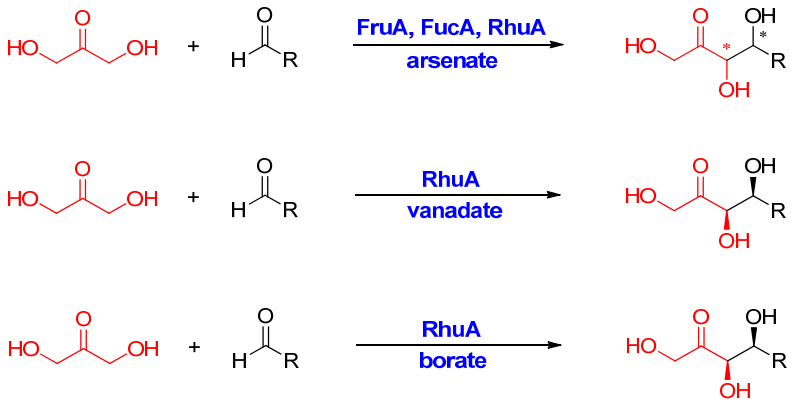

Scheme 1.5 *DHAP-dependent aldolases accept DHA as donor in the presence of arsenate, vanadate or borate.*

1.4.2 Discovery and design of new enzymes

Fructose 6-phosphate aldolase (FSA) from *E. coli*, the first example of enzymes using dihydroxyacetone (DHA) as donor substrate, is one of major discoveries in this field (**Scheme 1.6**).[62] Besides DHA, FSA also can accept hydroxyacetone (HA), hydroxybutanone (HB) and even glycolaldehyde (GA) as donor substrates.[35, 63-65] This broad donor substrate specificity is remarkable, especially the acceptance of GA as an donor substrate, which offers the unprecedented opportunity of enzymatic cross-aldol addition reactions of glycolaldehyde to aldehydes, thereby opening new promising biocatalytic strategies for the immediate and stereoselective synthesis of aldoses (instead of ketoses derived from usual ketone donors) and related complex analogs or derivatives. Structurally related transaldolase B variants (TalB-F178Y and TalB-F178Y/R181E) of *E. coli* are designed aldolases and also can accept DHA, HA and HB as donor substrates.[66] FSA, TalB-F178Y and TalB-F178Y/R181E give aldol products with (3S,4R)-configuration and can be considered as an alternative to FruA.

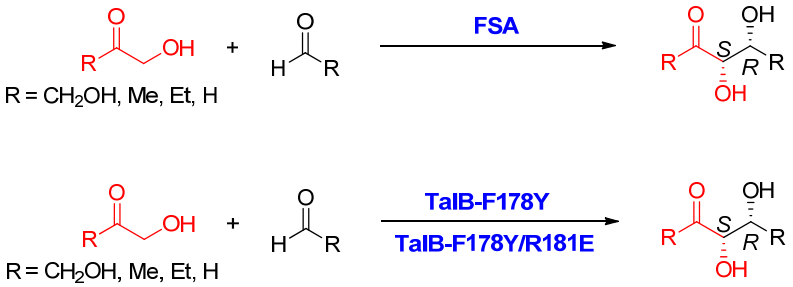

Scheme 1.6 *FSA, TalB-F178Y and TalB-F178Y/R181E mediated aldol reactions.*

Recently, a bifunctional aldolase/kinase enzyme (FruA-DHAK-FruA) was constructed by gene fusion, which consists of a monomeric FruA and a homodimeric DHAK (**Scheme 1.7**).[67] The fusion protein retains both kinase and aldolase activity and has been applied for the

stereoselective C-C bond formation starting from DHA as the initial donor and an aldehyde with 20-fold increase in the reaction rate compared to the multi-enzyme system of the free parent enzymes. However, a phosphatase is still needed to remove phosphate group from aldol adducts.

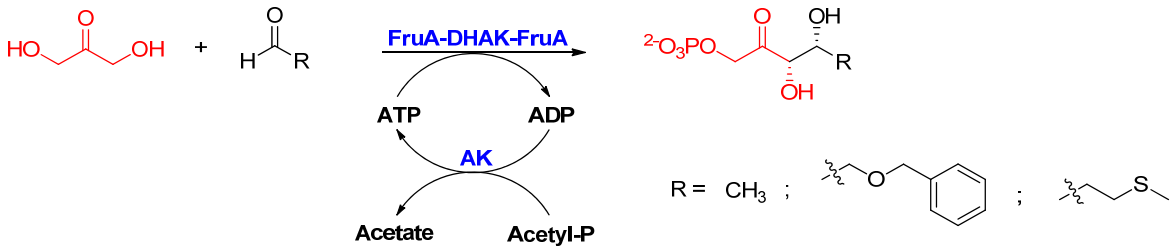

Scheme 1.7 *Application of FruA-DHAK-FruA to stereoselective C-C bond formation.*

1.4.3 Directed evolution of enzymes

A directed evolution approach was successfully applied to engineer RhuA to avoid the use of DHAP (**Scheme 1.8**). Thus, after random mutagenesis and a proper selection system, RhuA-N29D was able to accept DHA as a donor and furnish aldol adducts with (3R,4S) configuration.[68] Thus, RhuA-N29D is stereocomplementary to FSA, TalB-F178Y and TalB-F178Y/R181E. However, the acceptor scope of RhuA-N29D catalyzed aldol addition of DHA to aldehyde still hasn't been fully explored.

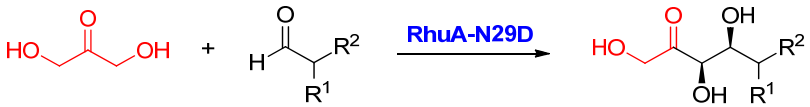

	yield (%)
R^1 = (R)-CH3; R^2 = -NHCbz	45 %
R^1 = H; R^2 = -NHCbz	68 %
R^1 = H; R^2 = -OBn	63 %
R^1 = H; R^2 = -NHCHO	92 %

Scheme 1.8 *RhuA-N29D mediated aldol addition of DHA to aldehydes.*

In summary, these DHAP independent methods only can provides (*3S, 4R*) and (*3R, 4S*) configuration products. Access to (3*R*, 4*R*) and (3*S*, 4*S*) products still has to use DHAP as donor. And none of these methods has ever been realized on more than lab scale.

1.5 In vitro one-pot four-enzyme synthesis of ketoses with FruA

In glycolysis, FruA catalyzes the reversible degradation of D-fructose 1,6-bisphosphate to D-glyceraldehyde 3-phosphate (GAP) and DHAP. However, the equilibrium constant for this reaction strongly favors the synthesis direction, which makes FruA synthetically useful as a biocatalyst.[69] FruA from rabbit muscle (RAMA) is widely used, due to its commercial availability, high activity, and relaxed aldehyde substrate specificity.[36, 70, 71] Unfortunately, RAMA suffered from low operational stability and loss of activity during synthesis.[72] In contrast, FruA from bacterial sources, such as FruA from Staphylococcus carnosus (FruA$_{S.car}$), is exceptionally temperature and pH stable.[72, 73]

We developed a one-pot four-enzyme approach for the synthesis of rare sugars using FruA$_{S.car}$ (**Table 1.1**). In this one-pot reaction sequence, DHAP was firstly generated from the oxidation of L-GP by glycerol phosphate oxidase (GPO).[51, 74] The by-product of this oxidation, H_2O_2, which shows toxicity to GPO, was thus selectively degraded by catalase. The DHAP generated *in situ* was then coupled with aldehyde by aldolase to give the sugar-1-phosphate, which not only prevents product inhibition of GPO by DHAP and thus promotes the conversion of L-GP, but also suppresses any decomposition of the labile DHAP since it does not accumulate in the reaction mixture.[51] Lastly, the phosphate group was removed under acidic conditions by acid phosphatase (AP) to provide sugars in a one-pot fashion. As summarized in **Table 1.1**, FruA$_{S.car}$ accepted D- and L-glyceraldehydes, and various aliphatic aldehydes as acceptors, and

demonstrated excellent stereoselectivity. Only one diastereomer with (3*S*, 4*R*) configuration was isolated for each reaction.

This one-pot four-enzyme approach generates DHAP *in situ* from cheap DL-GP, which can reduce the synthetic cost, and provides a straight forward method for the synthesis of ketoses. However, the usage of four isolated enzymes is the major issue.

Table 1.1 *One-pot four-enzyme synthesis of ketoses with FruA*

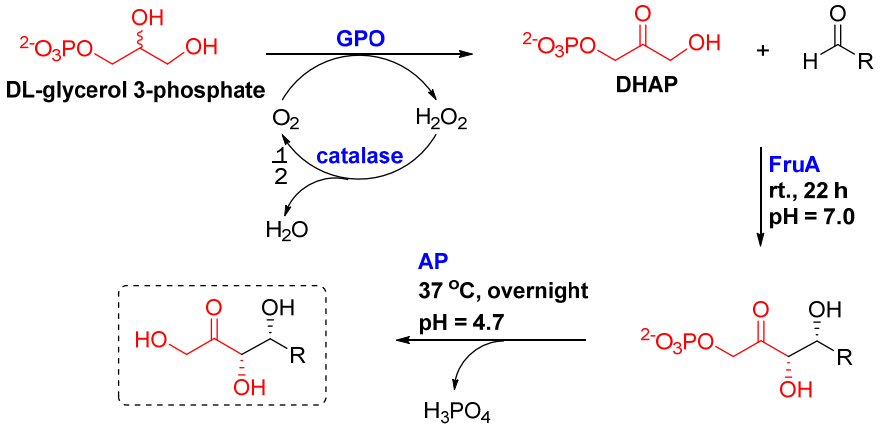

Entry	Enzyme	Acceptor	Product	Isolated yield
1	$FruA_{S.car}$	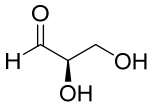	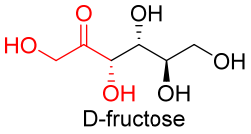 D-fructose	60 %
2	$FruA_{S.car}$	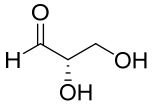	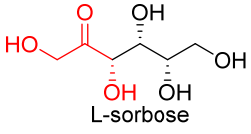 L-sorbose	28 %
3	$FruA_{S.car}$ RAMA		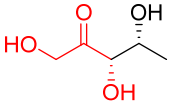	33 % 29 %
4	$FruA_{S.car}$ RAMA	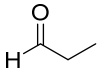	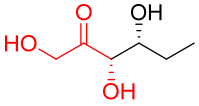	37 % 34 %
5	$FruA_{S.car}$ RAMA	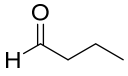		40 % 38 %
6	$FruA_{S.car}$ RAMA	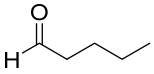	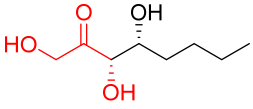	23 % 13 %

1.6 Transforming DHAP-dependent Aldolases Mediated Reactions from Flask into Cell-Based Synthesis

Synthetic biology, a recently emerging discipline which utilizes elaborate bio-engineered organisms as "programmable synthetic machinery" to execute transformations inside cells, has completely revolutionized the notion of the conventional enzymatic synthesis into an era of advanced manufacturing of chemicals in a highly efficient and sustainable fashion.[75-77] Advances in DNA technologies and bioinformatics enable the reconstruction and perfection of such genetic devices. Thus, synthetic biology could provide appealing opportunities and solutions to issues blocking large scale synthetic applications of DHAP-dependent aldolases by technically manipulating microbial hosts to execute the aldolase-catalyzed reactions inside cells and afford desired products.

DHAP is a metabolite in the universal glycolytic pathway. In glycolysis, glucose is metabolized into fructose 1,6-bisphosphate via three enzymatic steps, which is then split by FruA into two inter-convertible triose phosphates, DHAP and GAP.[78] The concentration ratio of DHAP to GAP is 96 % to 4 % due to favored formation of DHAP by TIM.[79] By introducing and overexpressing an aldolase and a phosphatase genes in *E. coli* cells, a "side way" or "external biosynthetic pathway" can be set up to hijack DHAP from the glycolytic pathway and couple it with an externally added aldehyde to provide phosphorylated aldol adduct. The formed aldol adduct will then be dephosphorylated by an overexpressed phosphatase and secreted out to the fermentation media to give desired product (**Scheme. 1.9**).

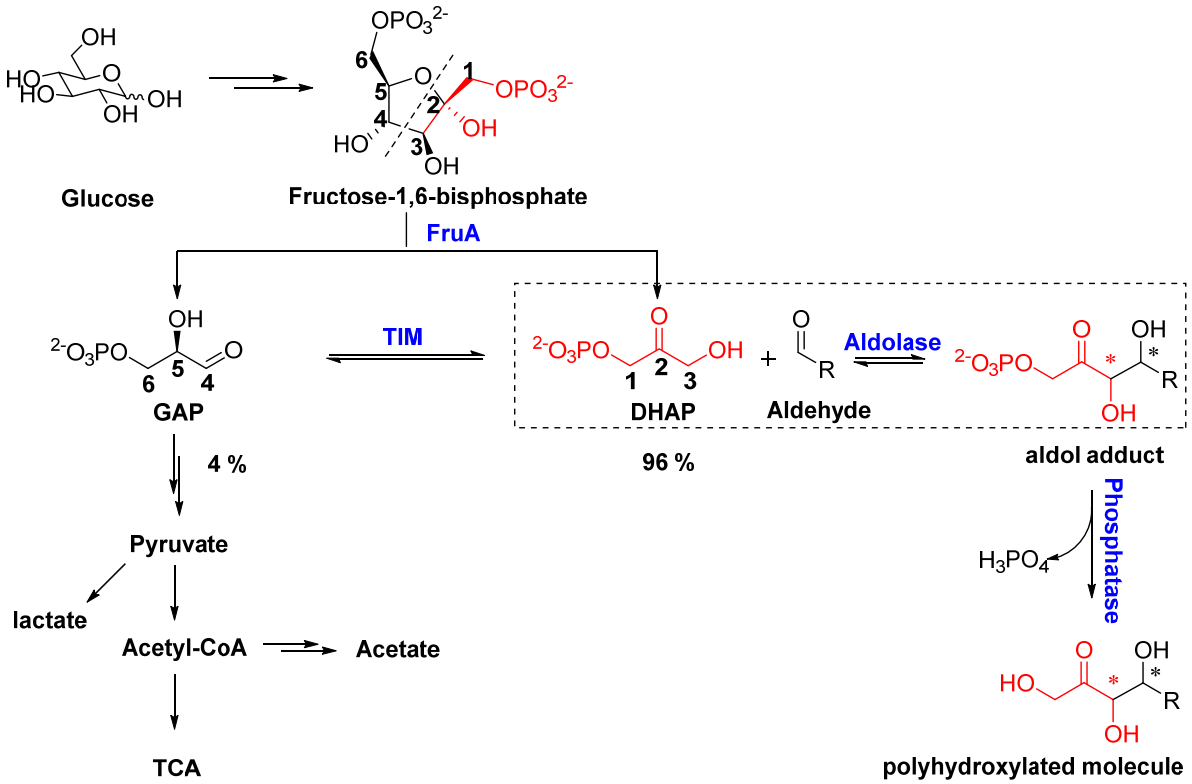

Scheme 1.9 *Hijacking DHAP from the glycolytic pathway.*

To fulfill such transformation (**Figure 1.1**), three major issues need to be addressed. First, a suitable aldolase gene must be introduced and overexpressed in the host cell. The expressed aldolase would couple glycolysis pathway with aldol reaction to afford phosphorylated aldol adducts. Second, an appropriate phosphatase gene needs to be introduced and overexpressed. High intracellular accumulation of phosphorylated aldol adducts is expected to be toxic or, at least, a burden to cells. The phosphatase should be able to selectively dephosphorylate resultant aldol adducts under physiological conditions but without any interference to other phosphorylated metabolic intermediates, which may have a negative influence on the whole engineered system. After dephosphorylation, final product would be secreted out of host cells. This will shift glycolysis and aldol reaction towards product formation and make purification of

final product much easier. Additionally, the removed phosphate could be recycled inside cells. Third, bacteria growth and product synthesis must be well balanced. Hijacking DHAP from glycolysis will greatly reduce energy production, disrupt redox balance, and reduce growth in host cells. A suitable condition must be explored to maximize production while maintain bacteria growth.

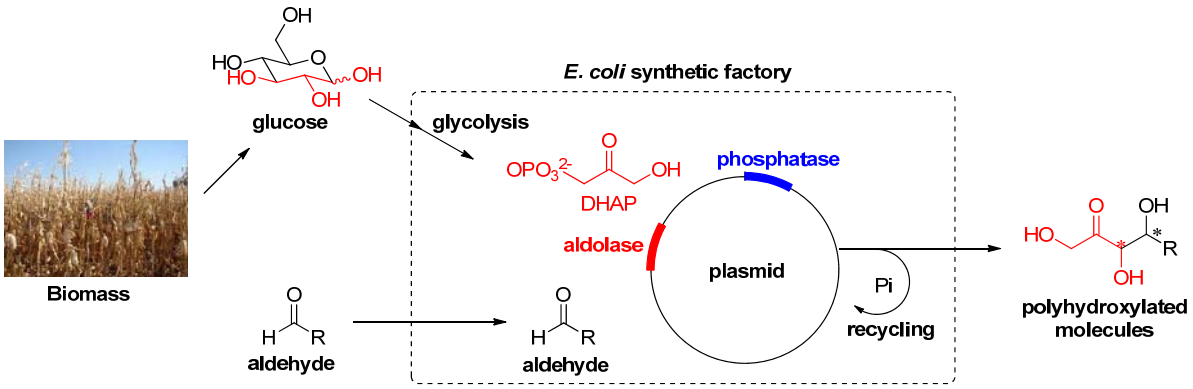

Figure 1.1 *Green and sustainable E. coli synthetic machinery.*

1.6.1 Validation of the E. coli synthetic machinery design

We are very interested in FruA, one class of DHAP-dependent aldolase, owing to its high stereoselectivity and relaxed aldehyde substrate specificity. FruA from *Staphylococcus carnosus* (FruA$_{S.car}$) encoded by gene *fda* displays unusual stability across a wide range of temperature and pH conditions while remains quite relaxed acceptor specificity.[72, 73] At the same time, FruA$_{S.car}$ has been demonstrated to exhibit high stereoselectivity in aldol reactions, selectively furnishing aldol products with (3*S*,4*R*)-*threo* configuration.[55, 72] Thus, we chose FruA$_{S.car}$ as aldolase. YqaB from *E. coli* (YqaB$_{E.coli}$) encoded by gene *yqaB* could dephosphorylate D-fructose-1-phosphate but shows no activity towards aldose phosphates, ketose terminal phosphates or other phosphorylated metabolic intermediates.[80] Our *in vitro* study also showed that YqaB$_{E.coli}$ could

dephosphorylate D-sorbose-1-phosphate, D-psicose-1-phosphate, L-tagatose-1-phosphate, L-fructose-1-phosphate but showed almost no activity toward DHAP under neutral conditions. Therefore, we chose YqaB$_{E.coli}$ as phosphatase. Meanwhile, we chose 3-trifluoroacetamido propanal **1** as model aldehyde acceptor owing to its excellent solubility in water.

To construct recombinant *E. coli* strain, *fda* and *yqaB* genes were cloned into pCDFDuet-1 (Novagen), a vector which allows high-level expression of two proteins under induction of isopropyl β-D-1-thiogalactopyranoside (IPTG). The resulted plasmid pCDF-fda-Y was transformed into *E. coli* BL21Star (DE3) to provide recombinant *E.coli* strain FruA-Y, which was grown aerobically at 37 ^{o}C, 220 rpm in LB broth medium until OD_{600} value reached 1.0. Then temperature was switched to 30 ^{o}C and IPTG was added to induce co-expression of FruA and YqaB for 12 h. Subsequently, **1** and glucose were fed. To our delight, after purification, 234 mg **2** was provided with 11.3 % yield.

1.6.2 Optimization of fermentation conditions for maximum product synthesis

After validation of such transformation, we set out to optimize fermentation conditions by using **1** as model acceptor. Several key parameters critical to fermentation yield were investigated (**Table 1**.2). Glucose is energy source and carbon source of living cell system, while high concentration of glucose will lead to catabolite repression. In order to determine the optimal initial glucose concentration in medium, a variety of glucose concentrations, ranging from 2 g/L to 12 g/L, were examined (entries 1-6). After glucose concentration is over 4 g/L threshold, yield of **2** would not increase anymore and keep almost constant until it reached 12 g/L, at which point yield of **2** began to decrease. Therefore, initial glucose concentration was chosen to be 4 g/L.

Notably, if glucose was fed during cell proliferation phase or induction stage, yield of **2** would decrease dramatically.

Addition of IPTG would affect growth of cells and expression of target genes. Therefore, IPTG was added at different levels of cell density, determined by corresponding OD_{600} value, to investigate effect of IPTG addition time point on fermentation yield. After 12 h induction, OD_{600} value of all cell cultures reached around 2.3. As illustrated in entries 2, 7-11, yield of **2** increased almost in a linear relationship with the increase of cell OD_{600} values until OD_{600} equaled to 1.8, at which point yield of 2 reached a plateau at 41.7 %. Thus, the optimum time point of IPTG addition is the time at which OD_{600} value is equal to or larger than 1.8.

LB Broth medium is a nutritionally rich medium and supplies essential growth factors that *E. coli* would otherwise have to synthesize. While ECAM (see recipe in supporting information) is a mineral salt medium and provides all kinds of metals and essential trace elements for *E. coli*. Thus, in order to probe effect of cultural medium on output of the *E. coli* strain, LB Broth and ECAM media were examined, as well as their combinations. As demonstrated in Table 1.1 entries 11-15, LB Broth turned out to be far superior to ECAM with respect to yield of **2** (entry 11 vs. 15). However, an appropriate combination of these two media can increase yield of **2**. When these two media were mixed in a 3:1 volumetric ratio, yield of **2** was increased from 41.7 % to 49.8 % (entry 11 vs. entry 12). Yield of **2** was further increased to 50.0 % by mixing LB Broth and ECAM in a 1:1 volumetric ratio (entry 13). Further increase of ECAM ratio led to decrease of production yield (entry 14). Therefore, the optimal medium is combination of LB Broth and ECAM in a 1:1 volumetric ratio. In addition, when *E. coli* strain BL21Star (DE3) was used to perform fermentation under optimized conditions, no product was detected (entry 16), which indicated that the background reactions were negligible.

Table 1.2 *Condition Optimization for maximum production.*

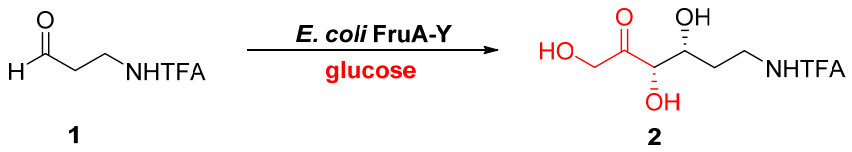

1 **2**

Entry[a]	Medium	Glucose (g/L)[b]	Cell density[c] OD_{600}	Incubation time (h)	Yield[d]
1	LB Broth	2	1.0	12	19.7 %
2	LB Broth	4	1.0	12	27.6 %
3	LB Broth	6	1.0	12	27.5 %
4	LB Broth	8	1.0	12	27.6 %
5	LB Broth	10	1.0	12	27.4 %
6	LB Broth	12	1.0	12	15.4 %
7	LB Broth	4	1.2	11	30.1 %
8	LB Broth	4	1.4	10	33.5 %
9	LB Broth	4	1.6	9	36.7 %
10	LB Broth	4	1.8	8	41.7 %
11	LB Broth	4	1.95	8	41.7 %
12	LB Broth/ECAM (3/1, v/v)	4	> 1.8	8	49.8 %
13	LB Broth/ECAM (1/1, v/v)	4	> 1.8	8	50.0 %
14	LB Broth/ECAM (1/3, v/v)	4	> 1.8	8	40.4 %
15	ECAM	4	> 1.8	11	28.5 %
16[e]	LB Broth/ECAM (1/1, v/v)	4	> 1.8	8	0 %

[a] Fermentation conditions: strain FruA-Y was grown aerobically at 37 °C, 220 rpm in 200 mL medium until OD_{600} reached certain value. Then temperature was switched to 30 °C and IPTG was added to induce co-expression of FruA and YqaB for 12 h. Subsequently, 8 mmol **1** and

glucose were fed. [b] Initial glucose concentration in medium. [c] At this cell density, IPTG was added. [d] HPLC yield based on acceptor **1**. [e] *E. coli* strain BL21Star (DE3) was used.

1.6.3 Production of polyhydroxylated molecules via E. coli FruA-Y strain

After identified optimal fermentation conditions, we set out to investigate the scope and limitations of such FruA-Y *E. coli* synthetic factory by using a variety of cell membrane permeable aldehydes as acceptors. FruA-Y strain demonstrated superb promiscuity towards different aldehyde acceptors. As indicated in **Table 1.3**, a set of small aldehydes were taken up by FruA-Y *E. coli* cells and subjected to aldol reaction with glycolytic intermediate DHAP, followed by *in situ* dephosphorylation， to yield desired aldol products. When **1** was used as acceptor, 2.47 g **2** was provided with 23.8 % yield as a single stereoisomer (*dr* > 95:5). However, concentration of **2** in fermentation medium was 5.18 g/L (determined by HPLC) and corresponding yield was 50.0 % (entry 1). The low isolated yield is mainly attributed to loss of product during purification. Along the same line, 3-trichloroacetamido propanal gave 4.41 g (3*S*,4*R*)-6-trichloroacetamido-1,3,4-trihydroxyhexan-2-one with 35.7 % yield and 92:8 *dr* (entry 2); 3-Difluoroacetamido propanal gave 2.26 g (3*S*,4*R*)-6-difluoroacetamido-1,3,4-trihydroxyhexan-2-one with 23.4 % yield and 92:8 *dr* (entry 3); 3-(methylthio)propanal gave 327 mg (3*S*,4*R*)-1,3,4-trihydroxy-6-(methylthio)hexan-2-one with 2.8 % yield and 92:8 *dr* (entry 4); 4,4,4-trifluorobutanal gave 716 mg (3*S*,4*R*)-7,7,7-trifluoro-1,3,4-trihydroxyheptan-2-one with 4.7 % yield and 87:13 *dr* (entry 5). Low fermentation yields of 3-(methylthio)propanal and 4,4,4-trifluorobutanal are mainly due to vaporization of aldehyde acceptors during incubation and their poor cell membrane permeability. When D-glyceraldehyde was used as acceptor, 947 mg of D-fructose was afforded with 26.3 % yield. However, HPLC yield before purification was 65.6 %

(entry 6). In addition, when (*R*)-3-trifluoroacetamido-2-hydroxypropanal and (*S*)-3-trifluoroacetamido-2-hydroxypropanal were used as acceptors, 827 mg **3** and 513 mg **4** were afforded respectively (entries 7-8).

Table 1.3 *Production of polyhydroxylated molecules via E. coli strain FruA-Y.*

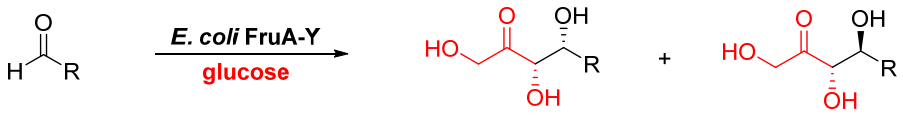

Entry[a]	Acceptor	Product	Incubation time (h)	Isolated yield	*dr*[b]
1	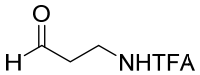	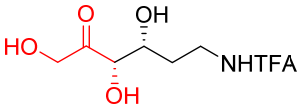	8	2.47 g / 23.8 % (5.18g / 50.0 %)[c]	> 95:5
2	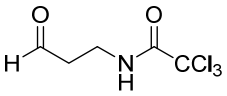	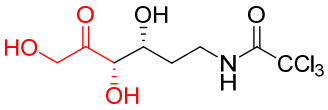	10	4.41 g / 35.7 %	92:8
3	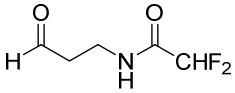	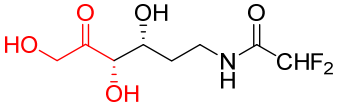	10	2.26 g / 23.4 %	92:8
4[d]	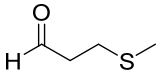	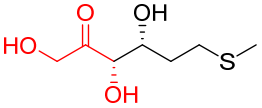	24	327 mg / 2.8 %	92:8
5[e]	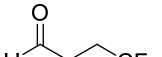	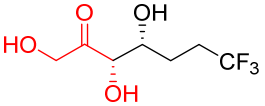	20	716 mg / 4.7 %	87:13
6[f]	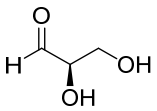	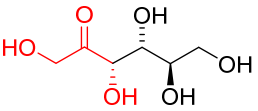	20	947 mg / 26.3 % (2.36 g / 65.6 %)[c]	> 95:5[g]
7[h]	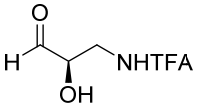	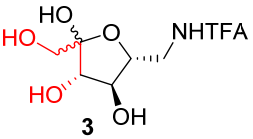 **3**	10	827 mg / 11.0 %	ND
8[h]	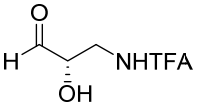	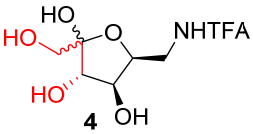 **4**	10	513 mg / 6.8 %	ND

[a] Fermentation conditions: strain FruA-Y was grown aerobically at 37 ºC, 220 rpm in 1 L LB Broth/ECAM (1/1, v/v) medium until OD_{600} reached 1.8-2.0. Then temperature was switched to 30 ºC and IPTG was added to induce co-expression of FruA and YqaB for 12 h. Subsequently, aldehyde acceptor and glucose were fed. [b] Determined by ^{1}H NMR. [c] HPLC yield based on aldehyde acceptor. [d] 60 mmol aldehyde was used. [e] 70 mmol aldehyde was used. [f] 1 L ECAM was used as medium and 20 mmol aldehyde was used. [g] Determined by HPLC. [h] 27.3 mmol aldehyde was used. ND, not determined.

1.6.4 Synthesis of D-fagomine, 1-Deoxymannojirimycin (DMJ), 1-Deoxynojirimycin (DNJ)

D-fagomine, 1-Deoxymannojirimycin (DMJ), 1-Deoxynojirimycin (DNJ) and their derivatives are effective inhibitors of glycosidases and glycosyltransferases, and exert profound effect on *N*-linked glycoprotein processing and maturation, as well as cell-cell and cell-virus recognition.[81] Therefore, they have gained considerable clinical importance in the treatment of cancer, type II diabetes, viral diseases such as HIV, hepatitis B and C, Gaucher's disease, and other glycosphingolipid storage disorders.[82-85] For example, D-fagomine can effectively reduce blood glucose peak when taken together with sucrose or starch, without stimulating insulin release, and help to eliminate the excess of enterobacteria and lower weight gain by selectively agglutinating fimbriated enterobacteria and inhibiting their adhesion to the intestinal mucosa.[86, 87] Miglitol, N-hydroxyethyl DNJ, is currently used as potent second-generation digestive α-glucosidase inhibitor for treatment of type II diabetes; Miglustat, N-butyl DNJ, is currently used for treatment of Type 1 Gaucher disease (GD1) and Niemann-Pick type C (NPC) disease.[88-90] By simple deprotection and reductive amination, product **2**, **3** and **4** were transformed to D-

fagomine, DMJ and DNJ respectively with high yields and no other diastereomers were detected by ^{1}H NMR analysis (**Scheme 1.10**).

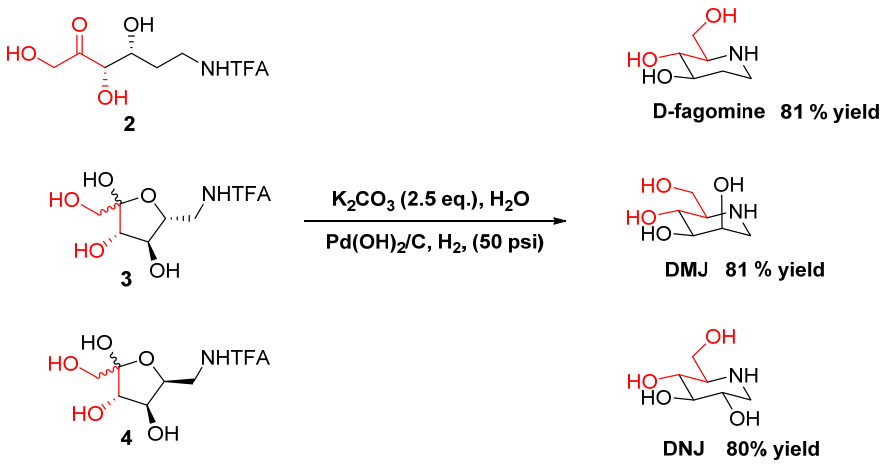

Scheme 1.10 *Synthesis of D-fagomine, DMJ and DNJ.*

1.6.5 Production of polyhydroxylated molecules via E. coli FucA-Y and RhaD-Y strains

To further expand applications of such *E. coli* synthetic machinery, recombinant *E. coli* strains FucA-Y and RhaD-Y were constructed following the same procotol of FruA-Y with *fucA* gene encoding L-fuculose-1-phosphate aldolase (FucA) from *Thermus. thermophilus* HB8 and *rhaD* gene encoding L- rhamnulose-1-phosphate aldolase (RhaD) from *E. coli*. For FucA-Y strain, D-glyceraldehyde gave 960 mg D-psicose with 35.6 % yield and 92:8 *dr* (**Table 1.4**, entry 1); **1** gave 665 mg (3*R*,4*R*)-6-trifluoroacetamido-1,3,4-trihydroxy-hexan-2-one **5** with 12.8 % yield and 87:13 *dr* (**Table 1.4**, entry 2). For RhaD-Y strain, D-glyceraldehyde provided 281 mg D-piscose and 286 mg D-sorbose with 10.4 % and 10.6 % yield respectively (**Table 1.4**, entry 3); **1** yielded 1.16 g (3*R*,4*S*)-6-trifluoroacetamido-1,3,4-trihydroxy-hexan-2-one **6** with 22.4 % yield and 89:11 *dr* (**Table 1.4**, entry 4). The successful application of D-glyceraldehyde and **1** in

strains FucA-Y and RhaD-Y indicated that many other aldehydes also could be applied in these two *E. coli* strains.

Table 1.4 *Production of polyhydroxylated molecules via E. coli strains FucA-Y and RhuA-Y.*

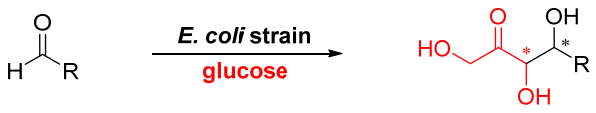

Entry[a]	Strain	Acceptor	Product	Incubation time (h)	Isolated yield	*dr*
1[b]	FucA-Y	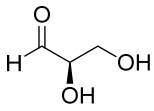	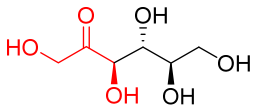 D-psicose	20	960 mg 35.6 %	92:8[d]
2[c]	FucA-Y	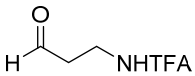	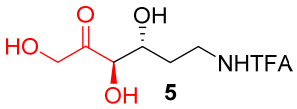 **5**	12	665 mg 12.8 %	87:13[e]
3[b]	RhuA-Y	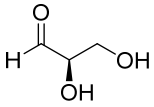	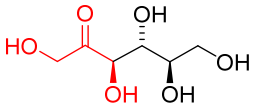 D-psicose 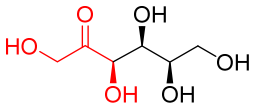 D-sorbose	20	281 mg 10.4 % 286 mg 10.6 %	49:51[d]
4[c]	RhuA-Y	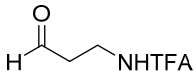	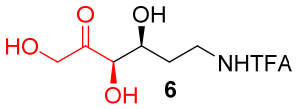 **6**	6	1.16g 22.4 %	89:11[e]

[a] Fermentation conditions: same as Table 2. [b] 1 L ECAM was used as medium and 15 mmol aldehyde was used [c] 1 L LB Broth/ECAM (1/1, v/v) was used as medium and 20 mmol aldehyde was used. [d] Determined by HPLC. [e] Determined by ^{1}H NMR.

1.6.6 Comparing the in vivo and in vitro stereoselectivities of FruA, FucA, and RhuA

To compare the *in vivo* and *in vitro* stereoselectivities of FruA, FucA and RhuA, **2**, **5**, and **6** were synthesize via *in vitro* one-pot four-enzyme system (**Table 1.5**). GPO catalyzed the *in*

situ generation of DHAP from DL-glycerol 3-phosphate. Then, aldolases coupled DHAP with aldehyde **1** to give phosphorylated aldol adducts, which were dephosphorylated by acid phosphatase (AP) to give aldol product **2**, **5**, **6**. FruA gave **2** exculsively (*dr* > 95:5, entry 1), FucA provided **5** with 87:13 *dr* (entry 2), and RhaD yielded **6** with 89:11 *dr* (entry 3). The stereoselectivities of FruA, FucA and RhaD are in consistence with the *in vivo* results. Therefore, these engineered *E. coli* strains can serve as a general and effective method for the practical production of polyhydroxylated molecules.

Table 1.5 *One-pot four-enzyme synthesis of* ***2***, ***5***, ***6***

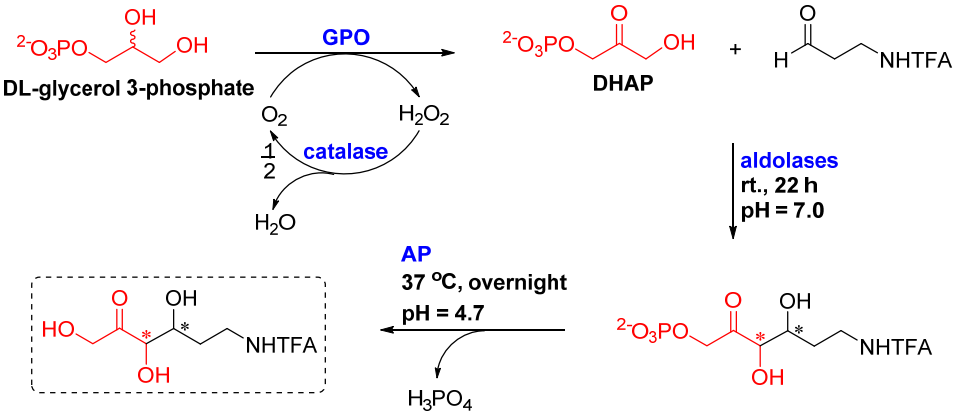

Entry	Aldolase	Acceptor	Product	Isolated yield	*dr*[a] *in vitro*	*dr*[a] *in vivo*
1	FruA	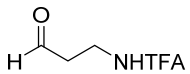	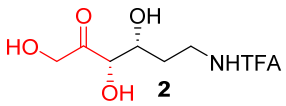 **2**	53 %	> 95:5	> 95:5
2	FucA	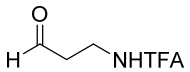	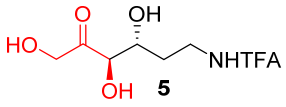 **5**	48 %	87:13	87:13
3	RhuA	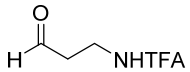	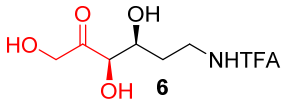 **6**	42 %	89:11	89:11

[a] Determined by ^{1}H NMR.

1.6.7 Confirming the E. coli synthetic machinery design by ^{13}C labeling experiment.

To confirm that C1, C2, C3 three carbons of products were derived from supplemented glucose via DHAP of glycolytic pathway, FruA-Y was fed with [U-$^{13}C_6$] glucose as sole carbon source and **1** as aldehyde acceptor (**Scheme 1.11**). Fermentation was carried out in the same protocol as described previously by using citric acid-free ECAM as culture medium. After purification, product was characterized by ^{1}H, ^{13}C NMR, which indicated that C1, C2, C3 three carbons truly came from [U-$^{13}C_6$] glucose as integral of the three carbons are much stronger than other carbons due to 100 % ^{13}C abundance.

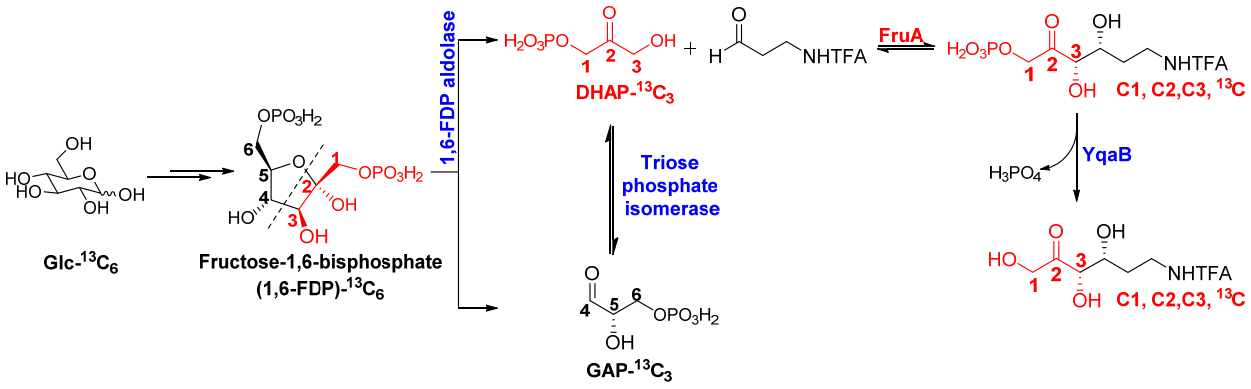

Scheme 1.11 *Production of [1,2,3-$^{13}C_3$]* ***2*** *by using Glc-$^{13}C_6$ as the sole carbon source.*

1.7 Pathway modeling and analysis

In order to further enhance the production efficiency of current "*E. coli* synthetic machinery", we tried to develop a mathematical model to analyze the *E. coli* glycolytic reaction networks with the aldol biosynthetic pathway. Through the mathematical model, we can analyze the dynamics of the reaction networks, and identify the bottleneck reaction steps/pathways. Then, we can explore the parameter space and design space to identify what type of modifications in the pathway would result in an increase in final production. Such a prediction

will guide the optimization of *E. coli* strains (design and construct new *E. coli* strains based on the results of modeling analysis) to improve production efficiency.

Using optimization-based methods to predict fluxes in metabolic flux balance models has been a successful approach for *E. coli*,[91] enabling construction of in silico models,[92] inference of some regulatory motifs,[93] and design of metabolic pathways for optimum performance.[94]

The basic principles of Flux Balance Analysis (FBA) models are well established. If it is postulated that the cell maximizes a certain metabolic objective, *I*, then the flux distribution (*v*) can be predicted through solving an optimization problem (**Equation 1.1**). V is the vector of fluxes (*v*). *c* is a vector of weights indicating how much each reaction contributes to the objective function. c^T is the transpose of *c*.

$$\max_V I = c^T \cdot V$$

Equation 1.1

At steady state, the changes in the metabolites is zero (**Equation 1.2**) and the equations can be reduce to a set of linear algebraic equations. V is the vector of m fluxes (*v*) and S is the *n*m* matrix of stoichiometric coefficients of the n metabolites in reactions.

$$\frac{d[Z]}{dt} = S * V = 0$$

Equation 1.2

FBA essentially combine metabolic flux steady state analysis with an assumed/identified metabolic objective function. It has been particularly successful in modeling E. coli, by assuming

maximum biomass formation in a variety of conditions.[95-97] Therefore, we choose to use FBA to study the biosynthetic pathway model and develop in silico models of the reaction schemes to help understand the biosynthetic systems as well as predict optimal alternatives.

Central carbon metabolic pathway (containing the phosphotransferase system (PTS), glycolysis, pentose-phosphate pathway (PPP)) is the most important among metabolic pathways in all microorganisms since it produces energy and precursors for biosynthesis. Therefore, we designed a mathematical model consisting of the central carbon metabolic pathway and DHAP-dependent aldolases mediated biosynthetic pathway. As shown in **Scheme 1.12**, the constructed model consists of 25 metabolites participating in 28 reactions catalyzed by 22 enzymes.

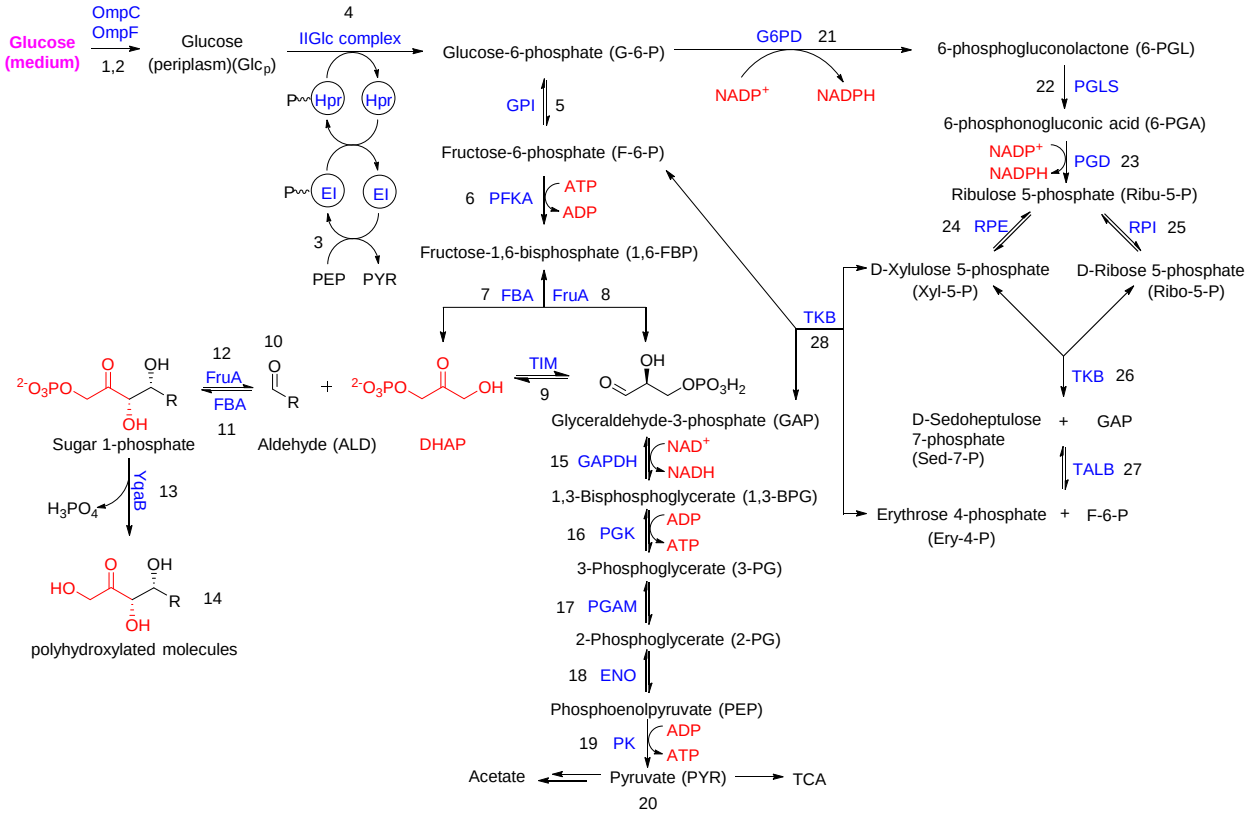

OmpC: outer membrane porin C; OmpF: outer membrane porin F; IIGlc complex: glucose Enzyme II transporter complex; Hpr: histidyl phosphorylatable protein; EI: enzyme I;GPI: glucose-6-phosphate isomerase; PFKA: 6-phosphofructokinase; FBA: fructose bis-phosphate aldolase; TIM: triose phosphate isomerase; GAPDH: glyceraldehyde-3-phosphate dehydrogenase; PGK: phosphoglycerate kinase; PGAM: phosphoglycerate mutase; ENO: enolase; PK: pyruvate kinase; G6PD: Glucose-6-phosphate 1-dehydrogenase;PGLS: 6-phosphogluconolactonase; PGD: 6-phosphogluconate dehydrogenase; RPE: ribulose phosphate 3-epimerase; RPI: ribose-5-phosphate isomerase A; TKB: transketolase B; TALB: transaldolase B;

Scheme 1.12 *Reaction networks of E. coli central carbon metabolism.*

The reaction network of constructed model was simplified in term of reaction fluxes (v). As shown in **Scheme 1.13**, the simplified model contains 42 internal fluxes ($v_1 - v_{42}$) and 4 external fluxes (α, β, γ, δ).

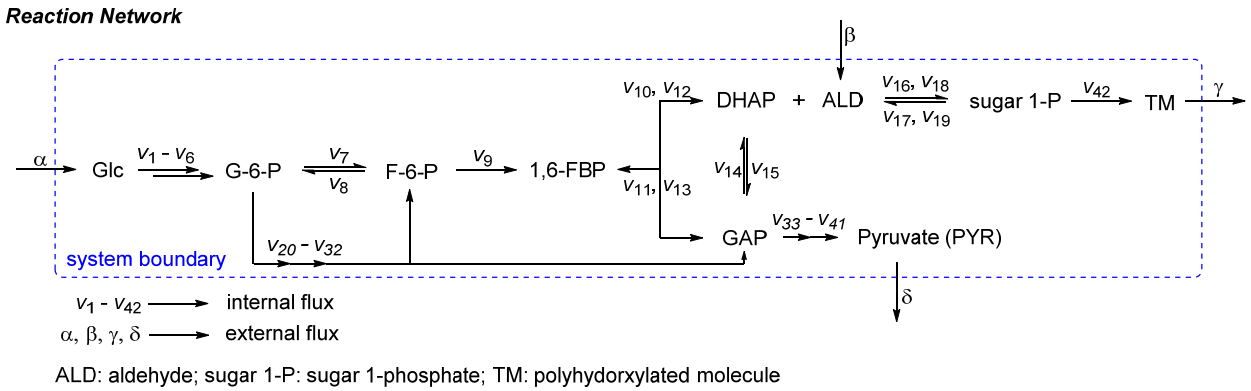

Scheme 1.13 *Simplified reaction network.*

According to the simplified reaction network, the mass balance equations of each metabolites were reduce to a set of linear algebraic equations, which were then mathematically represented as a stoichiometric matrix S_{25x46}, with each row representing one metabolite and each column representing the participation of one particular reaction flux across the mass balance of all metabolites (**Figure 1.2 A**). **V** is the vector of fluxes and **X** is the vector of metabolites. At steady state, the changes in the metabolites is zero. Therefore, $d\mathbf{X}/dt = \mathbf{S}*\mathbf{X}^T = 0$, and $\mathbf{X}_{ss}$ (concentration of metabolites at steady state) is the solution of this equation. Therefore, given one set of fluxes V_0, the corresponding concentration of metabolites X_{ss0} can be deduced from solving the mass balance equation at steady state. However, the total number of enzyme kinetic parameters for the 46 fluxes is 136, and almost one third of them are unknown. Without complete enzyme kinetic parameters, we couldn't solve the mass balance equation. Thus, we suspended the mathematical modeling.

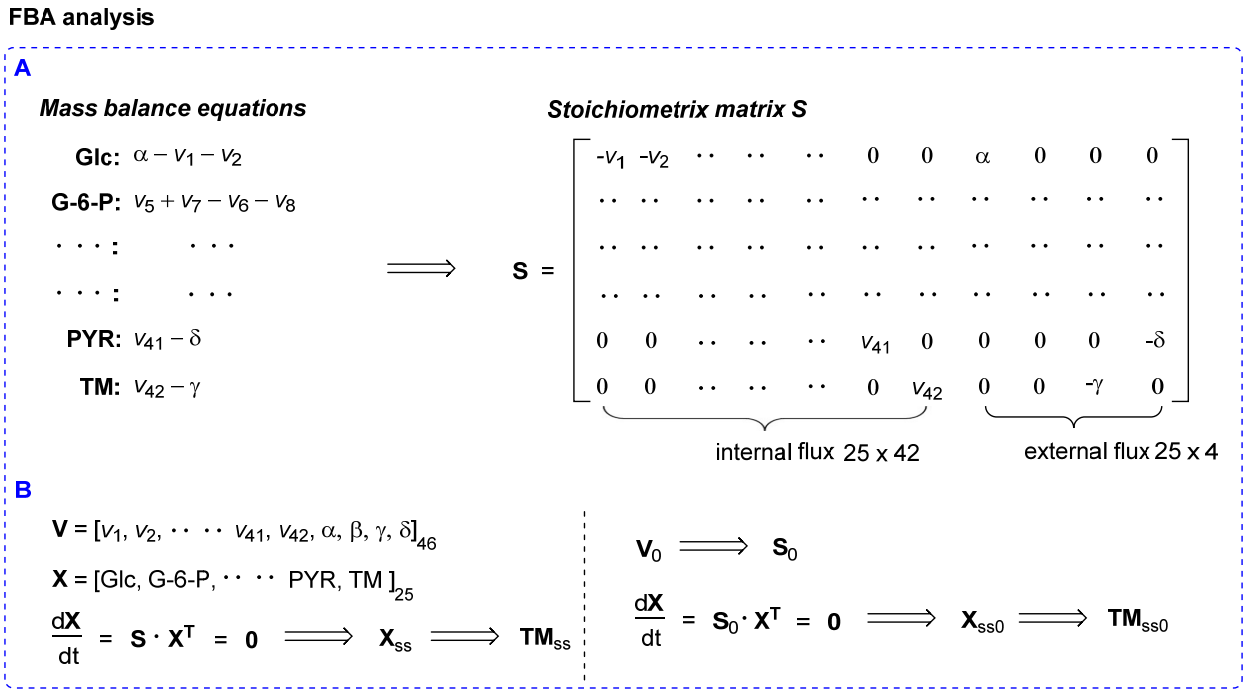

Figure 1.2 *FBA analysis of constructed model.*

1.8 Conclusions

Transforming DHAP-dependent aldolases mediated aldol reactions from flask into cell-based synthesis addressed several key issues plaguing large scale synthetic utility of DHAP-dependent aldolases: 1) it solves the problem of DHAP availability by *in vivo* hijacking DHAP from glycolysis pathway of bacterial system, 2) it circumvents purification of recombinant aldolases and phosphatase, and 3) it dephosphorylates resultant aldol adducts *in vivo*, thus eliminating the additional step for phosphate removal and achieving *in vivo* phosphate recycling. Operational simplicity, low cost and easy to scale up of fermentation renders such transformation holds enormous value in synthesis of biologically relevant polyhydroxylated molecules on an industrial scale.

Moreover, in the final products, the 3 carbons corresponding to the DHAP structure come from biomass, the cheapest, sustainable source. And the fermentation process is fully executed in environmental friendly conditions. This is in sharp contrast with the conventional non-green chemical or *in vitro* enzymatic synthesis that either uses toxic organic solvents or expensive reaction starting materials from non-sustainable petroleum industry.

Finally, this approach of hijacking valuable biochemical (DHAP) from metabolic pathway (glycolysis) and transforming enzymatic reactions (DHAP-dependent aldolases catalyzed aldol reactions) from flasks to *E. coli* cells may open the flood gate that large number of biochemicals in microbial metabolic pathways can be utilized.

1.9 References

1. Gijsen, H.J.M. & Wong, C.-H. Unprecedented Asymmetric Aldol Reactions with Three Aldehyde Substrates Catalyzed by 2-Deoxyribose-5-phosphate Aldolase. *J. Am. Chem. Soc.* **116**, 8422-8423 (1994).

2. Wong, C.-H., Garcia-Junceda, E., Chen, L., Blanco, O., Gijsen, H.J.M. & Steensma, D.H. Recombinant 2-Deoxyribose-5-phosphate Aldolase in Organic Synthesis: Use of Sequential Two-Substrate and Three-Substrate Aldol Reactions. *J. Am. Chem. Soc.* **117**, 3333-3339 (1995).

3. Chopra, T.J., O'Neill, P.M. & Wilkes, P.B. 32pp. (Pfizer Products Inc., USA . 2008).

4. Hu, S., Tao, J. & Xie, Z. 34pp. (Pfizer Inc., USA . 2006).

5. O'Sullivan, S. & O'Neill, J. 17pp. (Pfizer Science and Technology Ireland Limited, Ire. . 2007).

6. Tully, W. 20pp. (Pfizer Science and Technology Ireland Limited, Ire. . 2002).

7. Tully, W., Madigan, E. & O'Connell, J. 12pp. (Pfizer Science and Technology Ireland Limited, Ire. . 2002).

8. Machajewski, T.D. & Wong, C.H. The Catalytic Asymmetric Aldol Reaction. *Angew. Chem., Int. Ed.* **39**, 1352-1375 (2000).

9. Brovetto, M., Gamenara, D., Saenz Méndez, P. & Seoane, G.A. C−C Bond-Forming Lyases in Organic Synthesis. *Chem. Rev.* **111**, 4346-4403 (2011).

10. Wong, C.H. & Whitesides, G.M. Enzymes in synthetic organic chemistry. (Pergamon, Oxford).

11. Fessner, W.-D. in Modern Aldol Reactions 201-272 (Wiley-VCH Verlag GmbH, 2008).

12. Bednarski, M.D., Simon, E.S., Bischofberger, N., Fessner, W.D., Kim, M.J., Lees, W., Saito, T., Waldmann, H. & Whitesides, G.M. Rabbit muscle aldolase as a catalyst in organic synthesis. *J. Am. Chem. Soc.* **111**, 627-635 (1989).

13. Whalem, L.J. & Wong, C.-H. Enzymes in organic synthesis: aldolase-mediated synthesis of iminocyclitols and novel heterocycles. *Aldrichimica Acta* **39**, 63-71 (2006).

14. Sugiyama, M., Hong, Z., Greenberg, W.A. & Wong, C.-H. 405-419 (John Wiley & Sons, Inc., 2010).

15. Laborda, P., Sayago, F.J., Cativiela, C., Parella, T., Joglar, J. & Clapes, P. Aldolase-Catalyzed Synthesis of Conformationally Constrained Iminocyclitols: Preparation of

Polyhydroxylated Benzopyrrolizidines and Cyclohexapyrrolizidines. *Org. Lett.* **16**, 1422-1425 (2014).

16. Concia, A.L., Gomez, L., Parella, T., Joglar, J. & Clapes, P. Casuarine Stereoisomers from Achiral Substrates: Chemoenzymatic Synthesis and Inhibitory Properties. *J. Org. Chem.* **79**, 5386-5389 (2014).

17. Lin, C.-I., McCarty, R.M. & Liu, H.-w. The biosynthesis of nitrogen-, sulfur-, and high-carbon chain-containing sugars. *Chem. Soc. Rev.* **42**, 4377-4407 (2013).

18. Jarosz, S. From higher carbon sugars to carbocyclic sugar mimics. *Curr. Org. Chem.* **12**, 985-994 (2008).

19. El, B.L., Ahbala, M., Bolte, J. & Lemaire, M. Straightforward chemo-enzymatic synthesis of new aminocyclitols, analogues of valiolamine and their evaluation as glycosidase inhibitors. *Tetrahedron: Asymmetry* **17**, 2684-2688 (2006).

20. El, B.L., Assaf, Z., Camps, B.F., Veschambre, H., Thery, V., Bolte, J. & Lemaire, M. Fructose-1,6-Bisphosphate Aldolase-Mediated Synthesis of Aminocyclitols (Analogues of Valiolamine) and their Evaluation as Glycosidase Inhibitors. *ChemCatChem* **1**, 463-471 (2009).

21. Gijsen, H.J.M. & Wong, C.-H. Synthesis of a cyclitol via a tandem enzymic aldol-intramolecular Horner-Wadsworth-Emmons reaction. *Tetrahedron Lett.* **36**, 7057-7060 (1995).

22. El, B.L., Crestia, D., Gallienne, E., Demuynck, C., Bolte, J. & Lemaire, M. A straightforward synthesis of an aminocyclitol based on an enzymatic aldol reaction and a highly stereoselective intramolecular Henry reaction. *Tetrahedron: Asymmetry* **15**, 2951-2954 (2004).

23. Fessner, W.-D. & Helaine, V. Biocatalytic synthesis of hydroxylated natural products using aldolases and related enzymes. *Curr. Opin. Biotechnol.* **12**, 574-586 (2001).

24. Chenevert, R., Lavoie, M. & Dasser, M. Use of aldolases in the synthesis of non-carbohydrate natural products. Stereoselective synthesis of aspicilin C-3--C-9 fragment. *Can. J. Chem.* **75**, 68-73 (1997).

25. Phung, A.N., Zannetti, M.T., Whited, G. & Fessner, W.D. Stereospecific biocatalytic synthesis of pancratistatin analogues. *Angew. Chem., Int. Ed.* **42**, 4821-4824 (2003).

26. Charmantray, F., Dellis, P., Helaine, V., Samreth, S. & Hecquet, L. Chemoenzymatic synthesis of 5-thio-D-xylopyranose. *Eur. J. Org. Chem.*, 5526-5532 (2006).

27. Gomez, L., Garrabou, X., Joglar, J., Bujons, J., Parella, T., Vilaplana, C., Cardona, P.J. & Clapes, P. Chemoenzymatic synthesis, structural study and biological activity of novel indolizidine and quinolizidine iminocyclitols. *Org. Biomol. Chem.* **10**, 6309-6321 (2012).

28. Concia, A.L., Gomez, L., Parella, T., Joglar, J. & Clapes, P. Casuarine Stereoisomers from Achiral Substrates: Chemoenzymatic Synthesis and Inhibitory Properties. *J. Org. Chem.* **79**, 5386-5389 (2014).

29. Sanchez-Moreno, I., Iturrate, L., Doyagueez, E.G., Martinez, J.A., Fernandez-Mayoralas, A. & Garcia-Junceda, E. Activated α,β-Unsaturated Aldehydes as Substrate of Dihydroxyacetone Phosphate (DHAP)-Dependent Aldolases in the Context of a Multienzyme System. *Adv. Synth. Catal.* **351**, 2967-2975 (2009).

30. Laborda, P., Sayago, F.J., Cativiela, C., Parella, T., Joglar, J. & Clapes, P. Aldolase-Catalyzed Synthesis of Conformationally Constrained Iminocyclitols: Preparation of Polyhydroxylated Benzopyrrolizidines and Cyclohexapyrrolizidines. *Org. Lett.* **16**, 1422-1425 (2014).

31. Soler, A., Garrabou, X., Hernandez, K., Gutierrez, M.L., Busto, E., Bujons, J., Parella, T., Joglar, J. & Clapes, P. Sequential Biocatalytic Aldol Reactions in Multistep Asymmetric Synthesis: Pipecolic Acid, Piperidine and Pyrrolidine (Homo)Iminocyclitol Derivatives from Achiral Building Blocks. *Adv. Synth. Catal.* **356**, 3007-3024 (2014).

32. Brovetto, M., Gamenara, D., Saenz Mendez, P. & Seoane, G.A. C-C Bond-Forming Lyases in Organic Synthesis. *Chem. Rev.* **111**, 4346-4403 (2011).

33. Clapes, P. & Garrabou, X. Current Trends in Asymmetric Synthesis with Aldolases. *Adv. Synth. Catal.* **353**, 2263-2283 (2011).

34. Samland, A.K. & Sprenger, G.A. Microbial aldolases as C-C bonding enzymes - unknown treasures and new developments. *Appl. Microbiol. Biotechnol.* **71**, 253-264 (2006).

35. Sugiyama, M., Hong, Z., Liang, P.-H., Dean, S.M., Whalen, L.J., Greenberg, W.A. & Wong, C.-H. D-Fructose-6-Phosphate Aldolase-Catalyzed One-Pot Synthesis of Iminocyclitols. *J. Am. Chem. Soc.* **129**, 14811-14817 (2007).

36. Bednarski, M.D., Simon, E.S., Bischofberger, N., Fessner, W.D., Kim, M.J., Lees, W., Saito, T., Waldmann, H. & Whitesides, G.M. Rabbit muscle aldolase as a catalyst in organic synthesis. *J. Am. Chem. Soc.* **111**, 627-635 (1989).

37. Colbran, R.L., Jones, J.K.N., Matheson, N.K. & Rozema, I. A synthesis of dihydroxyacetone phosphate from dihydroxyacetone. *Carbohydr. Res.* **4**, 355-358 (1967).

38. Pederson, R.L., Esker, J. & Wong, C.H. An improved synthesis of dihydroxyacetone phosphate. *Tetrahedron* **47**, 2643-2648 (1991).

39. Jung, S.-H., Jeong, J.-H., Miller, P. & Wong, C.-H. An Efficient Multigram-Scale Preparation of Dihydroxyacetone Phosphate. *J. Org. Chem.* **59**, 7182-7184 (1994).

40. Gefflaut, T., Lemaire, M., Valentin, M.-L. & Bolte, J. A Novel Efficient Synthesis of Dihydroxyacetone Phosphate and Bromoacetol Phosphate for Use in Enzymic Aldol Syntheses. *J. Org. Chem.* **62**, 5920-5922 (1997).

41. Ferroni, E.L., DiTella, V., Ghanayem, N., Jeske, R., Jodlowski, C., O'Connell, M., Styrsky, J., Svoboda, R., Venkataraman, A. & Winkler, B.M. A Three-Step Preparation of Dihydroxyacetone Phosphate Dimethyl Acetal. *J. Org. Chem.* **64**, 4943-4945 (1999).

42. Meyer, O., Rohmer, M. & Grosdemange-Billiard, C. Short and efficient synthesis of a stock material of dihydroxyacetone phosphate from glycidol. *Tetrahedron Lett.* **45**, 7921-7923 (2004).

43. Charmantray, F., El Blidi, L., Gefflaut, T., Hecquet, L., Bolte, J. & Lemaire, M. Improved Straightforward Chemical Synthesis of Dihydroxyacetone Phosphate through Enzymatic Desymmetrization of 2,2-Dimethoxypropane-1,3-diol. *J. Org. Chem.* **69**, 9310-9312 (2004).

44. Meyer, O., Ponaire, S., Rohmer, M. & Grosdemange-Billiard, C. Lewis Acid Mediated Regioselective Ring Opening of Benzylglycidol with Dibenzyl Phosphate: Short and Attractive Synthesis of Dihydroxyacetone Phosphate. *Org. Lett.* **8**, 4347-4350 (2006).

45. Schuemperli, M., Pellaux, R. & Panke, S. Chemical and enzymatic routes to dihydroxyacetone phosphate. *Appl. Microbiol. Biotechnol.* **75**, 33-45 (2007).

46. Wong, C.H. & Whitesides, G.M. Synthesis of sugars by aldolase-catalyzed condensation reactions. *J. Org. Chem.* **48**, 3199-3205 (1983).

47. Crans, D.C. & Whitesides, G.M. Glycerol kinase: synthesis of dihydroxyacetone phosphate, sn-glycerol-3-phosphate, and chiral analogs. *J. Am. Chem. Soc.* **107**, 7019-7027 (1985).

48. Yanase, H., Okuda, M., Kita, K., Sato, Y., Shibata, K., Sakai, Y. & Kato, N. Enzymic preparation of [1,3-13C]dihydroxyacetone phosphate from [13C]methanol and hydroxypyruvate using the methanol-assimilating system of methylotrophic yeasts. *Appl. Microbiol. Biotechnol.* **43**, 228-234 (1995).

49. Itoh, N., Tujibata, Y. & Liu, J.Q. Cloning and overexpression in Escherichia coli of the gene encoding dihydroxyacetone kinase isoenzyme I from Schizosaccharomyces pombe, and its application to dihydroxyacetone phosphate production. *Appl. Microbiol. Biotechnol.* **51**, 193-200 (1999).

50. Sanchez-Moreno, I., Francisco Garcia-Garcia, J., Bastida, A. & Garcia-Junceda, E. Multienzyme system for dihydroxyacetone phosphate-dependent aldolase catalyzed C-C bond formation from dihydroxyacetone. *Chem. Commun.*, 1634-1635 (2004).

51. Fessner, W.D. & Sinerius, G. Enzymes in organic synthesis. 7. Synthesis of dihydroxyacetone phosphate (and isosteric analogs) by enzymic oxidation: sugars from glycerol. *Angew. Chem.* **106**, 217-220 (1994).

52. Schoevaart, R., van Rantwijk, F. & Sheldon, R.A. A Four-Step Enzymatic Cascade for the One-Pot Synthesis of Non-natural Carbohydrates from Glycerol. *J. Org. Chem.* **65**, 6940-6943 (2000).

53. Hettwer, J., Oldenburg, H. & Flaschel, E. Enzymic routes to dihydroxyacetone phosphate or immediate precursors. *J. Mol. Catal. B: Enzym.* **19-20**, 215-222 (2002).

54. Charmantray, F., Dellis, P., Samreth, S. & Hecquet, L. An efficient chemoenzymatic route to dihydroxyacetone phosphate from glycidol for the in situ aldolase-mediated synthesis of monosaccharides. *Tetrahedron Lett.* **47**, 3261-3263 (2006).

55. Li, Z., Cai, L., Wei, M. & Wang, P.G. One-pot four-enzyme synthesis of ketoses with fructose 1,6-bisphosphate aldolases from Staphylococcus carnosus and rabbit muscle. *Carbohydr. Res.* **357**, 143-146 (2012).

56. Fessner, W.D. & Walter, C. Enzymes in organic synthesis. 3. Artificial metabolism applied to the one-pot asymmetric synthesis of branched saccharides. *Angew. Chem.* **104**, 643-645 (1992).

57. Drueckhammer, D.G., Durrwachter, J.R., Pederson, R.L., Crans, D.C., Daniels, L. & Wong, C.H. Reversible and in situ formation of organic arsenates and vanadates as organic phosphate mimics in enzymatic reactions: mechanistic investigation of aldol reactions and synthetic applications. *J. Org. Chem.* **54**, 70-77 (1989).

58. Schoevaart, R., van Rantwijk, F. & Sheldon, R.A. Facile Enzymatic Aldol Reactions with Dihydroxyacetone in the Presence of Arsenate. *J. Org. Chem.* **66**, 4559-4562 (2001).

59. Crans, D.C., Sudhakar, K. & Zamborelli, T.J. Interaction of rabbit muscle aldolase at high ionic strengths with vanadate and other oxoanions. *Biochemistry* **31**, 6812-6821 (1992).

60. Sugiyama, M., Hong, Z., Whalen, L.J., Greenberg, W.A. & Wong, C.-H. Borate as a phosphate ester mimic in aldolase-catalyzed reactions: practical synthesis of L-Fructose and L-Iminocyclitols. *Adv. Synth. Catal.* **348**, 2555-2559 (2006).

61. Garrabou, X., Calveras, J., Joglar, J., Parella, T., Bujons, J. & Clapes, P. Highly efficient aldol additions of DHA and DHAP to N-Cbz-amino aldehydes catalyzed by L-

rhamnulose-1-phosphate and L-fuculose-1-phosphate aldolases in aqueous borate buffer. *Org. Biomol. Chem.* **9**, 8430-8436 (2011).

62. Schurmann, M. & Sprenger, G.A. Fructose-6-phosphate aldolase is a novel class I aldolase from Escherichia coli and is related to a novel group of bacterial transaldolases. *J. Biol. Chem.* **276**, 11055-11061 (2001).

63. Castillo, J.A., Calveras, J., Casas, J., Mitjans, M., Vinardell, M.P., Parella, T., Inoue, T., Sprenger, G.A., Joglar, J. & Clapes, P. Fructose-6-phosphate Aldolase in Organic Synthesis: Preparation of D-Fagomine, N-Alkylated Derivatives, and Preliminary Biological Assays. *Org. Lett.* **8**, 6067-6070 (2006).

64. Concia, A.L., Lozano, C., Castillo, J.A., Parella, T., Joglar, J. & Clapes, P. D-fructose-6-phosphate aldolase in organic synthesis: Cascade chemical-enzymatic preparation of sugar-related polyhydroxylated compounds. *Chem. - Eur. J.* **15**, 3808-3816 (2009).

65. Garrabou, X., Castillo, J.A., Guerard-Helaine, C., Parella, T., Joglar, J., Lemaire, M. & Clapes, P. Asymmetric Self- and Cross-Aldol Reactions of Glycolaldehyde Catalyzed by D-Fructose-6-phosphate Aldolase. *Angew. Chem., Int. Ed.* **48**, 5521-5525 (2009).

66. Schneider, S., Sandalova, T., Schneider, G., Sprenger, G.A. & Samland, A.K. Replacement of a Phenylalanine by a Tyrosine in the Active Site Confers Fructose-6-phosphate Aldolase Activity to the Transaldolase of Escherichia coli and Human Origin. *J. Biol. Chem.* **283**, 30064-30072 (2008).

67. Iturrate, L., Sanchez-Moreno, I., Oroz-Guinea, I., Perez-Gil, J. & Garcia-Junceda, E. Preparation and Characterization of a Bifunctional Aldolase/Kinase Enzyme: A More Efficient Biocatalyst for C-C Bond Formation. *Chem. - Eur. J.* **16**, 4018-4030 (2010).

68. Garrabou, X., Joglar, J., Parella, T., Crehuet, R., Bujons, J. & Clapes, P. Redesign of the Phosphate Binding Site of L-Rhamnulose- 1-Phosphate Aldolase towards a Dihydroxyacetone Dependent Aldolase. *Adv. Synth. Catal.* **353**, 89-99 (2011).

69. Goldberg, R.N. & Tewari, Y.B. Thermodynamics of enzyme-catalyzed reactions: Part 4. Lyases. *J. Phys. Chem. Ref. Data* **24**, 1669-1698 (1995).

70. Fessner, W.-D. & Helaine, V. Biocatalytic synthesis of hydroxylated natural products using aldolases and related enzymes. *Curr. Opin. Biotechnol.* **12**, 574-586 (2001).

71. Gefflaut, T., Blonski, C., Perie, J. & Willson, M. Class I aldolases: Substrate specificity, mechanism, inhibitors and structural aspects. *Prog. Biophys. Mol. Biol.* **63**, 301-340 (1995).

72. Brockamp, H.P. & Kula, M.R. Staphylococcus carnosus aldolase as catalyst for enzymic aldol reactions. *Tetrahedron Lett.* **31**, 7123-7126 (1990).

73. Brockamp, H.P. & Kula, M.R. Purification and characterization of a class I fructose 1,6-bisphosphate aldolase from Staphylococcus carnosus. *Appl. Microbiol. Biotechnol.* **34**, 287-291 (1990).

74. Fessner, W.-D. & Walter, C. Enzymic C-C bond formation in asymmetric synthesis. *Top. Curr. Chem.* **184**, 97-194 (1997).

75. Khalil, A.S. & Collins, J.J. Synthetic biology: applications come of age. *Nature Reviews. Genetics* **11**, 367-379 (2010).

76. Endy, D. Foundations for engineering biology. *Nature* **438**, 449-453 (2005).

77. Purnick, P.E.M. & Weiss, R. The second wave of synthetic biology: from modules to systems. *Nat. Rev. Mol. Cell Biol.* **10**, 410-422 (2009).

78. Romano, A.H. & Conway, T. Evolution of carbohydrate metabolic pathways. *Res. Microbiol.* **147**, 448-455 (1996).

79. Harris, T.K., Cole, R.N., Comer, F.I. & Mildvan, A.S. Proton transfer in the mechanism of triosephosphate isomerase. *Biochemistry* **37**, 16828-16838 (1998).

80. Kuznetsova, E., Proudfoot, M., Gonzalez, C.F., Brown, G., Omelchenko, M.V., Borozan, I., Carmel, L., Wolf, Y.I., Mori, H., Savchenko, A.V., Arrowsmith, C.H., Koonin, E.V., Edwards, A.M. & Yakunin, A.F. Genome-wide Analysis of Substrate Specificities of the Escherichia coli Haloacid Dehalogenase-like Phosphatase Family. *J. Biol. Chem.* **281**, 36149-36161 (2006).

81. Wardrop, D.J. & Waidyarachchi, S.L. Synthesis and biological activity of naturally occurring α-glucosidase inhibitors. *Nat. Prod. Rep.* **27**, 1431-1468 (2010).

82. Asano, N. Naturally occurring iminosugars and related compounds: Structure, distribution, and biological activity. *Curr. Top. Med. Chem.* **3**, 471-484 (2003).

83. Asano, N. Glycosidase inhibitors: update and perspectives on practical use. *Glycobiology* **13**, 93R-104R (2003).

84. Robina, I., Moreno-Vargas, A.J., Carmona, A.T. & Vogel, P. Glycosidase inhibitors as potential HIV entry inhibitors? *Curr. Drug Metab.* **5**, 329-361 (2004).

85. Dwek, R.A., Butters, T.D., Platt, F.M. & Zitzmann, N. Targeting glycosylation as a therapeutic approach. *Nat. Rev. Drug Discovery* **1**, 65-75 (2002).

86. Gomez, L., Molinar-Toribio, E., Calvo-Torras, M.A., Adelantado, C., Juan, M.E., Planas, J.M., Canas, X., Lozano, C., Pumarola, S., Clapes, P. & Torres, J.L. D-Fagomine lowers postprandial blood glucose and modulates bacterial adhesion. *Br. J. Nutr.* **107**, 1739-1746 (2012).

87. Ramos-Romero, S., Molinar-Toribio, E., Gomez, L., Perez-Jimenez, J., Casado, M., Clapes, P., Pina, B. & Torres, J.L. Effect of D-fagomine on excreted enterobacteria and weight gain in rats fed a high-fat high-sucrose diet. *Obesity* **22**, 976-979 (2014).

88. Horne, G., Wilson, F.X., Tinsley, J., Williams, D.H. & Storer, R. Iminosugars past, present and future: medicines for tomorrow. *Drug Discov. Today* **16**, 107-118 (2011).

89. Nash, R.J., Kato, A., Yu, C.Y. & Fleet, G.W. Iminosugars as therapeutic agents: recent advances and promising trends. *Future Med. Chem.* **3**, 1513-1521 (2011).

90. Zhang, Z.-X., Wu, B., Wang, B., Li, T.-H., Zhang, P.-F., Guo, L.-N., Wang, W.-j., Zhao, W. & Wang, P.G. Facile and stereo-controlled synthesis of 2-deoxynojirimycin, Miglustat and Miglitol. *Tetrahedron Lett.* **52**, 3802-3804 (2011).

91. Kauffman, K.J., Prakash, P. & Edwards, J.S. Advances in flux balance analysis. *Curr. Opin. Biotechnol.* **14**, 491-496 (2003).

92. Price, N.D., Papin, J.A., Schilling, C.H. & Palsson, B.O. Genome-scale microbial in silico models: the constraints-based approach. *Trends Biotechnol.* **21**, 162-169 (2003).

93. Palsson, J.L.R.a.B.Ø. Thirteen Years of Building Constraint-Based In Silico Models of Escherichia coli. *Journal of Bacteriology* **185**, 2692-2699 (2003).

94. Vassily Hatzimanikatis, L.W. The systems engineering of cellular processes. . *Computer Aided Chemical Engineering* **21**, 71–80 (2006).

95. Edwards JS, I.R., Palsson BO In silico predictions of Escherichia coli metabolic capabilities are consistent with experimental data. *Nat. Biotechnol.* **19**, 125-130 (2001).

96. Mahadevan, R., Edwards, J.S. & Doyle, F.J., III Dynamic flux balance analysis of diauxic growth in Escherichia coli. *Biophys. J.* **83**, 1331-1340 (2002).

97. Palsson, A.V.a.B.O. Stoichiometric Flux Balance Models Quantitatively Predict Growth and Metabolic by- Product Secretion in Wild-Type Escherichia-Coli W3110. *Appl. Environ. Microbiol.* **60**, 3724–3731 (1994).

2 CHAPTER 2 STUDY THE MECHANISM OF CHEMICAL DESIALYLATION IN THE LIFE PROCESSES

2.1 Introduction

Sialic acids exist in abundance in glycan chains of glycoproteins and glycolipids on the surface of all eukaryotic cells and some prokaryotic cells. Their presence affects the molecular properties and structure of glycoconjugates, modifying their functions and interactions with other molecules.[1, 2] Sialic acid residues on glycoproteins and glycolipids have been recognized as critical factors modulating molecular recognitions and signaling inside the cell, between the cells, between the cells and the extracellular matrix, and between the cells and exogenous pathogens.[3, 4]

The sialylation status, referring to the expression levels and linkages of sialic acids on the cell surface, is determined by the dynamic balance between sialylation and desialylation (removal of sialic acids), which dramatically impacts the status, property and function of cells (**Figure 2.1**). Sialylation is mainly regulated through expression and activity of sialyltransferases, enzymes that transfer sialic acid residues onto oligosaccharides and glycoconjugates. And most sialyltransferases have been identified, cloned and characterized from multiple species.[5, 6] On the contrary, there is much limited understanding about the regulation of desialylation. The mainstream idea attributes desialylation to the sialidases,[7, 8]

enzymes that catalyze the removal of terminal sialic acid residues from sialosides and sialoglycoconjugates. However, mammalian sialidases are very unstable outside the cell and their extracellular activities are very low. Meanwhile, more and more emerging evidences, including our own, support the existence of chemical desialylation process in which the desialylation is brought by reactive oxygen species (ROS) and reaction nitrogen species (RNS) under some pathological conditions.

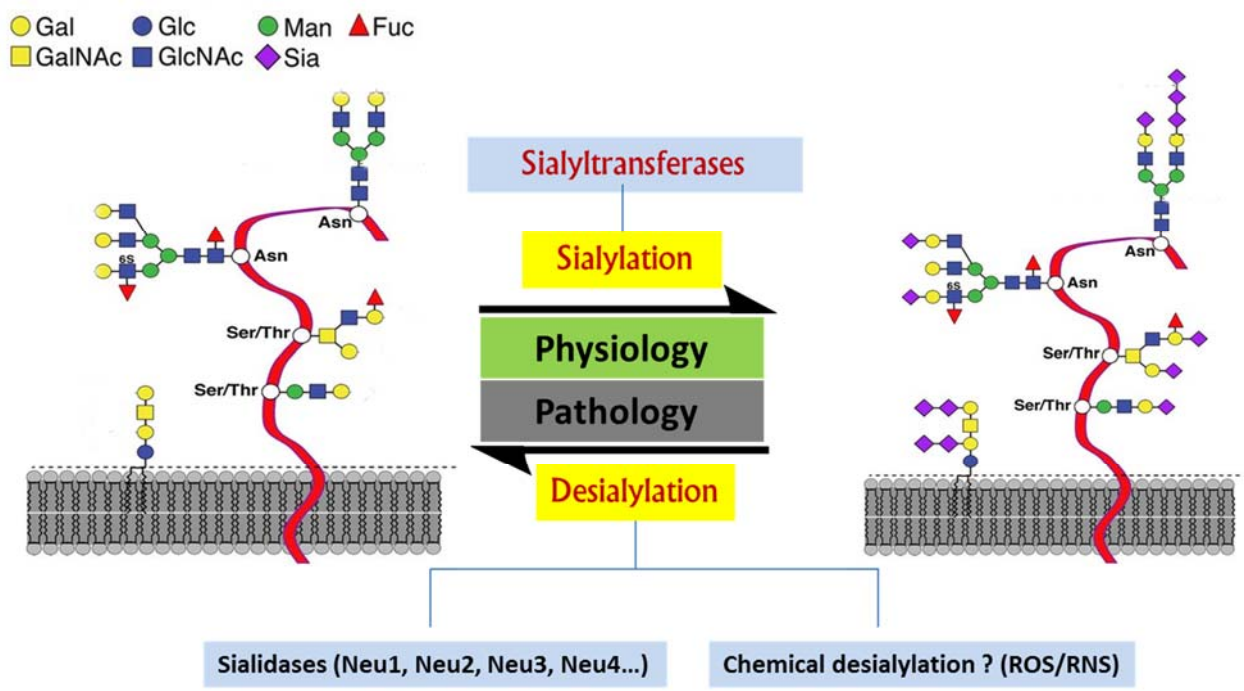

Figure 2.1 *Dynamics of Sialylation status—sialylation and desialylation*

2.2 Structural diversity and biological functions of sialic acids

Sialic acids are a diverse family of α-keto acidic monosaccharides widely expressed on all cell surfaces of animals (e.g., more than 10 million molecules per human erythrocyte) and to a less extent in plants and bacteria. *N*-acetylneuraminic acid (Neu5Ac), *N*-glycolylneuraminic acid

(Neu5Gc), and deaminoneuraminic acid (KDN) are the most well-known members of the sialic acid family (**Figure 2.2**). In addition to these three basic forms, more than 50 distinct sialic acid structures have been identified in nature, arising from acetylation, methylation, lactylation, sulfation, and phosphorylation of the C-4, C-5, C-7, C-8, or C-9 hydroxyl groups. Sialic acids exist predominantly as terminal monosaccharides linked to galactose (Gal) or *N*-acetylgaloctosamine (GalNAc) residues in glycan chains through α-2,3- or α-2,6-linkages. They can also form a homopolymer of α-2,8-linked polysialic acid (PSA).[9-12]

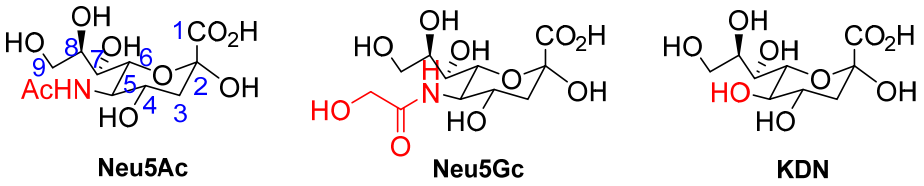

Figure 2.2 *Three basic forms of naturally occurring sialic acids*

Given their remarkable diversity in structure, glycosidic linkage, and underlying glycan chains, as well their exposed location, sialic acids play important roles in many physiological and pathological processes, including platelet clearance, regulation of the immune response, microbe binding that leads to infections, brain development, and the progression and spread of human malignancies (**Figure 2.3**).[13, 14] Besides to function as recognition sites, sialic acids also can act as biological mask to shield recognition sites. Recently, it also has been reported that sialic acids can act as antioxidant to scavenge free radicals and protect DNA.[15]

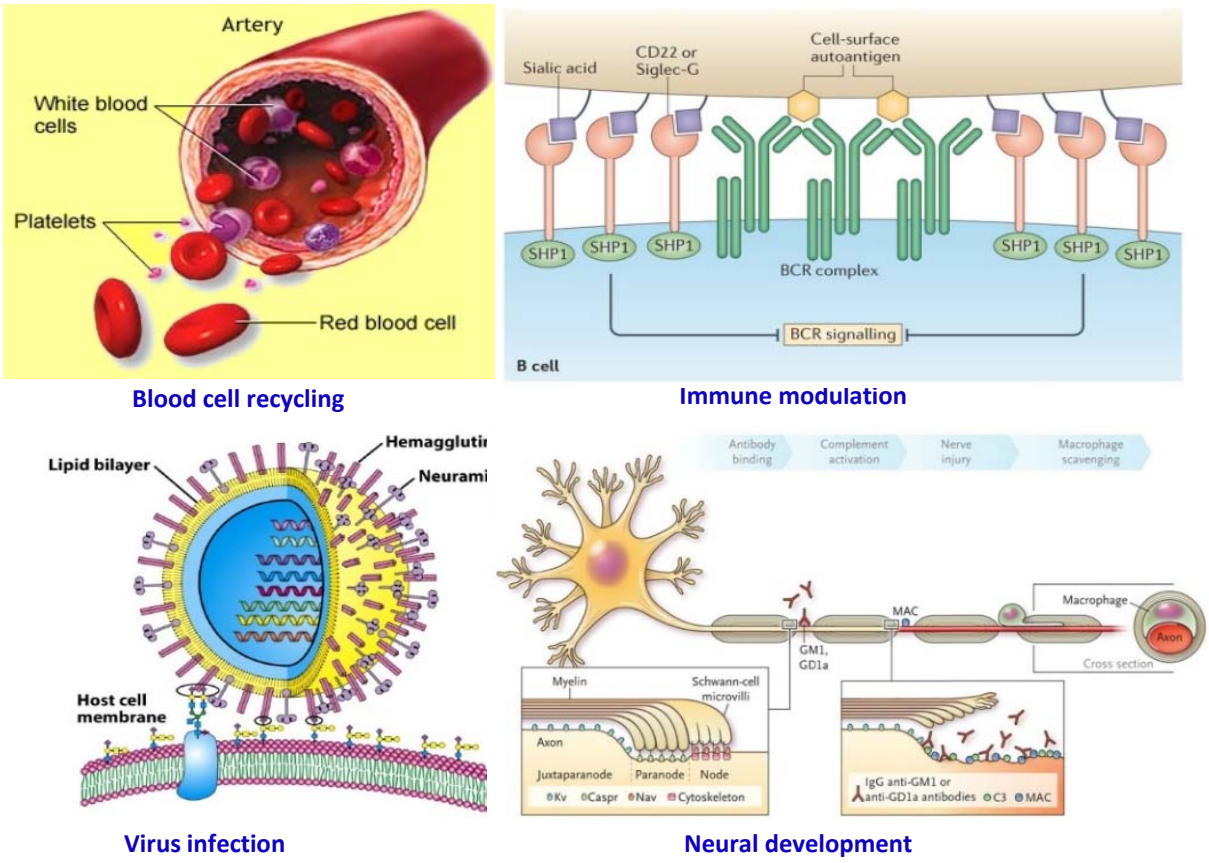

Figure 2.3 *Biological functions of sialic acids.*

2.3 Biosynthesis of sialoglycoconjugates

Neu5Ac and KDN are the precursors of all known mammalian sialic acids. In mammals, Neu5Ac and KDN are synthesized in the cytosol. Sialic acid synthase catalyzes aldol condensation of ManNAc-6-P or Man-6-P with phosphoenolpyruvate (PEP) to yield Neu5Ac-9-P and KDN-9-P. Subsequently, the condensation products are dephosphorylated by phosphatase to give free Neu5Ac and KDN (**Scheme 2.1**). The free Neu5Ac and KDN enter the nucleus and are activated by CMP-Sia synthase to form CMP-Neu5Ac and CMP-KDN, which then return to the cytoplasm, and part of CMP-Neu5Ac is converted to CMP-Neu5Gc by CMP-Neu5Ac hydroxylase. Then, CMP-Sias (CMP-Neu5Ac, CMP-KDN and CMP-Neu5Gc) are transported

into the lumen of Golgi, and Sias are transferred onto newly synthesized glycoconjugates passing through Golgi by sialyltransferases. Finally, if necessary, the nascent sialoglycoconjugate is further modified by sialic acid modification enzymes before it is delivered to the cell surface. However, some modifications are installed onto CMP-Sias before the transfer of Sias to glycoconjugates.

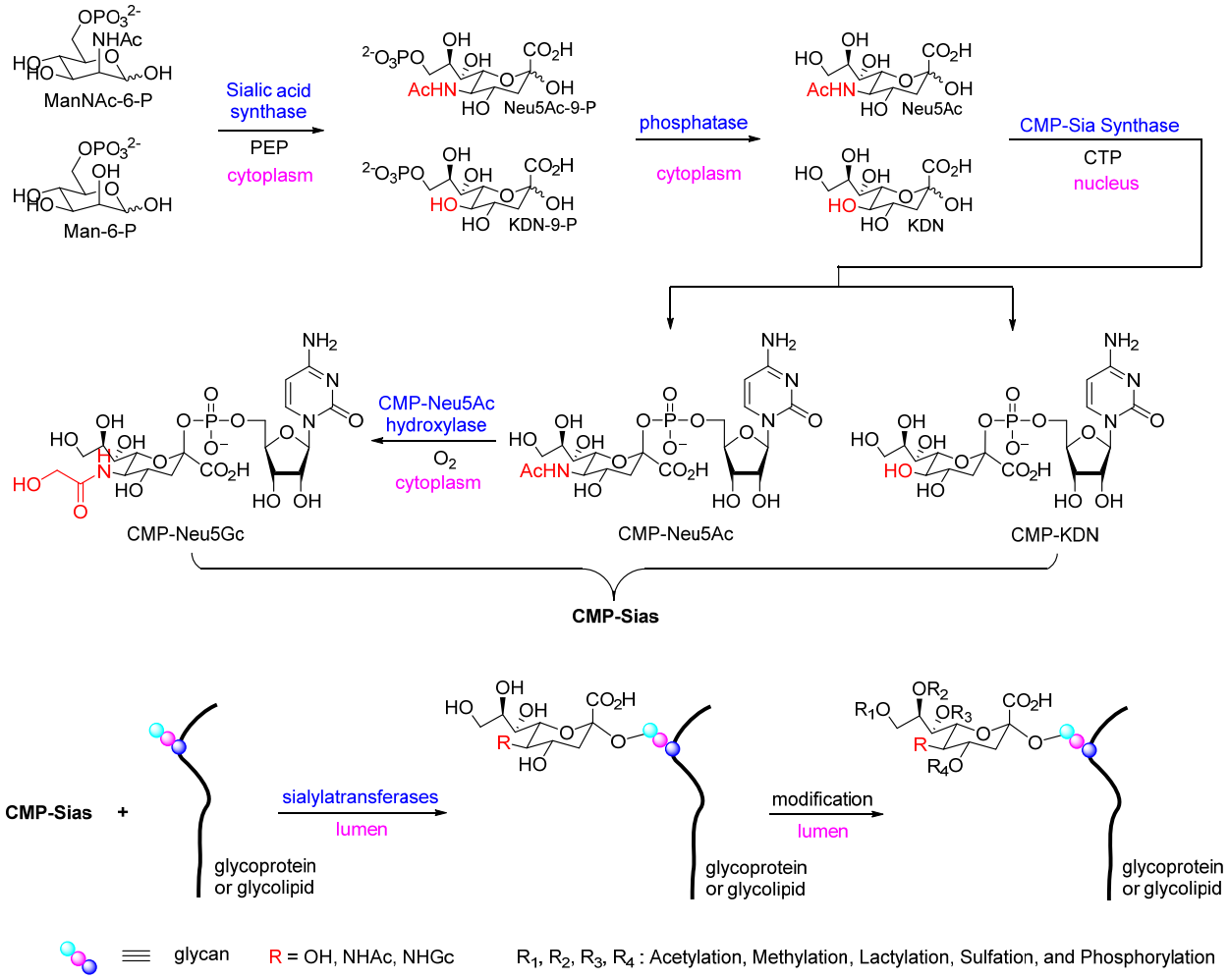

Scheme 2.1 *Biosynthesis of sialoglycoconjugates.*

2.4 Desialylation is an essential life process and highly associated with human diseases

Desialylation is an essential part of sialic acid metabolism. Sialic acids attached to a glycoconjugate must eventually be removed at some point in the life cycle of the molecule. During recycling of cell-surface molecules, sialoglycoconjugates are desialylated in endosomal/lysosomal compartments, and the desialylated glycoconjugates can either be further degraded or return to the Golgi to undergo re-sialylation and then be delivered back to the cell surface. The released sialic acid in lysosomal is delivered back to the cytoplasm, where it is either efficiently reutilized (via CMP-Sia) or degraded. For a long time, Sialyltransferases were thought to be mainly responsible for the creation and maintenance of a temporal and spatial diversity of sialylated moieties. However, the growing evidence suggests that in mammalian cells, at least equally important roles belong to desialylation and abnormal of desialylation is highly associated with human diseases.[16-18]

2.5 Mammalian sialidases

Sialidases may either initiate the catabolism of sialoglycoconjugates or just cleave their sialic acid residues, and thereby regulate cell-surface sialic acid presentation. To date, four types of mammalian sialidases have been identified and characterized (**Table 2.1**), and are classified upon their subcellular localization, namely the intra-lysosomal sialidase (NEU1, localized at the lysosomal inner membranes), the cytosolic sialidase (NEU2, in cytosol), the plasma membrane-associated sialidase (NEU3, localized in plasma membranes), and the lysosomal or mitochondrial membrane-associated sialidase (NEU4, localized in endoplasmic reticulum membranes (ER), lysosomal or mitochondrial membranes).[19, 20] However, recent observations have revealed that the subcellular localization can vary with particular cell stimuli. NEU1 is

ubiquitously expressed with the highest expression in kidney, pancreas, skeletal muscle, liver, lungs, placenta, and brain. NEU2 is found predominantly in muscle tissues. NEU3 has the highest expression in adrenal gland, skeletal muscle, heart, testis, and thymus. NEU4 has the highest expression in brain, skeletal muscle, heart, placenta, and liver.[21]

Table 2.1 *General properties of mammalian sialidases.*

	Major subcellular localization	Major expression tissues	substrate specificity	relative expression level
NEU1	lysosomal inner membranes	kidney, pancreas, skeletal muscle, liver, lungs, placenta, and brain	glycopeptides oligosaccharides	100
NEU2	cytosol	muscle	α-2,3-sialylated oligosaccharides glycopeptides gangliosides	5-10
NEU3	plasma membranes	adrenal gland, skeletal muscle, heart, testis, and thymus	gangliosides.	5-10
NEU4	endoplasmic reticulum membranes, lysosomal or mitochondrial membranes	brain, skeletal muscle, heart, placenta, and liver	oligosaccharides glycoproteins gangliosides	0.01-0.025

Set the expression level of NEU1 to 100.

In term of substrate specificity, NEU1 is active primarily against sialylated glycopeptides and oligosaccharides with lower activity against gangliosides. NEU2 is active against α-2,3-sialylated oligosaccharides, glycopeptides, and gangliosides. NEU3 is active mainly towards gangliosides. NEU4 is active against all types of sialylated glycoconjugates including oligosaccharides, glycoproteins, and gangliosides. With respect to expression levels, NEU1 has the highest expression level among the four sialidases, although the expression levels of four sialidases are very low. NEU3 and NEU4 are generally expressed at 1/10 to 1/20 of the level of NEU1. NEU2 is expressed at extremely low level, only 1/4,000 to 1/10,000 of the level of NEU1.[22]

Up-regulation of NEU3 has been detected in prostate,[23] colon,[24] renal[25] and ovarian cancers.[26] On the other hand, cancer cells and tissues tend to show down-regulation of NEU1 and NEU4,[19, 27-29] although the molecular mechanisms of such regulations are still unknown. In addition, mammalian sialidases couldn't recognize modified sialic acid residues (*O*-acetylation, methylation, lactylation, sulfation, and phosphorylation),[30, 31] which further complicates the regulatory mechanism of desialylation. However, ROS- and RNS-mediated chemical desialylation could cleave sialic acid residues directly, no matter they are modified or not, which provided a new dimension for the regulation of cell surface sialylation status.

In the past decades, more and more emerging evidences, including our own, support the existence of chemical desialylation in the life process.

2.6 Evidences for non-sialidase desialylation in the life process.

In fact, the first direct evidence for chemical desialylation in the life process comes from our lab (*Glycobiology,* **2005** 15, 1094-1101). In 2005, in collaboration with Taniguchi's lab, we discovered that the reactive oxygen species (ROS), generated by a combination of hypoxanthine and xanthine oxidase (HX/XO), led to the specific cleavage of Neu5Ac from cell surface sialyl lewis^x (sLe^x) without up-regulation of sialidases (**Figure 2.4**).[32]

After the cells were treated by HX/XO, desialylation was observed by flow cytometry with a sialic acid-specific lectin (SSA), (**Figure 2.5 a**). The result showed that HX/XO decrease the amount of sialic acid on the cell surface. A concomitant increase of free sialic acid was observed by HPLC in the supernatant (**Figure 2.5 b**). Cleavage of sialic acid by ROS was also verified by the degradation of 4-methylumbelliferyl-Neu5Ac (4-MU-Neu5Ac) by HX/XO in the presence of hydrogen peroxide and iron ion (**Figure 2.5 c**). These findings suggested that non-

reducing terminal sialic acid residues were one of the most susceptible targets for ROS, and provided the basis for our further mechanistic study.[33]

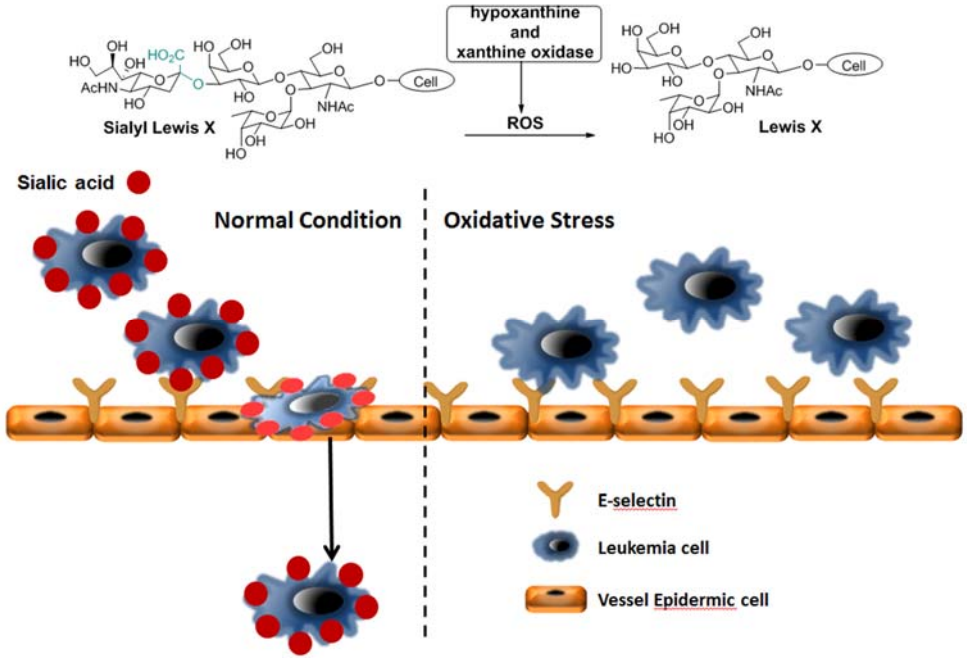

Figure 2.4 *ROS reduces the cell adhesion of leukemia cell*

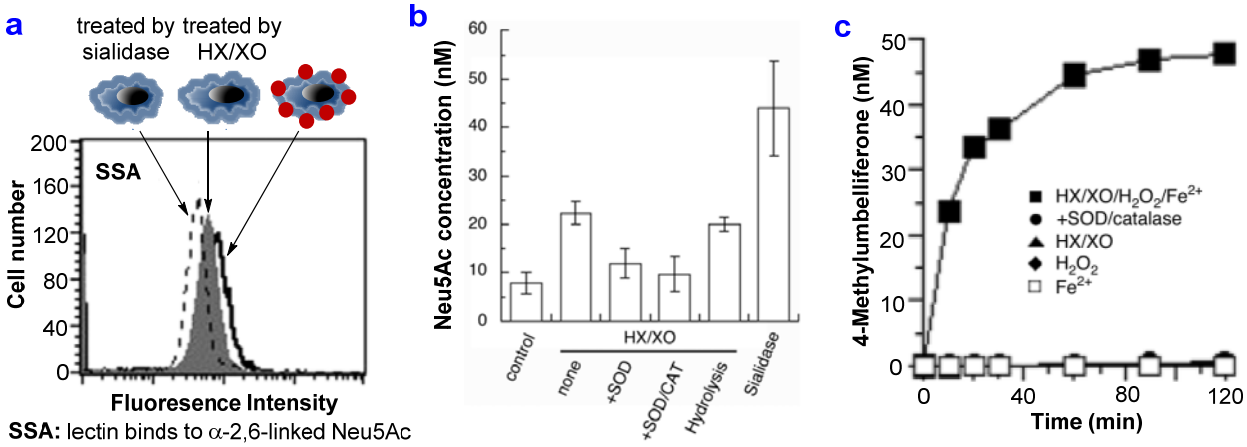

Figure 2.5 a) *Flow cytometric analysis of HX/XO mediated desialylation;* ***b)*** *Sialic acid concentration in the supernatant;* ***c)*** *The degradation of 4-methylumbelliferyl-Neu5Ac.*

Subsequent study was based on the Long–Evans Cinnamon (LEC) rat which is developing into hepatitis as the result of abnormal copper accumulation in liver. The findings of this study show that copper, hydrogen peroxide, and lipid peroxides accumulate to drastically high levels in LEC rat serum. The desialylation of sialylated glycoproteins in the LEC rat serum was examined by lectin blot and lectin ELISA. The result showed that sialic acid on the conjugates was decreased in acute hepatitis as time went by. Further analysis on glycoform of transferrin demonstrated that bi-sialylated and asialo-agalacto biantennary sugar chains existed on transferrin in the acute hepatitis rats (**Figure 2.6**). In addition, treatment of non-hepatitis rat serum with copper ions and hydrogen peroxide decreased tri-sialylated sugar chain of the normal transferrin and increased bi-sialylated and asialylated biantennary sugar chains. This was the first evidence which directly supported the connection between non-sialidase desialylation and ROS *in vivo*, and indicated that non-sialidase desialylation may contribute the development of acute hepatitis.[34]

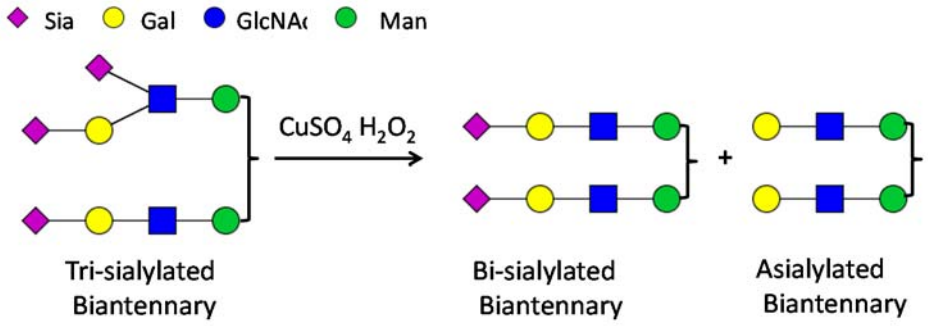

Figure 2.6 *The glycoform change in the LEC rat*

Recently, a method has been developed by Nakagomi's lab to detect the existence of oxidation product of N-acetylneuraminic acid (Neu5Ac), 4-(acetylamino)-2,4-dideoxy-D-

glycero-D-galacto-octonic acid (ADOA).[35] 4-(*N*, *N*-dimethylaminosulfonyl)-7-(2-aminoethylamino)-2,1,3-benzoxadiazole (DBD-ED) with strong fluorescence was utilized to label Neu5Ac and ADOA in the serum. The modified Neu5Ac and ADOA were separated by a hydrophilic interaction liquid chromatography column (HILIC) and determined by fluorometric detection. The results revealed that the concentrations of Neu5Ac and ADOA ranged from 6.30 M to 25.50 M, and from 0.14 M to 0.49 M in the normal salivary samples, respectively (**Figure 2.7**). The heavy smokers who suffer from oxidative stress in their body have much higher concentrations of Neu5Ac (17.77- 87.00 M) and ADOA (0.64–3.43 M) than their counterparts in saliva. This is the very first time to detect ADOA in biological samples.[35] And ADOA could be the long-seeking biomarker for non-sialidase desialylation, which could result from desialylation during oxidative stress and inflammation.[35-37]

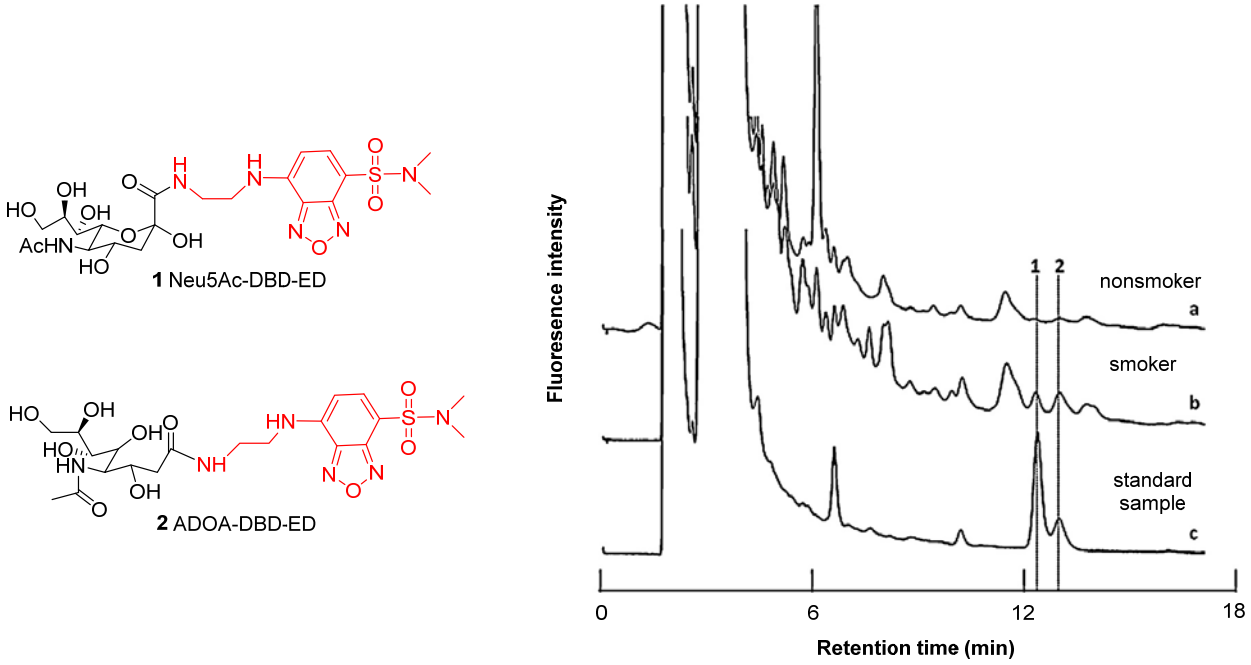

Figure 2.7 *HPLC profiles of Neu5Ac-DBD-ED (peak 2) and ADOA-DBD-ED (peak 1)*

2.7 Synthesis of sialic acid conjugates for the study of chemical desialylation

For the study of chemical desialylation, a library of sialic acid conjugates (**Figure 2.8**) were synthesized including unnatural Neu5Ac derivatives (**7**-**11**), Neu5Ac, Neu5Gc and KDN conjugated oligosaccharides (**12**-**20**), Neu5Ac conjugated glycopeptide (**21**) and glycoproteins (**22**, **23**). In **7** and **8**, Neu5Ac linked to a small methyl group. In **9**, a strong electron withdrawing group CF_3 was introduced. In **10**, a bulky adamantanyl group was introduced. In **11**, an electron donating allyl group was introduced. **7**-**11** were used to study the electronic and steric effect of underlying residue on desialylation (**7** vs **9** vs **11**, **7** vs **10**), as well as the difference between α and β linkage (**7** vs **8)**. **12** and **13**, **14** and **15**, **16** and **17** were used to compare the desialylation of Neu5Ac, Neu5Gc and KDN, as well as the difference between α-2, 3- and α-2, 6-linkages. **18**, **19** and **20** were used to compare the desialylation of α-2, 8-linked and α-2, 3- and α-2, 6-linked Neu5Ac. **21**, **22**, **23** were used to study the desialylation of glycopeptide and glycoprotein.

As shown in **Scheme 2.2**, **7**-**11** were chemically synthesized according to the literature.[38-41] **12**-**20** were efficiently synthesized by transferring sialic acid residues onto 1-β-methyl lactoside (Lac-β-OMe) through one-pot multi-enzyme strategy.[42-44] As shown in **Scheme 2.3**, Neu5Ac was activated to CMP-Neu5Ac by sialic acid synthase (NmCSS), and then transferred onto Lac-β-OMe by α-2,3-sialyltransferase (PmsT1) and α-2,6-sialyltransferase (Pd2,6ST) to give **12** and **13** respectively. **12** and **13** were further sialylated by an α-2,8-sialyltransferase (CstII) to yield **18** and **19**. **20** was synthesized by transferring an α-2,6-linked Neu5Ac to **12**. **14** and **15**, **16** and **17** were synthesized by transferring Neu5Gc and KDN onto Lac-β-OMe by PmsT1 and Pd2,6ST. **21** was isolated from egg yolk.[45] **22** and **23** were synthesized by coupling NHS activated sugar-linker conjugates with BSA (**Scheme 2.4**).

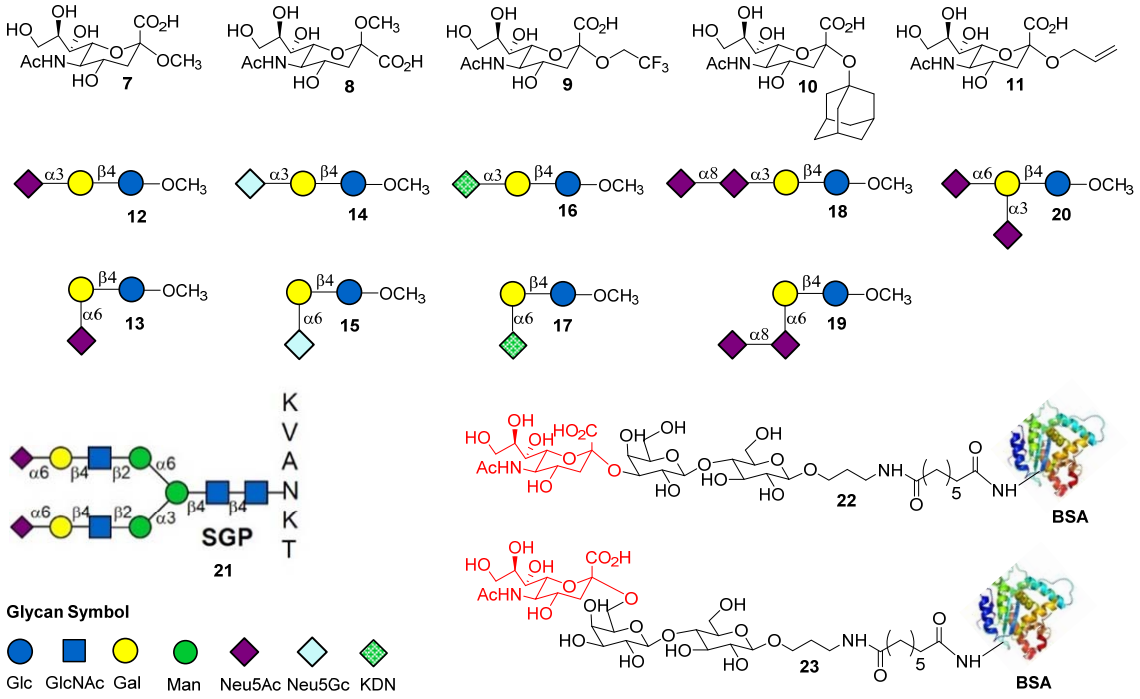

Figure 2.8 *Sialic acid conjugates library for the study of chemical desialylation.*

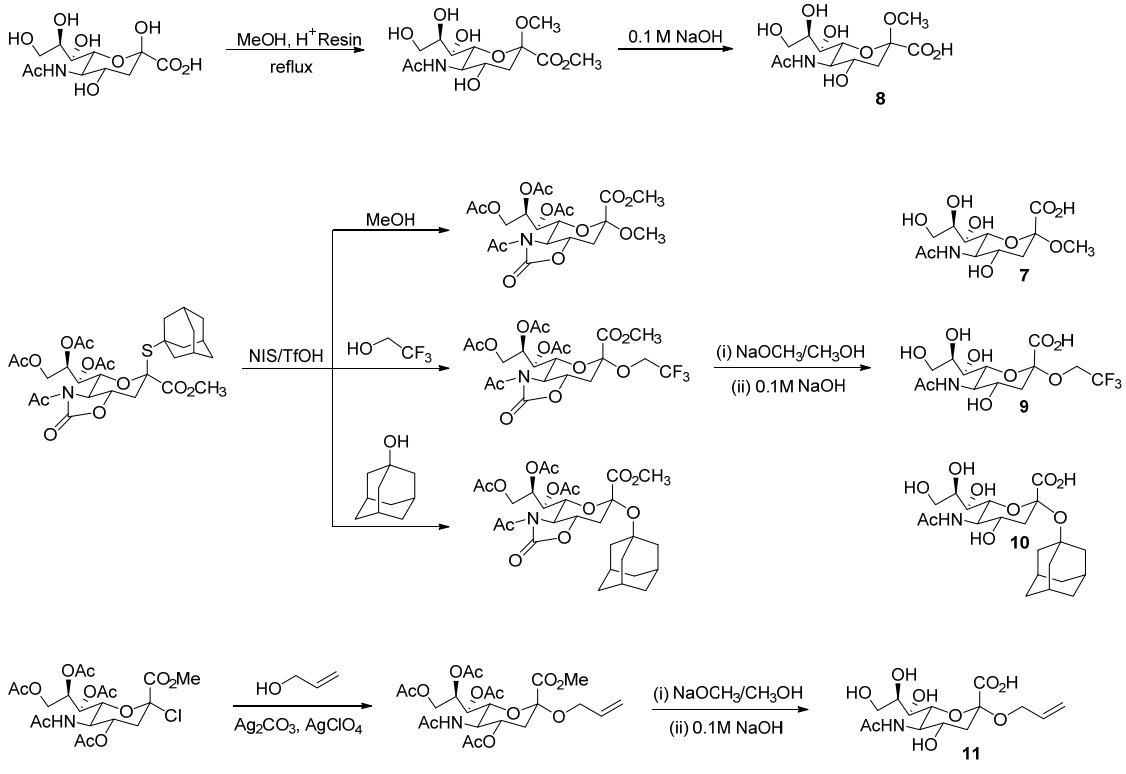

Scheme 2.2 *Chemical synthesis of* ***7-11****.*

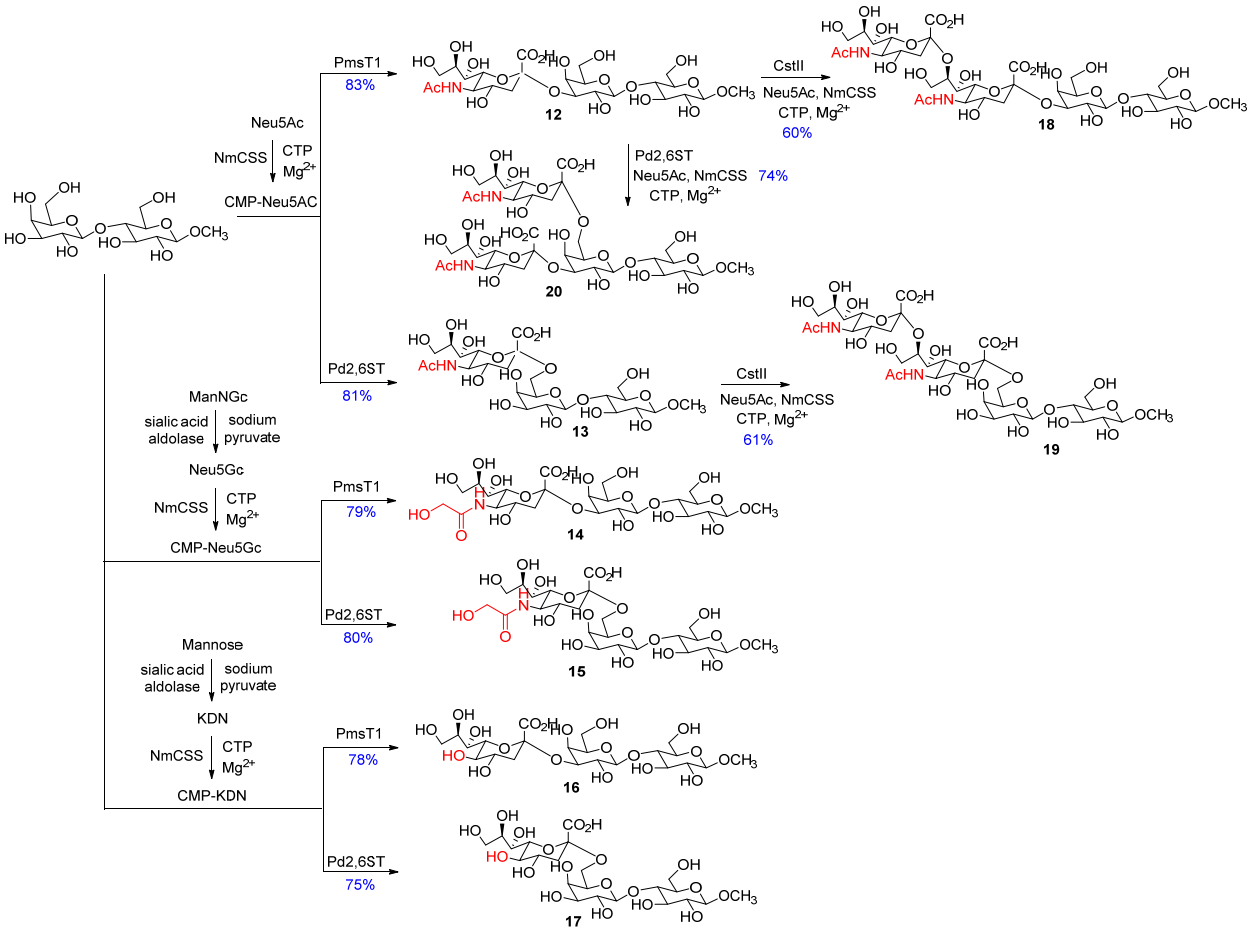

Scheme 2.3 *Enzymatic synthesis of* ***12-20****.*

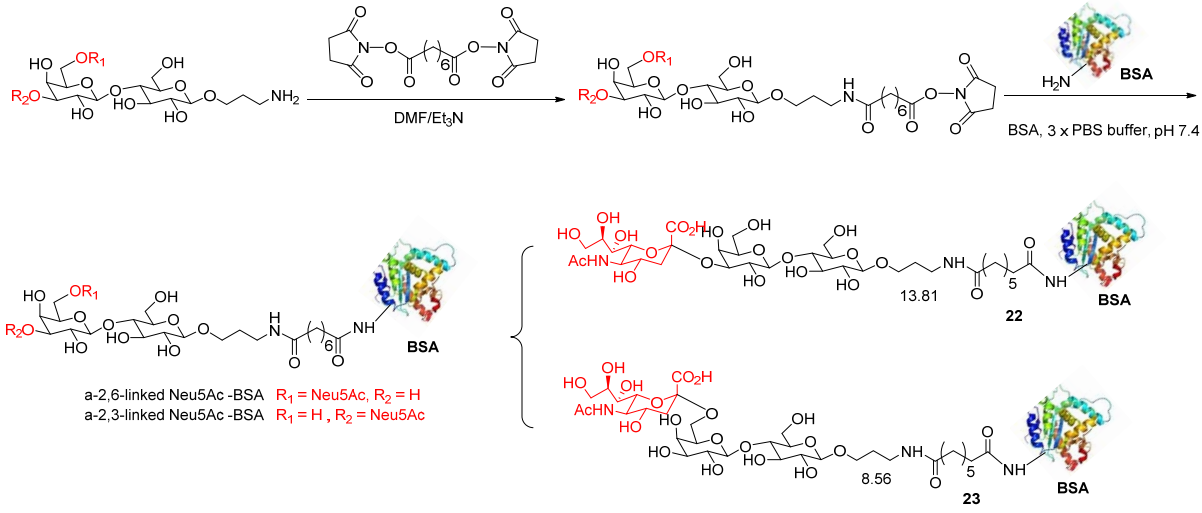

Scheme 2.4 *Synthesis of* ***22*** *and* ***23****.*

2.8 Chemical desialylation

Direct oxidative decarboxylation of Neu5Ac to ADOA with H_2O_2 was reported by Tomita lab[46] and Yamazaki lab (**Scheme 2.5a**),[47] and the mechanism was proposed to go through Baeyer-Villiger rearrangement.[47] The cyclic Neu5Ac equilibrates with the open chain form. The α-keto of open chain form can be attacked by H_2O_2, followed by Baeyer-Villiger rearrangement and decarboxylation, to yield ADOA (**Scheme 2.5c**). When α-2,8-linked homodimer of Neu5Ac-Neu5Ac was treated with H_2O_2, only Neu5Ac-α-2,8-ADOA was afforded,[48] which demonstrated that the reducing terminal Neu5Ac could be oxidized by H_2O_2, but non-reducing terminal Neu5Ac couldn't be oxidized by H_2O_2 (**Scheme 2.5b**). The failure to oxidize terminal Neu5Ac residue of Neu5Ac-α-2,8-ADOA probably is due to that the formation of open chain form is blocked. Therefore, attack of H_2O_2 to α-carbonyl group was blocked.

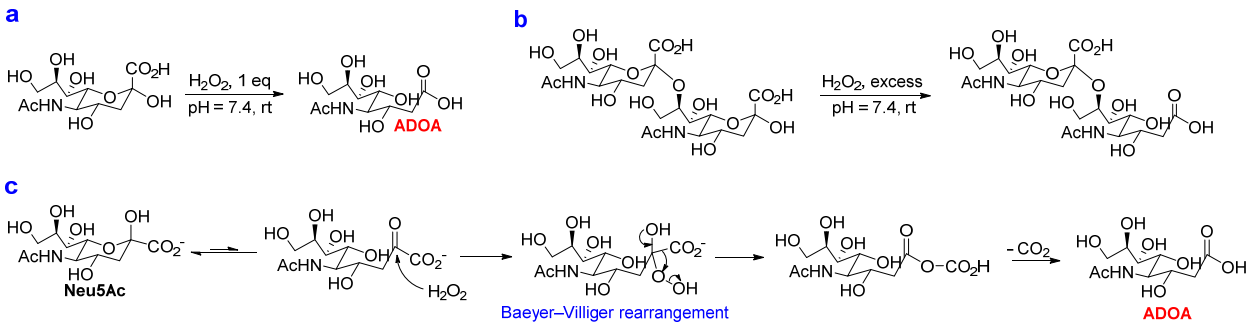

Scheme 2.5 *Oxidation of Neu5Ac and Neu5Ac conjugates by H_2O_2.*

However, C. Neyra *et al* recently reported that polysialic acid could be depolymerized by H_2O_2 at 70 °C (**Scheme 2.6**), and they proposed the involvement of hydroxyl radical in the depolymerization.[49] But, the detailed mechanism of such depolymerization is unknown.

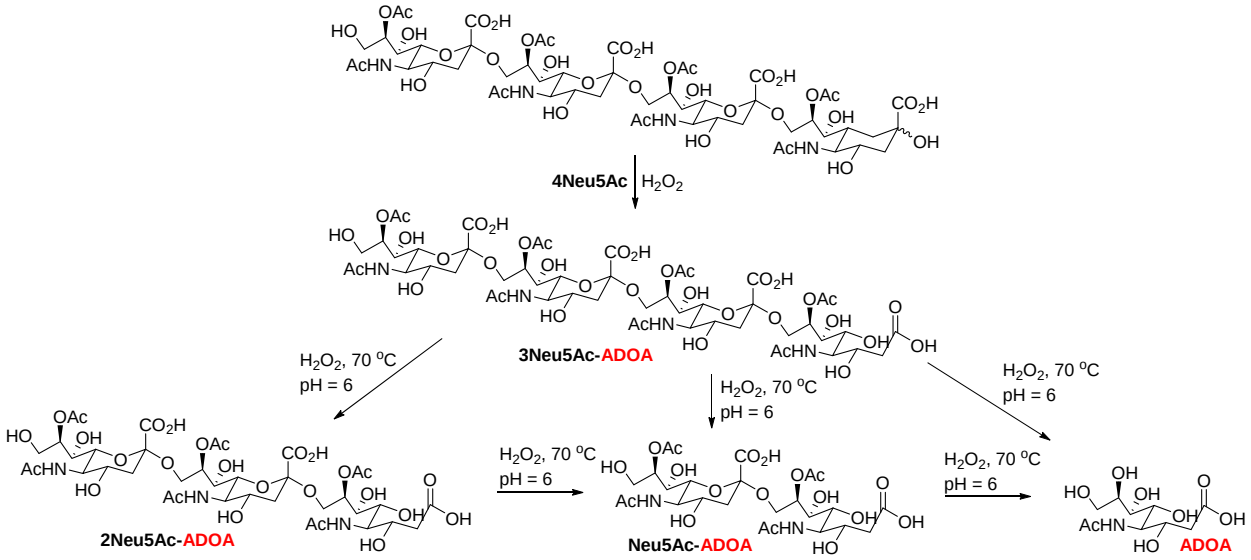

Scheme 2.6 *Depolymerization of polysialic acid.*

ROS/RNS are products of normal cellular metabolism, and play important roles in cell signaling.[50, 51] But high concentration of ROS/RNS would generate oxidative stress and cause damage to DNA/RNA, proteins and lipids.[52] ROS/RNS mediated damage to DNA/RNA, proteins and lipids are widely studied and well characterized. However, the effects of ROS/RNS to carbohydrates, especially sialic acid conjugates, are barely studied.[53-58] Previous studies indicated that ROS/RNS involved in the desialylation of sialic acid conjugates under pathological conditions such as inflammation, cardiovascular diseases, diabetes mellitus, Hodgkin's lymphoma, dengue infection and sepsis. However, the detailed chemistry of ROS/RNS-mediated desialylation is still unknown. In biological system, the most common ROS/RNS species are $O_2^{\bullet -}$, H_2O_2, OH•, OCl^-, •NO, $•NO_2$, and $ONOO^-$.

Therefore, we carried out some preliminary studies on the reaction of sialic acid conjugates with H_2O_2. It was reported that normal cells could survive in H_2O_2 aqueous with the concentration of H_2O_2 up to 240 μM.[59] Thus, we treated sialic acid conjugates (**12**, **13**, **21**, **22**,

23) with 200 μM H_2O_2 at pH 7.4 and rt for 12 h, then analyzed the products with LC-MS/MS. As summarized in **Table 2.2**, all sialic acid conjugates could be desialylated by H_2O_2 with ADOA as the major product and Neu5Ac as the minor product, though the total conversion is low. These results suggest that H_2O_2 can mediate desialylation of cellular sialic acid conjugates under oxidative stress.

Table 2.2 *H_2O_2 mediated desialylation.*

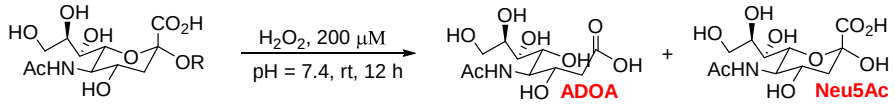

Substrate	yield ADOA	yield Neu5Ac
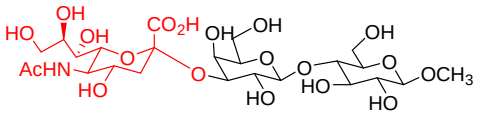 **12**	5.9 %	0.8%
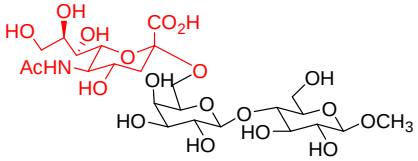 **13**	3.5%	0.1%
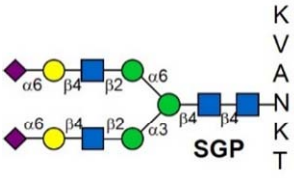 **21**	0.6%	0.006%
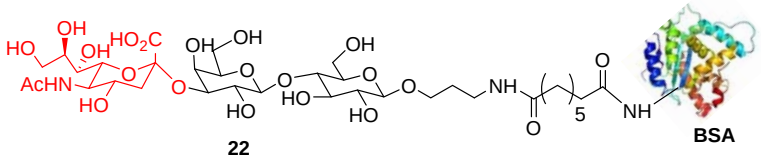 **22**	7.5%	0.3%
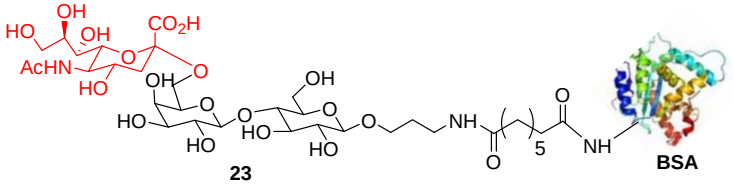 **23**	1.5%	0.2%

We also performed some preliminary experiments on the reaction of sialic acid conjugates with ROS. all ROS species in biological systems are derived from $O_2^{\bullet -}$,[60] and OH•, is the most reactive specie of ROS.[61-63] Thus, **22** was treated with different ROS generating systems including HX/XO ($O_2^{\bullet -}$), HX/XO/Fe^{2+}, H_2O_2/Fe^{2+} (OH•) and HX/XO/H_2O_2/Fe^{2+} (**Table 2.3**). LC–MS/MS analysis showed that these ROS generating systems could directly remove terminal Neu5Ac to yield ADOA and Neu5Ac, especially the combination system of HX/XO/H_2O_2/Fe^{2+}. These results suggested that ROS can directly remove terminal sialic acid residues of cellular sialic acid conjugates.

Table 2.3 *Desialylation of glycoprotein by ROS.*

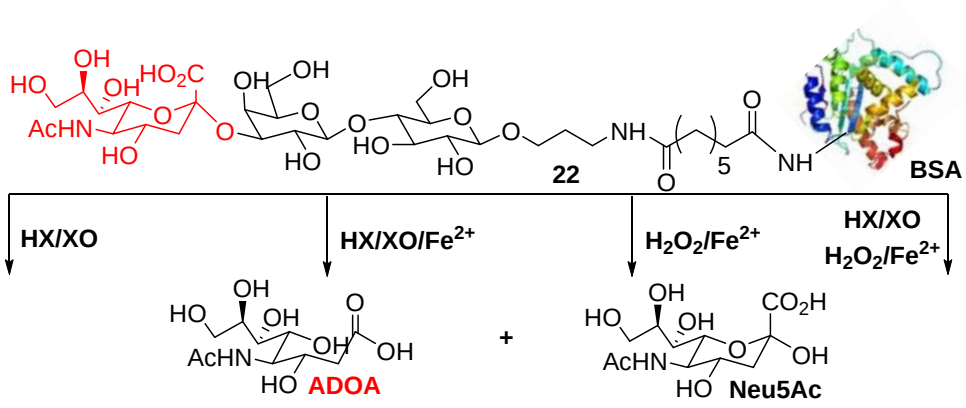

Sample name	α-2,3-Neu5Ac-Lactose-linker-BSA 22			
	HX/XO	HX/XO/Fe^{2+}	H_2O_2/Fe^{2+}	HX/XO/H_2O_2/Fe^{2+}
ADOA (ng/mL)	88	98	210	567
Neu5Ac (ng/mL)	86	106	20	31
ADOA/Neu5Ac	1	1	11	18

Based on these results and previous studies on oxidation of sialic acids, the probable mechanism of ROS mediated desialylation was proposed to go through radical decarboxylation.

As depicted in **scheme 2.7**, ROS abstract one electron from carboxylate group of sialic acid residue to generate carboxyl radical **I**, which is highly active and spontaneously decarboxylates to give the corresponding alkyl radical **II**. Due to anomeric effect, **II** can easily be further oxidized to generate oxocarbenium **III**, which is then attacked by water to give lactone **IV**. After hydrolysis of **IV**, ADOA was provided.

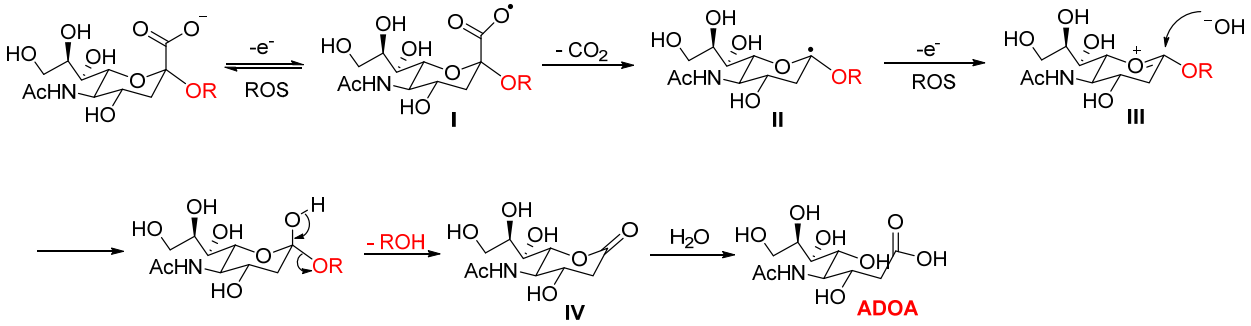

Scheme 2.7 *Proposed mechanism of ROS mediated desialylation.*

2.9 Mimicking ROS-mediated desialylation by electrochemical oxidation

Kolbe electrolysis (or Kolbe oxidation) is a standard oxidative decarboxylation reaction, as well as a classical radical reaction.[64-66] Hofer-Moest reaction is an extension of Kolbe oxidation.[67-70] Under electrolytic condition, carboxylic acid loses one electron to generate carboxyl radical, which is highly active and spontaneously decarboxylates to give the corresponding alkyl radical. Then the alkyl radical further loses one electron to generate alkyl cation, which reacts with a nucleophile to give decarboxylative coupling product (**Scheme 2.8**). The proposed mechanism of ROS mediated desialylation highly resembles the mechanism of Hofer-Moest reaction. Therefore, we used electrochemical oxidation to mimic ROS/RNS mediated desialylation.

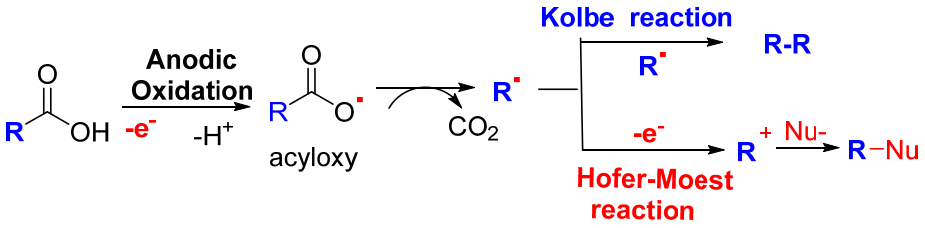

Scheme 2.8 *Kolbe oxidation and Hofer-Moest reaction.*

Boron doped diamond (BDD) is an excellent electrode material with wide potential window in aqueous solution, low background currents (low capacitance), reduced fouling, non-corroding at high temperatures, pressures and in challenging environments, and excellent biocompatibility, which make it an intriguing material for electroanalysis and electrochemical research.[71-75] Therefore, we used BBD electrode to mimic the oxidative desialylation of sialic acid conjugates.

12 was dissolved in $NaClO_4$ (0.2 M) aqueous solution and the pH of the solution was adjusted to 7.4 by 0.1 M NaOH. Then two BBD electrodes were inserted to the stirred solution and 2.8 V voltage was applied at room temperature. During electrolysis, the pH of the solution was maintained to 7.4 by adding 0.1 M NaOH. After complete consumption of **12**, the reaction mixture was concentrated and purified by silica gel flash chromatography, then Bio-Gel P-2 gel filtration to give ADOA with 37% yield.

2.9.1 Optimization of electrochemical desialylation

After validation of such electrochemical mimicry of oxidative desialylation, we set out to optimize electrolysis conditions by using **12** as the model substrate. Several key parameters

critical to electrolysis were investigated (**Table 2.4**). Voltage is critical for electrochemical oxidation. At high voltage, sialic acid conjugates can be efficiently desialylated. However, the product ADOA also can be further oxidized at high voltage, which will make the electrochemical desialylation very complex to analyze. In order to determine the optimal voltage, the electrochemical desialylation was conducted under a variety of voltages, ranging from 2.0 V to 2.8 V (entries 1-5). At 2.0 V, no reaction at all. At 2.2 V, **12** could be slowly desialylated and ADOA was provided as the major product. At 2.4 V, **12** was efficiently desialylated and ADOA was provided with 62% yield. At 2.6 V and 2.8 V, **12** was quickly desialylated, however, the yield of ADOA decreased, which may be caused by further oxidization of ADOA or other side-reactions for oxidation of **12**. Therefore, the stability of ADOA under different voltage was examined. As shown in **Figure 2.9**, at 2.4 V, ADOA couldn't be oxidized at all. At 2.6 V, ADOA was slowly oxidized (less than 5 % for 12 h). At 2.8 V, ADOA was substantially oxidized. Therefore, the best voltage for electrochemical desialylation of sialic acid conjugates is 2.4 V.

$NaClO_4$, KNO_3 and NaH_2PO_4/Na_2HPO_4 are three common electrolytes used for electrolysis in water. Therefore, KNO_3 and NaH_2PO_4/Na_2HPO_4 were examined. When KNO_3 was used as electrolyte, **12** was desialylated at 2.4 V and ADOA was provided with 54% yield. However, the electrolysis time was elongated to 72 h. When NaH_2PO_4/Na_2HPO_4 was used as electrolyte, **12** was desialylated very slowly (less than 10% in 12 h) at 2.4 V. Therefore, the voltage was increased to 2.6 V, and 12 was completely desialylated in 16 h and ADOA was provided with 46% yield. Therefore, $NaClO_4$ was chosen as the electrolyte.

Table 2.4 *Optimization of electrolysis conditions.*

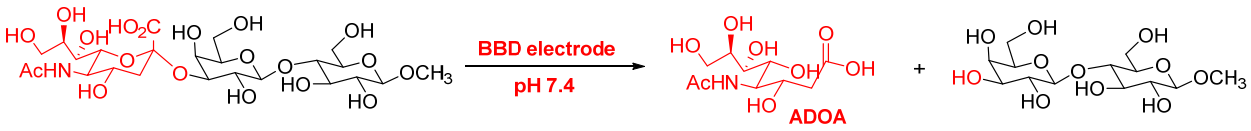

Entry	Electrolyte	Voltage	Time/h	Conversion	ADOA yield
1	$NaClO_4$	2.0 V	24	0%	0%
2	$NaClO_4$	2.2 V	24	15%	12%
3	$NaClO_4$	2.4 V	24	> 95%	62%
4	$NaClO_4$	2.6 V	18	100%	60%
5	$NaClO_4$	2.8 V	13	100%	47%
6	KNO_3	2.4 V	72	> 95%	54%
7	NaH_2PO_4/Na_2HPO_4	2.6 V	16	100%	46%

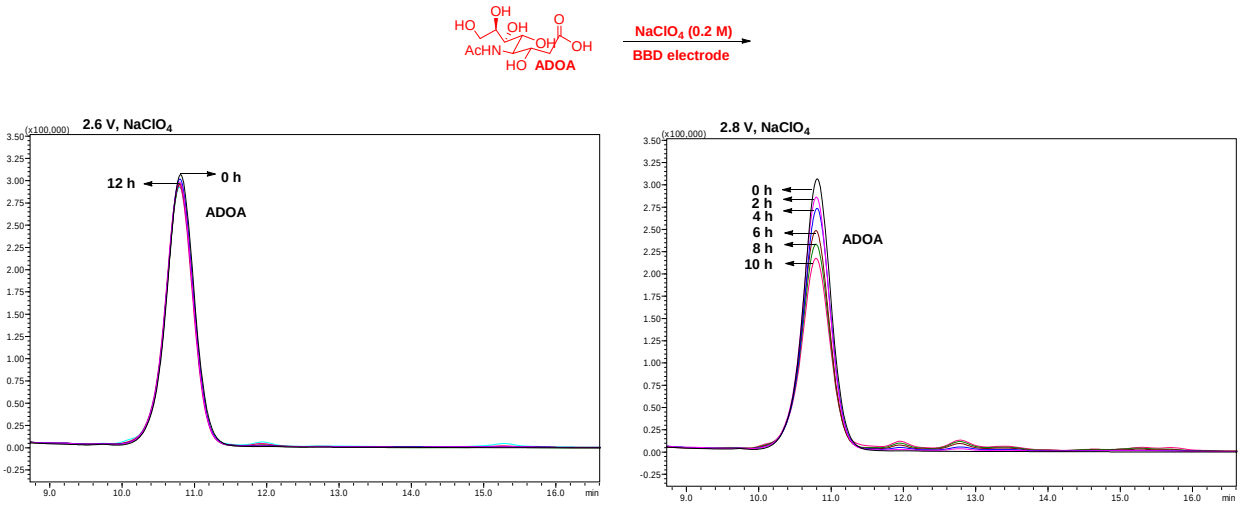

Figure 2.9 *Stability of ADOA under different voltage.*

2.9.2 Electrochemical desialylation of sialic acid conjugates

After identified the optimal conditions, the synthesized sialic acid conjugates in Figure 2.8 were applied to electrochemical desialylation. In order to study the effect of underlying residue on electrochemical desialylation, Ne5Ac and its derivatives were electrolyzed first (**Table 2.5**, entries 1-5). Methyl α-Neu5Ac **7** could be efficiently desialylated at 2.6 V and ADOA was generated with 57% yield in 47 h (entry 1). In contrast, the β-anomer **8** couldn't be electrolyzed until the voltage was increased to 3.0 V (entry 2), which indicates that there is a huge difference in activity between α- and β-anomers. In **9**, a strong electron withdrawing group CF_3 was introduced, which made **9** easier to be electrolyzed and ADOA was provided with 65% yield in 20 h (entry 3). In **10**, a bulky 1-adamantyl group was introduced, which made **10** easier to be electrolyzed and ADOA was provided with 56% yield in 15 h (entry 4).When free Neu5Ac was electrolyzed, the voltage needed to be increased to 2.8 V and ADOA was provided with 47% yield (entry 5). In water, free Neu5Ac is an equilibrium mixture of α- and β-anomers, which consists of 92.1% β-anomer and 7.5% α-anomer at pH 8.0.[76] Since β-anomer is much more difficult to be electrolyzed, α-anomer was oxidized and then β-anomer was converted to α-anomer. Therefore, 2.8 V is the voltage for eletrolysis of α-anomer.

Then, Neu5Ac conjugated oligosaccharides **12**, **13**, **18**, **19** and **20** were electrolyzed to study the effect of sialic acid linkages on desialylation. **12** could be efficiently desialylated at 2.4 V and ADOA was provided with 62% yield (entry 6). **13** was more difficult to be electrolyzed. Therefore, the voltage was increased to 2.6 V and ADOA was provided with 56% yield (entry 7). Both **14** and **15** could be efficiently desialylated at 2.6 V and ADOA was provided with 90% yield in 32 h (entry 8) and 92% yield in 24 h (entry 9) respectively.

Table 2.5 *Electrochemical desialylation of sialic acid conjugates.*

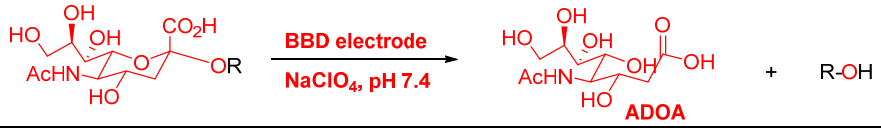

Entry	Substarte	Voltage	Yield	Time/h
1	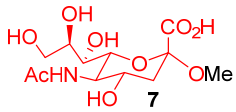 7	2.6 V	57 %	47
2	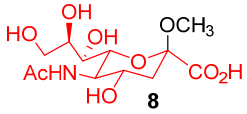 8	3.0 V	33 %	15
3	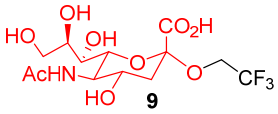 9	2.6 V	65 %	20
4	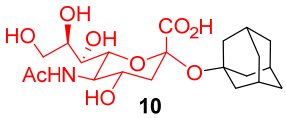 10	2.6 V	56 %	15
5	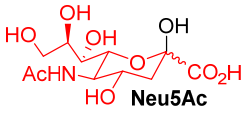 Neu5Ac	2.8 V	42 %	46
6	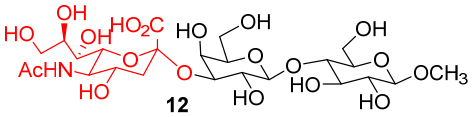 12	2.4 V	62 %	24
7	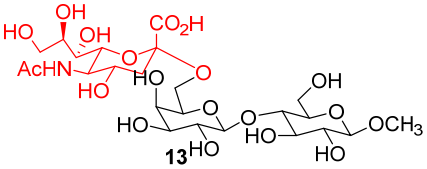 13	2.6 V	56 %	18
8	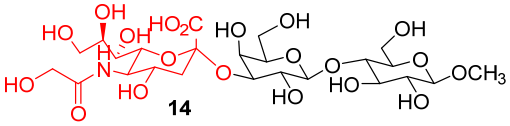 14	2.6 V	90 %	32
9	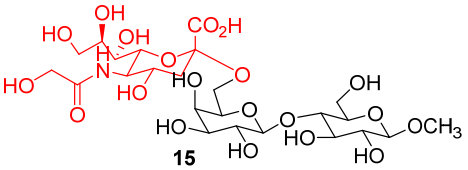 15	2.6 V	92 %	24
10	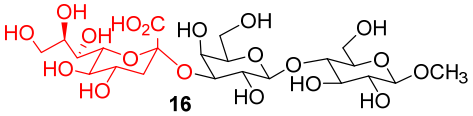 16			
11	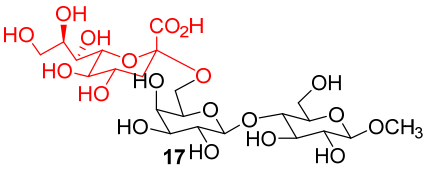 17			

Compared to monosialylated **12** and **13**, the activities of disialylated **18**, **19** and **20** were even lower. Therefore, high voltage and long electrolysis time were employed. For **18**, **19** and **20**, ADOA was provided with 45%, 49% and 60% yields respectively (**Table 2.6**, entries 1-3).

Table 2.6 *Electrochemical desialylation of sialic acid conjugates.*

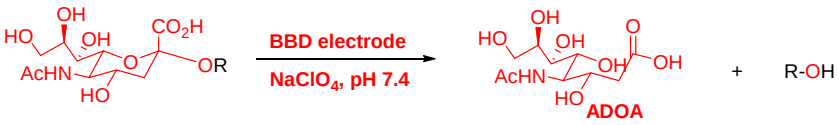

Entry	Substarte	Voltage	Yield	Time/h
1	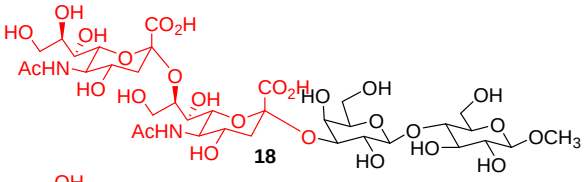 **18**	**2.6 V**	**45 %**	**41**
2	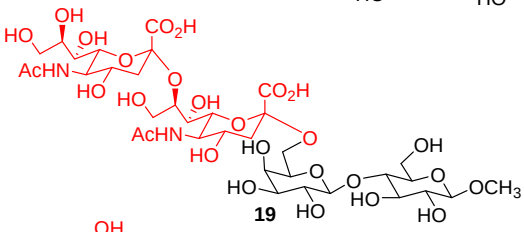 **19**	**2.6 V**	**49 %**	**52**
3	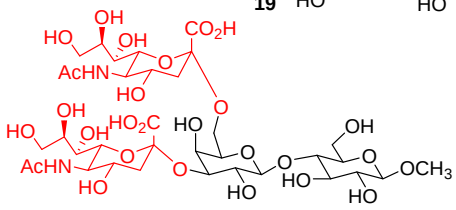 **20**	**2.6 V**	**60 %**	**47**
4	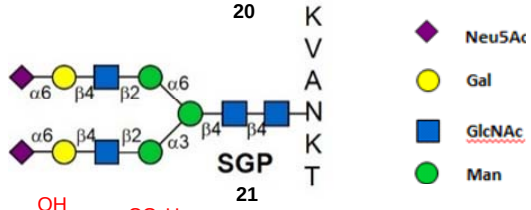 **21**			
5	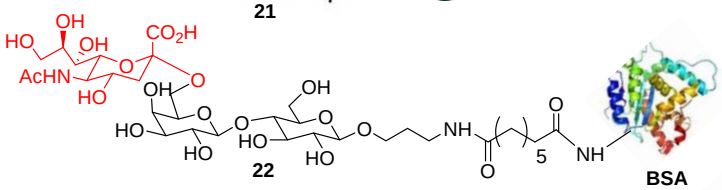 **22** BSA			
6	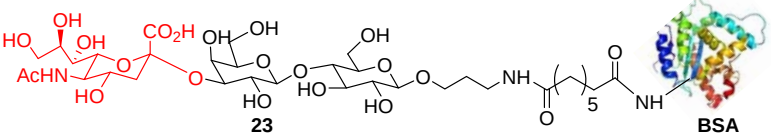 **23** BSA			

Since **18**, **19** and **20** were desialylated, their desialylation processes were studied in detail. As shown in **Figure 2.10**, **18** can be sequentially desialylated from the terminal, or cleaved at the internal α-2,3-linkage directly to give Neu5Ac-ADOA, which can be further oxidized to give two ADOA. According to the Mass result, Neu5Ac-ADOA was detected and Neu5Ac-Lac-OMe wasn't detected. Therefore, **18** was desialylated by cleavage at the internal α-2,3-linkage directly, which indicated that α-2,3-linked Neu5Ac was easier to be desialylated than α-2,8-linked Neu5Ac.

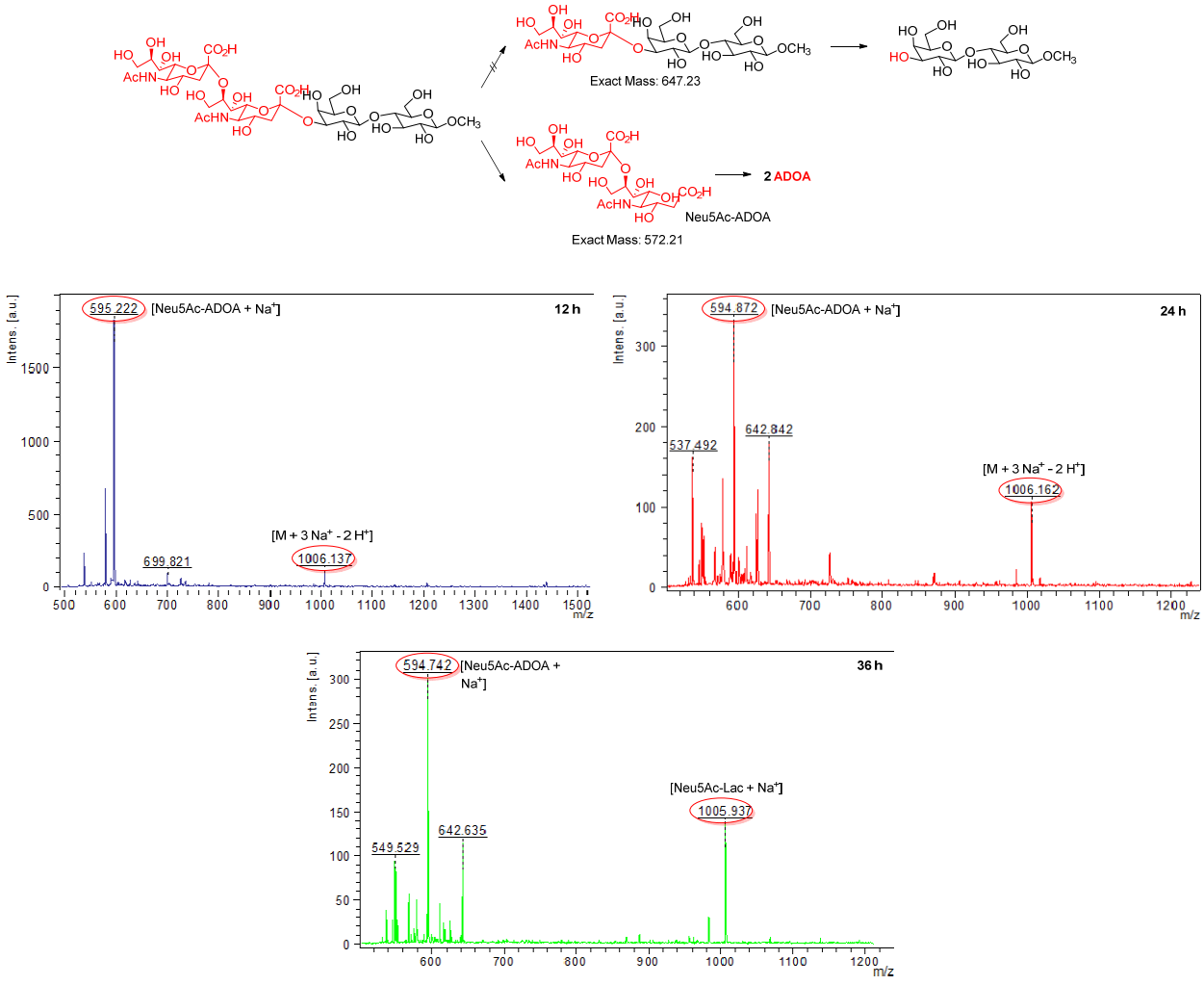

Figure 2.10 *Electrochemical desialylation of* ***18****.*

For **19**, the two Neu5Ac residues also can be sequentially desialylated from the terminal, or cleaved at the internal α-2,6-linkage directly to give Neu5Ac-ADOA (**Figure 2.11**). According to the Mass result, Neu5Ac-Lac-OMe was detected and Neu5Ac-ADOA wasn't detected. Therefore, **18** was sequentially desialylated from the terminal, which indicated that α-2,8-linked Neu5Ac was easier to be desialylated than α-2,6-linked Neu5Ac.

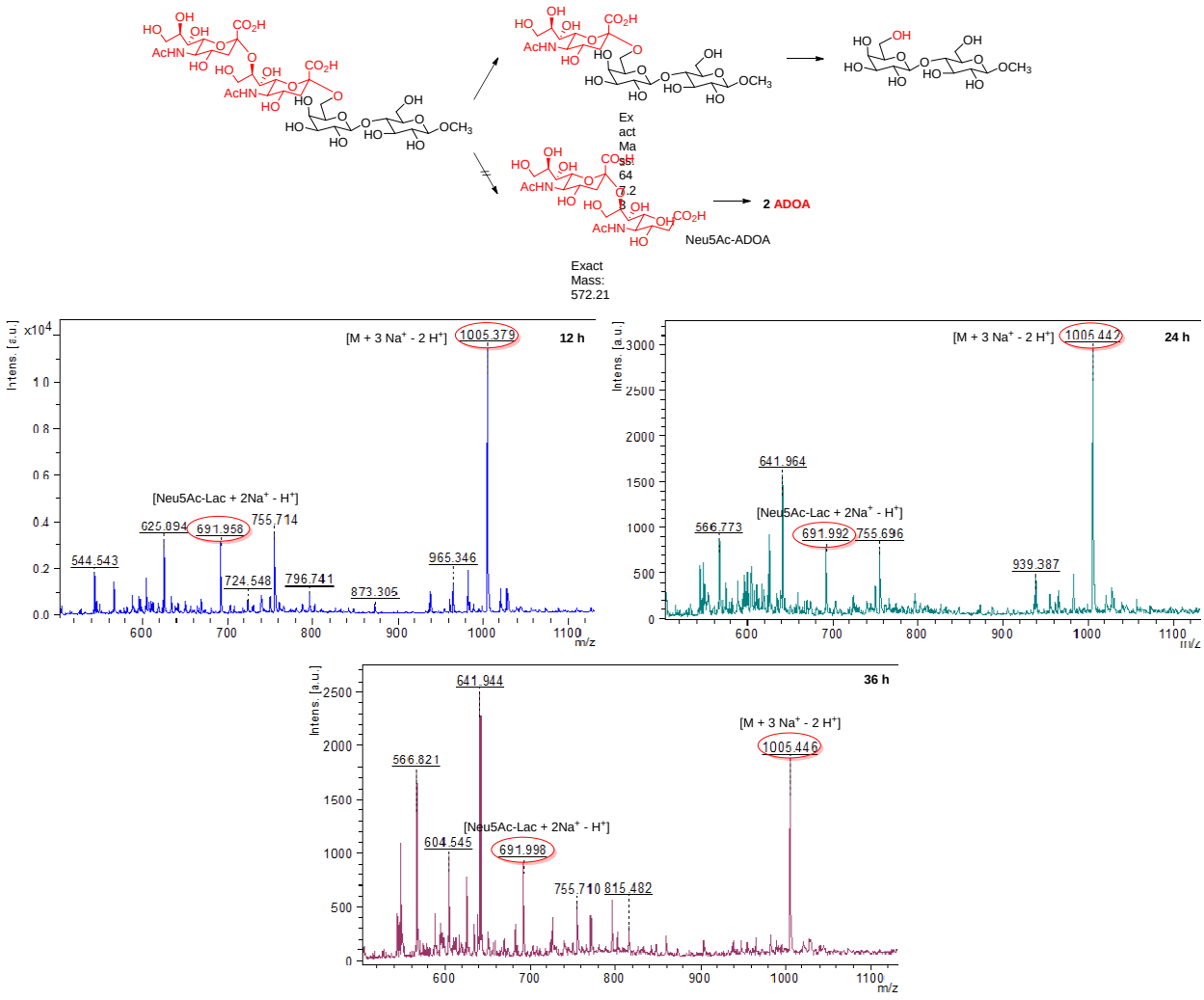

Figure 2.11 *Electrochemical desialylation of* ***19****.*

According to the desialylation of **18** and **19**, the two Neu5Ac residues on **20** can either be desialylated at 3 positon first, then 6 position, or be desialylated simultaneously (**Scheme 2.9**). However, the molecular mass of intermediates in both two pathways is same. Therefore, the desialylation pathway could be identified by mass spectrometer. Currently, we are trying to use CE to determine the desialylation pathway of **20**.

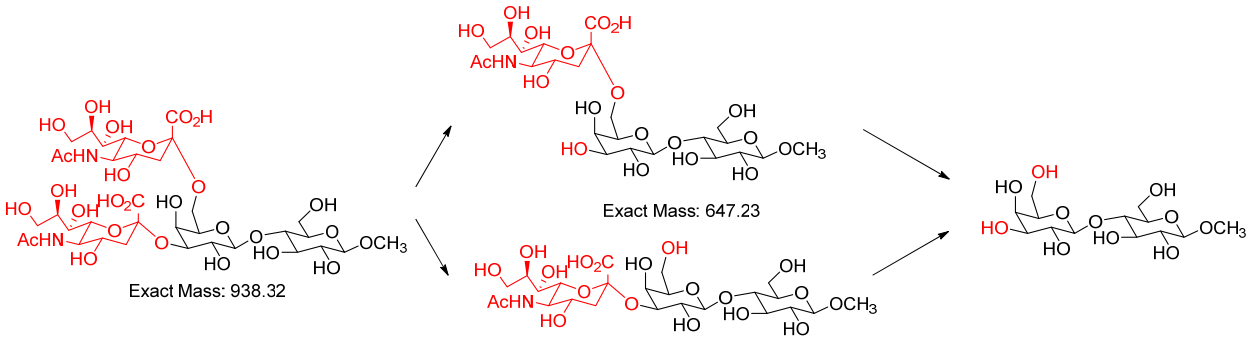

Scheme 2.9 *Electrochemical desialylation of* ***20****.*

Neu5Gc conjugated oligosaccharides **14** and **15**, KDN conjugated oligosaccharides **16** and **17**, glycopeptide **21**, glycoprotein **22** and **23** are still under electrolysis.

2.9.3 Proposed mechanism of electrochemical desialylation

The mechanism of electrochemical desialylation was proposed to follow the Hofer-Moest reaction mechanism. Under electrolytic condition, carboxylate group of sialic acid loses one electron to generate carboxyl radical **I**, which is highly active and spontaneously decarboxylate to give the corresponding alkyl radical **II** (**Scheme 2.10a**). Due to anomeric effect (**Scheme 2.10b II**), **II** further loses one electron to give oxocarbenium **III**, which is attacked by water to give lactone **IV**. After hydrolysis of **IV**, ADOA was provided. The favored electrolytic

desialylation of α-linked sialic acid to β-linked sialic acid is due to anomeric effect. When the carboxylate group is in axial position (α-linked sialic acid, **I**), the *p* orbital of endocyclic oxygen is parallel to the σ^* orbital of axial C-carboxylate bond; the lone electron pair on *p* orbital can migrate to σ^* orbital, therefore, the electron density of carboxylic oxygen is rich, which is easy to be oxidized (**Scheme 2.10b I**).[77] Meanwhile, the formed alkyl radical **II** also can be stabilized by this lone electron pair migration (**Fig. 7b II**). However, when the carboxylate group is in equatorial position (β-linked sialic acid), the *p* orbital and σ^* orbital aren't parallel and this lone electron pair migration is blocked. Therefore, it is difficult to be oxidized.[78] Introduction of bulky group makes the formation of **II** and **III** more energy favorable, thus increasing the desialylation activity (**Table 2.5**, entry 4).

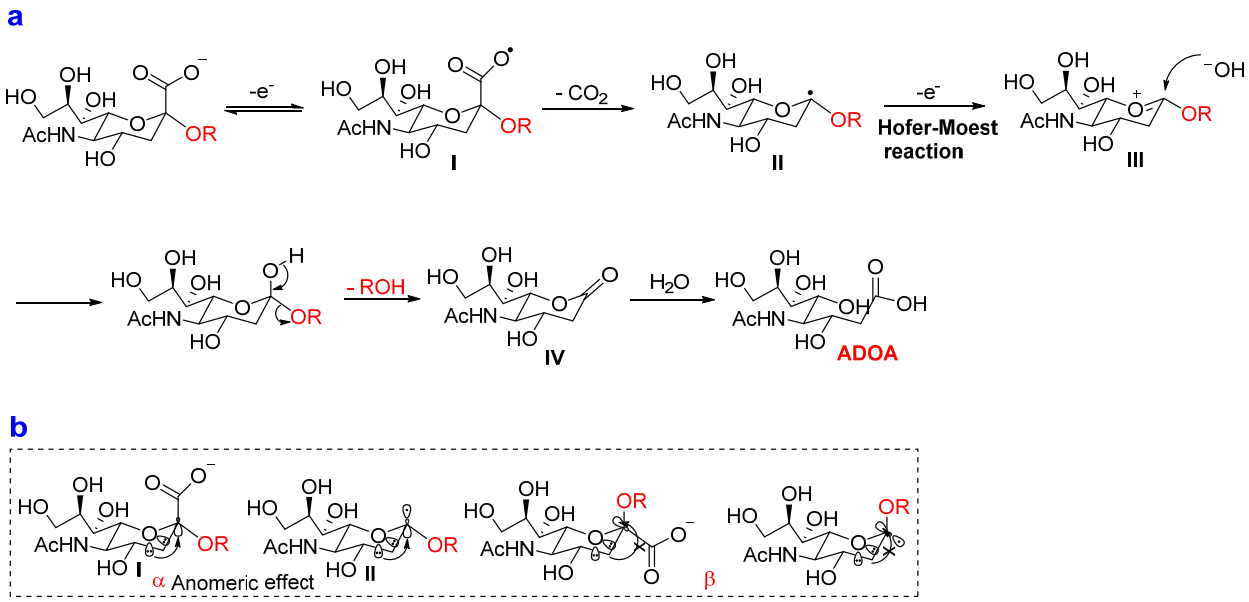

Scheme 2.10 *Proposed mechanism of electrochemical desialylation.*

2.9.4 Trapping intermediates of electrochemical desialylation

In order to prove the proposed desialylation mechanism, methyl ester **24** was electrolyzed. However, no reaction was detected even though the voltage was increased to 2.8 V (**Scheme 2.11**), which is in sharp contrast to the desialylation of carboxylic acid **7** (**Table 2.5**, entry 1). Thus, the carboxylic acid group on sialic acid residue is essential for the desialylation, which is in consistence with our proposed mechanism.

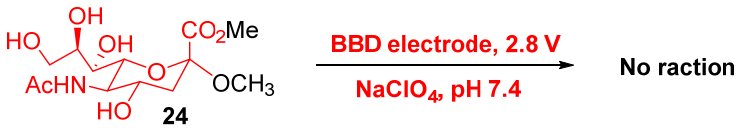

Scheme 2.11 *Electrochemical desialylation of* ***24***.

Then, we tried to trap intermediates of the proposed desialylation mechanism. Intermediate **I** is highly active and undergoes decarboxylation spontaneously. The lifetime of **I** is extremely short, which makes it difficult to be captured. On the other hand, intermediate **II** and **III** are relatively stable. Therefore, **II** and **III** should be able to be trapped. **II** can be trapped by TEMPO to yield **25**,[79] or by allyltrimethylsilane to yield **26** (**Scheme 2.12a**).[80-82] **III** also can be captured by some nucleophiles other than water (such as azide, **Scheme 2.12b**).[83] The proposed mechanism also can be tested by electrochemical oxidation of **11**. According to the proposed mechanism, electrochemical decarboxylation of **11** will generate intermediate **V**, which will automatically undergo intramolecular radical cyclization to generate cyclic product **27** (**Scheme 2.12c**). Therefore, if cyclic product 27 was detected, that means the proposed mechanism is correct. We first tried to capture **III** with NaN_3, but failed. It turned out that azide was reduced

under the electrolysis conditions. Currently, we are trying to trap II with TEMPO and allyltrimethylsilane, and **11** also is under electrolysis.

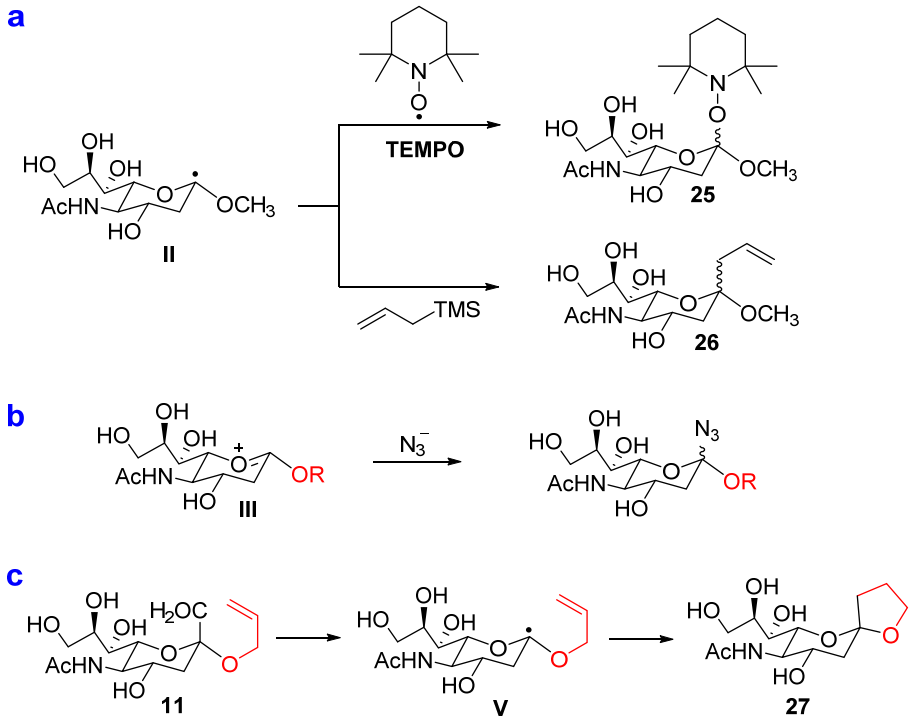

Scheme 2.12 *Trapping intermediates of electrochemical desialylation.*

2.10 Probe chemical desialylation on cellular level

With the knowledge gained from *in vitro* chemical desialylation, we plan to briefly explore chemical desialylation at cellular level. The main roadblock to evaluate chemical desialylation of whole cell is the interference of background and inducible enzymatic desialylation of the cells. Apparently, this interference can be suppressed by sialidase inhibitors, and many good sialidase inhibitors have been developed including the famous commercial drugs Temiflu, Zanamivir and Oseltamivir for influenza infection.[84-86] However, these sialidase inhibitors are mainly for bacterial sialidases and their inhibitory activities toward mammalian

sialidases are quite low.[22] In addition, complete inhibition of sialidases also may impact the viability and functions of cells. Therefore, using sialidase inhibitors to exclude the interference of enzymatic desialylation is not a good choice. Recently, Krishna Kumar *et al* reported that mammalian sialidases couldn't hydrolyze some *N*-acyl derivatives of sialic acid, such as *N*-pentynoyl sialic acid (Neu5Al).[87] Thus, we plan to probe chemical desialylation of cell via metabolic glycoengineering. *in vivo*.[88, 89] When the cell is fed with peracetylated *N*-(4-pentynoyl) mannosamine (Ac_4ManNAl), Ac_4ManNAl will enter the cytoplasm of cells, and be deacetylated by esterases. Subsequently, the deacetylated ManNAl will be converted to Neu5Al, which will be transferred onto glycoconjugates and eventually present on the cell surface following the biosynthetic pathway of sialoglycoconjugates (**Figure 2.13**). Then, the cell will be treated with various ROS/RNS. The released desialylation product will be capture by biotinylated tag via click reaction, then enriched via streptavidin column and analyzed by HPLC. Since Neu5Al couldn't be desialylated by sialidases, all captured desialylation products are from the chemical desialylation. Therefore, this metabolic glycoengineering approach allows selective detection of chemical desialylation on cells, which supports the existence of chemical desialylation in the life processes directly.

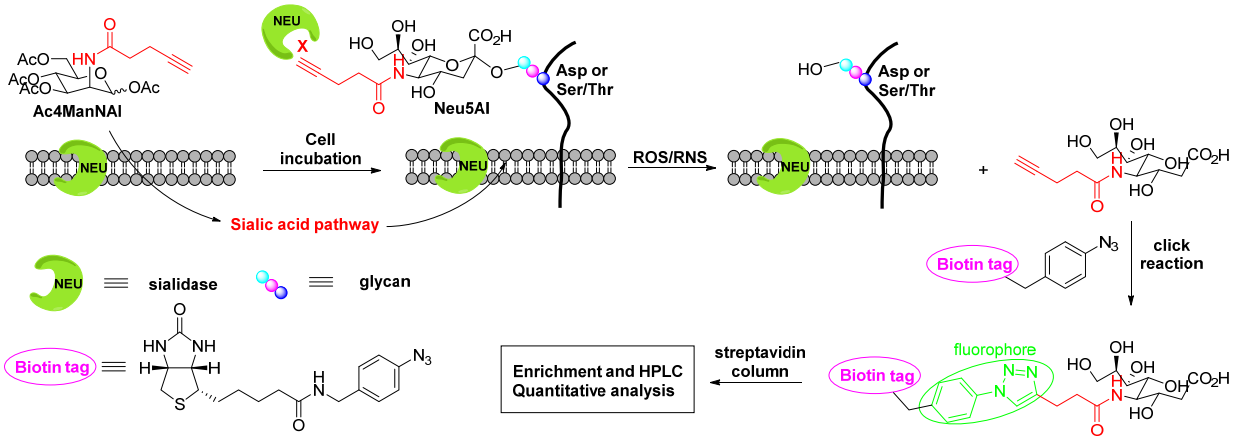

Figure 2.12 *Probe chemical desialylation of cell through metabolic glycoengineering.*

2.11 Conclusions

We have successfully used electrochemical oxidation of sialic acid conjugates to mimic ROS mediated chemical desialylation. Such electrochemical desialylation mimicry reveals that 1) β-linked sialic acid is much more difficult to de desialylated than α-linked sialic acid, 2) electron withdrawing residue and bulky underlying residue can facilitate the desialylation, 3) α-2,3-linked sialic acid is easier to be desialylated than α-2,6- and α-2,8-linked sialic acid, which is in consistence with the glycosidic linkage preference of NEU1[90] and NEU2.[91] This information is highly valuable for identifying the ROS species participated in ROS mediated desialylation and unveiling corresponding mechanisms. ROS mediated desialylation was proposed to go through radical decarboxylation, and we are trapping intermediates to prove the mechanism. In addition, the desialylation product ADOA may become a biomarker for chemical desialylation from oxidative stress.

2.12 References

1. Tiralongo, J., Martinez-Duncker, I. & Editors Sialobiology: Structure, Biosynthesis And Function. Sialic Acid Glycoconjugates In Health And Disease. (Bentham Science Publishers Ltd., 2014).

2. Varki, A. & Schauer, R. 199-227 (Cold Spring Harbor Laboratory Press, 2009).

3. Schauer, R. Sialic acids as regulators of molecular and cellular interactions. *Curr. Opin. Struct. Biol.* **19**, 507-514 (2009).

4. Crocker, P.R., Clark, E.A., Filbin, M., Gordon, S., Jones, Y., Kehrl, J.H., Kelm, S., Le Douarin, N., Powell, L., Roder, J., Schnaar, R.L., Sgroi, D.C., Stamenkovic, K., Schauer, R., Schachner, M., van den Berg, T.K., van der Merwe, P.A., Watt, S.M. & Varki, A. Siglecs: a family of sialic-acid binding lectins. *Glycobiology* **8**, v (1998).

5. Harduin-Lepers, A. 139-187 (Bentham Science Publishers Ltd., 2014).

6. Li, Y. & Chen, X. Sialic acid metabolism and sialyltransferases: natural functions and applications. *Appl. Microbiol. Biotechnol.* **94**, 887-905 (2012).

7. Achyuthan, K.E. & Achyuthan, A.M. Comparative enzymology, biochemistry and pathophysiology of human exo-alpha-sialidases (neuraminidases). *Comparative biochemistry and physiology. Part B, Biochemistry & molecular biology* **129**, 29-64 (2001).

8. Schauer, R. Chemistry, metabolism, and biological functions of sialic acids. *Adv. Carbohydr. Chem. Biochem.* **40**, 131-234 (1982).

9. Angata, T. & Varki, A. Chemical Diversity in the Sialic Acids and Related α-Keto Acids: An Evolutionary Perspective. *Chem. Rev.* **102**, 439-470 (2002).

10. Boons, G.-J. & Demchenko, A.V. Recent Advances in O-Sialylation. *Chem. Rev.* **100**, 4539-4566 (2000).

11. Chen, X. & Varki, A. Advances in the biology and chemistry of sialic acids. *ACS Chem. Biol.* **5**, 163-176 (2010).

12. Kiefel, M.J. & von Itzstein, M. Recent Advances in the Synthesis of Sialic Acid Derivatives and Sialylmimetics as Biological Probes. *Chem. Rev.* **102**, 471-490 (2002).

13. Dennis, J., Waller, C., Timpl, R. & Schirrmacher, V. Surface sialic acid reduces attachment of metastatic tumour cells to collagen type IV and fibronectin. *Nature* **300**, 274-276 (1982).

14. Varki, A. Glycan-based interactions involving vertebrate sialic-acid-recognizing proteins. *Nature* **446**, 1023-1029 (2007).

15. Gavella, M. & Lipovac, V. Protective effects of exogenous gangliosides on ROS-induced changes in human spermatozoa. *Asian J Androl* **15**, 375-381 (2013).

16. Du, J., Meledeo, M.A., Wang, Z., Khanna, H.S., Paruchuri, V.D. & Yarema, K.J. Metabolic glycoengineering: sialic acid and beyond. *Glycobiology* **19**, 1382-1401 (2009).

17. Traving, C. & Schauer, R. Structure, function and metabolism of sialic acids. *Cellular and molecular life sciences : CMLS* **54**, 1330-1349 (1998).

18. Varki, A. Sialic acids in human health and disease. *Trends Mol. Med.* **14**, 351-360 (2008).

19. Miyagi, T., Takahashi, K., Hata, K., Shiozaki, K. & Yamaguchi, K. Sialidase significance for cancer progression. *Glycoconjugate J.* **29**, 567-577 (2012).

20. Miyata, M., Kambe, M., Tajima, O., Moriya, S., Sawaki, H., Hotta, H., Kondo, Y., Narimatsu, H., Miyagi, T., Furukawa, K. & Furukawa, K. Membrane sialidase NEU3 is highly expressed in human melanoma cells promoting cell growth with minimal changes in the composition of gangliosides. *Cancer Sci.* **102**, 2139-2149 (2011).

21. Pshezhetsky, A.V. & Ashmarina, L.I. Desialylation of surface receptors as a new dimension in cell signaling. *Biochemistry (Moscow)* **78**, 736-745 (2013).

22. Hata, K., Koseki, K., Yamaguchi, K., Moriya, S., Suzuki, Y., Yingsakmongkon, S., Hirai, G., Sodeoka, M., von Itzstein, M. & Miyagi, T. Limited inhibitory effects of oseltamivir and zanamivir on human sialidases. *Antimicrob. Agents Chemother.* **52**, 3484-3491 (2008).

23. Kawamura, S., Sato, I., Wada, T., Yamaguchi, K., Li, Y., Li, D., Zhao, X., Ueno, S., Aoki, H., Tochigi, T., Kuwahara, M., Kitamura, T., Takahashi, K., Moriya, S. & Miyagi, T. Plasma membrane-associated sialidase (NEU3) regulates progression of prostate cancer to androgen-independent growth through modulation of androgen receptor signaling. *Cell Death Differ.* **19**, 170-179 (2012).

24. Kakugawa, Y., Wada, T., Yamaguchi, K., Yamanami, H., Ouchi, K., Sato, I. & Miyagi, T. Up-regulation of plasma membrane-associated ganglioside sialidase (Neu3) in human colon cancer and its involvement in apoptosis suppression. *Proc. Natl. Acad. Sci. USA* **99**, 10718-10723 (2002).

25. Tringali, C., Lupo, B., Silvestri, I., Papini, N., Anastasia, L., Tettamanti, G. & Venerando, B. The plasma membrane sialidase NEU3 regulates the malignancy of renal carcinoma cells by controlling beta1 integrin internalization and recycling. *J. Biol. Chem.* **287**, 42835-42845 (2012).

26. Nomura, H., Tamada, Y., Miyagi, T., Suzuki, A., Taira, M., Suzuki, N., Susumu, N., Irimura, T. & Aoki, D. Expression of NEU3 (plasma membrane-associated sialidase) in clear cell adenocarcinoma of the ovary: its relationship with T factor of pTNM classification. *Oncol. Res.* **16**, 289-297 (2006).

27. Sawada, M., Moriya, S., Saito, S., Shineha, R., Satomi, S., Yamori, T., Tsuruo, T., Kannagi, R. & Miyagi, T. Reduced sialidase expression in highly metastatic variants of mouse colon adenocarcinoma 26 and retardation of their metastatic ability by sialidase overexpression. *International journal of cancer. Journal international du cancer* **97**, 180-185 (2002).

28. Miyagi, T., Sato, K., Hata, K. & Taniguchi, S. Metastatic Potential of Transformed Rat 3y1 Cell-Lines Is Inversely Correlated with Lysosomal-Type Sialidase Activity (Vol 349, Pg 255, 1994). *FEBS Lett.* **356**, 151-151 (1994).

29. Yamanami, H., Shiozaki, K., Wada, T., Yamaguchi, K., Uemura, T., Kakugawa, Y., Hujiya, T. & Miyagi, T. Down-regulation of sialidase NEU4 may contribute to invasive properties of human colon cancers. *Cancer Sci.* **98**, 299-307 (2007).

30. Khedri, Z., Li, Y., Muthana, S., Muthana, M.M., Hsiao, C.-W., Yu, H. & Chen, X. Chemoenzymic synthesis of sialosides containing C7-modified sialic acids and their application in sialidase substrate specificity studies. *Carbohydr. Res.* **389**, 100-111 (2014).

31. Khedri, Z., Muthana, M.M., Li, Y., Muthana, S.M., Yu, H., Cao, H. & Chen, X. Probe sialidase substrate specificity using chemo-enzymatically synthesized sialosides containing C9-modified sialic acid. *Chem. Commun.* **48**, 3357-3359 (2012).

32. Eguchi, H., Ikeda, Y., Ookawara, T., Koyota, S., Fujiwara, N., Honke, K., Wang, P.G., Taniguchi, N. & Suzuki, K. Modification of oligosaccharides by reactive oxygen species decreases sialyl Lewis x-mediated cell adhesion. *Glycobiology* **15**, 1094-1101 (2005).

33. Padra, J.T., Sundh, H., Jin, C., Karlsson, N.G., Sundell, K. & Linden, S.K. Aeromonas salmonicida binds differentially to mucins isolated from skin and intestinal regions of Atlantic salmon in an N-acetylneuraminic acid-dependent manner. *Infect. Immun.* **82**, 5235-5245 (2014).

34. Yasuda, J., Eguchi, H., Fujiwara, N., Ookawara, T., Kojima, S., Yamaguchi, Y., Nishimura, M., Fujimoto, J. & Suzuki, K. Reactive oxygen species modify oligosaccharides of glycoproteins in vivo: A study of a spontaneous acute hepatitis model rat (LEC rat). *Biochem. Biophys. Res. Commun.* **342**, 127-134 (2006).

35. Ota, T., Yasuda, M., Iijima, R., Yui, S., Fukuuchi, T., Yamaoka, N., Mawatari, K.-i., Kaneko, K. & Nakagomi, K. Development of a fluorescence analysis method for N-acetylneuraminic acid and its oxidized product ADOA. *J. Chromatogr. B* **932**, 152-157 (2013).

36. Iijima, R., Takahashi, H., Namme, R., Ikegami, S. & Yamazaki, M. Novel biological function of sialic acid (N-acetylneuraminic acid) as a hydrogen peroxide scavenger. *FEBS Lett.* **561**, 163-166 (2004).

37. Iijima, R., Takahashi, H., Ikegami, S. & Yamazaki, M. Characterization of the reaction between sialic acid (N-acetylneuraminic acid) and hydrogen peroxide. *Biol. Pharm. Bull.* **30**, 580-582 (2007).

38. Roy, R. & Laferrière, C.A. Synthesis of protein conjugates and analogues of N-acetylneuraminic acid. *Can. J. Chem.* **68**, 2045-2054 (1990).

39. Crich, D. & Li, W.J. alpha-selective sialylations at-78 degrees C in nitrile solvents with a 1-adamantanyl thiosialoside. *J. Org. Chem.* **72**, 7794-7797 (2007).

40. Stanley, M., Mayr, J., Huber, W., Vlasak, R. & Streicher, H. Synthesis and inhibitory activity of sialic acid derivatives targeted at viral sialate-O-acetylesterases. *Eur. J. Med. Chem.* **46**, 2852-2860 (2011).

41. Veronesi, P.A., Rodriguez, P.E.A., Veronesi, A.M. & Peschechera, E. 80pp. (Therapicon S.r.l., Italy . 2011).

42. Yu, H., Huang, S., Chokhawala, H., Sun, M., Zheng, H. & Chen, X. Highly efficient chemoenzymatic synthesis of naturally occurring and non-natural alpha-2,6-linked sialosides: a P. damsela alpha-2,6-sialyltransferase with extremely flexible donor-substrate specificity. *Angew. Chem., Int. Ed.* **45**, 3938-3944 (2006).

43. Chokhawala, H.A., Yu, H. & Chen, X. High-throughput substrate specificity studies of sialidases by using chemoenzymatically synthesized sialoside libraries. *ChemBioChem* **8**, 194-201 (2007).

44. Yu, H., Lau, K., Thon, V., Autran, C.A., Jantscher-Krenn, E., Xue, M., Li, Y., Sugiarto, G., Qu, J., Mu, S., Ding, L., Bode, L. & Chen, X. Synthetic Disialyl Hexasaccharides Protect Neonatal Rats from Necrotizing Enterocolitis. *Angew. Chem., Int. Ed.* **53**, 6687-6691 (2014).

45. Sun, B., Bao, W., Tian, X., Li, M., Liu, H., Dong, J. & Huang, W. A simplified procedure for gram-scale production of sialylglycopeptide (SGP) from egg yolks and subsequent semi-synthesis of Man3GlcNAc oxazoline. *Carbohydr. Res.* **396**, 62-69 (2014).

46. Sugiyama, N., Saito, K.-i., Fujikura, K., Sugai, K., Yamada, N., Goto, M., Ban, C., Hayasaka, E. & Tomita, K. Thermal and photochemical degradation of sodium N-acetylneuraminate. *Carbohydr. Res.* **212**, 25-36 (1991).

47. Narayanan, S. Sialic acid as a tumor marker. *Ann. Clin. Lab. Sci.* **24**, 376-384 (1994).

48. Crook, M.A., Pickup, J.C., Lumb, P.J., Giorgino, F., Webb, D.J., Fuller, J.H. & Group, E.I.C.S. Relationship between plasma sialic acid concentration and microvascular and macrovascular complications in type 1 diabetes: the EURODIAB Complications Study. *Diabetes Care* **24**, 316-322 (2001).

49. Neyra, C., Paladino, J. & Le Borgne, M. Mechanisms of depolymerization and activation of a polysialic acid and its tetramer by hydrogen peroxide. *Carbohydr. Polym.* **115**, 494-501 (2015).

50. Dickinson, B.C. & Chang, C.J. Chemistry and biology of reactive oxygen species in signaling or stress responses. *Nat. Chem. Biol.* **7**, 504-511 (2011).

51. Cai, T.B., Lu, D., Tang, X., Zhang, Y., Landerholm, M. & Wang, P.G. New glycosidase activated nitric oxide donors: glycose and 3-morphorlinosydnonimine conjugates. *J. Org. Chem.* **70**, 3518-3524 (2005).

52. Olsen, L.F., Issinger, O.-G. & Guerra, B. The Yin and Yang of redox regulation. *Redox Rep.* **18**, 245-252 (2013).

53. Duan, J. & Kasper, D.L. Oxidative depolymerization of polysaccharides by reactive oxygen/nitrogen species. *Glycobiology* **21**, 401-409 (2011).

54. Rees, M.D. & Davies, M.J. Heparan Sulfate Degradation via Reductive Homolysis of Its N-Chloro Derivatives. *J. Am. Chem. Soc.* **128**, 3085-3097 (2006).

55. Praly, J.-P. Structure of anomeric glycosyl radicals and their transformations under reductive conditions. *Adv. Carbohydr. Chem. Biochem.* **56**, 65-151 (2001).

56. Chatgilialoglu, C. Reactivity of nucleic acid sugar radicals. *Wiley Ser. React. Intermed. Chem. Biol.* **2**, 99-133 (2009).

57. Gimisis, T. & Chatgilialoglu, C. in Encyclopedia of Radicals in Chemistry, Biology and Materials (John Wiley & Sons, Ltd, 2012).

58. Rees, M.D., Hawkins, C.L. & Davies, M.J. Hypochlorite-Mediated Fragmentation of Hyaluronan, Chondroitin Sulfates, and Related N-Acetyl Glucosamines: Evidence for Chloramide Intermediates, Free Radical Transfer Reactions, and Site-Specific Fragmentation. *J. Am. Chem. Soc.* **125**, 13719-13733 (2003).

59. Temple, M.D., Perrone, G.G. & Dawes, I.W. Complex cellular responses to reactive oxygen species. *Trends Cell Biol.* **15**, 319-326 (2005).

60. Winterbourn, C.C. Reconciling the chemistry and biology of reactive oxygen species. *Nat. Chem. Biol.* **4**, 278-286 (2008).

61. Bray, W.C. & Gorin, M.H. FERRYL ION, A COMPOUND OF TETRAVALENT IRON. *J. Am. Chem. Soc.* **54**, 2124-2125 (1932).

62. Costas, M., Mehn, M.P., Jensen, M.P. & Que, L. Dioxygen activation at mononuclear nonheme iron active sites: Enzymes, models, and intermediates. *Chem. Rev.* **104**, 939-986 (2004).

63. Tshuva, E.Y. & Lippard, S.J. Synthetic models for non-heme carboxylate-bridged diiron metalloproteins: strategies and tactics. *Chem. Rev.* **104**, 987-1012 (2004).

64. Zersetzung der Valeriansäure durch den elektrischen Strom. *Justus Liebigs Ann. Chem.* **64**, 339-341 (1848).

65. Kolbe, H. Untersuchungen über die Elektrolyse organischer Verbindungen. *Justus Liebigs Ann. Chem.* **69**, 257-294 (1849).

66. Vijh, A.K. & Conway, B.E. Electrode Kinetic Aspects of the Kolbe Reaction. *Chem. Rev.* **67**, 623-664 (1967).

67. Sperry, J.B. & Wright, D.L. The application of cathodic reductions and anodic oxidations in the synthesis of complex molecules. *Chem. Soc. Rev.* **35**, 605-621 (2006).

68. Lebreux, F., Buzzo, F. & Marko, I. Studies in the Oxidation of Carboxylic Acids: New Twists for an Old Reaction. Synthesis of Various Cyclic Systems and Substituted Orthoesters. *ECS Transactions* **13**, 1-10 (2008).

69. Stapley, J.A. & BeMiller, J.N. The Ruff degradation: a review of previously proposed mechanisms with evidence that the reaction proceeds by a Hofer-Moest-type reaction. *Carbohydr. Res.* **342**, 407-418 (2007).

70. Atherton, G., Fleischmann, M. & Goodridge, F. Kinetic study of the Hofer-Moest reaction. *Transactions of the Faraday Society* **63**, 1468-1477 (1967).

71. MacPherson, J.V. A practical guide to using boron doped diamond in electrochemical research. *Phys. Chem. Chem. Phys.* **17**, 2935-2949 (2015).

72. Angus, J.C. 3-19 (John Wiley & Sons, Inc., 2011).

73. Einaga, Y., Foord, J.S. & Swain, G.M. Diamond electrodes: Diversity and maturity. *MRS Bull.* **39**, 525-532 (2014).

74. Einaga, Y. Diamond electrodes for electrochemical analysis. *J. Appl. Electrochem.* **40**, 1807-1816 (2010).

75. Luong, J.H.T., Male, K.B. & Glennon, J.D. Boron-doped diamond electrode: synthesis, characterization, functionalization and analytical applications. *Analyst (Cambridge, U. K.)* **134**, 1965-1979 (2009).

76. Klepach, T., Carmichael, I. & Serianni, A.S. 13C-Labeled N-Acetylneuraminic Acid in Aqueous Solution: Detection and Quantification of Acyclic Keto, Keto Hydrate, and Enol Forms by 13C NMR Spectroscopy. *J. Am. Chem. Soc.* **130**, 11892-11900 (2008).

77. Kancharla, P.K., Kato, T. & Crich, D. Probing the Influence of Protecting Groups on the Anomeric Equilibrium in Sialic Acid Glycosides with the Persistent Radical Effect. *J. Am. Chem. Soc.* **136**, 5472-5480 (2014).

78. Peixoto, S., Nguyen, T.M., Crich, D., Delpech, B. & Marazano, C. One-Pot Formation of Piperidine- and Pyrrolidine-Substituted Pyridinium Salts via Addition of 5-Alkylaminopenta-2,4-dienals to N-Acyliminium Ions: Application to the Synthesis of (+/-)-Nicotine and Analogs. *Org. Lett.* **12**, 4760-4763 (2010).

79. Kancharla, P.K., Navuluri, C. & Crich, D. Dissecting the Influence of Oxazolidinones and Cyclic Carbonates in Sialic Acid Chemistry. *Angew. Chem., Int. Ed.* **51**, 11105-11109 (2012).

80. Paulsen, H. & Matschulat, P. Synthese von C-Glycosiden der N-Acetylneuraminsäure und weiteren Derivaten. *Liebigs Ann. Chem.* **1991**, 487-495 (1991).

81. Nagy, J.O. & Bednarski, M.D. The chemical-enzymatic synthesis of a carbon glycoside of N-acetylneuraminic acid. *Tetrahedron Lett.* **32**, 3953-3956 (1991).

82. Waaglund, T. & Claesson, A. Stereoselective synthesis of the α-allyl C-glycoside of 3-deoxy-D-manno-2-octulosonic acid (KDO) by use of radical chemistry. *Acta Chem. Scand.* **46**, 73-76 (1992).

83. Nokami, T., Shibuya, A., Tsuyama, H., Suga, S., Bowers, A.A., Crich, D. & Yoshida, J.I. Electrochemical generation of glycosyl triflate pools. *J. Am. Chem. Soc.* **129**, 10922-10928 (2007).

84. Magano, J. Synthetic Approaches to the Neuraminidase Inhibitors Zanamivir (Relenza) and Oseltamivir Phosphate (Tamiflu) for the Treatment of Influenza. *Chem. Rev.* **109**, 4398-4438 (2009).

85. Feng, E., Shin, W.J., Zhu, X.L., Li, J., Ye, D.J., Wang, J., Zheng, M.Y., Zuo, J.P., No, K.T., Liu, X., Zhu, W.L., Tang, W., Seong, B.L., Jiang, H.L. & Liu, H. Structure-Based Design and Synthesis of C-1- and C-4-Modified Analogs of Zanamivir as Neuraminidase Inhibitors. *J. Med. Chem.* **56**, 671-684 (2013).

86. Shtyrya, Y.A., Mochalova, L.V. & Bovin, N.V. Influenza Virus Neuraminidase: Structure and Function. *Acta Naturae* **1**, 26-32 (2009).

87. Zamora, C.Y., Ryan, M.J., d'Alarcao, M. & Kumar, K. Sialidases as regulators of bioengineered cellular surfaces. *Glycobiology* **25**, 784-791 (2015).

88. Chang, P.V., Chen, X., Smyrniotis, C., Xenakis, A., Hu, T., Bertozzi, C.R. & Wu, P. Metabolic labeling of sialic acids in living animals with alkynyl sugars. *Angew. Chem., Int. Ed.* **48**, 4030-4033 (2009).

89. Hsu, T.-L., Hanson, S.R., Kishikawa, K., Wang, S.-K., Sawa, M. & Wong, C.-H. Alkynyl sugar analogs for the labeling and visualization of glycoconjugates in cells. *Proc. Natl. Acad. Sci. USA* **104**, 2614-2619 (2007).

90. Miyagi, T. & Tsuiki, S. Rat liver lysosomal sialidase. Solubilization, substrate specificity and comparison with the cytosolic sialidase. *Eur. J. Biochem.* **141**, 75-81 (1984).

91. Miyagi, T. & Tsuiki, S. Purification and characterization of cytosolic sialidase from rat liver. *J. Biol. Chem.* **260**, 6710-6716 (1985).

3 CHAPTER 3 EXPERIMENTAL PROCEDURES

3.1 Experiment procedures for transforming DHAP-dependent aldolases mediated aldol reaction from flask into cell-based synthesis

3.1.1 General information

^{1}H and ^{13}C NMR spectra were recorded on Bruker AV-400 MHz. Chemical shifts are expressed in ppm using residual $CDCl_3$ (7.26 ppm for ^{1}H NMR and 77 ppm for ^{13}C NMR) or CD_3OD (3.31 ppm for ^{1}H NMR and 49 ppm for ^{13}C NMR) or D_2O at 298 k as internal standard. High-resolution mass spectra were recorded under ESI-TOF Mass spectra conditions. Optical rotations were measured with JASCO P-1020 polarimeter. Analytical thin-layer chromatography (TLC) was performed on pre-coated plates (Silica Gel 60). Silica gel 60 (E. Merck) was employed for all flash chromatography. Reagents and starting materials obtained from commercial suppliers were used without further purification unless otherwise noted.

3.1.2 Bacterial strains and plasmids

Bacterial strains, plasmids and primers were summarized in Table S1. Pfx DNA polymerase was purchased from Invitrogen (CA, USA). Restriction enzymes and T4 ligase were purchased from Fermentas (MBI, Canada). *Thermus thermophiles* HB8 genomic DNA was purchased from ATCC (Manassas, VA). Plasmid pKKfda containing *fda* gene from *Staphylococcus carnosus* TM300 was a kind gift from professor Wolf-Dieter Fessner. Bio gel P-2 gel and Aminex HPX-87H column (300 × 7.8 mm) were purchased from Bio-Rad Laboratories, Inc. (Hercules, CA). XK column (100 × 2.6 cm) was purchased from GE Healthcare (Piscataway, NJ).

Plasmids, strains and primers used in this study

Materials	Relevant genotype or primer sequence	Source
Plasmids		
pCDFDuet-1	CloDF13 ori lacI T7lac Str^r	Novagen
pCDF-Y	pCDFDuet-1 harboring *yqaB* gene from *E. coli* MG1655	This work
pCDF-fucA-Y	pCDFDuet-1 harboring *fucA* gene from *T. thermophiles* HB8 and *yqaB* gene from *E. coli* MG1655	This work
pKK-fda	Plasmid pKK223-3 harboring *fda* gene from *S. carnosus*	Fessner W.D et al.(1999)
pCDF-fda-Y	pCDFDuet-1 harboring *fda* gene from *S. carnosus* and *yqaB* gene from *E. coli* MG1655	This work
pCDF-rhuA-Y	pCDFDuet-1 harboring *rhuA* gene from *E.coli* MG1655 and *yqaB* gene from *E.coli* MG1655	This work
Strains		
DH5α	lacZΔM15 hsdR recA	Gibco-BRL
MG1655	F- λ- ilvG rfb-50 rph-1	Lab stock
BL21Star (DE3)	F- ompT hsdSB(rB- mB-) gal dcm rne131 (DE3)	Invitrogen
E.coli FucA-Y	BL21Star (DE3) harboring plasmid pCDF-fucA-Y	This work
E.coli FruA-Y	BL21Star (DE3) harboring plasmid pCDF-fda-Y	This work
E.coli RhuA-Y	BL21Star (DE3) harboring plasmid pCDF-rhuA-Y	This work
Primers		
pCDF-Y-F	5'-GCGCCATATGTACGAGCGTTATGCAGGTT-3'(*Nde*I)	
pCDF-Y-R	5'-TATACTCGAGCAGCAAGCGAACATCCACG-3'(*Xho*I)	
pCDF-fucA-F	5'-TATAGGATCCGCGCGCCCGGTTGTACG-3'(*BamH*I)	
pCDF-fucA-R	5'-TATAAAGCTTTCATTCCCCACCCCCCAAG-3'(*Hind*III)	
pCDF-fda-F	5'-GCGCGGATCCGAACCAAGAACAATT-3'(*BamH*I)	
pCDF-fda-R	5'-GCGCCTGCAGTTAAGCTTTGTTTACTGAA-3'(*Pst*I)	
pCDF-rhuA-F	5'-GCGTGGATCCGCAAAACATTACTCAGT-3'(*BamH*I)	
pCDF-rhuA-R	5'-TATAAAGCTTTTACAGCGCCAGCGCACT-3'(*Hind*III)	

3.1.3 Construction of pCDF-fucA-Y, pCDF-fda-Y and pCDF-rhuA-Y plasmids

Primers pCDF-Y-F and pCDF-Y-R were used to amplify the *yqaB* gene by PCR using *E. coli* MG1655 genomic DNA as the template. The amplified *yqaB* gene was digested with *Nde*I and *Xho*I then inserted into the MCS-2 of pCDFDuet-1 plasmid with the same enzymes digested to generate plasmid pCDF-Y. Primers pCDF-fucA-F and pCDF-fucA-R were used to amplify

fucA gene encoding *T. thermophiles* HB8 L-fuculose-1-phosphate aldolase by PCR using *T. thermophiles* HB8 genomic DNA as the template. The amplified *fucA* gene was digested with *BamH*I and *Hind*III then ligated into MCS-1 of plasmid pCDF-Y with the same enzymes digested to generate plasmid pCDF-fucA-Y. Primers pCDF-fda-F and pCDF-fda-R were used to amplify the *fda* gene encoding fructose-1, 6-bisphosphate aldolase from *S.carnosus* TM300 by PCR with plasmid pkk-fda as the template. The amplified *fda* was digested by *BamH*I and *Pst*I then inserted into MCS-1 of plasmid pCDF-Y with the same enzymes digested to generate plasmid pCDF-fda-Y. Primers pCDF-rhuA-F and pCDF-rhuA-R were used to amplify the gene *rhuA* encoding L-rhamnulose-1-phosphate aldolase with *E.coli* MG1655 as the template. The *rhuA* gene amplified was digested with *BamH*I and *Hind*III then inserted into MCS-1 of plasmid pCDF-Y with the same enzymes digested to generate plasmid pCDF-rhuA-Y. These recombinant plasmids were all transformed into DH5α strain for amplifying and sequencing. *pCDF-fucA-Y, pCDF-fda-Y and pCDF-rhuA-Y plasmids* were transformed into *E.coli* strain BL21Star (DE3) respectively, resulting in the recombinant strains *E.coli* FucA-Y, *E.coli* FruA-Y and *E.coli* RhuA-Y.

3.1.4 Synthesis of aldehyde acceptors

3-trifluoroacetamido propanal[1, 2]

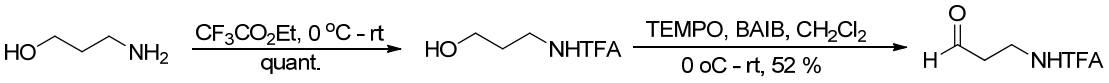

To a stirred solution of 3-aminopropan-1-ol (75 g, 1 mol, 1 equiv), ethyl trifluoroacetate (177.5 g, 1.5 mol, 1.25 equiv) was added dropwise at 0 °C. After completion of the addition, the mixture was warmed to room temperature and stirred overnight. When 3-aminopropan-1-ol was completely consumed, the resulting mixture was evaporated under reduced pressure to afford 3-trifluoroacetamido propan-1-ol, which was used for the TEMPO oxidation directly.

To a stirred solution of 3-trifluoroacetamido propan-1-ol (171 g, 1 mol, 1 equiv) in CH_2Cl_2 (1000 mL), TEMPO (15.6 g, 0.1 mol, 0.1 equiv) was added at 0 ^oC, followed by bis(acetoxy)iodobenzene (BAIB) (354 g, 1.1 mol, 1.1 equiv) in small portions. After the addition, the reaction mixture was warmed to room temperature and stirred at rt for 3 days. The reaction mixture was extracted with water (200 mL x 3). The aqueous phase was washed with hexane, then saturated with NaCl and extracted with CH_2Cl_2 (500 mL x 3). The organic phase was dried over anhydrous Na_2SO_4 and evaporated under reduced pressure. The residue was purified by vacuum distillation to give 3-trifluoroacetamido propanal 87.88 g with 52 % yield. ^1H NMR (400 MHz, $CDCl_3$) δ: 9.82 (s, 1H), 6.91 (s, 1H), 3.65 (dt, J = 6.0, 5.6 Hz, 2H), 2.83 (t, J = 5.6 Hz, 2H); ^{13}C NMR (100 MHz, $CDCl_3$) δ: 200.6, 157.3 (q, J = 37.0 Hz), 115.7 (q, J = 286.0 Hz), 42.5, 33.3; ^{19}F NMR (376 MHz, $CDCl_3$) δ: -76.1 (s, 3F).

3-trichloroacetamido propanal[3]

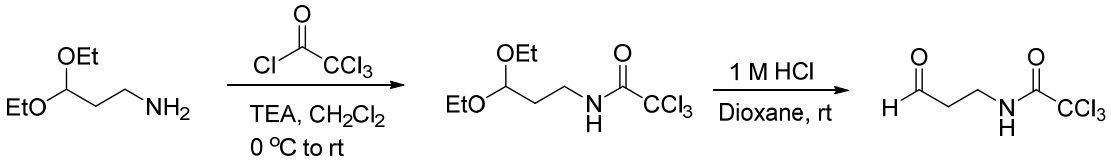

To the cooled (0 °C) solution of 3-aminopropionaldehyde diethylacetal (14.7 g, 100 mmol, 1 equiv) and TEA (11.13 g, 110 mmol, 1.1 equiv) in CH_2Cl_2 (150 mL), a solution of trichloroacetyl chloride (19.09 g, 105 mmol, 1.05 equiv) in CH_2Cl_2 (50 mL) was added dropwise. After completion of addition, the reaction mixture was allowed to warm to rt and stirred overnight. The resulting mixture was washed with water, dried over Na_2SO_4, and concentrated to provide 3-trichloroacetamido propionaldehyde diethylacetal. The crude 3-trichloroacetamido propionaldehyde diethylacetal was sufficiently pure and was used without further purification.

The mixture of 3-trichloroacetamido propionaldehyde diethylacetal in 1 M HCl in dioxane (100 mL) was stirred at room temperature until completion of the reaction (TLC monitored). The resulting reaction mixture was concentrated and the residue was dissolved in ethyl acetate, then washed with water, dried over Na_2SO_4, and concentrated *in vacuo* to afford 14.64 g 3-trichloroacetamido propanal with 67 % yield, which was sufficiently pure and was used for fermentation without further purification. ^{1}H NMR (400 MHz, $CDCl_3$) δ: 9.82 (s, 1H), 7.30 (s, 1H), 3.64 (dt, J = 6.0, 6.0 Hz, 2H), 2.84 (t, J = 5.8 Hz, 2H); ^{13}C NMR (100 MHz, $CDCl_3$) δ: 200.8, 162.0, 67.0, 42.6, 34.8.

3-difluoroacetamido propanal

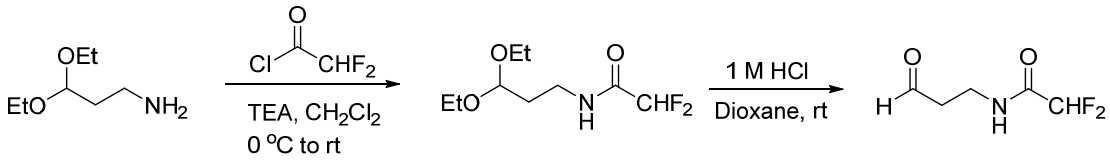

To the cooled (0 °C) solution of 3-aminopropionaldehyde diethylacetal (14.7 g, 100 mmol, 1 equiv) and TEA (11.13 g, 110 mmol, 1.1 equiv) in CH_2Cl_2 (150 mL), a solution of difluoroacetyl chloride (12.02 g, 105 mmol, 1.05 equiv) in CH_2Cl_2 (50 mL) was added dropwise. After completion of addition, the reaction mixture was allowed to warm to rt and stirred overnight. The resulting mixture was washed with water, dried over Na_2SO_4, and concentrated to provide 3-difluoroacetamido propionaldehyde diethylacetal. The crude 3-difluoroacetamido propionaldehyde diethylacetal was sufficiently pure and was used without further purification.

The mixture of 3-difluoroacetamido propionaldehyde diethylacetal in 1 M HCl in dioxane (100 mL) was stirred at room temperature until completion of the reaction (TLC monitored). The resulting reaction mixture was concentrated and the residue was dissolved in ethyl acetate, then washed with water, dried over Na_2SO_4, and concentrated *in vacuo* to afford 9.52 g 3-difluoroacetamido propanal with 63 % yield, which was sufficiently pure and was used

for fermentation without further purification. ^{1}H NMR (400 MHz, $CDCl_3$) δ: 9.77 (s, 1H), 7.03 (s, 1H), 5.85 (t, J = 54 Hz, 1H), 3.62-3.57 (m, 2H), 2.78 (s, 2H); ^{13}C NMR (100 MHz, $CDCl_3$) δ: 200.7, 162.7 (t, J = 25.3 Hz), 108.2 (t, J = 252.3 Hz), 42.8, 32.7.

(*R*)-3-trifluoroacetamido-2-hydroxypropanal[4]

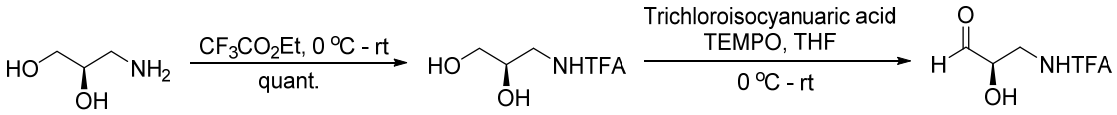

To a stirred solution of (*R*)-3-aminopropane-1, 2-diol (5 g, 54.95 mmol, 1 equiv) in methanol (50 mL), ethyl trifluoroacetate (9.75 g, 68.68 mmol, 1.25 equiv) was added dropwise at 0 °C. After the addition, the mixture was warmed to room temperature and stirred overnight. When (*R*)-3-aminopropane-1, 2-diol was completely consumed, the resulting mixture was evaporated under reduced pressure to afford (*R*)-3-trifluoroacetamido propan-1, 2-diol quantitatively, which was used for the IBX oxidation directly.

To a stirred solution of (*R*)-3-trifluoroacetamido propan-1, 2-diol (10.27 g, 54.95 mmol, 1 equiv) in EtOAc (500 mL), 2-iodoxybenzoic acid (76.3 g, 47 %, 82.5 mmol, 1.5 equiv) was added and refluxed overnight. The reaction mixture was quenched by filtering through celite. DD water (50 mL) was added to the filtrate and the organic solvent was removed under reduced pressure. The pH of the aldehyde solution was adjusted to 5 with $NaHCO_3$. After sterilization by filtering through 0.2 μm, nylon, sterile membrane, the resulting aldehyde solution was used for fermentation directly. The estimated yield was around 50 %.

(*S*)-3-trifluoroacetamido-2-hydroxypropanal

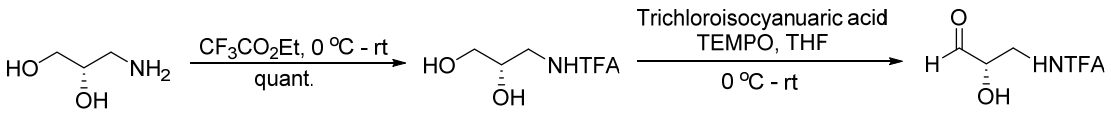

The (*S*)-3-trifluoroacetamido-2-hydroxypropanal was prepared analogously from commercial (*S*)-3-aminopropane-1, 2-diol. The estimated yield was around 50 %.

3.1.5 Media and fermentation procedures

20 mL overnight cultured recombinant *E.coli* strain was inoculated to 1 L LB Broth medium (LB broth 25 g/L, $NaH_2PO_4 \cdot H_2O$ 10.78 g/L, $Na_2HPO_4 \cdot 7H_2O$ 17.32 g/L, $MgSO_4$ 120.00 mg/L, $ZnSO_4$ 32.30 mg/L, $CaCl_2$ 11.10 mg/L, thiamine 10.00 mg/L, streptomycin 50.00 mg/L, glucose 4.00 g/L), or ECAM medium ($NaH_2PO_4 \cdot H_2O$ 10.78 g/L, $Na_2HPO_4 \cdot 7H_2O$ 17.32 g/L, KCl 4.27 g/L, $(NH_4)_2SO_4$ 2.33 g/L, citric acid 1 g/L, $MgSO_4$ 1 g/L, $CaCl_2$ 40 mg/L, thiamine 10 mg/L, EDTA 5 mg/L, $FeSO_4 \cdot 7H_2O$ 10 mg/L, $ZnSO_4 \cdot 7H_2O$ 2 mg/L, $MnSO_4 \cdot H_2O$ 2 mg/L, $CoCl_2 \cdot 6H_2O$ 0.2 mg/L, $CuSO_4 \cdot 5H_2O$ 0.1 mg/L, $Na_2MoO_4 \cdot 2H_2O$ 0.2 mg/L, H_3BO_3 0.1 mg/L, streptomycin 50.00 mg/L, glucose 4.00 g/L) or LB Broth/ECAM (1/1, v/v) medium (LB Broth 12.5 g/L, $NaH_2PO_4 \cdot H_2O$ 10.78 g/L, $Na_2HPO_4 \cdot 7H_2O$ 17.32 g/L, KCl 2.14 g/L, $(NH_4)_2SO_4$ 1.17 g/L, citric acid 0.5 g/L, $MgSO_4$ 0.5 g/L, $CaCl_2$ 20 mg/L, thiamine 5 mg/L, EDTA 2.5 mg/L, $FeSO_4 \cdot 7H_2O$ 5 mg/L, $ZnSO_4 \cdot 7H_2O$ 1 mg/L, $MnSO_4 \cdot H_2O$ 1 mg/L, $CoCl_2 \cdot 6H_2O$ 0.1 mg/L, $CuSO_4 \cdot 5H_2O$ 0.05 mg/L, $Na_2MoO_4 \cdot 2H_2O$ 0.1 mg/L, H_3BO_3 0.05 mg/L, streptomycin 50.00 mg/L, glucose 4.00 g/L) and grown aerobically at 37 ^oC, 220 rpm until the OD_{600} reached 1.80. Then the temperature was switched to 30 ^oC and isopropyl-1-thio-β-D-galactopyranoside (IPTG) was added at a final concentration of 1 mM to induce the co-expression of aldolase and phosphatase for 12 h. Then aldehyde aqueous solution (sterilized by filtering through 0.2 μm, nylon, sterile membrane) was added into the medium with an initial concentration of 20 mM. The consumption of glucose, aldehyde and generation of aldol product in the medium were monitored by HPLC (HPX-87H Ion Exchange Column, column temperature 60 ^oC, 5 mM H_2SO_4, 0.5 mL/min). Aldehyde (totally

40 mmol) and glucose were fed when necessary. The fermentation was stopped when the concentration of the aldol product reached a plateau.

When 3-trifluoroacetamido propanal, 3-trichloroacetamido propanal, 3-difluoroacetamido propanal, 3-(methylthio)propanal, 4,4,4-trifluorobutanal, (*R*)-3-trifluoroacetamido-2-hydroxypropanal and (*S*)-3-trifluoroacetamido-2-hydroxypropanal were used as the acceptor, LB Broth/ECAM (1/1, v/v) medium was used; when D-glyceraldehyde was used as the acceptor, ECAM medium was used for easier purification of aldol products.

3.1.6 Analytical methods

The progress of the fermentation was monitored by HPLC. Samples were taken at regular intervals to monitor the consumption of aldehyedes and generation of aldol products. After centrifugation, the supernatant was applied to HPLC column (Aminex HPX-87H, 300 × 7.8 mm) with 5 mM sulfuric acid as mobile phase and detected with Refractive Index Detector. The flow rate was 0.5 mL/min, and the column temperature was 60 ^{o}C.

Standard curve of **2**.

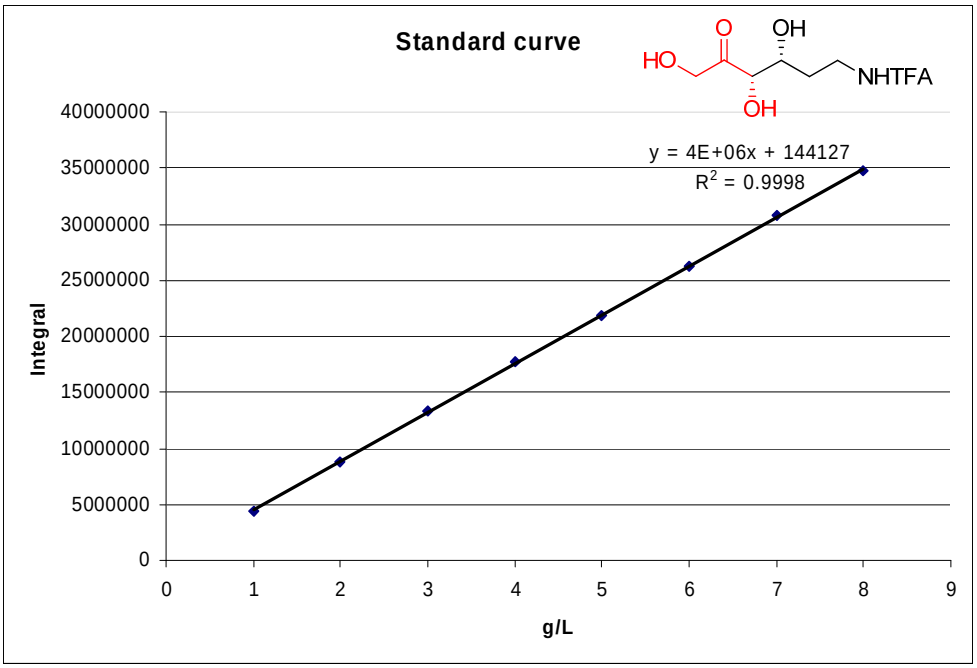

Standard curve of D-fructose.

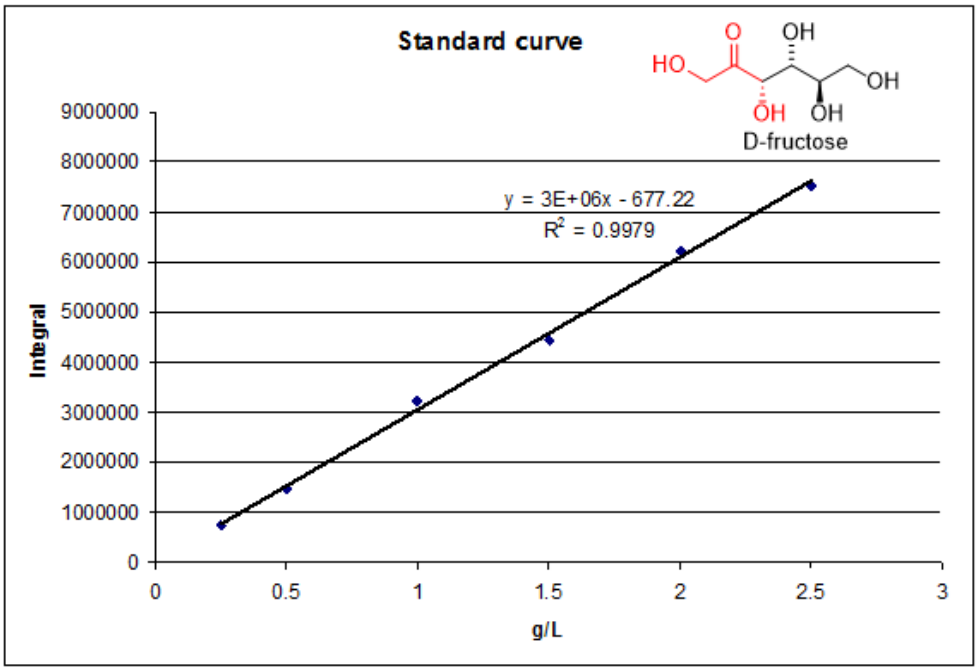

3.1.7 Product purification

The fermentation medium was centrifuged to remove *E. coli* cells and 2 L acetone was added to the supernatant to precipitate nucleic acid *etc*. When 3-trifluoroacetamido propanal, 3-trichloroacetamido propanal, 3-difluoroacetamido propanal, (*R*)-3-trifluoroacetamido-2-hydroxypropanal and (*S*)-3-trifluoroacetamido-2-hydroxypropanal were used as the acceptor, after removal of precipitate, the pH value of resulting supernatant was adjusted to 3 by concentrated hydrochloric acid, then silica gel was added and concentrated under reduced pressure. The resulting residue was loaded onto a pad of silica gel and washed with EtOAc/MeOH/HOAc (20/0.5/0.1, v/v/v). The filtrate was concentrated and the residue was purified by C-18 reverse phase silica gel column chromatography (water as the eluent), followed by silica gel column chromatography (CH_2Cl_2/MeOH, 10/1). For (*R*)-3-trifluoroacetamido-2-hydroxypropanal and (*S*)-3-trifluoroacetamido-2-hydroxypropanal, CH_2Cl_2/MeOH (6/1, v/v) was used to wash the residue. The filtrate was concentrated and the resulting residue was purified by preparative HPLC (C-18 reverse phase, mobile phase, 5 mM TFA).

When 3-(methylthio)propanal and 4,4,4-trifluorobutanal were used as the acceptor, after removal of precipitate, silica gel was added and the supernatant was concentrated under reduced pressure. The resulting residue was loaded onto a pad of silica gel and washed with EtOAc/MeOH/HOAc (20/0.5/0.1, v/v/v). The filtrate was concentrated and the residue was purified by C-18 reverse phase silica gel column chromatography (water as the eluent), followed by silica gel column chromatography (CH_2Cl_2/MeOH, 15/1).

When D-glyceraldehyde was used as the acceptor, after removal of precipitate, silica gel was added and the supernatant was concentrated under reduced pressure. The resulting residue was purified by silica gel column chromatography (EtOAc/iPrOH/H_2O 9/3/1 (v/v/v)), followed

by Bio gel P-2 column, a mixture of D-psicose and D-sorbose (or D-fructose and glucose) was obtained. This mixture was isolated by cation exchange resin column as described below.

3.1.8 Procedure for isolation of D-sorbose and D-psicose using cation exchange resin (Ca^{2+} form)

D-Sorbose and D-psicose mixture was dissolved in 3 mL ddH_2O and applied to a cation exchange resin (Ca^{2+} form, 100 × 2.6 cm) which was preheated to 65°C using a thermostatic jacket. The column was eluted with ddH_2O (flow rate ~1.5 mL/min) and the whole isolation process was performed at 65-70°C. Fractions were collected with an automatic fraction collector and identified by HPLC. D-Sorbose was eluted off first and D-psicose was eluted off in later fractions. Fractions containing pure D-sorbose or D-psicose were pooled and lyophilized to give pure D-sorbose and D-psicose. Pure D-fructose could also be isolated from glucose according to the procedure described above using cation exchange resin.

3.1.9 Synthesis of D-fagomine, DMJ, DNJ

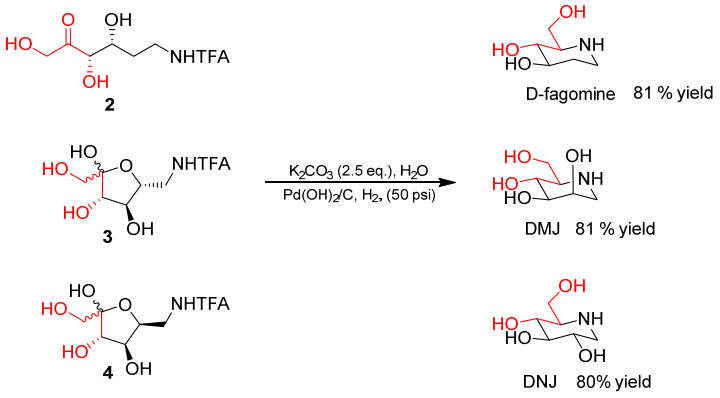

D-fagomine:

To a solution of **2** (259 mg, 1 mmol) and K_2CO_3 (345 mg, 2.5 mmol) in 10 mL water, $Pd(OH)_2/C$ (10 %) was added. The mixture was hydrogenated (50 psi H_2) at room temperature overnight. The mixture was filtered through 0.45 µm nylon membrane filter. The filtrate was concentrated

and the residue was purified by basic Al_2O_3 column chromatography (THF/MeOH/water/NH_4OH) to give 119 mg D-fagomine with 81 % yield.

DMJ:

Following the same procedure, **3** (150 mg, 0.55 mmol) was hydrogenated to give 72 mg DMJ with 81 % yield.

DNJ:

Following the same procedure, **4** (150 mg, 0.55 mmol) was hydrogenated to give 71 mg DNJ with 81 % yield.

3.1.10 One-pot four-enzyme synthesis of 2, 5, 6

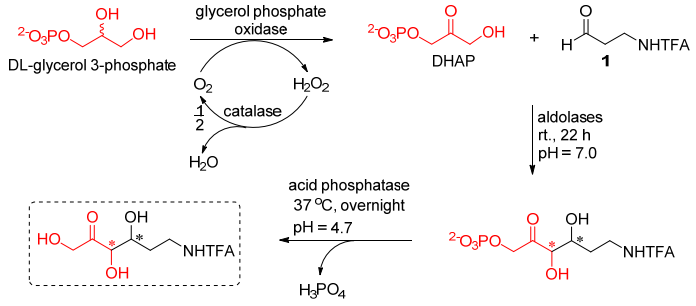

entry	aldolase	acceptor	product	isolated yield	*dr*[a]
1	FruA	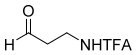	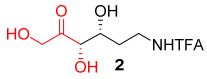 **2**	53 %	> 95:5
2	FucA	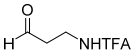	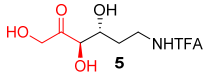 **5**	48 %	87:13
3	RhuA	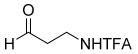	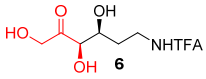 **6**	42 %	89:11

To a solution of DL-glycerol 3-phosphate magnesium salt (457.3 mg, 2 mmol) in 10 mL ddH2O, aldehyde **1** (253.5 mg, 1.5 mmol) was added at pH 7.0, followed by glycerol phosphate oxidase (70 U, 2 mg), catalase (1000 U, 1.2 μL), and aldolase (FruA from *Staphylococcus carnosus*, FucA from *Thermus. thermophilus* HB8 or RhuA from *E.* coli, final concentration 0.5 mg/mL). The mixture was shaken at rt for 22 h and the reaction was monitored by TLC

(developed by n-BuOH/AcOH/H2O: 2/1/1 (v/v/v) and stained with anisaldehyde sugar stain). The reaction mixture was heated for 10 min at 75 °C, then cooled to rt. Then, pH was adjusted to 4.7 with 6 M HCl and 11 µL acid phosphatase (18 U) was added and the mixture was shaken overnight at 37 °C. After cooling to rt, the pH was adjusted to 7.0 with 1 M NaOH and the mixture was diluted with methanol. The solution was filtered through celite and washed with methanol. The filtrate was concentrated under reduced pressure and the residue was purified by silica gel column chromatography (dichloromethane/methanol: 15/1 (v/v)) to afford product. After purification, 137.4 mg **2** was provided with 53 % yield, 124.4 mg **5** was provided with 48 % yield and 87:13 *dr*, and 108 mg **6** was provided with 42 % yield and 89:11 *dr*. Yields were calculated based on L-glycerol 3-phosphate (1 mmol).

3.1.11 Product characterizations

(3*S*, 4*R*)-6-trifluoroacetamido-1,3,4-trihydroxyhexan-2-one

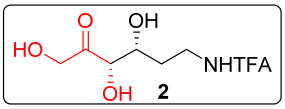

^{1}H NMR (400 MHz, CD_3OD) δ: 4.54 (d, *J* = 19.2 Hz, 1H), 4.44 (d, *J* = 19.6 Hz, 1H), 4.15 (s, 1H), 3.97 (t, *J* = 5.6 Hz, 1H), 3.46-3.38 (m, 2H), 1.85-1.80 (m, 2H); ^{13}C NMR (100 MHz, CD_3OD) δ: 213.3, 159.0 (q, *J* = 36.5 Hz), 117.5 (q, *J* = 284.7 Hz), 79.4, 71.1, 67.9, 37.9, 33.3; ^{19}F NMR (376 MHz, CD_3OD) δ: -77.4 (s, 3F); HRMS (ESI): $[M-H]^-$ calcd. for $C_8H_{11}F_3NO_5$, 258.0595; found, 258.0592.

(3*S*, 4*R*)-6-trichloroacetamido-1,3,4-trihydroxyhexan-2-one

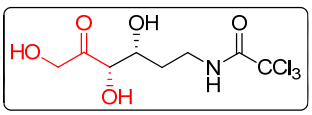

^{1}H NMR (400 MHz, CD_3OD) δ: 4.50 (d, *J* = 19.2 Hz, 1H), 4.40 (d, *J* = 19.2 Hz, 1H), 4.13 (s, 1H), 3.99-3.94 (m, 1H), 3.40 (t, *J* = 6.8 Hz, 2H), 1.82 (dt, *J* = 6.8, 6.8 Hz, 2H); ^{13}C NMR (100 MHz, CD_3OD) δ: 213.1, 164.2, 79.3, 71.2, 67.8, 39.5, 33.2; HRMS (ESI): $[M+Na]^+$ calcd. for $C_8H_{12}Cl_3NNaO_5$, 329.9673; found, 329.9668.

(3*S*, 4*R*)-6-difluoroacetamido-1,3,4-trihydroxyhexan-2-one

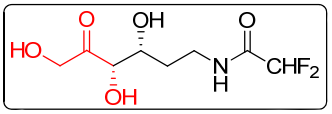

^{1}H NMR (400 MHz, CD_3OD) δ: 6.00 (t, *J* = 54.0 Hz, 1H), 4.51 (d, *J* = 19.3 Hz, 1H), 4.41 (d, *J* = 19.3 Hz, 1H), 4.13 (s, 1H), 3.98-3.93 (m, 1H), 3.36 (t, *J* = 6.8 Hz, 2H), 1.73 (dt, *J* = 6.8, 6.8 Hz, 2H); ^{13}C NMR (100 MHz, CD_3OD) δ: 213.3, 165.1 (t, *J* = 25.0 Hz), 109.9 (t, *J* = 240.7 Hz), 79.2, 71.1, 67.7, 37.3, 33.4; HRMS (ESI): $[M+Na]^+$ calcd. for $C_8H_{13}F_2NNaO_5$, 264.0654; found, 264.0648.

(3*S*, 4*R*)-1,3,4-trihydroxy-6-(methylthio)hexan-2-one

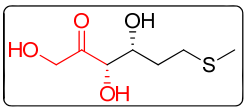

^{1}H NMR (400 MHz, CD_3OD) δ: 4.54 (d, *J* = 19.2 Hz, 1H), 4.44 (d, *J* = 19.2 Hz, 1H), 4.14 (d, *J* = 2 Hz, 1H), 4.07-4.04 (m, 1H), 2.67-2.52 (m, 2H), 2.09 (s, 3H), 1.88-1.81 (m, 2H); ^{13}C NMR (100 MHz, CD_3OD) δ: 213.4, 79.4, 72.2, 67.8, 33.7, 31.3, 15.3; HRMS (ESI): $[M+Na]^+$ calcd. for $C_7H_{14}NaO_4S$, 217.0505; found, 217.0500.

(3*S*, 4*R*)-7,7,7-trifluoro-1,3,4-trihydroxyheptan-2-one

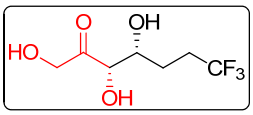

^{1}H NMR (400 MHz, CD_3OD) δ: 4.54 (d, *J* = 19.6 Hz, 1H), 4.45 (d, *J* = 19.6 Hz, 1H), 4.14 (s, 1H), 3.96 (s, 1H), 2.41-2.29 (m, 1H), 2.27-2.16 (m, 1H), 1.88-1.74 (m, 2H); ^{13}C NMR (100 MHz, CD_3OD) δ: 213.2, 128.9 (q, *J* = 273.4 Hz), 79.3, 72.0, 67.8, 31.2 (q, *J* = 28.6 Hz), 26.9; HRMS (ESI): $[M-H]^-$ calcd. for $C_7H_{10}F_3O_4$, 215.0537; found, 215.0536.

D-fructose[5]

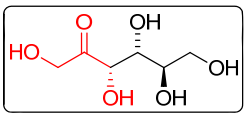

See reference 5.

3

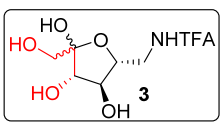

^{1}H NMR (400 MHz, D_2O) δ: 4.12-4.07 (m, 2H), 3.97-3.91 (m, 1H), 3.66-3.61 (m, 2H), 3.59-3.52 (m, 2H); ^{13}C NMR (100 MHz, D_2O) δ: 158.2 (q, *J* = 37.2

Hz), 114.8 (q, J = 284.1 Hz), 100.7, 77.0, 74.7, 74.1, 61.4, 41.0; ^{19}F NMR (376 MHz, CD_3OD) δ: -75.8 (s, 3F); HRMS (ESI): $[M-H]^-$ calcd. for $C_8H_{11}NO_6F_3$, 274.0540; found, 274.0538.

4

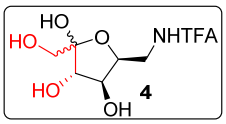

^{1}H NMR (400 MHz, D_2O) δ: 4.38-4.21 (m, 2H), 4.09-3.99 (m, 1H), 3.55-3.44 (m, 3H), 3.43-3.36 (m, 1H); ^{13}C NMR (100 MHz, D_2O) δ: 158.1 (q, J = 37.2 Hz), 114.9 (q, J = 284.1 Hz), 101.0, 74.6, 74.4, 74.0, 61.7, 39.1; ^{19}F NMR (376 MHz, CD_3OD) δ: -75.8 (s, 3F) ; HRMS (ESI): $[M-H]^-$ calcd for $C_8H_{11}NO_6F_3$, 274.0540; found, 274.0538.

D-fagomine

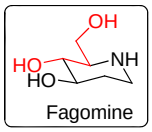

$[\alpha]_D^{25}$ = + 18.6 (c = 0.5 in H2O); 1H NMR (400 MHz, CD3OD) δ: 3.86 (dd, J = 11.0, 3.0 Hz, 1H), 3.60 (dd, J = 11.0, 6.6 Hz, 1H), 3.40 (ddd, J = 11.2, 8.6, 5.0 Hz, 1H), 3.10 (t, J = 9.2 Hz, 1H), 3.01 (ddd, J = 12.8, 4.4, 2.4 Hz, 1H), 2.62 (td, J = 12.8, 2.8 Hz, 1H), 2.47-2.42 (m, 1H), 1.96-1.89 (m, 1H), 1.52-1.42 (m, 1H); ^{13}C NMR (100 MHz, CD_3OD) δ: 75.1, 74.9, 63.2, 63.1, 44.5, 34.6; HRMS (ESI): $[M+H]^+$ calcd. for $C_6H_{14}NO_3$, 148.0968; found, 148.0967.

1-Deoxynojirimycin (DNJ)

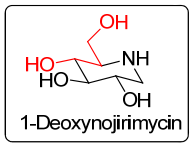

$[\alpha]_D^{25}$ = + 35.7 (c = 0.3 in H_2O); ^{1}H NMR (400 MHz, D_2O) δ: 3.85 (dd, J = 11.6, 3.0 Hz, 1H), 3.68 (dd, J = 11.6, 6.0 Hz, 1H), 3.44 (ddd, J = 10.8, 9.2, 5.2 Hz, 1H), 3.27 (t, J = 9.0 Hz, 1H), 3.18 (t, J = 9.4 Hz, 1H), 3.07 (dd, J = 12.2, 4.8 Hz, 1H), 2.68 (ddd, J = 9.6, 6.4, 2.8 Hz, 1H), 2.40 (t, J = 11.6 Hz, 1H),; ^{13}C NMR (100 MHz, D_2O) δ: 81.2, 74.1, 73.5, 64.0, 63.5, 51.4; HRMS (ESI): $[M+H]^+$ calcd. for $C_6H_{14}NO_4$, 164.0917; found, 164.0922.

1-Deoxymannojirimycin (DMJ)

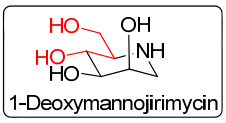

$[\alpha]_D^{25}$ = - 38.2 (c = 0.4 in H_2O); ^1H NMR (400 MHz, D_2O) δ: 3.96 (d, *J* = 1.5 Hz, 1H), 3.73 (d, *J* = 4.0 Hz, 2H), 3.56 (dd, *J* = 19.2, 9.5 Hz, 1H), 3.52 (dd, *J* = 9.5, 2.9 Hz, 1H), 2.97 (dd, *J* = 14.4, 2.7 Hz, 1H), 2.73 (dd, *J* = 14.0, 1.2 Hz, 1H), 2.45 (dt, *J* = 9.6, 4.0 Hz, 1H); ^{13}C NMR (100 MHz, D_2O) δ: 76.6, 71.2, 70.4, 62.8, 62.6, 50.3; HRMS (ESI): $[M+H]^+$ calcd. for $C_6H_{14}NO_4$, 164.0917; found, 164.0922.

(3*R*, 4*R*)-6-trifluoroacetamido-1,3,4-trihydroxyhexan-2-one

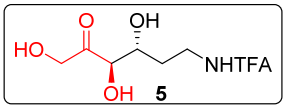

^1H NMR (400 MHz, CD_3OD) δ: 4.54 (d, *J* = 19.6 Hz, 1H), 4.44 (d, *J* = 19.2 Hz, 1H), 4.15 (d, *J* = 1.2 Hz, 1H), 3.97 (t, *J* = 5.6 Hz, 1H), 3.45-3.38 (m, 2H), 1.88-1.78 (m, 2H),; ^{13}C NMR (100 MHz, CD_3OD) δ: 213.3, 159.0 (q, *J* = 36.5 Hz), 117.5 (q, *J* = 284.7 Hz), 79.4, 71.1, 67.9, 37.9, 33.3; ^{19}F NMR (376 MHz, CD_3OD) δ: -77.4 (s, 3F); HRMS (ESI): $[M-H]^-$ calcd. for $C_8H_{11}F_3NO_5$, 258.0595; found, 258.0592.

(3*R*, 4*S*)-6-trifluoroacetamido-1,3,4-trihydroxyhexan-2-one

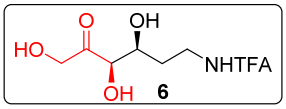

^1H NMR (400 MHz, CD_3OD) δ: 4.51 (d, *J* = 19.2 Hz, 1H), 4.41 (d, *J* = 19.6 Hz, 1H), 4.12 (s, 1H), 3.94 (t, *J* = 5.6 Hz, 1H), 3.41-3.36 (m, 2H), 1.84-1.74 (m, 2H); ^{13}C NMR (100 MHz, CD_3OD) δ: 213.3, 159.0 (q, *J* = 36.5 Hz), 117.5 (q, *J* = 284.7 Hz), 79.3, 71.1, 67.8, 37.9, 33.3; ^{19}F NMR (376 MHz, CD_3OD) δ: -77.4 (s, 3F); HRMS (ESI): $[M-H]^-$ calcd. for $C_8H_{11}F_3NO_5$, 258.0595; found, 258.0592.

D-psicose[6, 7]

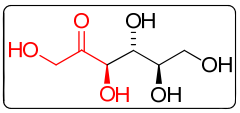

See references 6 and 7.

D-sorbose

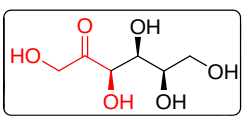

See references 6 and 7.

[1, 2, 3-$^{13}C_3$] (3*S*,4*R*)-6-trifluoroacetamido-1,3,4-trihydroxyhexan-2-one

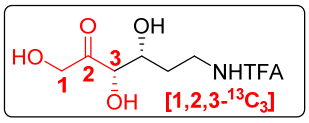

^{1}H NMR (400 MHz, CD_3OD) δ: 4.75-4.60 (m, 1H), 4.38-4.24 (m, 1.5H), 4.00-3.95 (m, 1.5H), 3.46-3.39 (m, 2H), 1.84-1.80 (m, 2H); ^{13}C NMR (100 MHz, CD_3OD) δ: 213.2 (dd, J = 42.7 41.4 Hz), 159.0 (q, J = 36.7 Hz), 117.5 (q, J = 284.8 Hz), 79.3 (dd, J = 43.1, 12.9 Hz), 71.1 (d, J = 39.6 Hz), 67.8 (dd, J = 40.9, 12.9 Hz), 37.9, 33.3; HRMS (ESI): $[M+Na]^+$ calcd. for $C_5{}^{13}C_3H_{12}F_3NO_5$, 285.0660; found, 285.0656.

3.1.12 Reference

1. Tang, R., Ji, W. & Wang, C. Synthesis and characterization of new poly(ortho ester amidine) copolymers for non-viral gene delivery. *Polymer* **52**, 921-932 (2011).

2. Einhorn, J., Einhorn, C., Ratajczak, F. & Pierre, J.-L. Efficient and Highly Selective Oxidation of Primary Alcohols to Aldehydes by N-Chlorosuccinimide Mediated by Oxoammonium Salts. *J. Org. Chem.* **61**, 7452-7454 (1996).

3. Kalisiak, J., Trauger, S.A., Kalisiak, E., Morita, H., Fokin, V.V., Adams, M.W.W., Sharpless, K.B. & Siuzdak, G. Identification of a New Endogenous Metabolite and the Characterization of Its Protein Interactions through an Immobilization Approach. *J. Am. Chem. Soc.* **131**, 378-386 (2009).

4. Concia, A.L., Lozano, C., Castillo, J.A., Parella, T., Joglar, J. & Clapes, P. D-fructose-6-phosphate aldolase in organic synthesis: Cascade chemical-enzymatic preparation of sugar-related polyhydroxylated compounds. *Chem. - Eur. J.* **15**, 3808-3816 (2009).

5. Barclay, T., Ginic-Markovic, M., Johnston, M.R., Cooper, P. & Petrovsky, N. Observation of the keto tautomer of D-fructose in D2O using 1H NMR spectroscopy. *Carbohydr. Res.* **347**, 136-141 (2012).

6. Wilson, J.J. & Lippard, S.J. Synthesis, Characterization, and Cytotoxicity of Platinum(IV) Carbamate Complexes. *Inorg. Chem.* **50**, 3103-3115 (2011).

7. He, W. & Lieberman, M. The synthesis and characterization of a side-by-side iron phthalocyanine dimer. *J. Porphyrins Phthalocyanines* **15**, 277-292 (2011).

3.1.13 NMR spectra

^{1}H-NMR spectrum of 3-trifluoroacetamido propanal in $CDCl_3$.

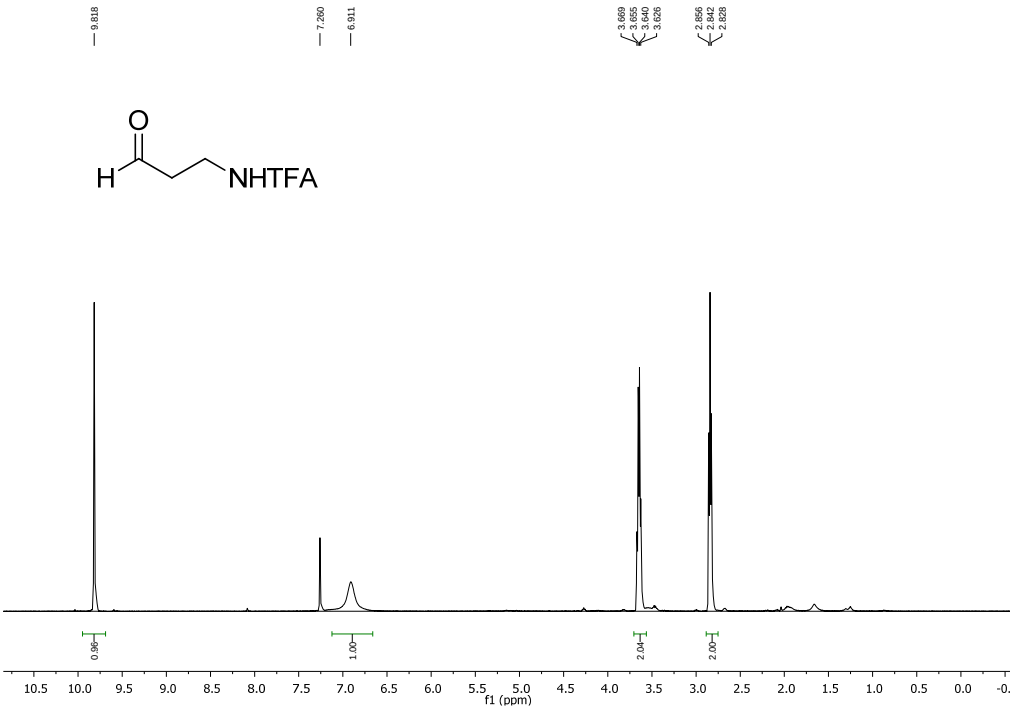

^{13}C-NMR spectrum of 3-trifluoroacetamido propanal in $CDCl_3$.

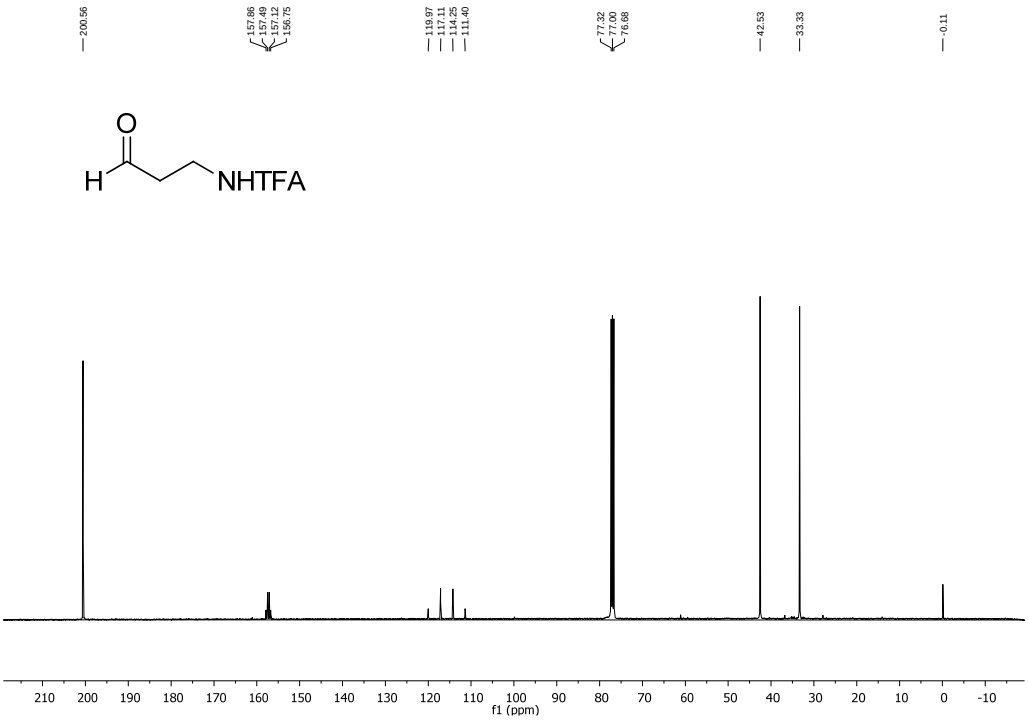

^{19}F-NMR spectrum of 3-trifluoroacetamido propanal in $CDCl_3$.

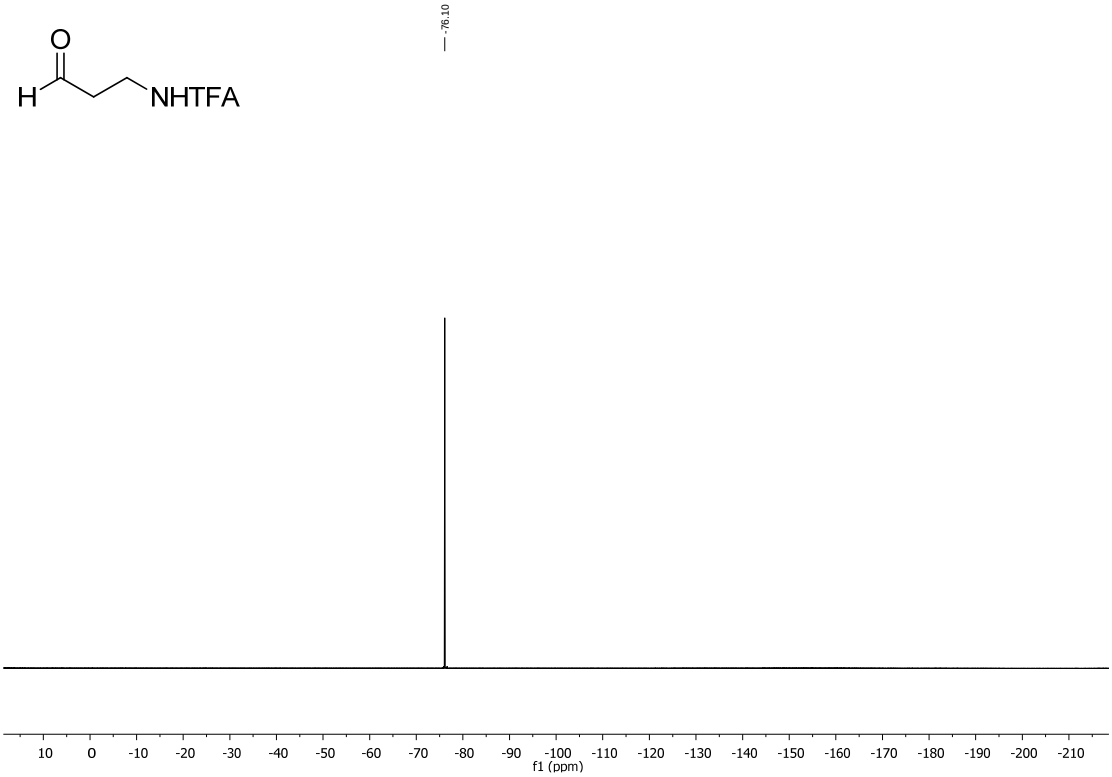

^{1}H-NMR spectrum of 3-trichloroacetamido propanal in $CDCl_3$.

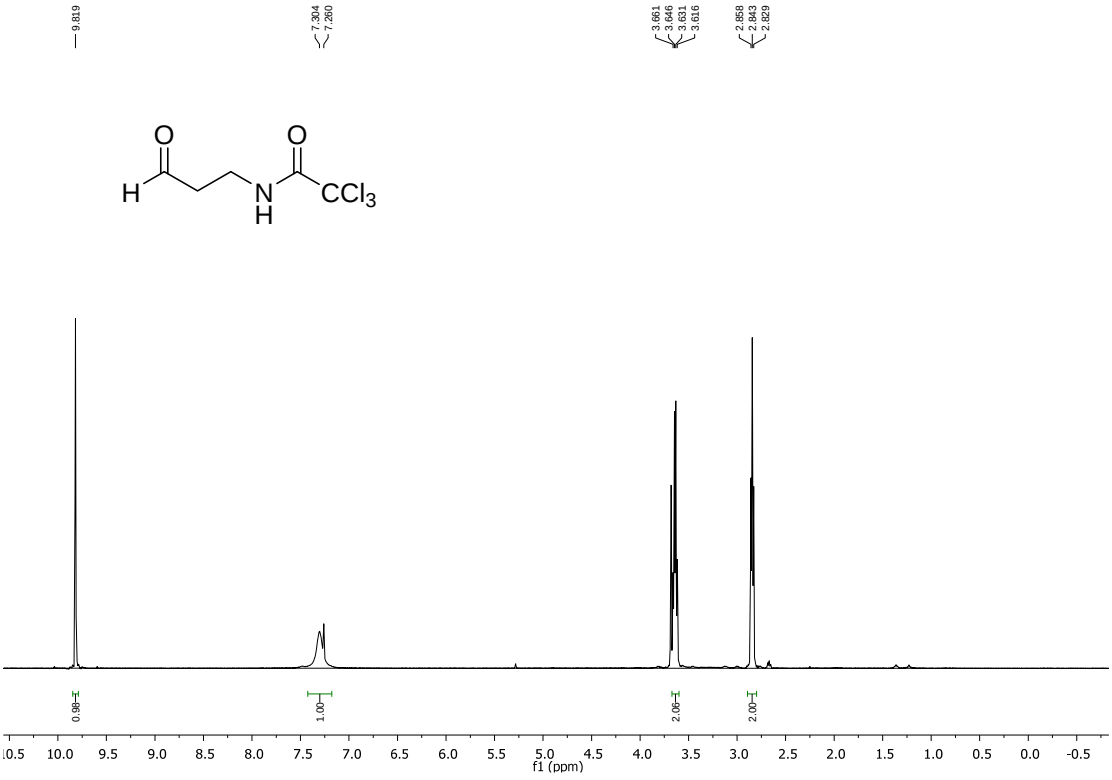

^{13}C-NMR spectrum of 3-trichloroacetamido propanal in $CDCl_3$.

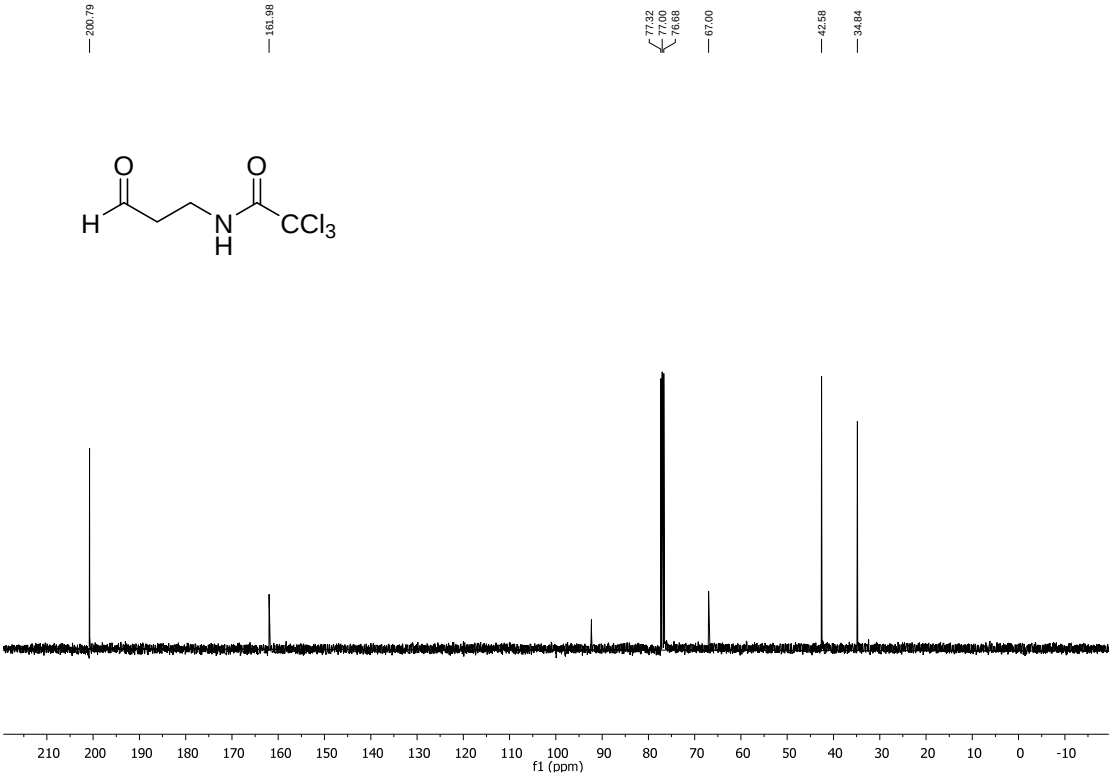

^{1}H-NMR spectrum of 3-difluoroacetamido propanal in $CDCl_3$.

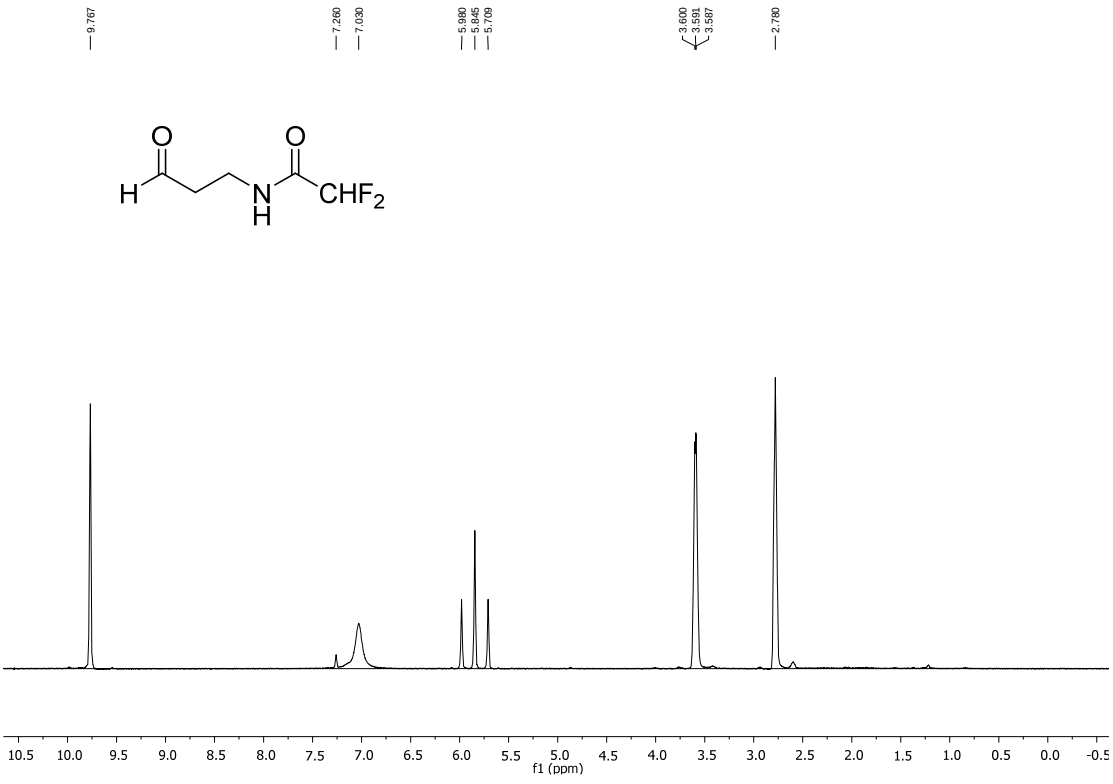

^{13}C-NMR spectrum of 3-difluoroacetamido propanal in $CDCl_3$.

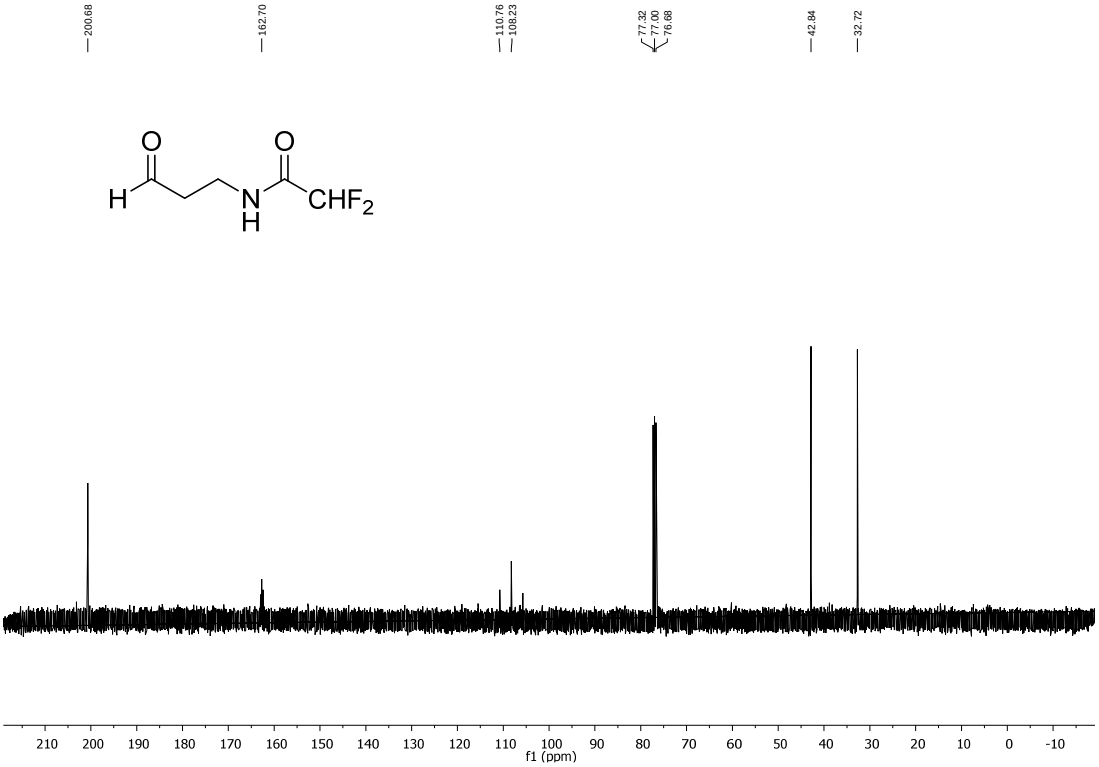

^{1}H-NMR spectrum of (3*S*, 4*R*)-6-trifluoroacetamido-1,3,4-trihydroxyhexan-2-one in CD_3OD.

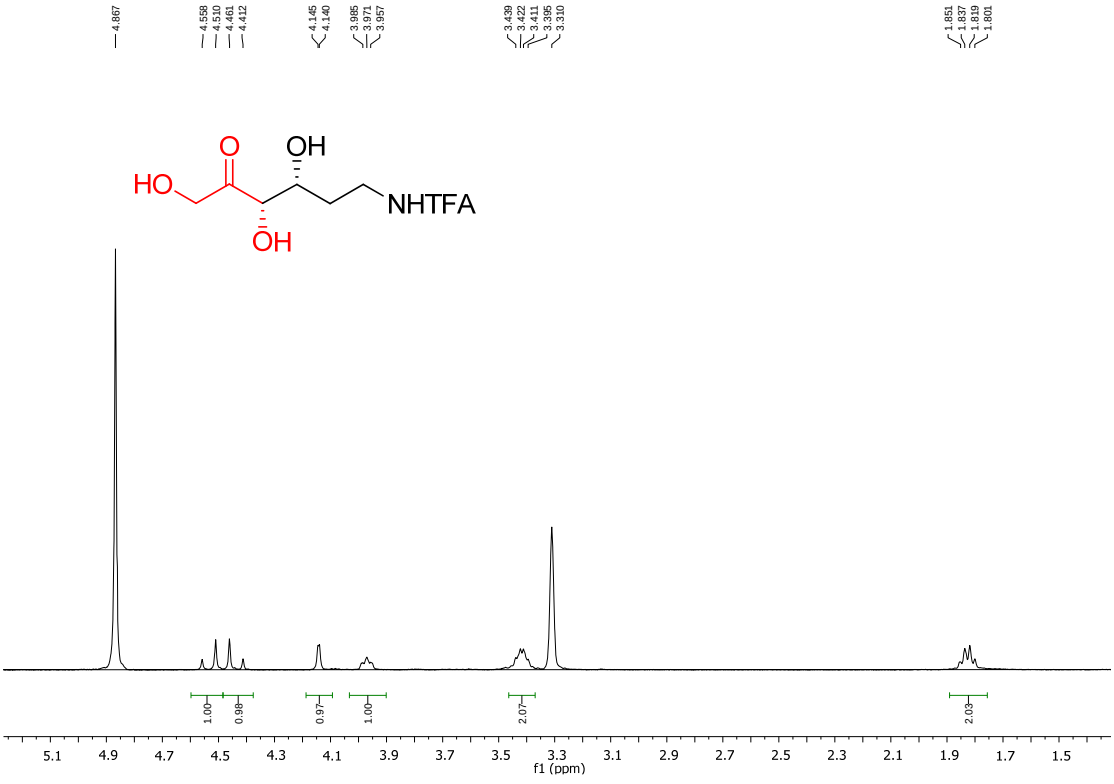

^{13}C-NMR spectrum of (3*S*, 4*R*)-6-trifluoroacetamido-1,3,4-trihydroxyhexan-2-one in CD_3OD.

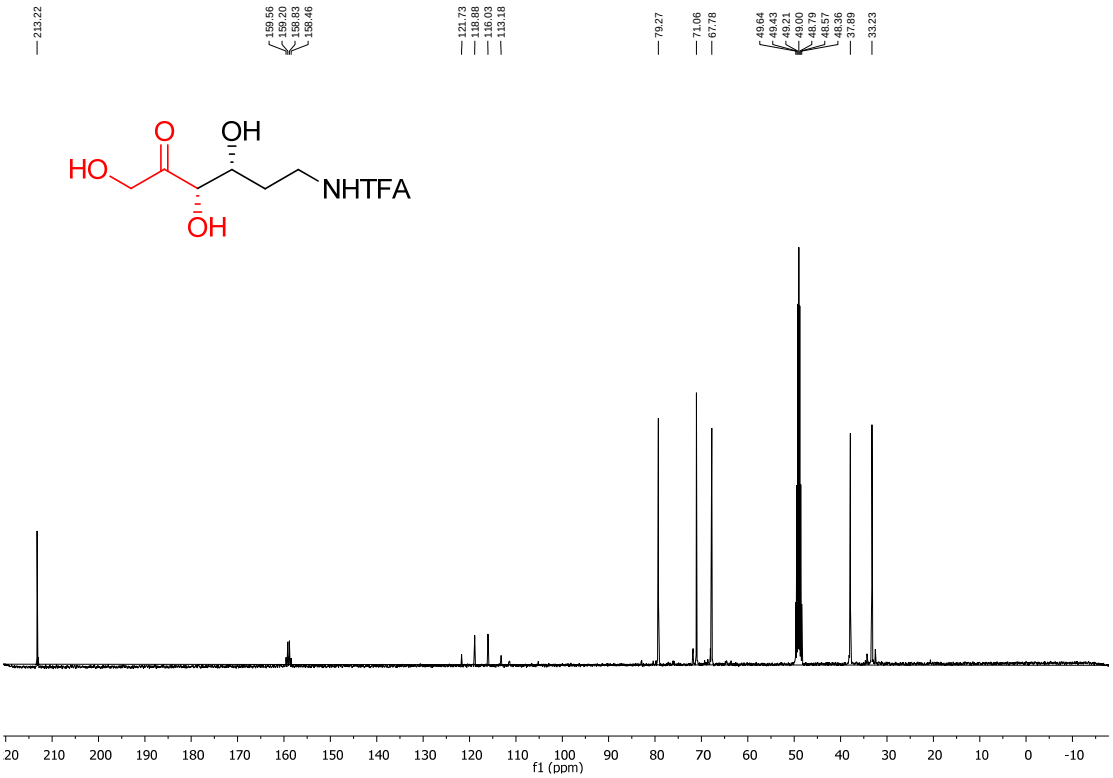

^{19}F-NMR spectrum of (3*S*, 4*R*)-6-trifluoroacetamido-1,3,4-trihydroxyhexan-2-one in CD_3OD.

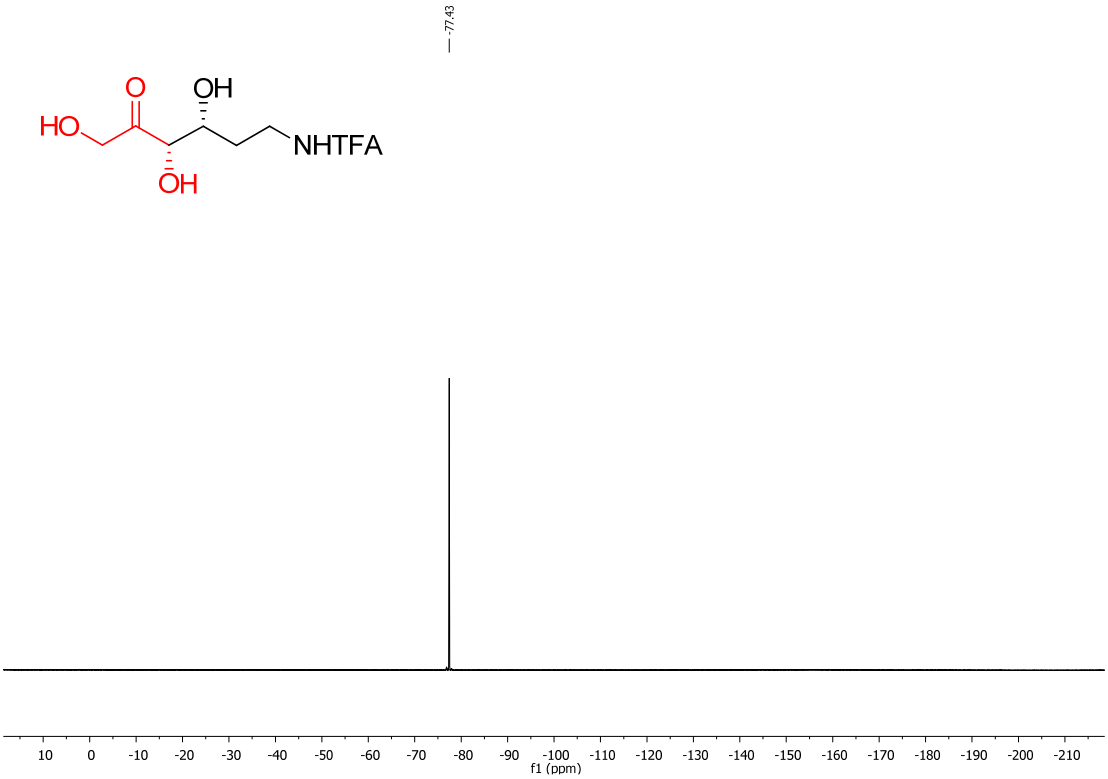

^{1}H-NMR spectrum of (3*S*, 4*R*)-6-trichloroacetamido-1,3,4-trihydroxyhexan-2-one in CD_3OD.

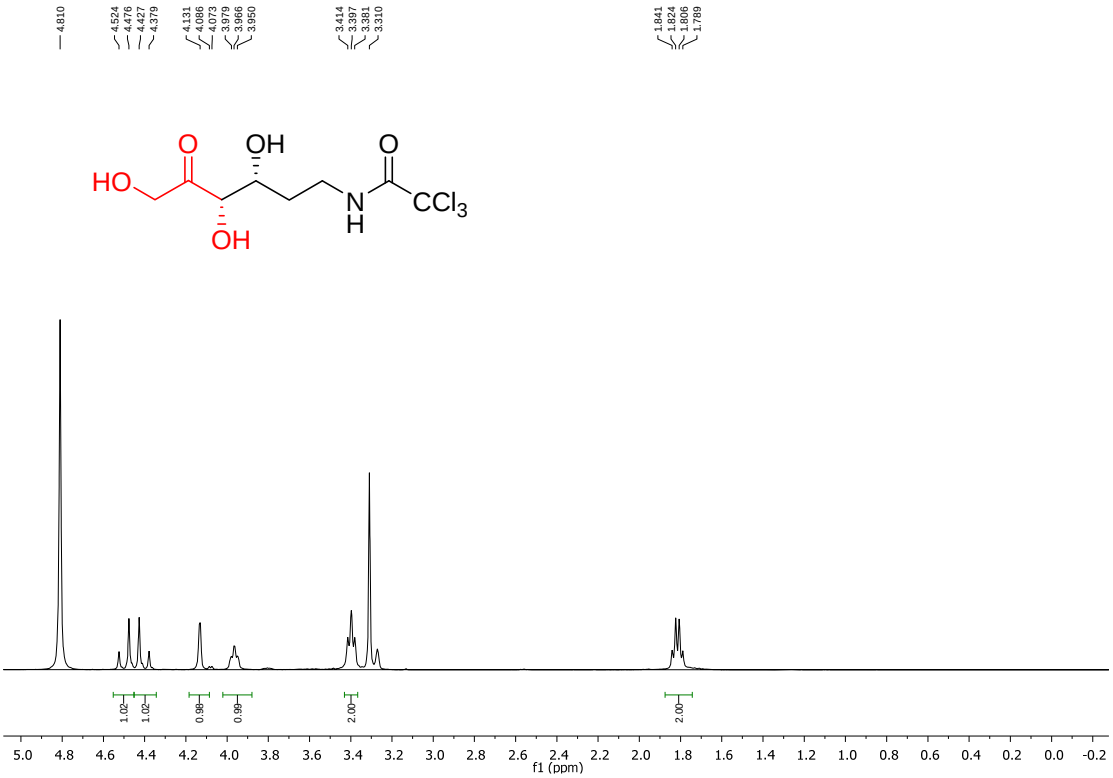

^{13}C-NMR spectrum of (3*S*, 4*R*)-6-trichloroacetamido-1,3,4-trihydroxyhexan-2-one in CD_3OD.

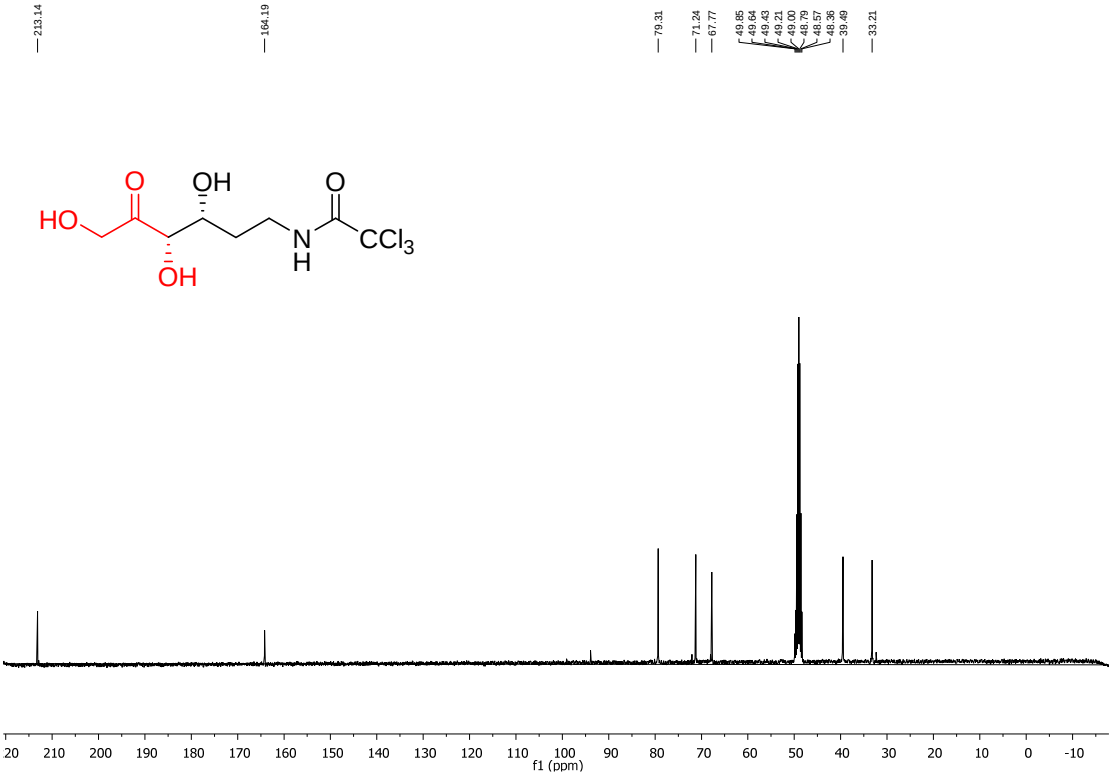

^{1}H-NMR spectrum of (3*S*, 4*R*)-6-difluoroacetamido-1,3,4-trihydroxyhexan-2-one in CD_3OD.

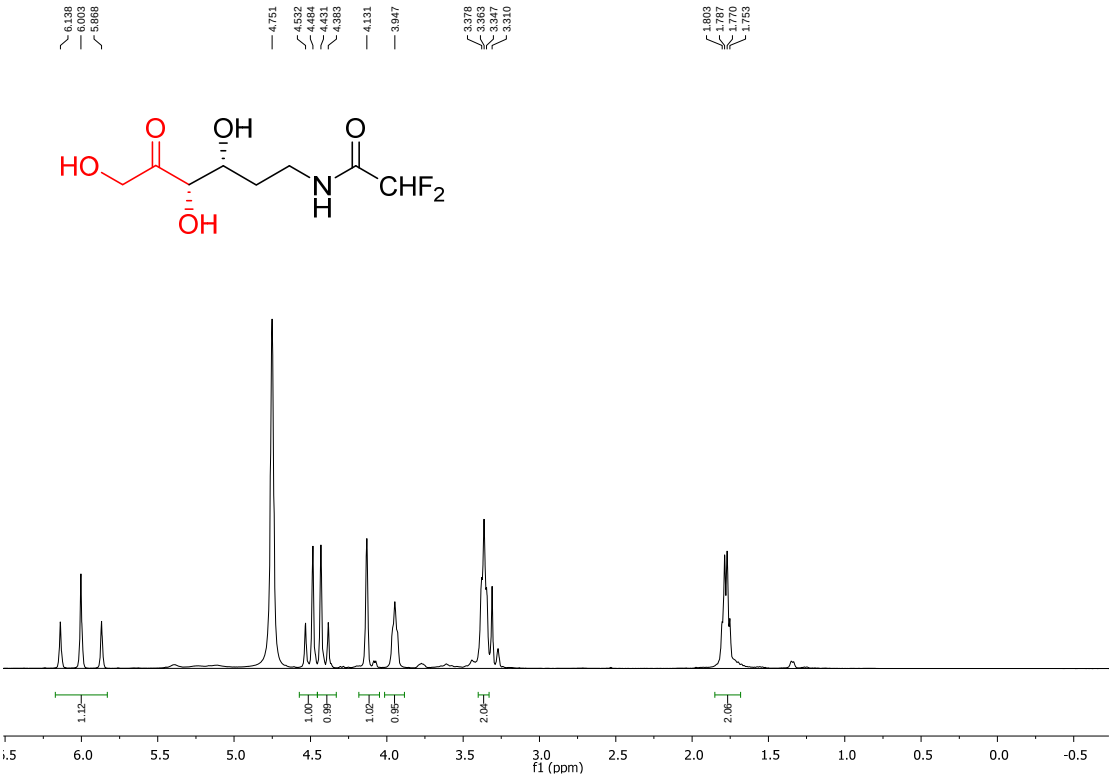

^{13}C-NMR spectrum of (3*S*, 4*R*)-6-difluoroacetamido-1,3,4-trihydroxyhexan-2-one in CD_3OD.

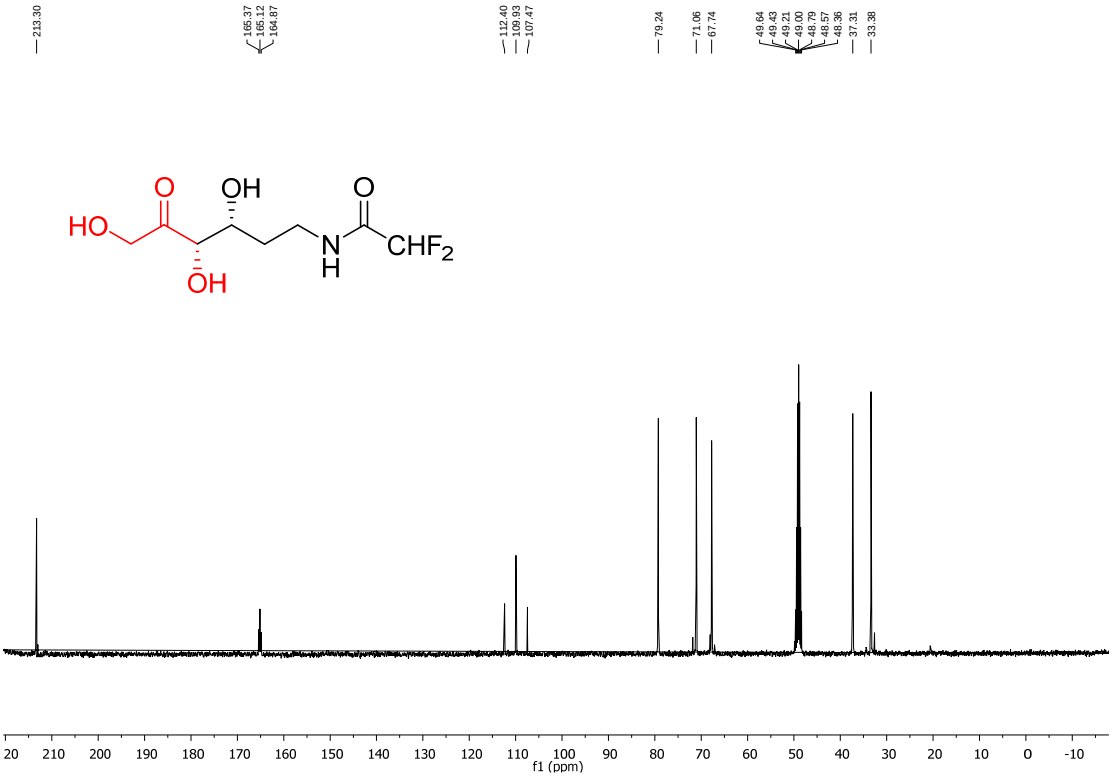

^{1}H-NMR spectrum of (3*S*, 4*R*)-1,3,4-trihydroxy-6-(methylthio)hexan-2-one in CD_3OD.

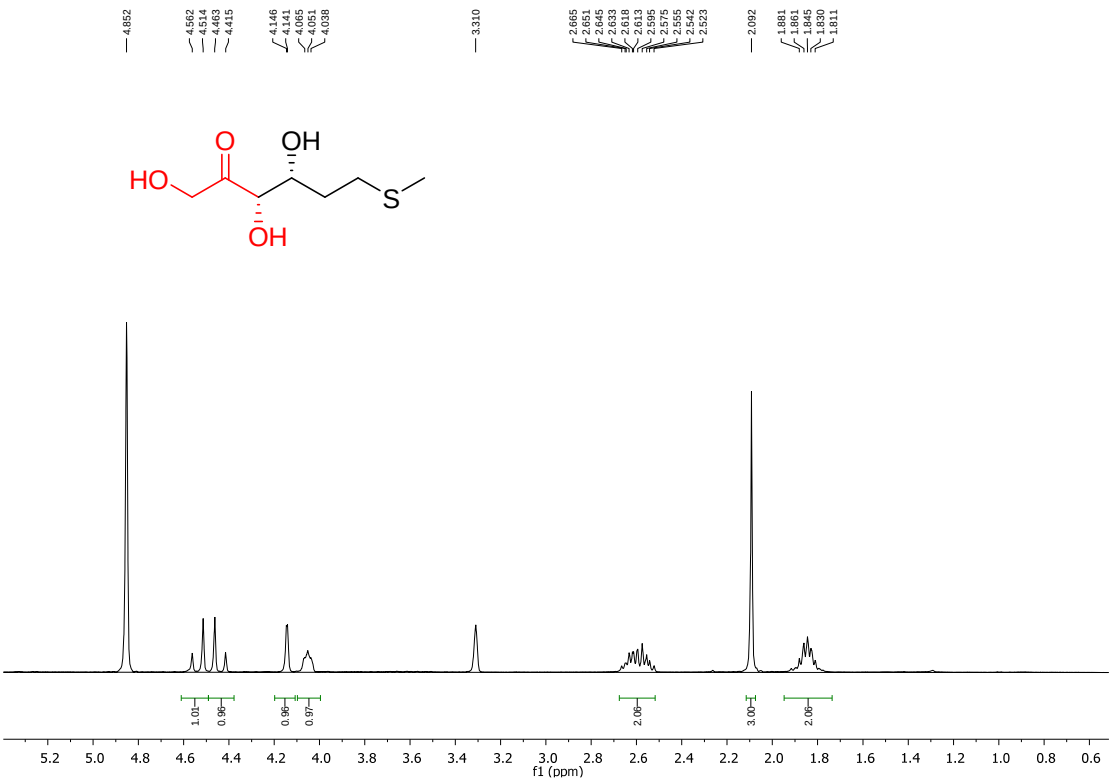

^{13}C-NMR spectrum of (3*S*, 4*R*)-1,3,4-trihydroxy-6-(methylthio)hexan-2-one in CD_3OD.

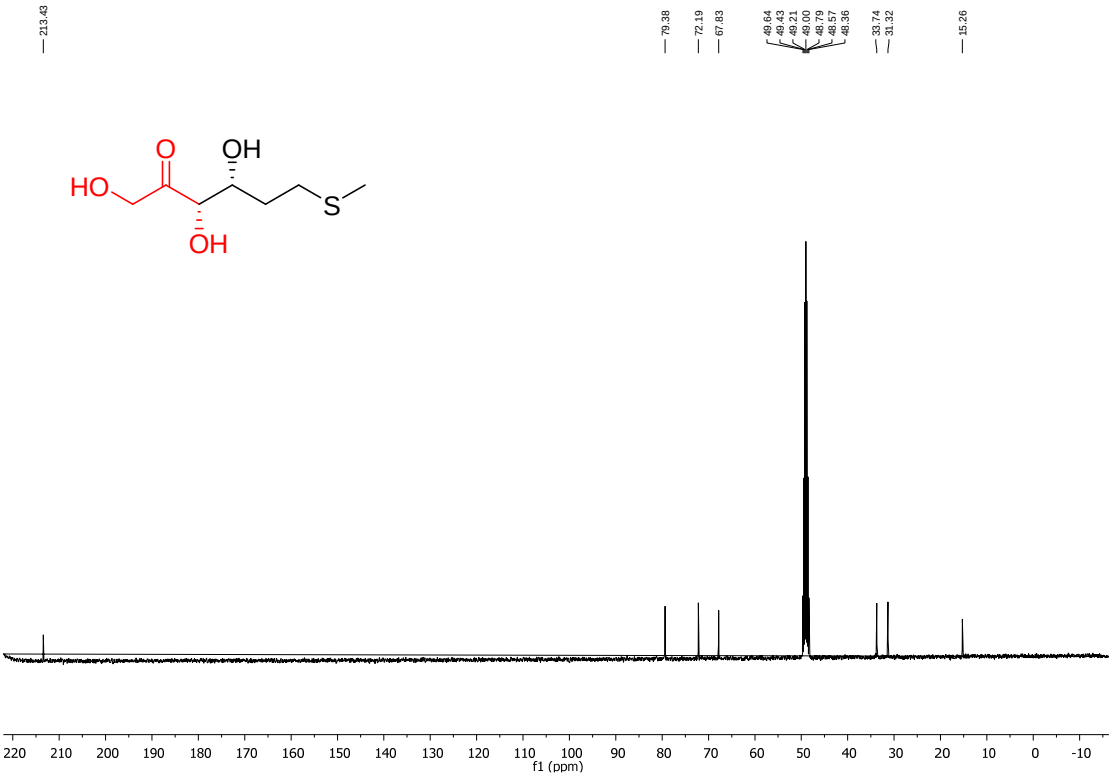

^{1}H-NMR spectrum of (3*S*, 4*R*)-7,7,7-trifluoro-1,3,4-trihydroxyheptan-2-one in CD_3OD

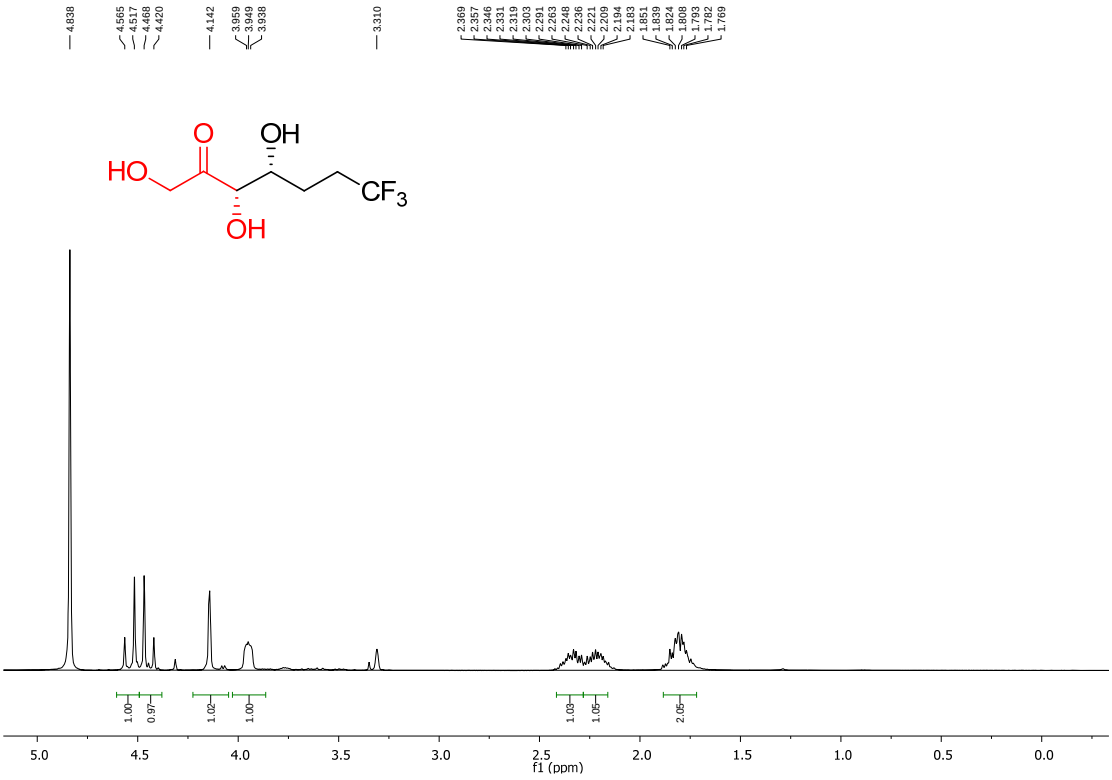

^{13}C-NMR spectrum of (3*S*, 4*R*)-7,7,7-trifluoro-1,3,4-trihydroxyheptan-2-one in CD_3OD

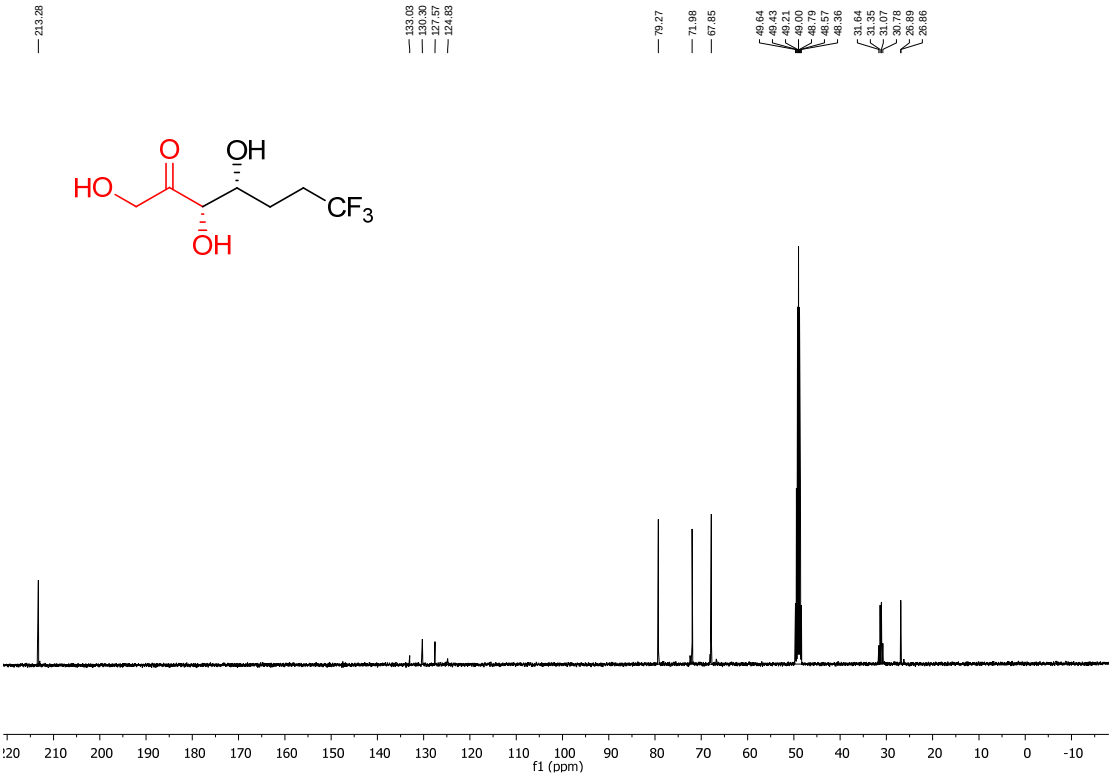

^{13}C-NMR spectrum of (3*S*, 4*R*)-7,7,7-trifluoro-1,3,4-trihydroxyheptan-2-one in CD_3OD.

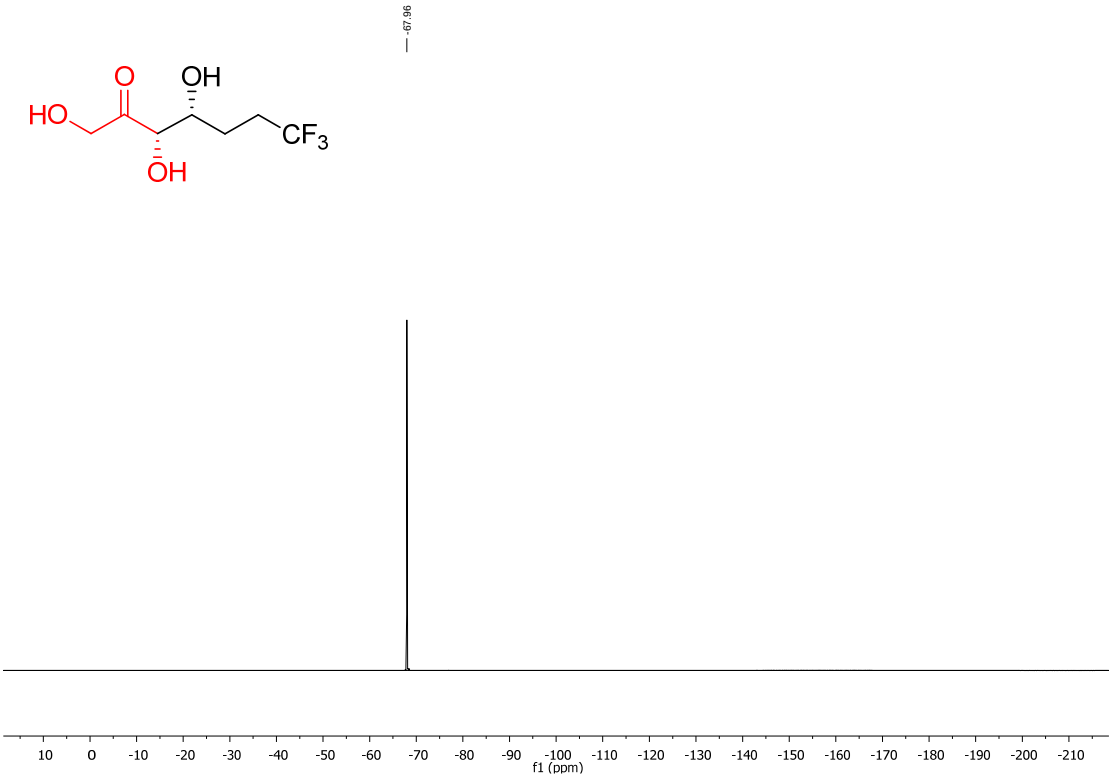

^{1}H-NMR spectrum of D-fructose standard in D_2O

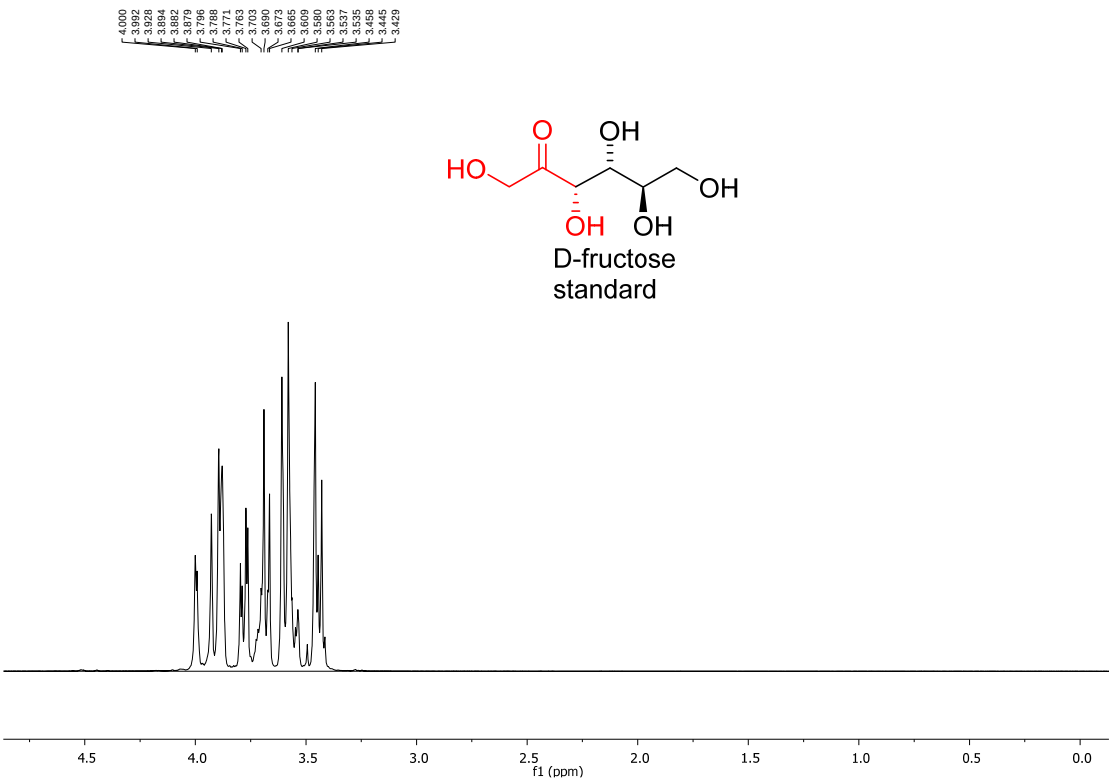

^{1}H-NMR spectrum of D-fructose from fermentation in D_2O

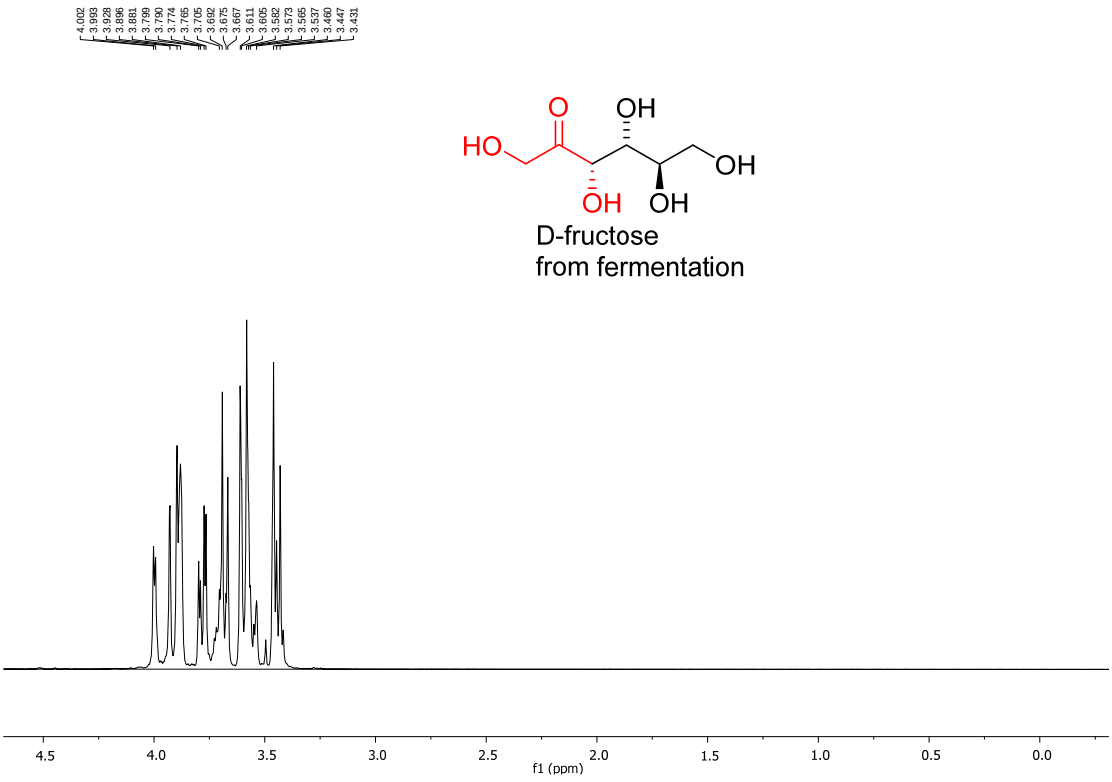

^{1}H-NMR spectrum of **3** in D_2O

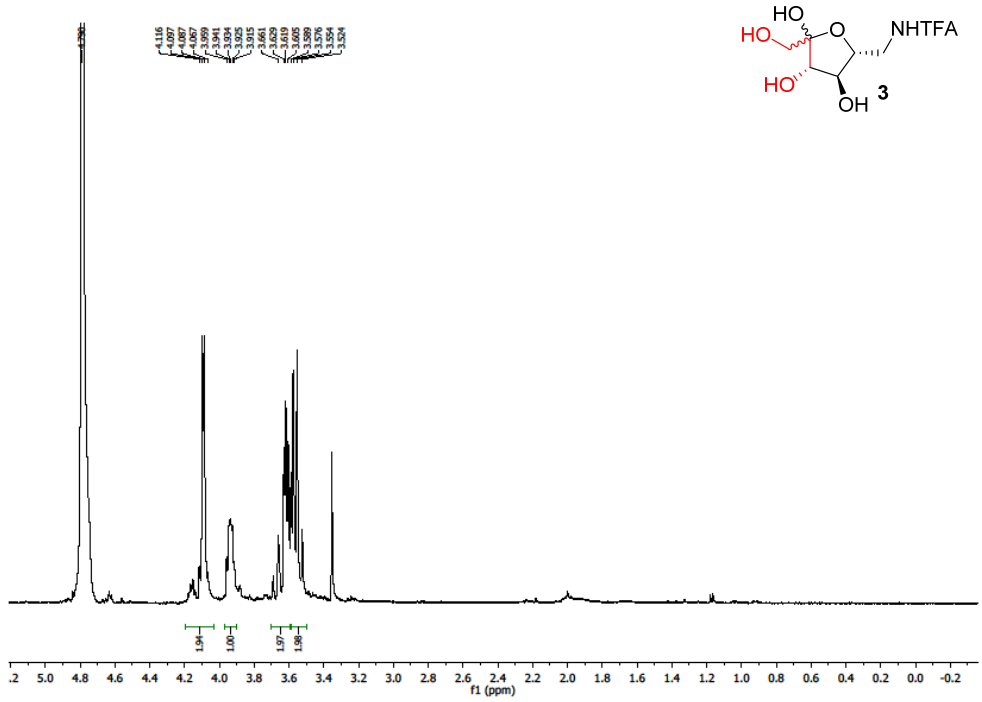

^{13}C-NMR spectrum of **3** in D_2O

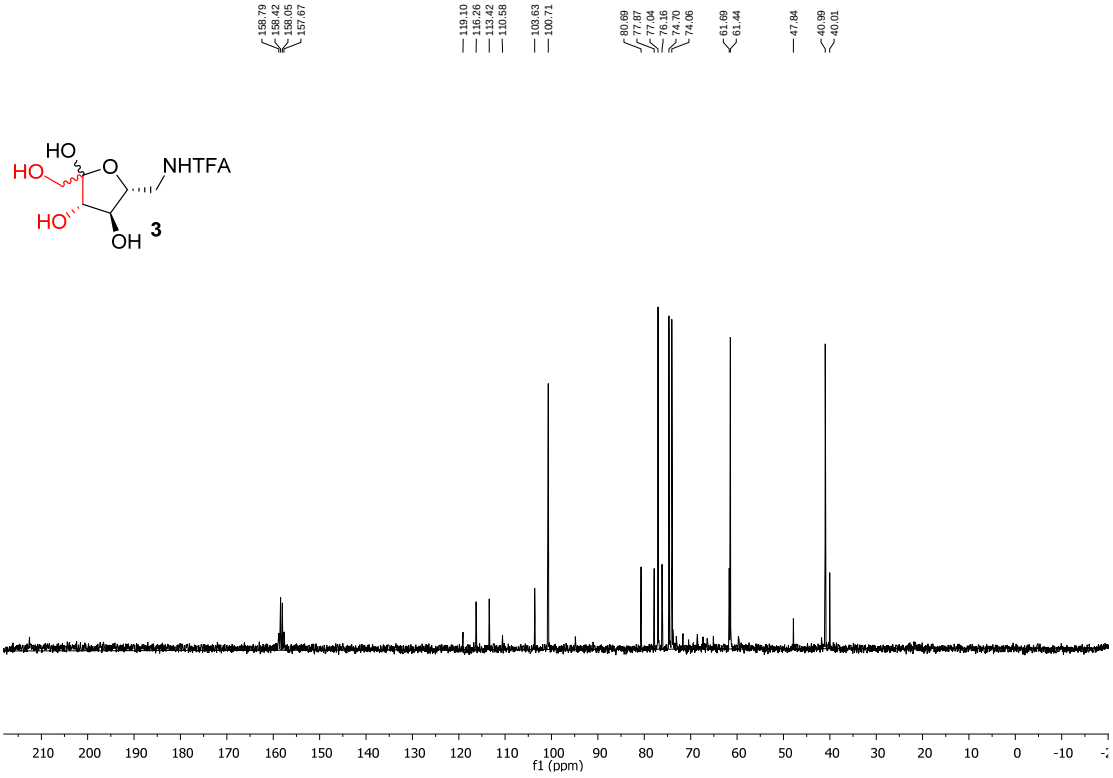

^{19}F-NMR spectrum of **3** in D_2O

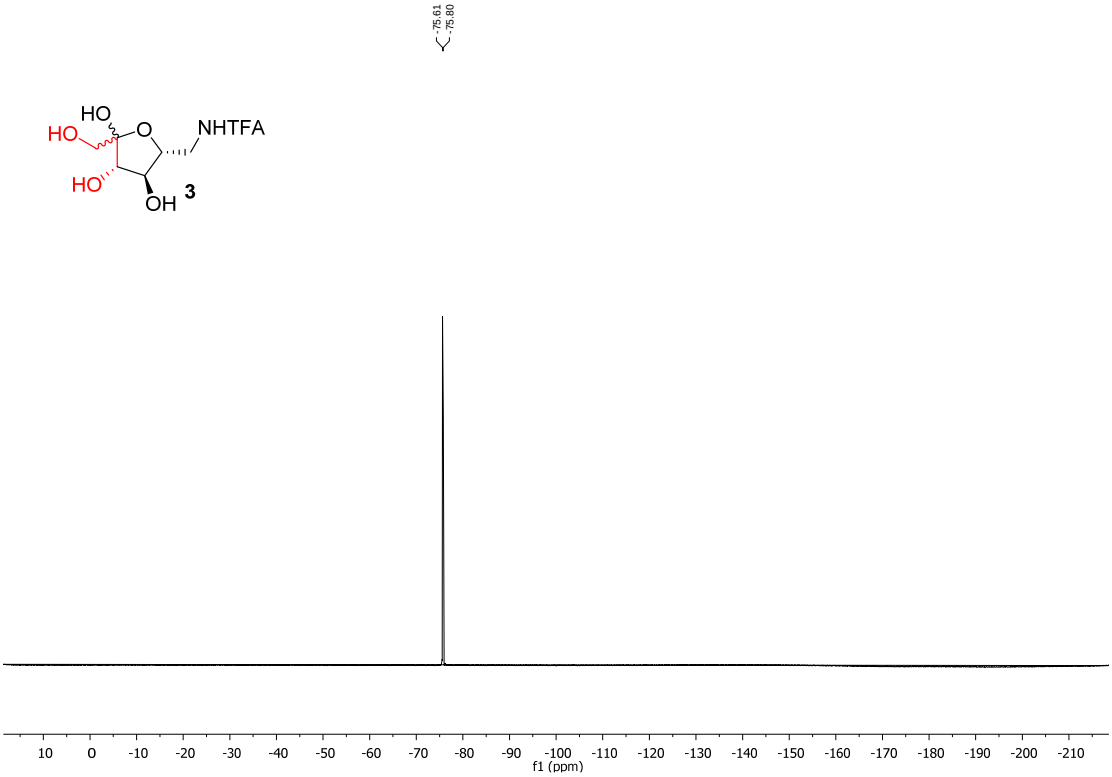

^{1}H-NMR spectrum of **4** in D_2O

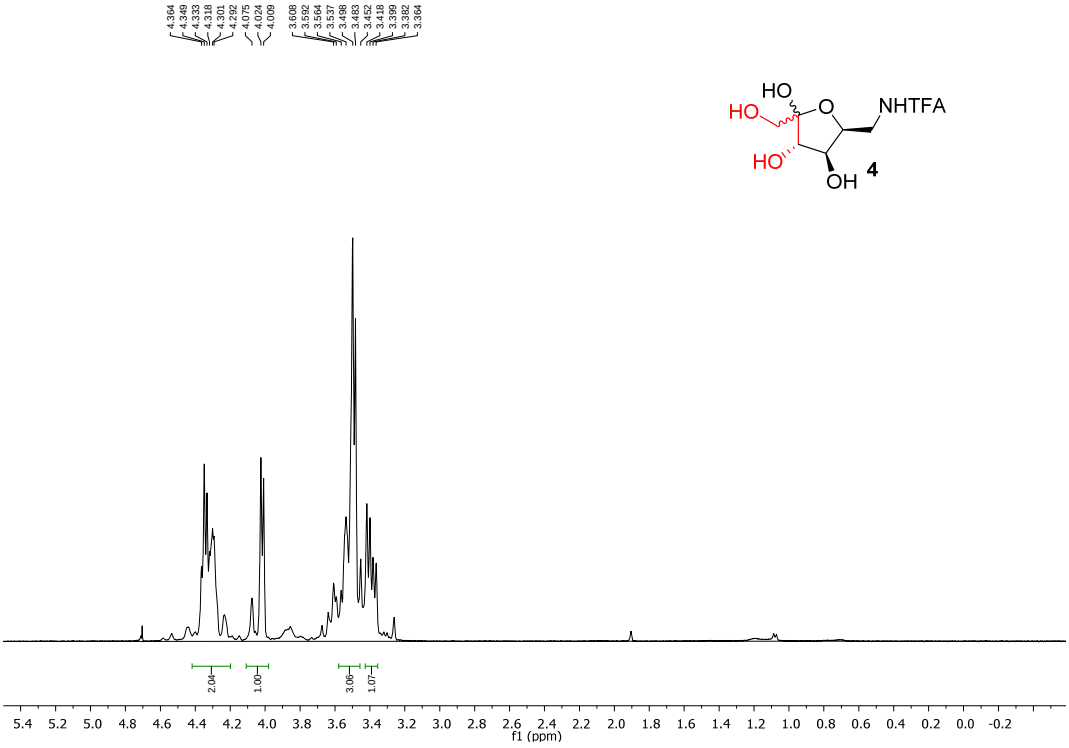

^{13}C-NMR spectrum of **4** in D_2O

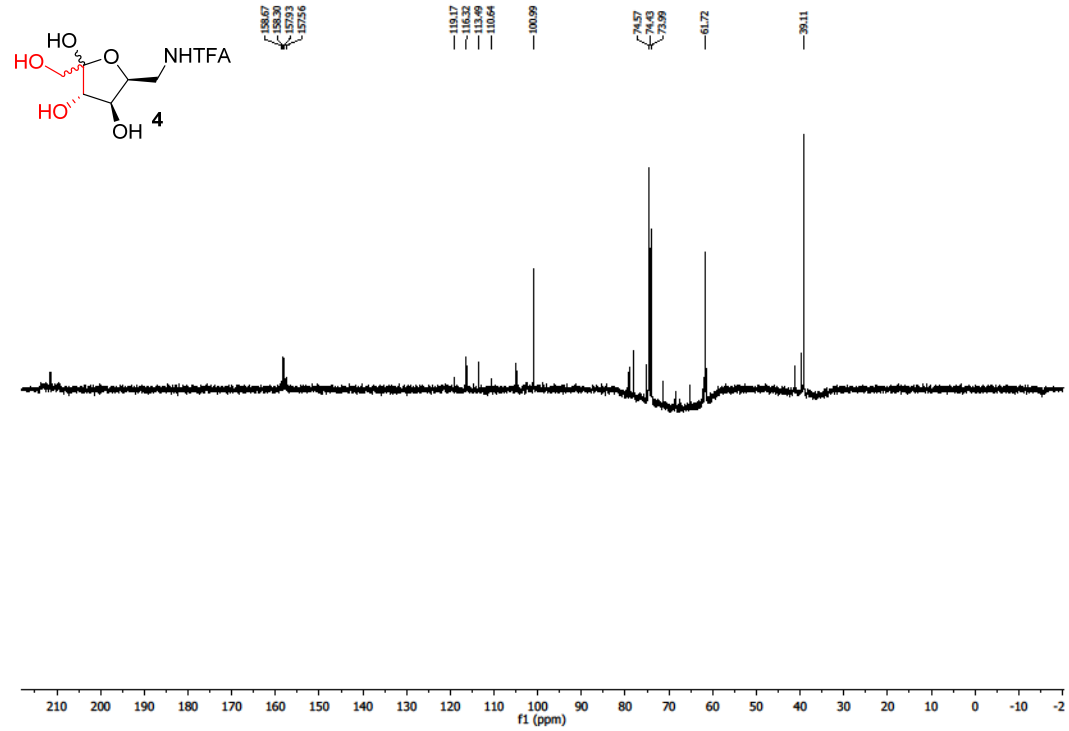

^{19}F-NMR spectrum of **4** in D_2O

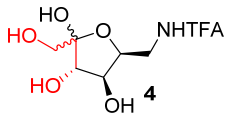

4

^{1}H-NMR spectrum of D-fagomine in CD_3OD.

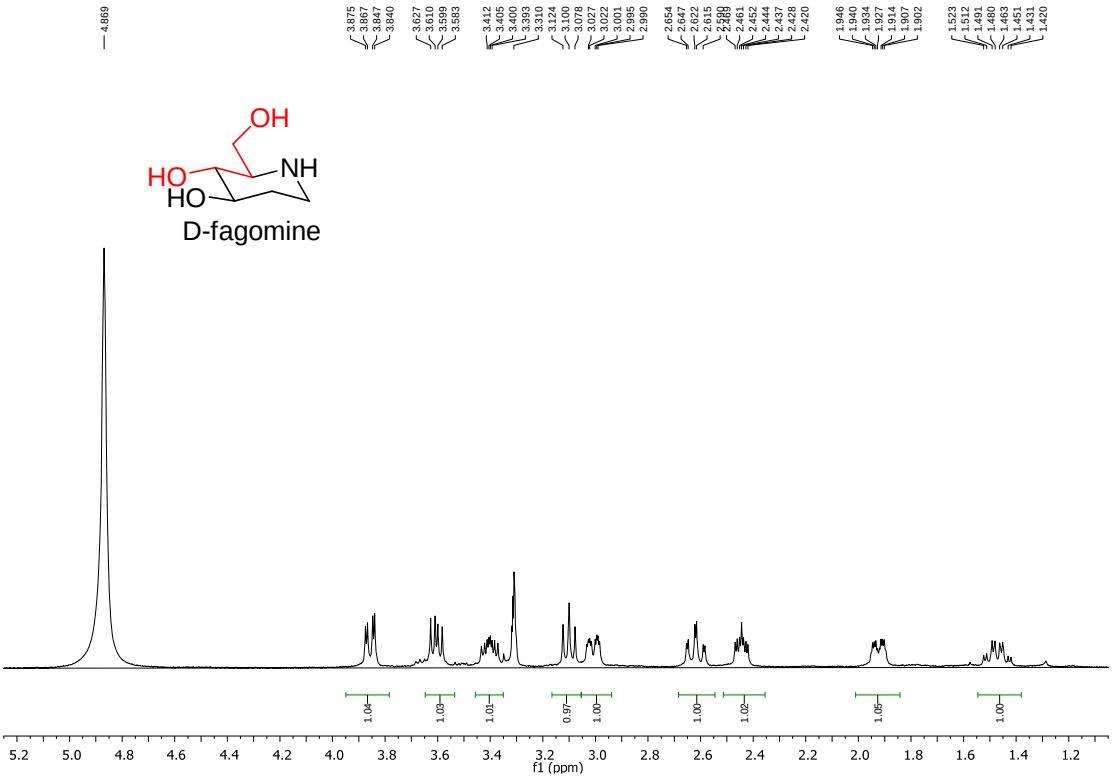

^{13}C-NMR spectrum of D-fagomine in CD_3OD.

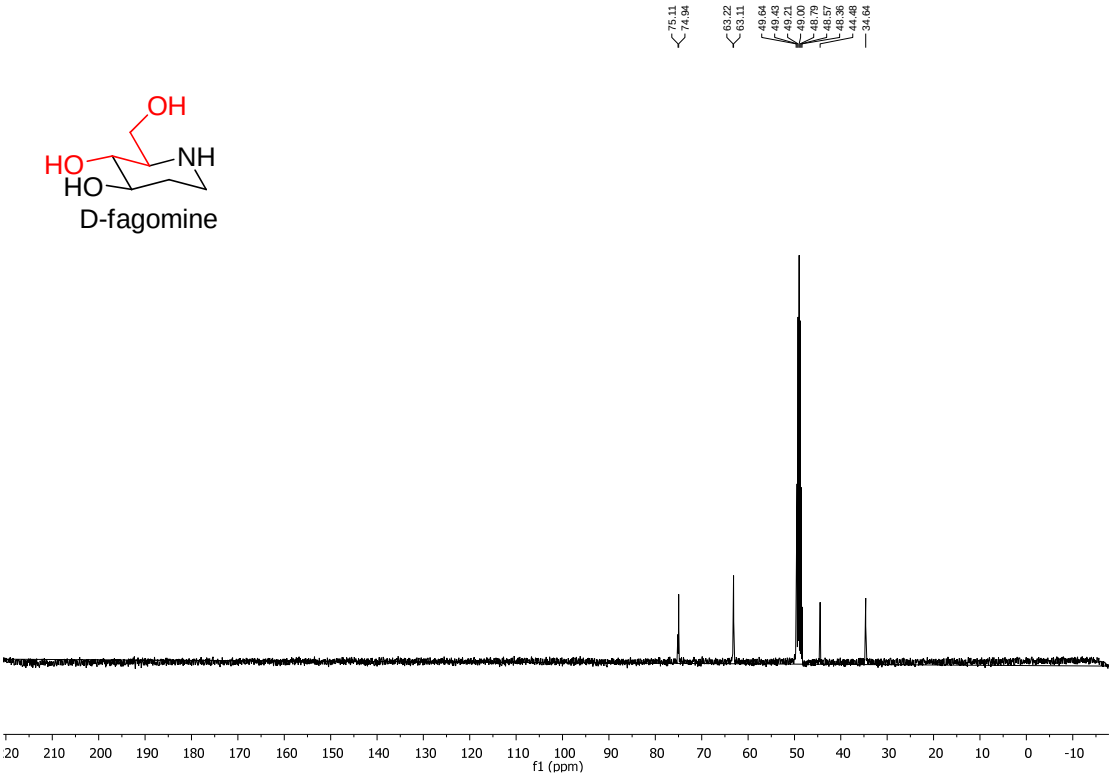

^{1}H-NMR spectrum of 1-Deoxynojirimycin in D_2O

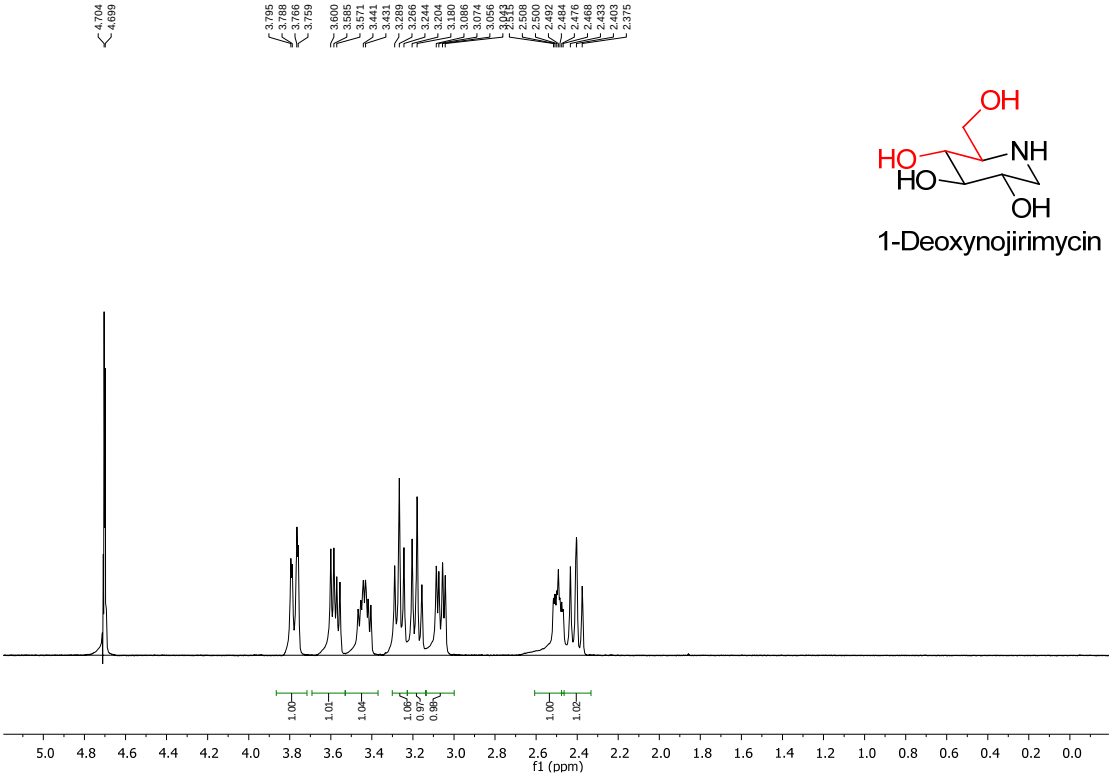

^{13}C-NMR spectrum of 1-Deoxynojirimycin in D_2O

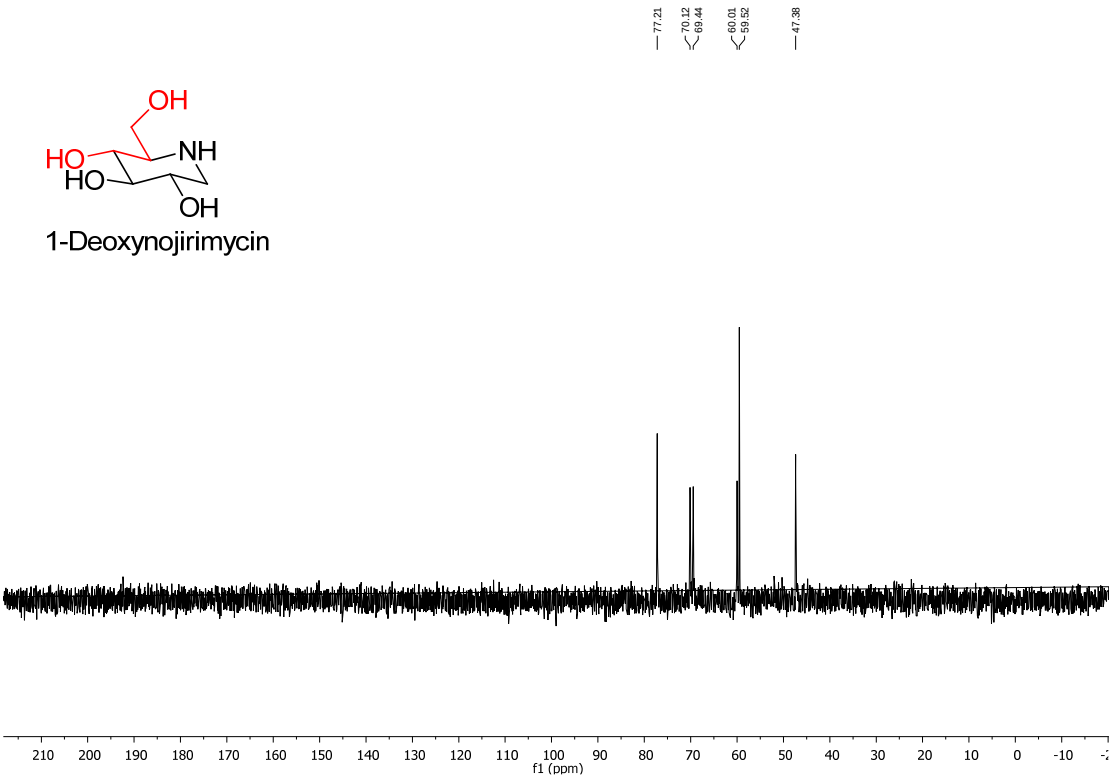

^{1}H-NMR spectrum of 1-Deoxymannojirimycin in D_2O

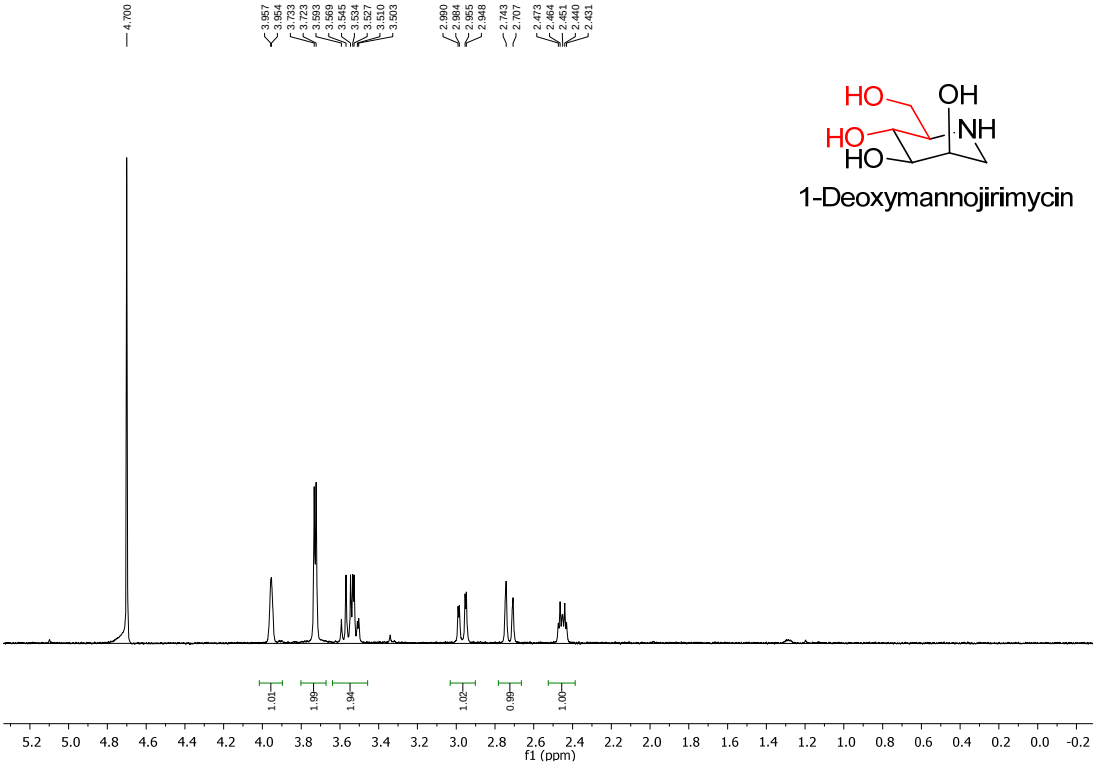

^{13}C-NMR spectrum of 1-Deoxymannojirimycin in D_2O

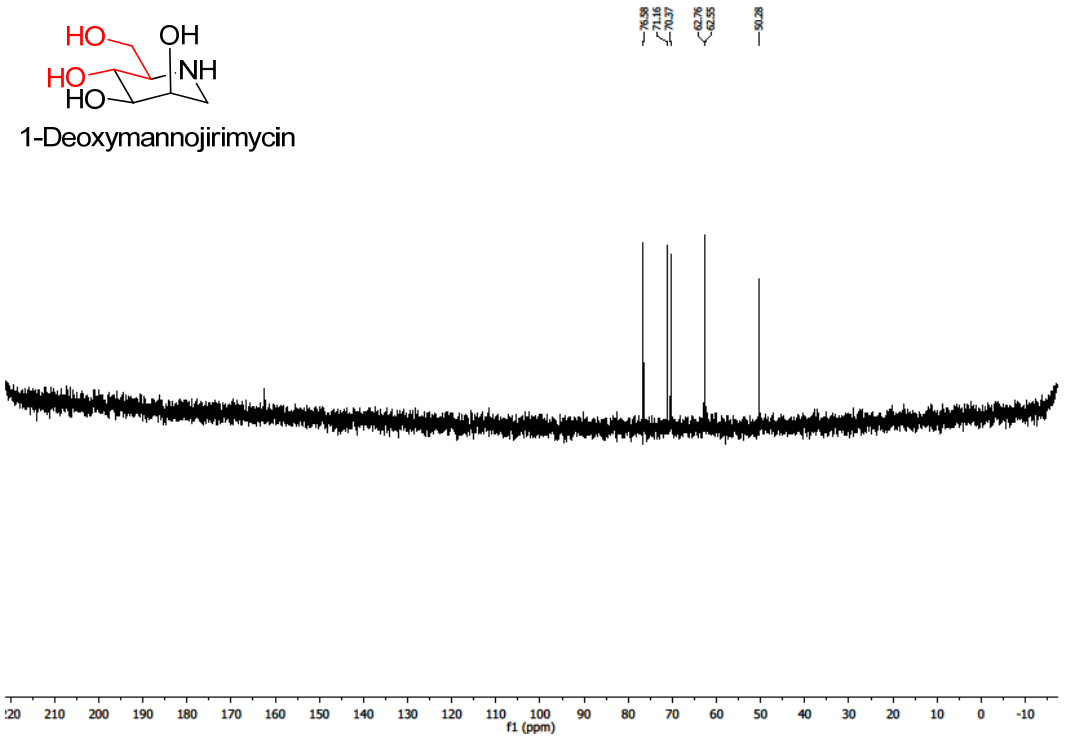

^{1}H-NMR spectrum of (3*R*, 4*R*)-6-trifluoroacetamido-1,3,4-trihydroxyhexan-2-one in CD_3OD.

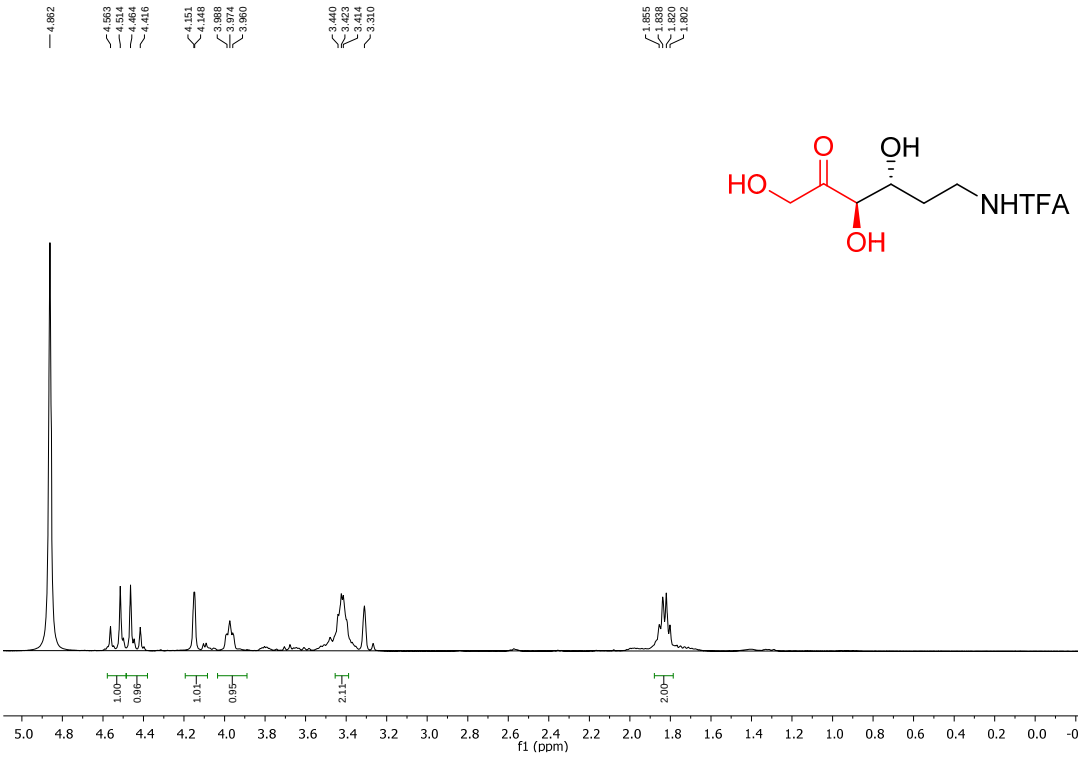

^{13}C-NMR spectrum of (3*R*, 4*R*)-6-trifluoroacetamido-1,3,4-trihydroxyhexan-2-one in CD_3OD.

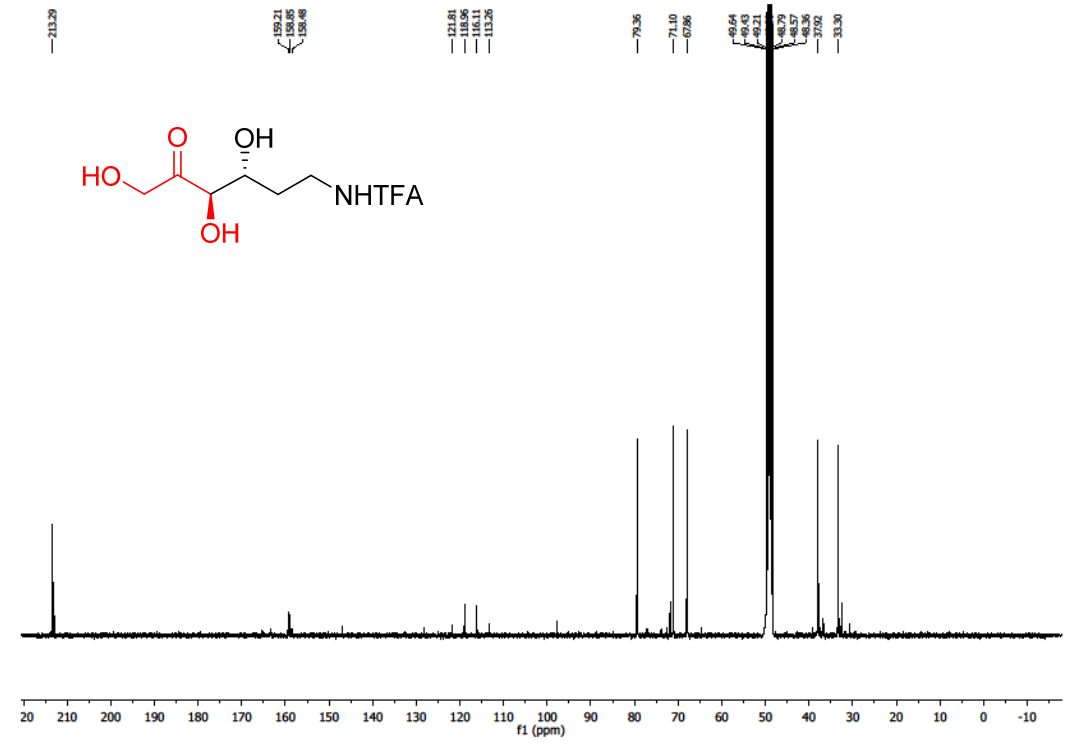

^{19}F-NMR spectrum of (3*R*, 4*R*)-6-trifluoroacetamido-1,3,4-trihydroxyhexan-2-one in CD_3OD.

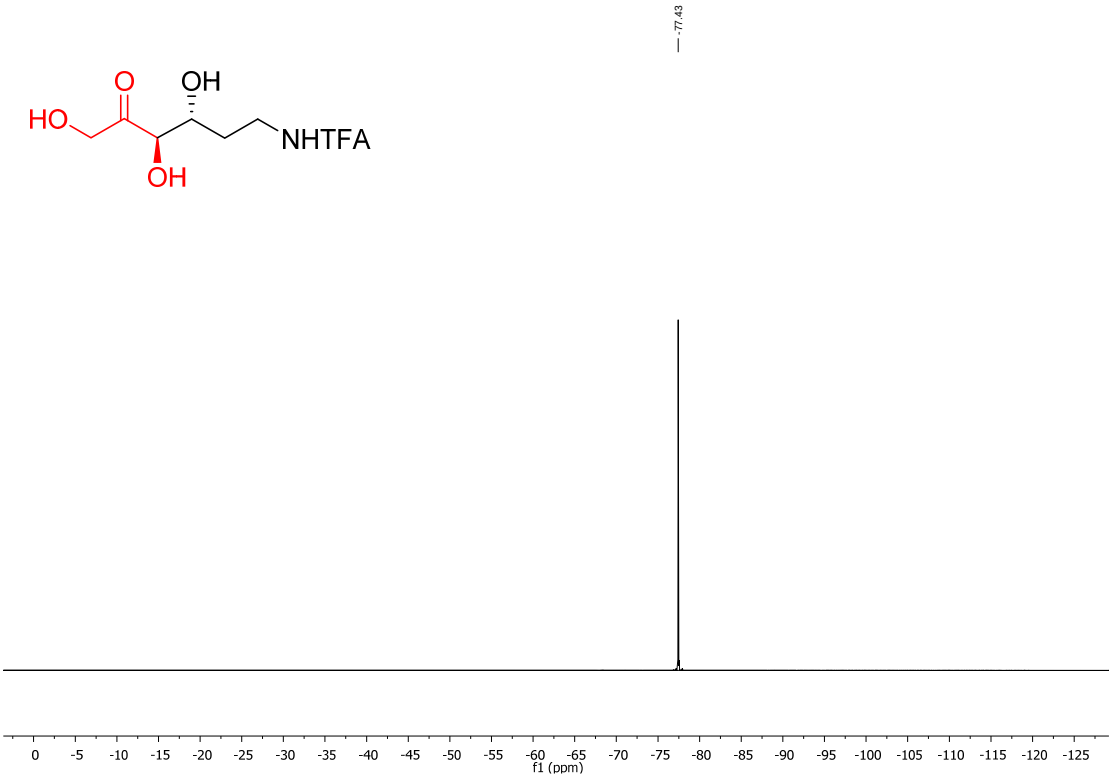

^{1}H-NMR spectrum of (3*R*, 4*S*)-6-trifluoroacetamido-1,3,4-trihydroxyhexan-2-one in CD_3OD.

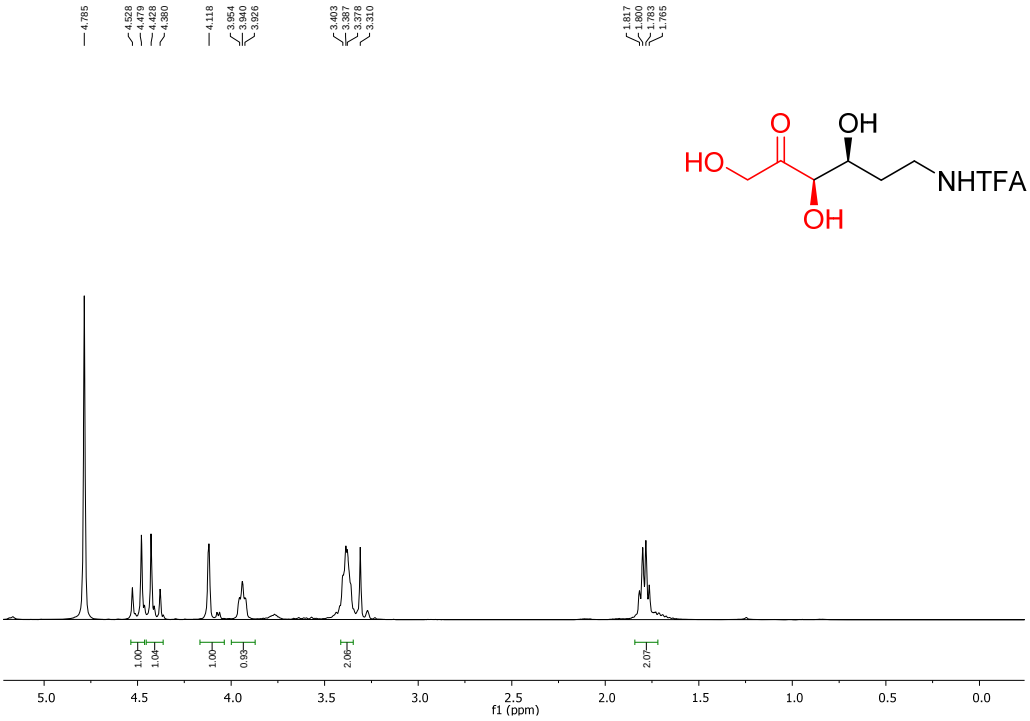

^{13}C-NMR spectrum of (3*R*, 4*S*)-6-trifluoroacetamido-1,3,4-trihydroxyhexan-2-one in CD_3OD.

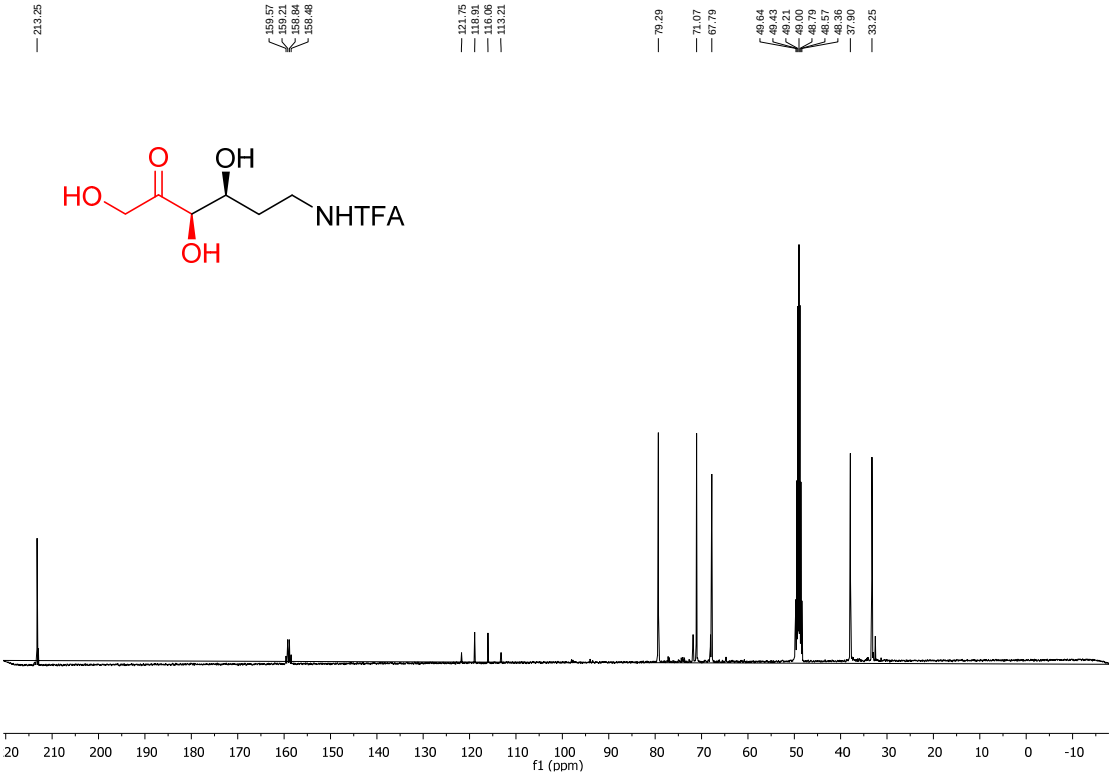

^{19}F-NMR spectrum of (3*R*, 4*S*)-6-trifluoroacetamido-1,3,4-trihydroxyhexan-2-one in CD_3OD.

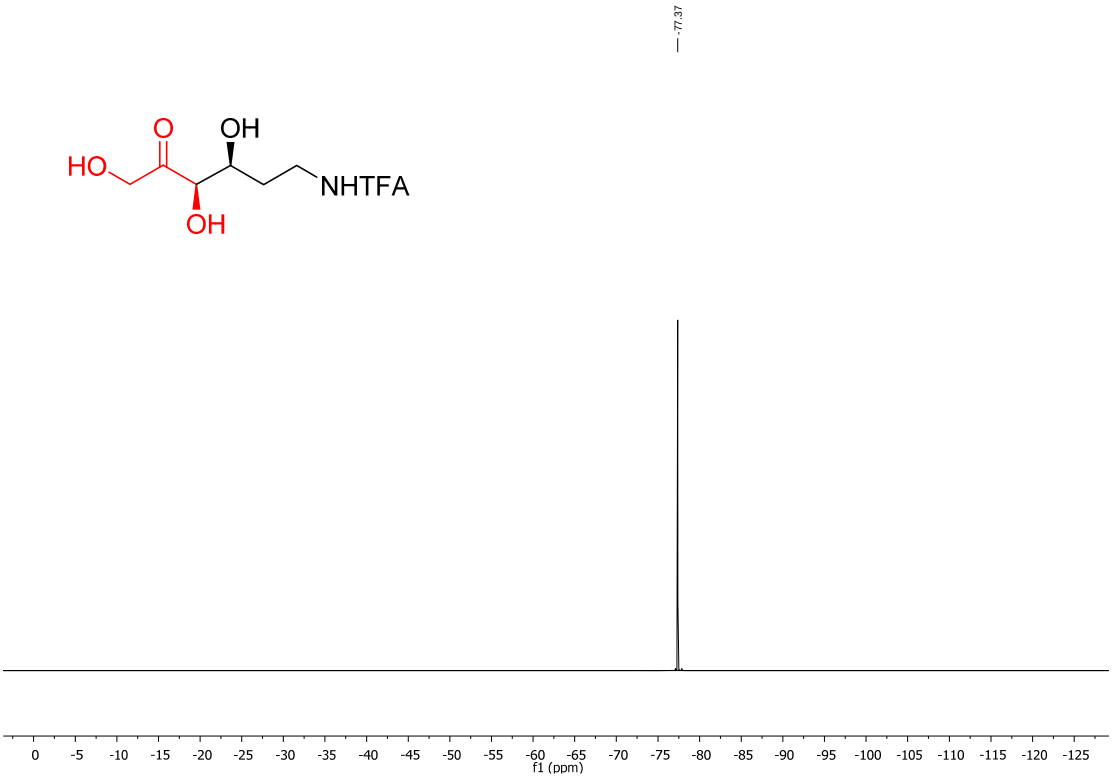

^{1}H-NMR spectrum of [1, 2, 3-$^{13}C_3$] (3*S*, 4*R*)-6-trifluoroacetamido-1,3,4-trihydroxyhexan-2-one in CD_3OD.

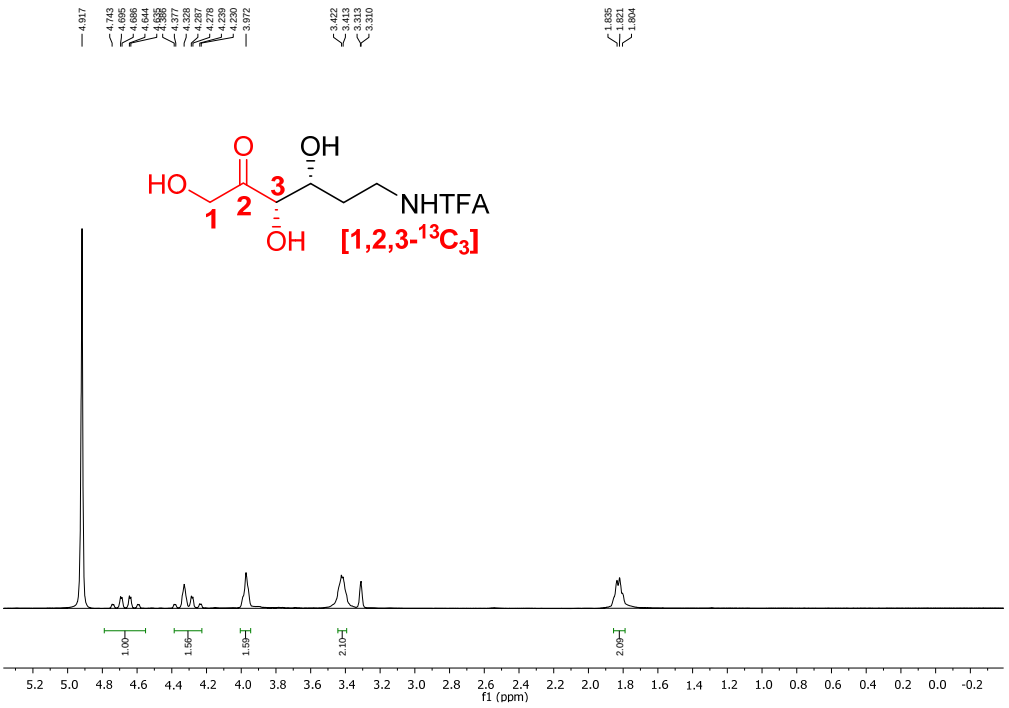

^{13}C-NMR spectrum of [1, 2, 3-$^{13}C_3$] (3*S*, 4*R*)-6-trifluoroacetamido-1,3,4-trihydroxyhexan-2-one in CD_3OD.

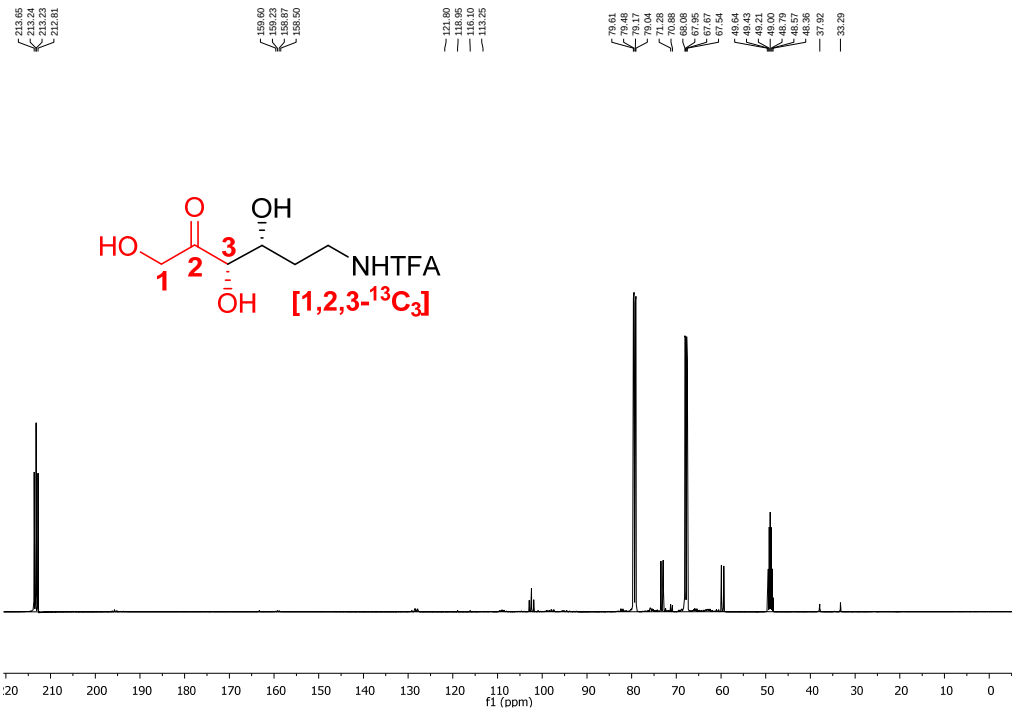

3.2 Experimental procedures for chemical desialylation

3.2.1 General information

All reagents were purchased from commercially sources and were used without further purification. Reactions were monitored by thin layer chromatography (TLC) using silica gel GF_{254} plates with detection by short wave UV light (λ = 254 nm) and staining with 10% phosphomolybdic acid in EtOH or *p*–anisaldehyde solution (ethanol/*p*–anisaldehyde/acetic acid/sulfuric acid 135:5:4:1.5), followed by heating on a hot plate. Column chromatography was conducted by silica gel (200–300 mesh) with hexane/ethyl acetate/2-propanol and ethyl acetate/methanol/water/acetic acid as eluents. ^{1}H NMR and ^{13}C NMR were recorded with Bruker AV 400 spectrometer at 400 MHz (^{1}H NMR), 100 MHz (^{13}C NMR) using $CDCl_3$ and D_2O as solvents. Chemical shifts were reported in δ (ppm) from $CDCl_3$ (7.26 ppm for ^{1}H NMR, 77.00 ppm for ^{13}C NMR), D_2O (4.70 ppm for ^{1}H NMR). Coupling constants were reported in hertz. High–resolution mass spectra (HRMS) were obtained on Thermo LTQ-Orbitrap Elite mass spectrometer. HPLC of analysis was performed by Shimadzu Prominence 20A coupled with UV detector at 210 nm and Aminex HPX-87H column (300 × 7.8 mm) with 5 mM sulfuric acid as mobile phase. The flow rate was 0.5 mL/min.

3.2.2 Synthesis of sialic acid conjugates

2-*O*-Methyl-β-D-*N*-acetyl-neuraminic acid 8[1]

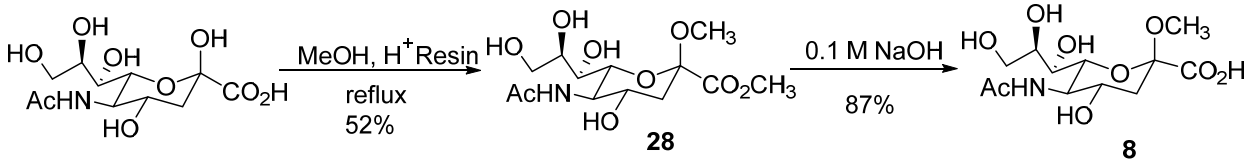

Sialic acid (3.09 g, 10 mmol) was dissolved in anhydrous methanol (200 mL). Amberlyst®15 hydrogen form ion-exchange resin (6.0 g) was added, and the suspension was

refluxed at 80 ºC for 48 h. TLC analysis showed complete conversion of starting material to a major product (ethyl acetate/methanol/water/acetic acid 5:2:1:0.2). The reaction mixture was cooled to room temperature and filtered to remove resin. The filtrate was concentrated in vacuum to give crude syrup **28,** which was then added a mixture of ethyl ether: methanol (3:1, w/w). The solution was kept at 4 ºC for 48 h. The solid substance was recovered by filtration and dried on oil pump to give **28** (1.75 g, 52%).

The methyl ester **28** (337.3 mg, 1 mmol) was saponified with 0.1 M NaOH (11 mL) overnight at room temperature, TLC analysis showed complete conversion of starting material to a major product (ethyl acetate/methanol/water/acetic acid 5:2:1:0.2). The solution pH was adjusted to pH ~2 with addition of Amberlyst®15 hydrogen form ion-exchange resin, and then filtered to remove resin. The filtrate was concentrated, passed through a BioGel P-2 Gel filtration column and lyophilized to afford **8** as white solid (281.6 mg, 87%). ^{1}H NMR (D_2O, 400 MHz): δ 1.50 (d, *J* = 12.0 Hz, 1 H), 1.91 (s, 3 H), 2.20 (dd, *J* = 4.8 Hz, 13.2 Hz, 1 H), 3.06 (s, 3 H), 3.40(d, *J* = 9.2 Hz, 1 H), 3.52 (dd, *J* = 5.6 Hz, 12 Hz, 1 H), 3.64-3.77 (m, 4 H), 3.84-4.88 (m, 1 H); ^{13}C NMR (D_2O, 100 MHz): δ 21.06, 38.71, 49.39, 50.91, 62.45, 65.99, 67.31, 68.91, 69.05, 99.33, 173.66, 174.30. ESI HRMS: m/z calcd for $C_{12}H_{20}NO_9$ $[M-H]^-$ 322.1138, found 322.1127.

2-*O*-Methyl-α-D-*N*-acetyl-neuraminic acid 7 acid[2, 3]

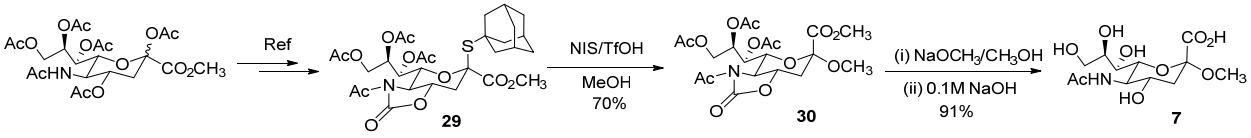

A solution of 1-Adamantanyl thiosialoside **29** (1.28 g, 2 mmol) and activated 4Å molecular sieves in anhydrous CH_2Cl_2/CH_3CN (2:1, 12 mL) was stirred for 30 min at rt, then anhydrous methanol (1 mL) was added. The reaction mixture was cooled to -78 ºC, NIS (1.13 g, 5 mmol) and TfOH (177 μL, 2 mmol) were added, and stirred at -78 ºC for 1 h. TLC analysis

showed complete conversion of starting material to a major product (hexane/ethyl acetate/2-propanol 20:20:1). The reaction was quenched by the addition of 0.2 mL triethylamine and filtered. The filtrate was concentrated in vacuum and purified by silica gel chromatography (hexane/ethyl acetate/2-propanol, 20:20:1) to afford **30** as a yellow solid (708 mg, 70%).

Compound **30** (505 mg, 1 mmol) was dissolved in anhydrous methanol (10 mL), catalytic amount of sodium methoxide was added to adjust pH to 9. Then the reaction mixture was stirred at rt for 2 h. TLC analysis showed complete conversion of starting material to a major product (ethyl acetate/methanol/water/acetic acid 5:1:0.5:0.1). The reaction mixture was neutralized with Amberlyst®15 hydrogen form ion-exchange resin, filtered and concentrated to afford to de-acetylated compound. Then, 0.1 M NaOH (11 mL) was added and stirred overnight at rt. TLC analysis showed complete conversion of starting material to a major product (ethyl acetate/methanol/water/acetic acid 5:2:1:0.2). The pH reaction mixture was adjusted 2 with Amberlyst®15 hydrogen form ion-exchange resin, and then filtered to remove resin. The filtrate was concentrated, passed through a BioGel P-2 Gel fitration column and lyophilized to afford **7** as white solid (293 mg, 91%). ^{1}H NMR (D_2O, 400 MHz): δ 1.54 (t, J = 12.0 Hz, 1 H), 1.94 (s, 3 H), 2.62 (dd, J = 4.4 Hz, 12.4 Hz, 1 H), 3.25 (s, 3 H), 3.50 (d, J = 8.8 Hz, 1 H), 3.52-3.60 (m, 2 H), 3.62 (d, J = 10.4 Hz, 1 H), 3.70 (d, J = 10.0 Hz, 1 H), 3.76-3.82 (m, 2 H); ^{13}C NMR (D_2O, 100 MHz): δ 21.01, 39.11, 50.55, 50.90, 61.60, 67.17, 70.63, 71.54, 99.64, 172.41, 174.03. ESI HRMS: m/z calcd for $C_{12}H_{20}NO_9$ $[M-H]^-$ 322.1138, found 322.1127.

9

Compound 9 was synthesized by following the same procedure with 2,2,2-trifluoroethanol as acceptor.

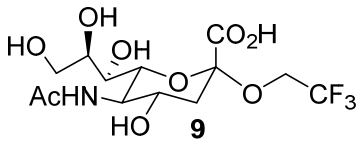

^{1}H NMR (D_2O, 400 MHz): δ 1.60 (t, *J* = 12.0 Hz, 1 H), 1.91 (s, 3 H), 2.65 (dd, *J* = 4.4 Hz, 12.4 Hz, 1 H), 3.32 (s, 3 H), 3.45-3.61 (m, 4 H), 3.69-3.75 (m, 3 H), 3.86-3.94 (m, 1 H), 4.02-4.13 (m, 1 H); ^{13}C NMR (D_2O, 100 MHz): δ 21.03, 38.61, 50.67, 60.43 (q, *J* = 35 Hz), 61.56, 67.05, 70.50, 71.78, 99.33, 122.66 (q, *J* = 275 Hz), 171.51, 174.04. ESI HRMS: m/z calcd for $C_{13}H_{19}F_3NO_9$ $[M-H]^-$ 390.1017, found 390.1054.

10

Compound 10 was synthesized by following the same procedure with 1-Adamantanol as acceptor.

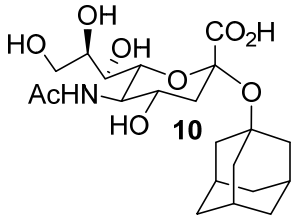

^{1}H NMR (D_2O, 400 MHz): δ 1.47 (s, 6 H), 1.50 (t, *J* = 12.0 Hz, 1 H), 1.83 (s, 6 H), 1.90 (s, 3 H), 1.97 (s, 3 H), 2.60 (dd, *J* = 4.4 Hz, 12.4 Hz, 1 H), 3.43-3.48 (m, 2 H), 3.52 (dd, *J* = 6.0 Hz, 12.4 Hz, 1 H), 3.62-3.66 (m, 2 H), 3.71-3.76 (m, 2 H); ^{13}C NMR (D_2O, 100 MHz): δ 20.95, 29.82, 34.45, 41.85, 42.79, 50.79, 61.33, 66.94, 67.06, 71.14, 71.90, 78.56, 98.56, 174.01, 174.51. ESI HRMS: m/z calcd for $C_{21}H_{33}NO_9$ $[M-H]^-$ 442.2082, found 442.2063.

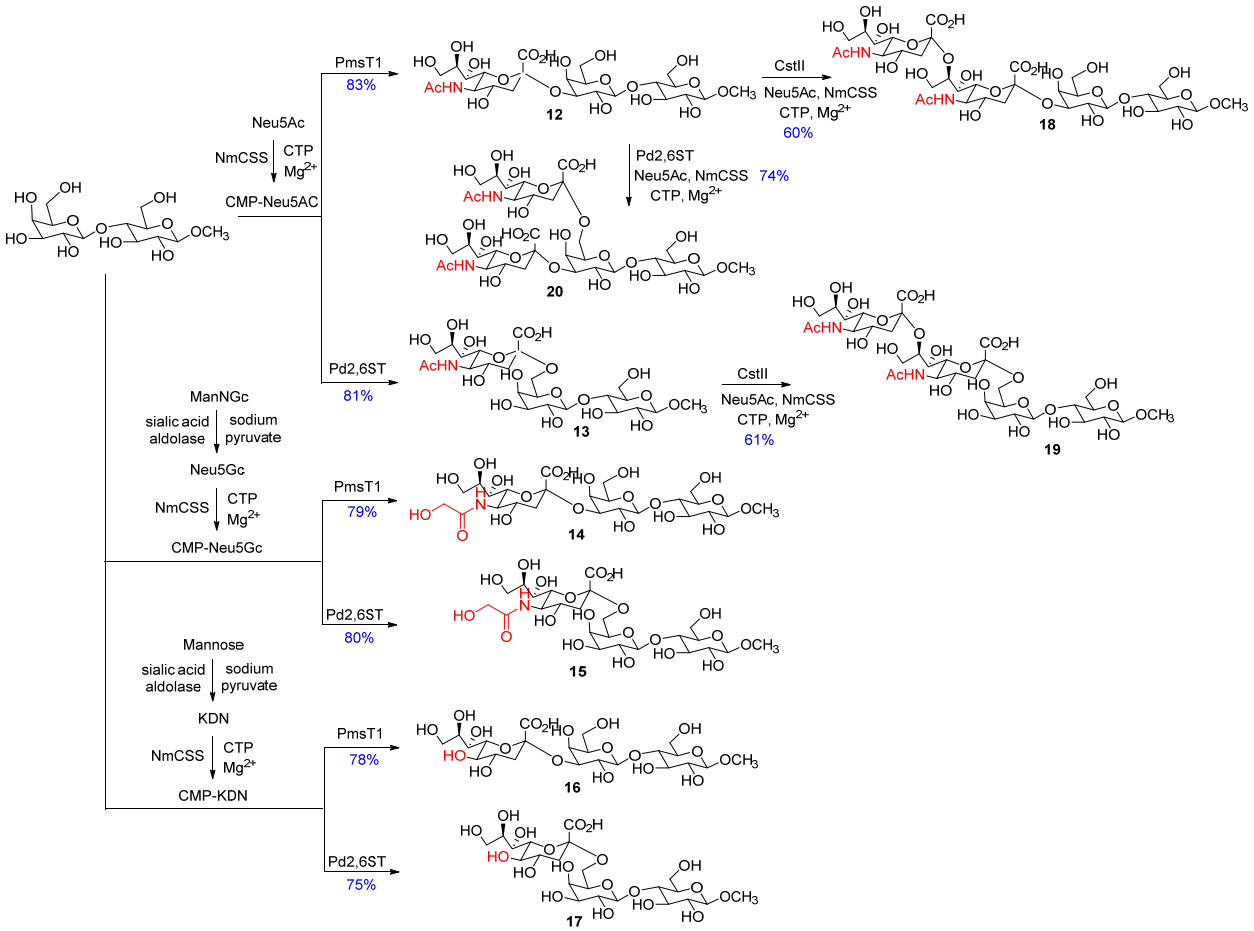

Neu5Ac-α-2,3-Lac-β-OCH_3 12[4, 5]

Lac-β-OCH_3 (10 mM), Neu5Ac (12 mM), cytidine-5'-triphosphate (CTP, 15 mM) and $MgCl_2$ (20 mM) were dissolved in water in a 50 mL centrifuge tube containing Tris-HCl buffer (100 mM). An N.meningitidis CMP-sialic acid synthetase NmCSS (0.5 mg) and an α-2,3 sialyltransferase PmST1 (0.2 mg) were added. Water was added to make the final volume of reaction mixture to 20 mL (pH, 8.5). The reaction was incubated 3 h at 37 °C with shaking (120 rpm). TLC analysis showed a major product (ethyl acetate/methanol/water/acetic acid 5:3:1.5:0.25). The reaction was stopped by adding the same volume of ice-cold ethanol and incubating at 4 °C for 30 min. The mixture was centrifuged to remove insoluble materials. The supernatant was concentrated by rotary evaporation and purified by Bio-Gel P-2 gel filtration

column. The desired product was collected and lyophilized to afford a white solid (107 mg, 83%). ^{1}H NMR (D_2O, 400 MHz): δ 1.78 (t, *J* = 12.0 Hz, 1 H), 2.02 (s, 3 H), 2.74 (dd, *J* = 4.8 Hz, 12.0 Hz, 1 H), 3.29 (t, *J* = 8.4 Hz, 1 H), 3.56-3.73 (m,14 H), 3.80-3.90 (m, 4 H), 3.94-4.00 (m, 2 H), 4.10 (dd, *J* = 2.8 Hz, 10.0 Hz, 1 H), 4.39 (d, *J* = 8.0 Hz, 1 H), 4.51 (d, *J* = 8.0 Hz, 1 H). ^{13}C NMR (D_2O, 100 MHz): δ 21.08, 38.60, 50.68, 56.22, 59.01, 60.01, 61.57, 66.46, 67.07, 67.30, 68.34, 70.76, 71.78, 71.84, 73.33, 73.73,74.13, 74.44, 77.18, 98.79, 101.62, 102.06, 172.84, 173.96;ESI HRMS: m/z calcd for $C_{24}H_{40}NO_{19}$ $[M-H]^-$ 646.2195, found 646.2168.

Neu5Ac-α-2,6-Lac-β-OCH_3 13

Lac-β-OCH_3 (10 mM), Neu5Ac (12 mM), CTP (15 mM) and $MgCl_2$ (20 mM) were dissolved in water in a 50 mL centrifuge tube containing Tris-HCl buffer (100 mM). NmCSS (0.5 mg) and an α-2,6 sialyltransferase (Pd2,6ST, 0.2 mg) were added. Water was added to make the final volume of reaction mixture to 20 mL (pH, 8.5). The reaction was incubated 3 h at 37 ºC with shaking (120 rpm). TLC analysis showed a major product (ethyl acetate/methanol/water/acetic acid 5:3:1.5:0.25). The reaction was stopped by adding the same volume of ice-cold ethanol and incubating at 4 ºC for 30 min. The mixture was centrifuged to remove insoluble materials. The supernatant was concentrated by rotary evaporation and purified by Bio-Gel P-2 gel filtration column. The desired product was collected and lyophilized to afford a white solid (105 mg, 81%). ^{1}H NMR (D_2O, 400 MHz): δ 1.72 (t, *J* = 12.0 Hz, 1 H), 2.02 (s, 3 H), 2.69 (dd, *J* = 4.4 Hz, 12.4 Hz, 1 H), 3.32 (t, *J* = 8.0 Hz, 1 H), 3.50-3.72 (m,13 H), 3.88-3.99 (m, 5 H), 3.92-3.99 (m, 3 H), 4.39-4.42(m, 2 H) ^{13}C NMR (D_2O, 100 MHz): *δ* 21.07, 39.06, 50.76, 56.14, 59.21, 61.61, 62.52, 67.33, 67.48, 69.76, 70.78, 71.34, 71.49, 71.67, 72.64, 73.60, 78.62, 99.24, 101.88, 102.21, 172.45, 173.87; ESI HRMS: m/z calcd for $C_{24}H_{40}NO_{19}$ $[M-H]^-$ 646.2195, found 646.2168.

Neu5Gc-α-2,3-Lac-β-OCH_3 14

Lac-β-OCH_3 (10 mM), ManNGc (12 mM), sodium pyruvate (60 mM), CTP (15 mM) and $MgCl_2$ (20 mM) were dissolved in water in a 50 mL centrifuge tube containing Tris-HCl buffer (100 mM). *E. coli* sialic acid aldolase (0.4 mg), NmCSS (0.5 mg) and PmST1 (0.2 mg) were added. Water was added to make the final volume of reaction mixture to 20 mL (pH, 8.5). The reaction was incubated 4 h at 37 ^oC with shaking (120 rpm). TLC analysis showed a major product (ethyl acetate/methanol/water/acetic acid 5:3:1.5:0.25). The reaction was stopped by adding the same volume of ice-cold ethanol and incubating at 4 ^oC for 30 min. The mixture was centrifuged to remove insoluble materials. The supernatant was concentrated by rotary evaporation and purified by Bio-Gel P-2 gel filtration column. The desired product was collected and lyophilized to afford a white solid (105 mg, 79%).

^1H NMR (D_2O, 400 MHz): δ 1.74 (t, J = 12.0 Hz, 1 H), 2.70 (dd, J = 4.4 Hz, 12.4 Hz, 1 H), 3.23 (t, J = 8.0 Hz, 1 H), 3.48–3.53 (m, 3 H), 3.50 (s, 3 H), 3.54-3.60 (m, 3 H), 3.61-3.72 (m, 5 H), 3.72-3.79 (m, 2 H), 3.80-3.87 (m, 2 H), 3.87-3.95 (m, 2 H), 4.02-4.08 (m, 3 H), 4.33 (d, J = 8.0 Hz, 1 H), 4.45 (d, J = 7.6 Hz, 1 H); ^{13}C NMR (D_2O, 100 MHz): δ 39.70, 51.38, 57.21, 60.05, 60.98, 61.02, 62.54, 67.45, 68.02, 68.09, 69.37, 71.82, 72.60, 72.78, 74.36, 74.77, 75.17, 75.47, 78.25, 99.81, 102.65, 103.08, 173.91, 175.77; ESI HRMS: m/z calcd for $C_{24}H_{40}NO_{20}$ $[M-H]^-$ 662.2149, found 662.2103.

Neu5Gc-α-2,6-Lac-β-OCH_3 15

Lac-β-OCH_3 (10 mM), ManNGc (12 mM), sodium pyruvate (60 mM), CTP (15 mM) and $MgCl_2$ (20 mM) were dissolved in water in a 50 mL centrifuge tube containing Tris-HCl buffer (100 mM). *E. coli* sialic acid aldolase (0.4 mg), NmCSS (0.5 mg) and Pd2,6ST (0.2 mg) were added. Water was added to make the final volume of reaction mixture to 20 mL (pH, 8.5). The

reaction was incubated 4 h at 37 ºC with shaking (120 rpm). TLC analysis showed a major product (ethyl acetate/methanol/water/acetic acid 5:3:1.5:0.25). The reaction was stopped by adding the same volume of ice-cold ethanol and incubating at 4 ºC for 30 min. The mixture was centrifuged to remove insoluble materials. The supernatant was concentrated by rotary evaporation and purified by Bio-Gel P-2 gel filtration column. The desired product was collected and lyophilized to afford a white solid (106 mg, 80%).

^{1}H NMR (D_2O, 400 MHz): δ 1.67 (t, *J* = 12.0 Hz, 1 H), 2.64 (dd, *J* = 4.4 Hz, 12.4 Hz, 1 H), 3.25 (t, *J* = 8.4 Hz, 1 H), 3.43-3.60 (m, 8 H), 3.49 (s, 3 H), 3.63-3.71 (m, 3 H), 3.72-3.82 (m, 4 H), 3.85-3.93 (m, 3 H), 4.03 (s, 2 H), 4.33 (d, *J* = 7.6 Hz, 1 H), 4.34 (d, *J* = 7.6 Hz, 1 H); ^{13}C NMR (D_2O, 100 MHz): *δ* 40.14, 51.49, 57.15, 59.39, 60.25, 60.99, 62.60, 63.57, 68.07, 68.31, 68.51, 70.78, 71.83, 72.24, 72.36, 72.68, 73.70, 74.62, 74.64, 79.68, 100.28, 102.90, 103.23, 173.49, 175.67; ESI HRMS: m/z calcd for $C_{24}H_{40}NO_{20}$ $[M-H]^-$ 662.2149, found 662.2103.

KDN-α-2,3-Lac-β-OCH_3 16

Lac-β-OCH_3 (10 mM), Mannose (12 mM), sodium pyruvate (60 mM), CTP (15 mM) and $MgCl_2$ (20 mM) were dissolved in water in a 50 mL centrifuge tube containing Tris-HCl buffer (100 mM). *E. coli* sialic acid aldolase (0.4 mg), NmCSS (0.5 mg) and PmST1 (0.2 mg) were added. Water was added to make the final volume of reaction mixture to 20 mL (pH, 8.5). The reaction was incubated 4 h at 37 ºC with shaking (120 rpm). TLC analysis showed a major product (ethyl acetate/methanol/water/acetic acid 5:3:1.5:0.25). The reaction was stopped by adding the same volume of ice-cold ethanol and incubating at 4 ºC for 30 min. The mixture was centrifuged to remove insoluble materials. The supernatant was concentrated by rotary evaporation and purified by Bio-Gel P-2 gel filtration column. The desired product was collected and lyophilized to afford a white solid (95 mg, 78%).

^{1}H NMR (D_2O, 400 MHz): δ 1.66 (t, *J* = 12.0 Hz, 1 H), 2.62 (dd, *J* = 4.4 Hz, 12.4 Hz, 1 H), 3.22 (t, *J* = 8.0 Hz, 1 H), 3.45-3.57 (m, 7 H), 3.49 (s, 3 H), 3.60-3.66 (m, 4 H), 3.72-3.83 (m, 4 H), 3.87 (s, 1 H), 3.92 (d, *J* = 12.0 Hz, 1 H), 4.00 (dd, *J* = 2.4 Hz, 10.0 Hz, 1 H), 4.32 (d, *J* = 8.0 Hz, 1 H), 4.43 (d, *J* = 8.0 Hz, 1 H); ^{13}C NMR (D_2O, 100 MHz): δ 38.28, 56.19, 59.03, 60.01, 61.62, 66.37, 66.70, 68.33, 68.73, 69.23, 71.05, 71.76, 72.89, 73.34, 73.76, 74.17, 74.43, 77.21, 98.76, 101.64, 102.07, 173.02; ESI HRMS: m/z calcd for $C_{22}H_{37}O_{19}$ $[M-H]^-$ 605.1935, found 605.1906.

KDN-α-2,6-Lac-β-OCH_3 17

Lac-β-OCH_3 (10 mM), Mannose (12 mM), sodium pyruvate (60 mM), CTP (15 mM) and $MgCl_2$ (20 mM) were dissolved in water in a 50 mL centrifuge tube containing Tris-HCl buffer (100 mM). *E. coli* sialic acid aldolase (0.4 mg), NmCSS (0.5 mg) and an Pd2,6ST (0.2 mg) were added. Water was added to make the final volume of reaction mixture to 20 mL (pH, 8.5). The reaction was incubated 7 h at 37 °C with shaking (120 rpm). TLC analysis showed a major product (ethyl acetate/methanol/water/acetic acid 5:3:1.5:0.25). The reaction was stopped by adding the same volume of ice-cold ethanol and incubating at 4 °C for 30 min. The mixture was centrifuged to remove insoluble materials. The supernatant was concentrated by rotary evaporation and purified by Bio-Gel P-2 gel filtration column. The desired product was collected and lyophilized to afford a white solid (91 mg, 75%).

^{1}H NMR (D_2O, 400 MHz): δ 1.60 (t, *J* = 12.0 Hz, 1 H), 2.55 (dd, *J* = 4.4 Hz, 12.4 Hz, 1 H), 3.22 (t, *J* = 8.4 Hz, 1 H), 3.42-3.52 (m, 6 H), 3.47 (s, 3 H), 3.53-3.60 (m, 4 H), 3.67-3.74 (m, 3 H), 3.78-3.83 (m, 3 H), 3.85-3.92 (m, 2 H), 4.30 (d, *J* = 3.2 Hz, 1 H), 4.32 (d, *J* = 3.2 Hz, 1 H); ^{13}C NMR (D_2O, 100 MHz): δ 38.70, 56.14, 59.23, 61.67, 62.57, 67.04, 67.49, 68.84, 69.18, 69.75, 71.05, 71.33, 71.67, 72.52, 72.72, 73.60, 78.73, 99.24, 101.92, 102.23, 172.68; ESI HRMS: m/z calcd for $C_{22}H_{37}O_{19}$ $[M-H]^-$ 605.1935, found 605.1906.

Neu5Ac-α-2,8-Neu5Ac-α-2,3-Lac-β-OCH_3 18[6]

Neu5Ac-α-2,3-Lac-β-OMe (10 mM), Neu5Ac (12 mM), CTP (15 mM) and $MgCl_2$ (20 mM) were dissolved in water in a 50 mL centrifuge tube containing Tris-HCl buffer (100 mM). NmCSS (2.5 mg) and Campylobacter jejuni α-2,8-sialyltransferase (CstII, 2 mg) were added. Water was added to make the final volume of reaction mixture to 10 mL (pH, 8.5). The reaction was incubated 20 h at 37 °C with shaking (120 rpm). TLC analysis showed a major product (ethyl acetate/methanol/water/acetic acid 5:3:1.5:0.25). The reaction was stopped by adding the same volume of ice-cold ethanol and incubating at 4 °C for 30 min. The mixture was centrifuged to remove insoluble materials. The supernatant was concentrated by rotary evaporation and purified by Bio-Gel P-2 gel filtration column. The desired product was collected and lyophilized to afford a white solid (56 mg, 60%).

^{1}H NMR (D_2O, 400 MHz): δ 1.64 (t, *J* = 12.0 Hz, 2 H), 1.92 (s, 3 H), 1.96 (s, 3 H), 2.57 (dd, *J* = 3.8 Hz, 12.2 Hz, 1 H), 2.67 (dd, *J* = 4.4 Hz, 12.4 Hz, 1 H), 3.20 (t, *J* = 8.4 Hz, 1 H), 3.45-3.65 (m, 14 H), 3.47 (s, 3 H), 3.70-3.80 (m, 6 H), 3.84-3.93 (m, 2 H), 3.97-4.09 (m, 3 H), 4.30 (d, *J* = 8.0 Hz, 1 H), 4.41 (d, *J* = 8.0 Hz, 1 H); ^{13}C NMR (D_2O, 100 MHz): δ 21.00, 21.28, 38.59, 39.47, 50.71, 51.22, 56.18, 58.18, 58.94, 60.07, 60.50, 61.53, 66.45, 66.89, 67.09, 67.46, 68.26, 70.72, 71.63, 71.79, 72.97, 73.27, 73.78, 74.19, 74.43, 76.97, 77.14, 99.17, 99.52, 101.64, 102.07, 172.30, 172.41, 173.95; ESI HRMS: m/z calcd for $C_{35}H_{57}N_2O_{27}$ $[M-H]^-$ 937.3154, found 937.3111.

Neu5Ac-α-2,8-Neu5Ac-α-2,6-Lac-β-OCH_3 19

Neu5Ac-α-2,6-Lac-β-OMe (10 mM), Neu5Ac (12 mM), CTP (15 mM) and $MgCl_2$ (20 mM) were dissolved in water in a 50 mL centrifuge tube containing Tris-HCl buffer (100 mM). NmCSS (2.5 mg) and CstII (2 mg) were added. Water was added to make the final volume of

reaction mixture to 10 mL (pH, 8.5). The reaction was incubated 20 h at 37 ºC with shaking (120 rpm). TLC analysis showed a major product (ethyl acetate/methanol/water/acetic acid 5:3:1.5:0.25). The reaction was stopped by adding the same volume of ice-cold ethanol and incubating at 4 ºC for 30 min. The mixture was centrifuged to remove insoluble materials. The supernatant was concentrated by rotary evaporation and purified by Bio-Gel P-2 gel filtration column. The desired product was collected and lyophilized to afford a white solid (57 mg, 61%). ^{1}H NMR (D_2O, 400 MHz): δ 1.57 (t, *J* = 12.0 Hz, 1 H), 1.63 (t, *J* = 12.0 Hz, 1 H), 1.92 (s, 3 H), 1.96 (s, 3 H), 2.51 (dd, *J* = 4.0 Hz, 12.4 Hz, 1 H), 2.67 (dd, *J* = 4.4 Hz, 12.4 Hz, 1 H), 3.21 (t, *J* = 8.4 Hz, 1 H), 3.42-3.58 (m, 12 H), 3.47 (s, 3 H), 3.68-3.74 (m, 6 H), 3.75-3.84 (m, 4 H), 3.88 (d, *J* = 12.4 Hz, 1 H), 4.01 (dd, *J* = 2.8 Hz, 12.0 Hz, 1 H), 4.09 (s, 1 H), 4.30 (s, 1 H), 4.32 (s, 1 H); ^{13}C NMR (D_2O, 100 MHz): δ 21.01, 21.27, 39.08, 39.47, 50.70, 51.24, 56.11, 59.25, 60.57, 61.54, 62.77, 66.81, 67.11, 67.47, 68.61, 69.76, 70.70, 71.30, 71.64, 72.72, 73.12, 73.62, 73.65, 77.52, 78.73, 99.40, 99.90, 101.87, 102.26, 172.29, 172.34, 173.91, 173.94; ESI HRMS: m/z calcd for $C_{35}H_{57}N_2O_{27}$ $[M-H]^-$ 937.3154, found 937.3111.

Neu5Ac-α-2,8-(Neu5Ac-α-2,3-)Lac-β-OCH_3 20

Neu5Ac-α-2,3-Lac-β-OCH_3 (10 mM), Neu5Ac (12 mM), CTP (15 mM) and $MgCl_2$ (20 mM) were dissolved in water in a 50 mL centrifuge tube containing Tris-HCl buffer (100 mM). NmCSS (2.5 mg) and an Pd2,6ST (2 mg) were added. Water was added to make the final volume of reaction mixture to 10 mL (pH, 8.5). The reaction was incubated 24 h at 37 ºC with shaking (120 rpm). TLC analysis showed a major product (ethyl acetate/methanol/water/acetic acid 5:3:1.5:0.25). The reaction was stopped by adding the same volume of ice-cold ethanol and incubating at 4 ºC for 30 min. The mixture was centrifuged to remove insoluble materials. The

supernatant was concentrated by rotary evaporation and purified by Bio-Gel P-2 gel filtration column. The desired product was collected and lyophilized to afford a white solid (69 mg, 74%). ^{1}H NMR (D_2O, 400 MHz): δ 1.62 (t, J = 12.0 Hz, 1 H), 1.68 (t, J = 12.0 Hz, 1 H), 1.90 (s, 6 H), 2.58 (dd, J = 4.4 Hz, 12.4 Hz, 1 H), 2.62 (dd, J = 4.4 Hz, 12.4 Hz, 1 H), 3.20 (t, J = 8.4 Hz, 1 H), 3.42-3.60 (m, 13 H), 3.45 (s, 3 H), 3.68-3.78 (m, 8 H), 3.82–3.90 (m, 3 H), 4.00 (dd, J = 2.8 Hz, 9.6 Hz, 1 H), 4.29 (d, J = 8.0 Hz, 1 H), 4.39 (d, J = 8.0 Hz, 1 H); ^{13}C NMR (D_2O, 100 MHz): δ 21.01, 38.38, 38.95, 50.60, 50.71, 56.10, 59.19, 61.54, 61.60, 62.44, 66.52, 67.03, 67.32, 68.18, 70.62, 71.46, 71.62, 71.81, 72.41, 73.58, 74.18, 78.62, 98.84, 99.12, 101.87, 101.92, 172.27, 172.66, 173.81, 173.90; ESI HRMS: m/z calcd for $C_{35}H_{57}N_2O_{27}$ $[M-H]^-$ 937.3154, found 937.3111.

SGP 21

SGP was isolated from egg yolk.[7]

α-2,3-linked Neu5Ac–BSA 22 and α-2,6-linked Neu5Ac–BSA 23

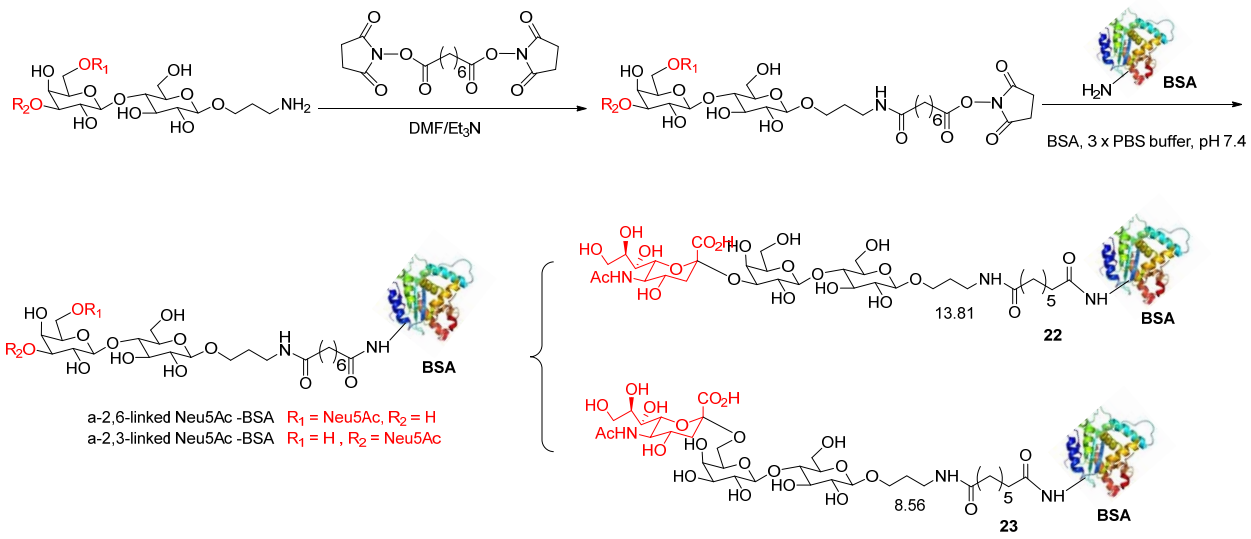

The NHS activated sugar-linker conjugates were mixed with BSA at a molar ratio of 50:1 in 3 x PBS buffer (pH 7.4). The solution was incubated overnight at room temperature. Then the

resultant solution was ultrafiltered and washed with 1 x PBS buffer using Amicon Centrifugal Filter Devices (Ultracel 10, 000). The glycoproteins solution was lyophilized to give a white solid. Based on the change of molecular weight between BAS and sugar-BSA conjugates (**22**, **23**), the loading number of sugars on BSA was calculated. On average, each BSA in **22** contains 13.8 sugars and each BSA in **23** contains 8.6 sugars.

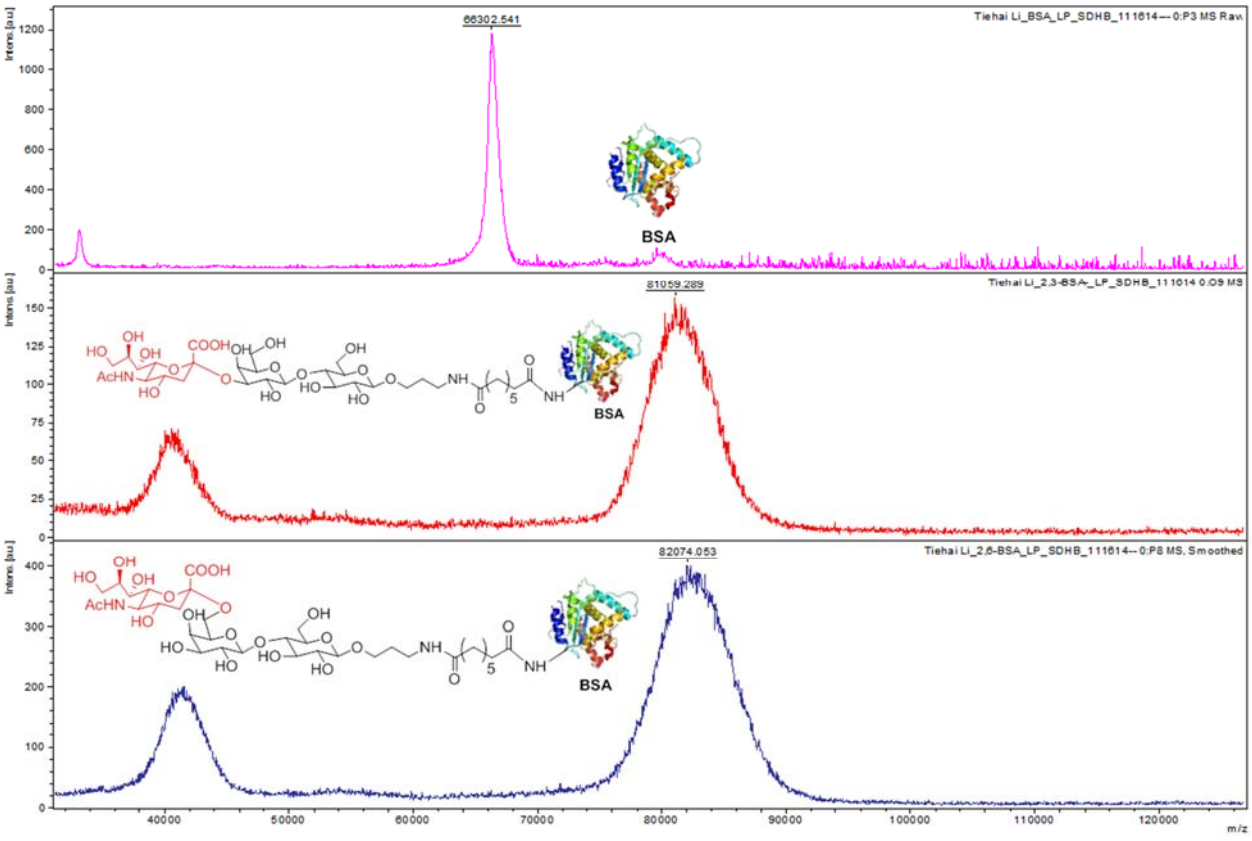

MALDI-TOF spectra of BSA, **22** and **23**.

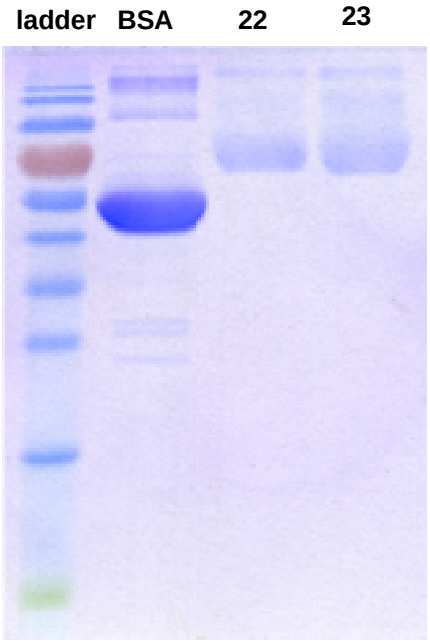

SDS PAGE of BSA, **22** and **23**.

3.2.3 Synthesis of ADOA, 31, and 32 as analytical standards

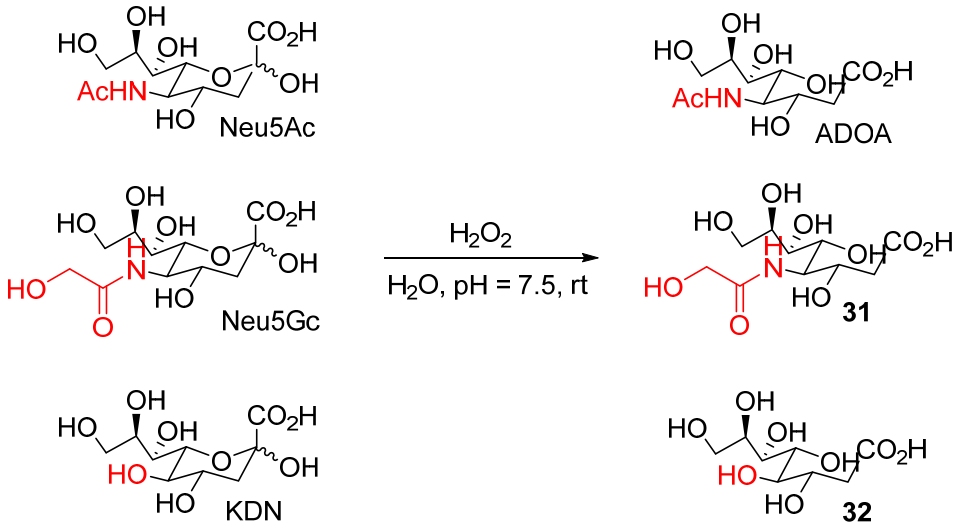

ADOA

Neu5Ac (309 mg, 1 mmol) was dissolved in 10 mL ddH_2O, and the pH of the solution was adjusted to 7.5 by 0.1 M NaOH. Then, H_2O_2 (1.5 eq) was added and the reaction mixture was stirred at rt. After complete consumption of Neu5Ac, the reaction mixture was concentrated

and purified by Bio-Gel P2 gel filtration column. The desired product was collected and lyophilized to afford 265 mg ADOA with 94% yield. ^{1}H NMR (D_2O, 400 MHz): δ 1.93 (s, 3 H), 2.21 (d, *J* = 6.6 Hz, 2 H), 3.33 (d, *J* = 9.0 Hz, 1 H), 3.49 (dd, *J* = 6.4 Hz, *J* = 12.0 Hz, 1 H), 3.60-3.64 (m, 1 H), 3.71 (d, *J* = 12.0 Hz, 1 H), 3.81 (s, 2 H), 4.35 (t, *J* = 6.8 Hz, 1 H); ^{13}C NMR (D_2O, 100 MHz): δ 20.81, 40.40, 52.45, 62.19, 65.64, 66.65, 68.31, 69.58, 173.37, 178.71. ESI HRMS: m/z calcd for $C_{10}H_{18}NO_8$ $[M-H]^-$ 280.1111, found 280.1021.

31

31 was synthesized by following the same procedure with 87% yield. ^{1}H NMR (D_2O, 400 MHz): δ 2.29 (d, *J* = 6.0 Hz, 2 H), 3.42 (d, *J* = 8.8 Hz, 1 H), 3.58 (dd, *J* = 5.8 Hz, 11.4 Hz, 1 H), 3.69 (d, *J* = 11.6 Hz, 1 H), 3.79 (d, *J* = 12.0 Hz, 1 H), 3.94 (d, *J* = 10.0 Hz, 1 H), 3.98 (d, *J* = 12.0 Hz, 1 H), 4.10 (s, 1 H), 4.47 (t, *J* = 14.5 Hz, 1 H); ^{13}C NMR (D_2O, 100 MHz): 40.64, 52.24, 59.92, 62.23, 65.80, 66.78, 68.43, 69.71, 174.12; ESI HRMS: m/z calcd for $C_{10}H_{18}NO_9$ $[M-H]^-$ 296.0987, found 296.0931.

32

32 was synthesized by following the same procedure with 91% yield. ^{1}H NMR (D_2O, 400 MHz): δ 3.34 (dd, *J* = 4.8 Hz, 14.8 Hz, 1 H), 3.41 (dd, *J* = 9.2 Hz, 14.8 Hz, 1 H), 3.44 (d, *J* = 9.2 Hz, 1 H), 3.54 (dd, *J* = 6.0 Hz, 11.6 Hz, 1 H), 3.62-3.71 (m, 2 H), 3.72-3.79 (m, 2 H), 4.18 (t, *J* = 6.4 Hz, 1 H); ^{13}C NMR (D_2O, 100 MHz): δ 40.58, 62.24, 66.71, 67.45, 68.25, 69.86, 70.38, 179.29; ESI HRMS: m/z calcd for $C_8H_{15}O_8$ $[M-H]^-$ 239.0772, found 239.0737.

3.2.4 Standard curves of ADOA, 31 and 32

Standard curve of ADOA

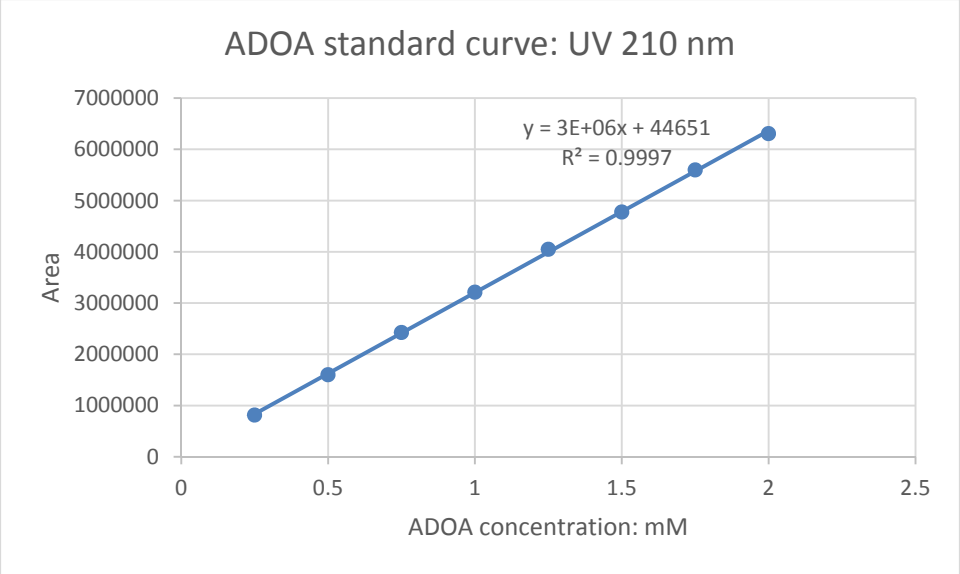

Standard curve of **31**

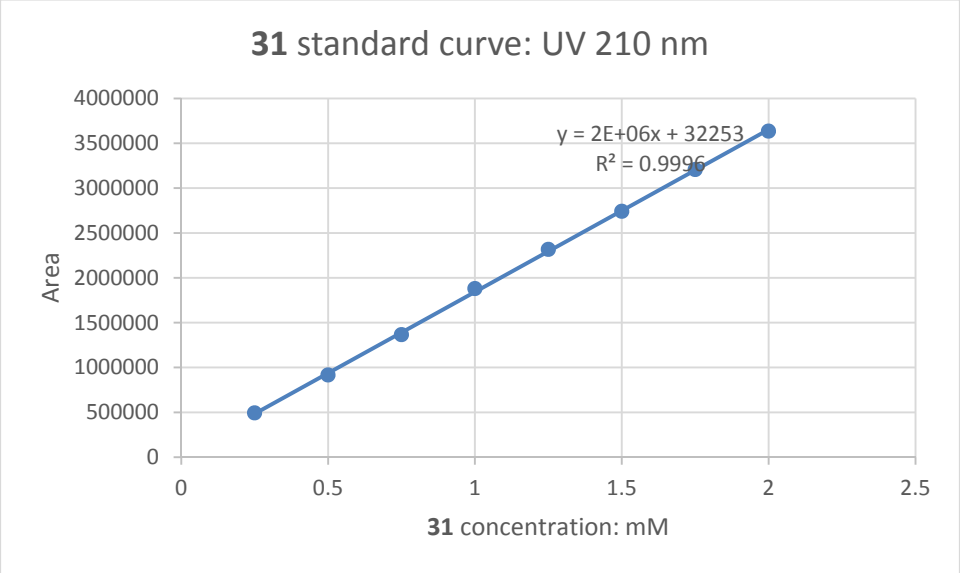

Standard curve of **32**

3.2.5 Desialylation of sialic acid conjugates by hydrogen peroxide

12 (8 mM), **13** (8 mM), SGP **21** (4 mM) , **22** (0.06 mM) and **23** (0.056mM) were treated by H_2O_2 (2 μL) in 0.1 x PBS buffer (pH 7.4, total volume 100 μL) for 8 h at 37°C, and lyophilized to give white solids for analysis.

The lyophilized samples were dissolved in 200 μL ddH_2O, and mix 5 μL of samples with 5 μL of internal standard (a solution of $^{13}C_3$-Neu5Ac and $^{13}C_3$-ADOA). Then 5 μL of the mixture was injected to LC-MS/MS system. Neu5Ac, ADOA and IS were separated by a Primesep D column (2.1 x 100mm, 5 μm; SIELC Technologies, Prospect Heights, IL, USA). The gradient elution time program was used, in which phase A is deionized water containing 10 mM ammonium formate and 0.1% formic acid, and phase B is a mixture of 90% acetonitrile, 10% water, 3 mM ammonium formate, and 0.04% formic acid. The MS detection was carried out in negative electrospray ionization and multiple reactions monitoring (MRM) mode.

3.2.6 Procedure of electrochemical desialylation

To a stirred solution of sialic acid conjugate (5 mM) and $NaClO_4$ (0.2 M) in 3 mL ddH_2O, 0.1 M NaOH was added to adjust the pH to 7.5. Then two BBD electrodes were inserted, and a direct current power (2.4 - 3.0 V) was applied at rt.

The progress of the electrochemical desialylation was monitored by HPLC. Samples (15 μL) were taken at regular intervals to monitor the consumption of sialic acid conjugate and generation of ADOA (or **31**, **32**). The samples were diluted 3 times and then applied to HPLC analysis directly (column: Aminex HPX-87H, 300 × 7.8 mm; eluent: 5 mM sulfuric acid solution; flow rate: 0.5 mL/min; column temperature 60 °C; detector: UV 210 nm).

3.2.7 References

1. Veronesi, P.A., Rodriguez, P.E.A., Veronesi, A.M. & Peschechera, E. 80pp. (Therapicon S.r.l., Italy . 2011).

2. Roy, R. & Laferrière, C.A. Synthesis of protein conjugates and analogues of N-acetylneuraminic acid. *Can. J. Chem.* **68**, 2045-2054 (1990).

3. Crich, D. & Li, W.J. alpha-selective sialylations at-78 degrees C in nitrile solvents with a 1-adamantanyl thiosialoside. *J. Org. Chem.* **72**, 7794-7797 (2007).

4. Yu, H., Huang, S., Chokhawala, H., Sun, M., Zheng, H. & Chen, X. Highly efficient chemoenzymatic synthesis of naturally occurring and non-natural alpha-2,6-linked sialosides: a P. damsela alpha-2,6-sialyltransferase with extremely flexible donor-substrate specificity. *Angew. Chem., Int. Ed.* **45**, 3938-3944 (2006).

5. Chokhawala, H.A., Yu, H. & Chen, X. High-throughput substrate specificity studies of sialidases by using chemoenzymatically synthesized sialoside libraries. *ChemBioChem* **8**, 194-201 (2007).

6. Yu, H., Lau, K., Thon, V., Autran, C.A., Jantscher-Krenn, E., Xue, M., Li, Y., Sugiarto, G., Qu, J., Mu, S., Ding, L., Bode, L. & Chen, X. Synthetic Disialyl Hexasaccharides Protect Neonatal Rats from Necrotizing Enterocolitis. *Angew. Chem., Int. Ed.* **53**, 6687-6691 (2014).

7. Sun, B., Bao, W., Tian, X., Li, M., Liu, H., Dong, J. & Huang, W. A simplified procedure for gram-scale production of sialylglycopeptide (SGP) from egg yolks and subsequent semi-synthesis of Man3GlcNAc oxazoline. *Carbohydr. Res.* **396**, 62-69 (2014).

3.2.9 NMR spectra

^{1}H-NMR spectrum of ADOA in D_2O.

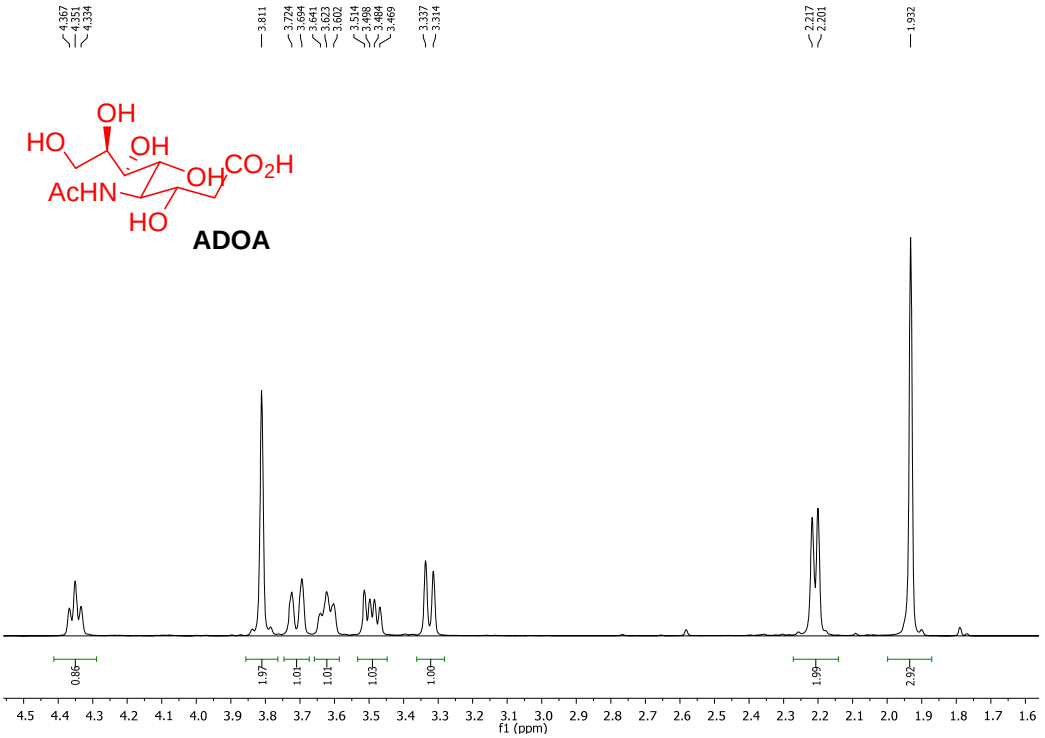

^{13}C-NMR spectrum of ADOA in D_2O.

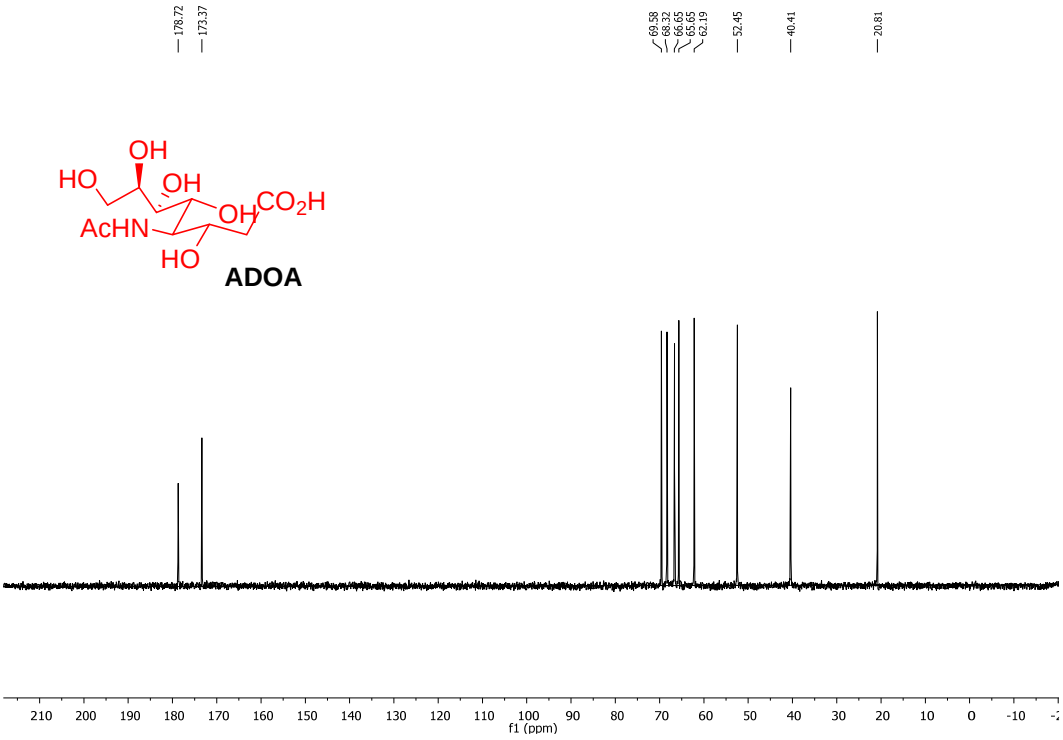

^{13}C HSQC-NMR spectrum of ADOA in D_2O.

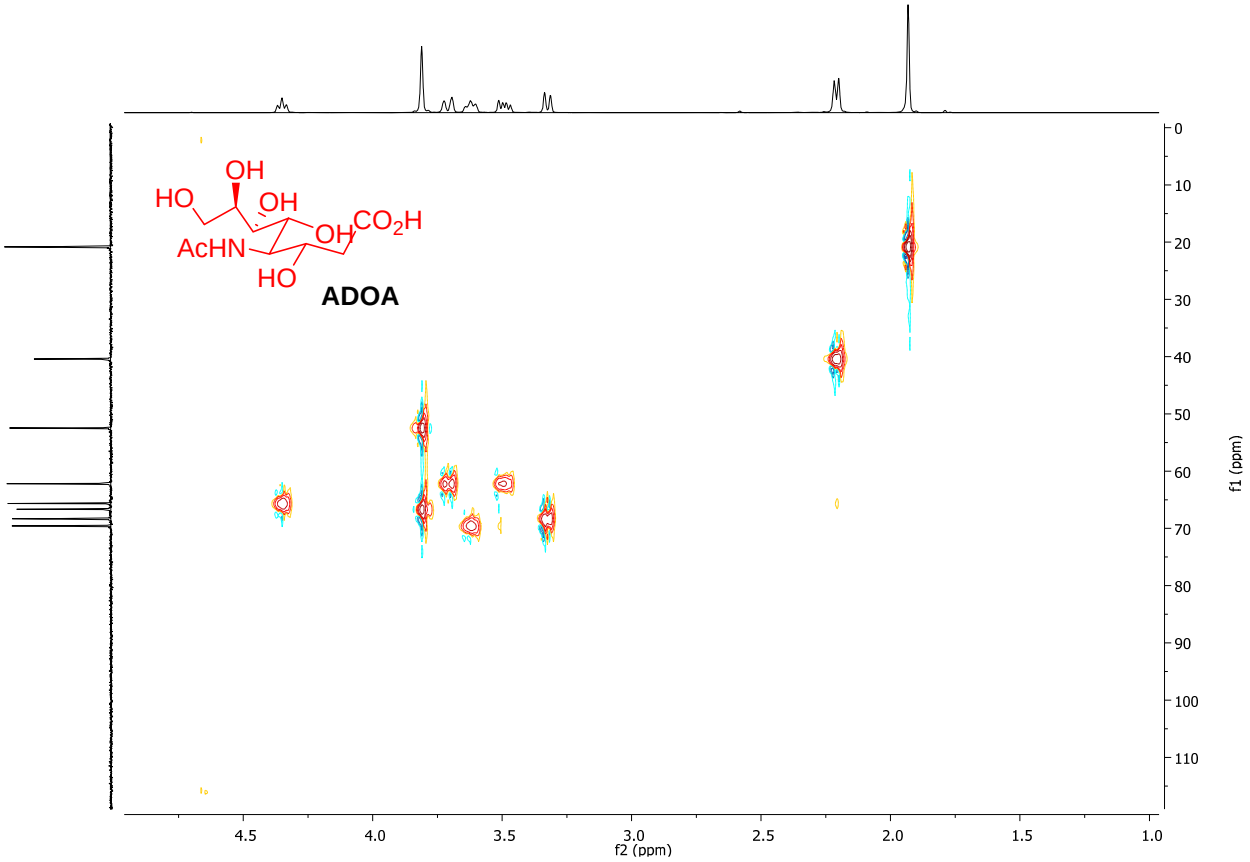

^{1}H-NMR spectrum of **31** in D_2O.

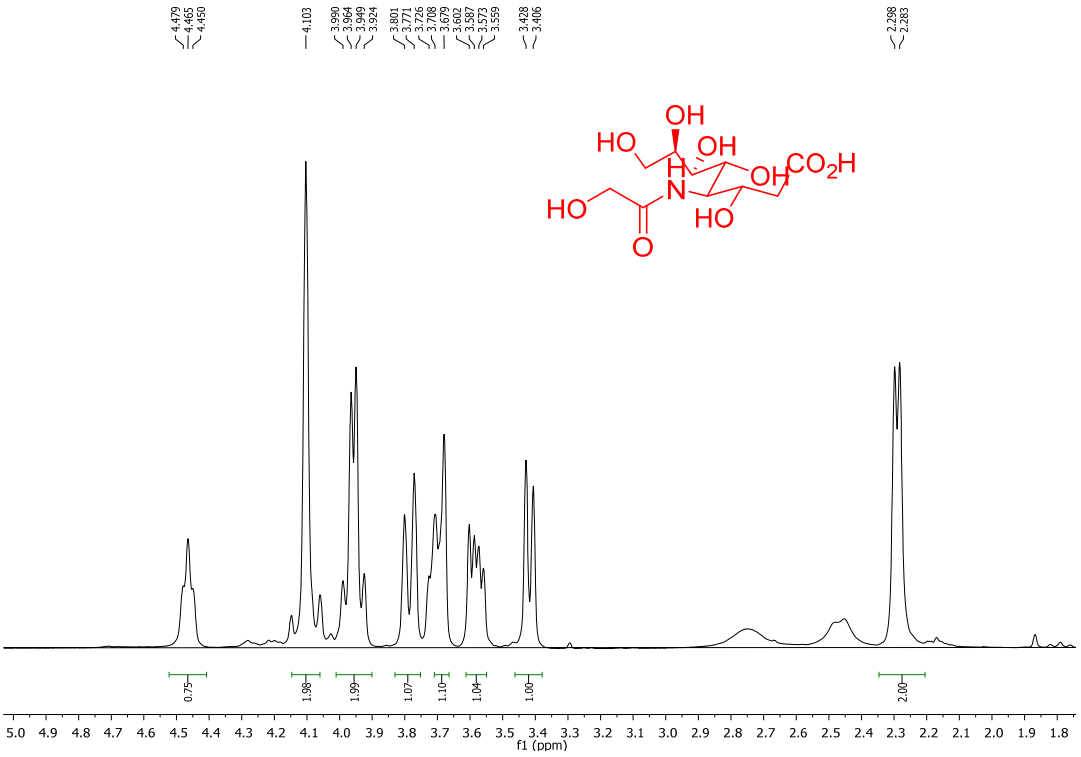

^{13}C-NMR spectrum of **31** in D_2O.

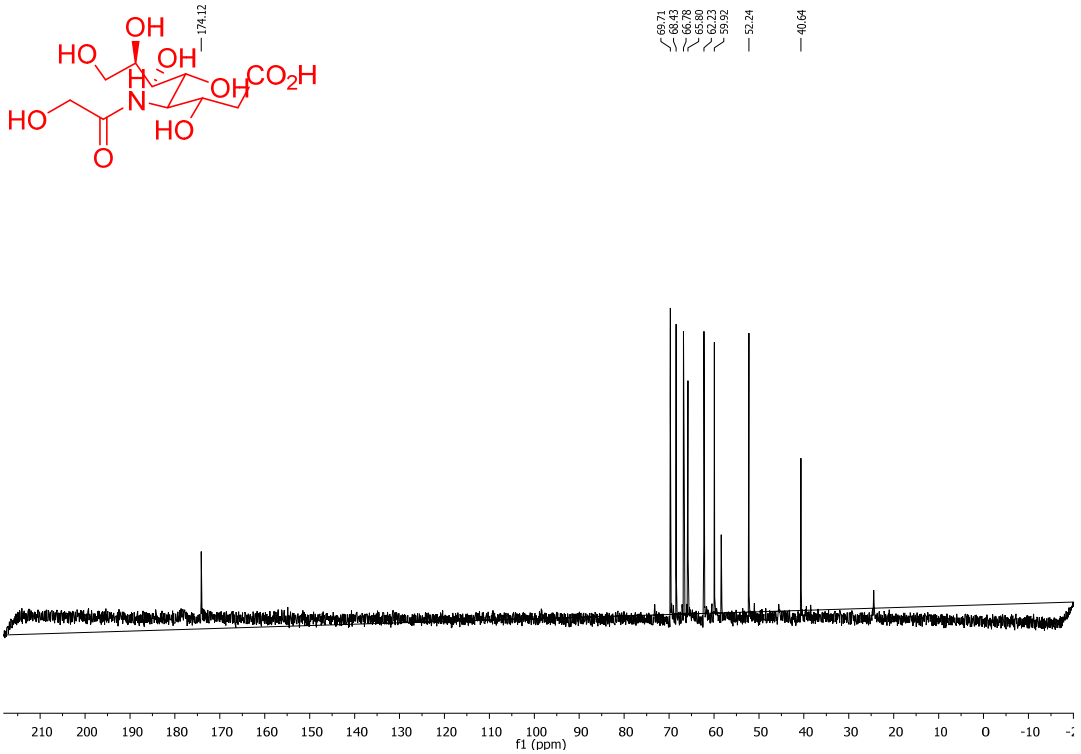

^{13}C HSQC-NMR spectrum of **31** in D_2O.

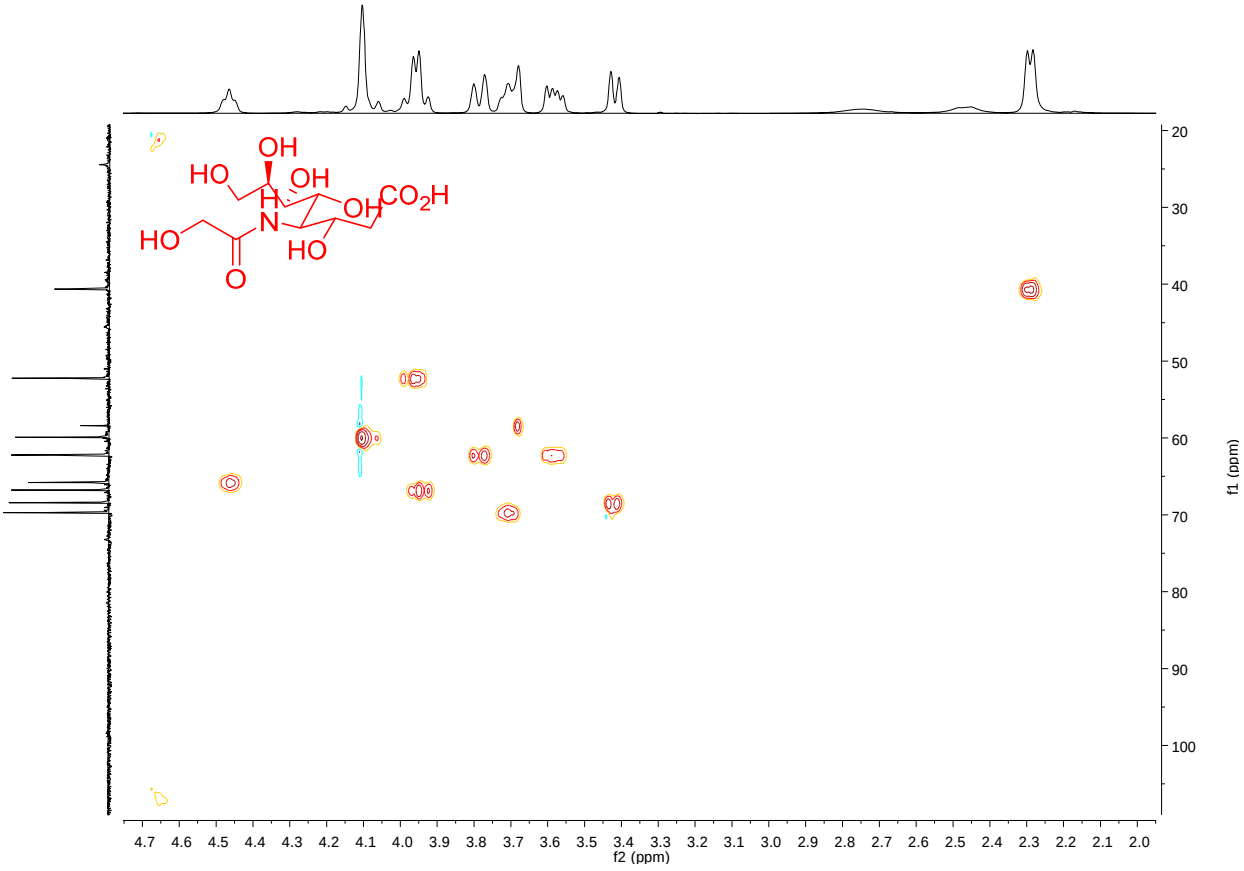

^{1}H-NMR spectrum of **32** in D_2O.

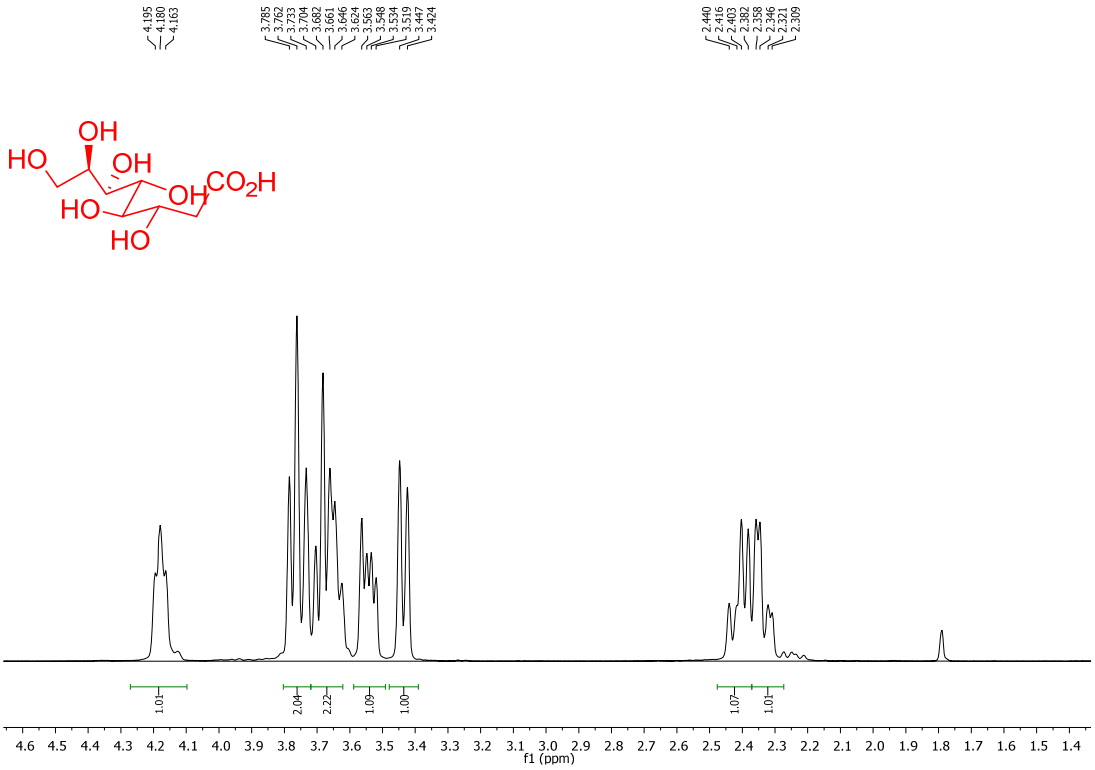

^{13}C-NMR spectrum of **32** in D_2O.

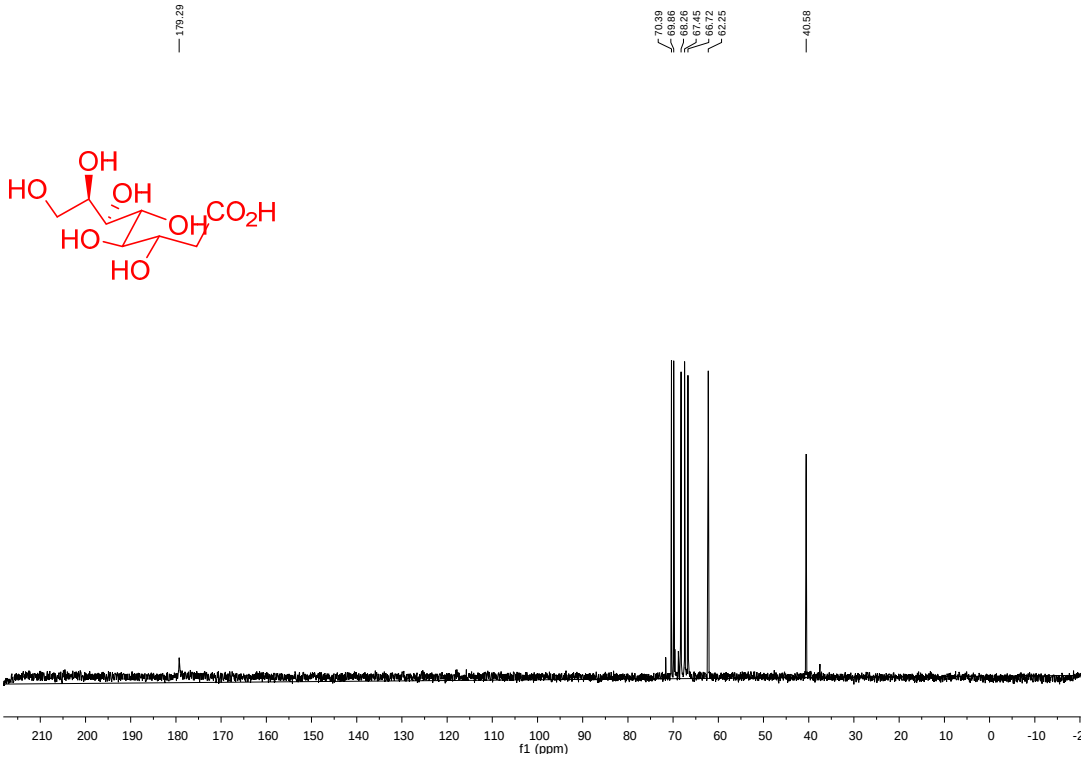

^{13}C HSQC-NMR spectrum of **32** in D_2O.

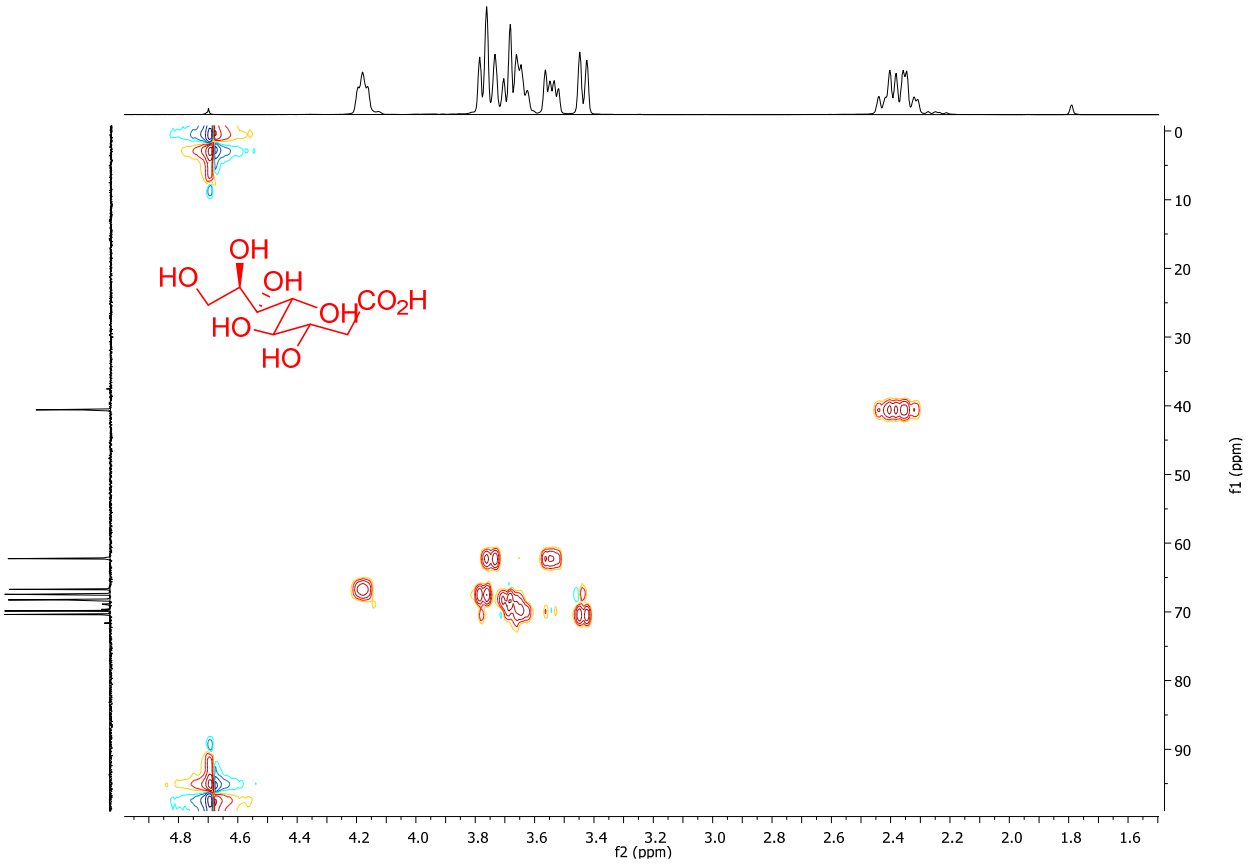

^{1}H-NMR spectrum of **7** in D_2O.

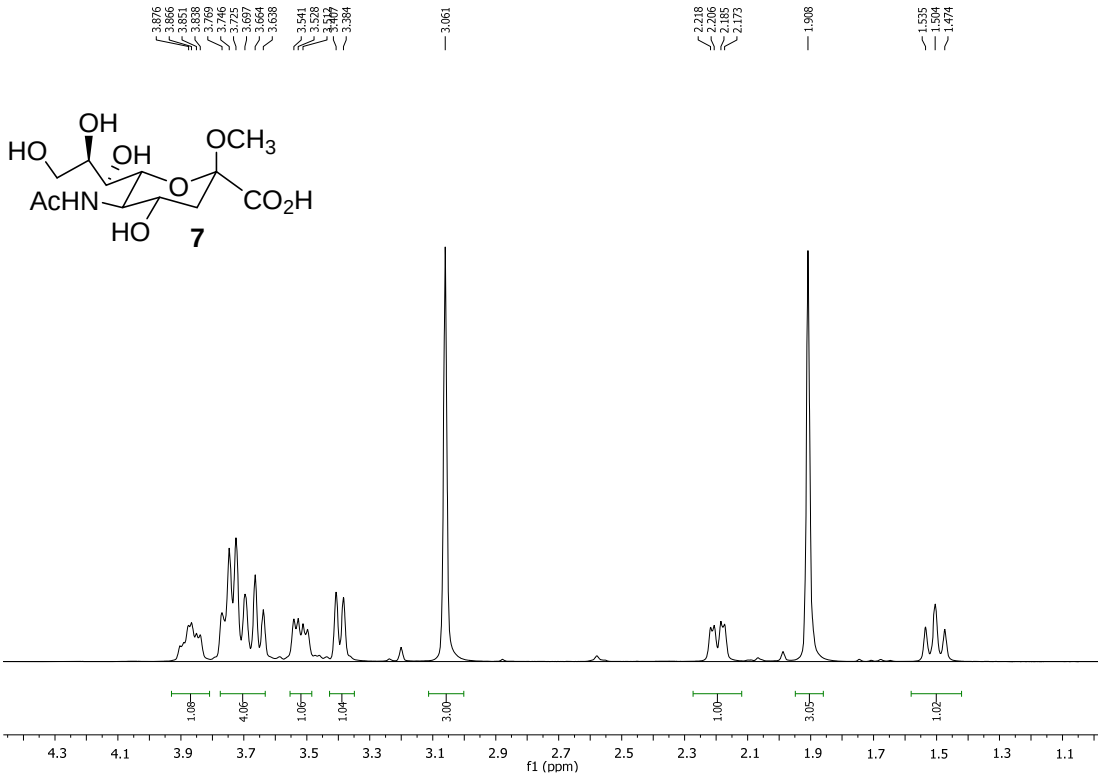

^{13}C-NMR spectrum of **7** in D_2O.

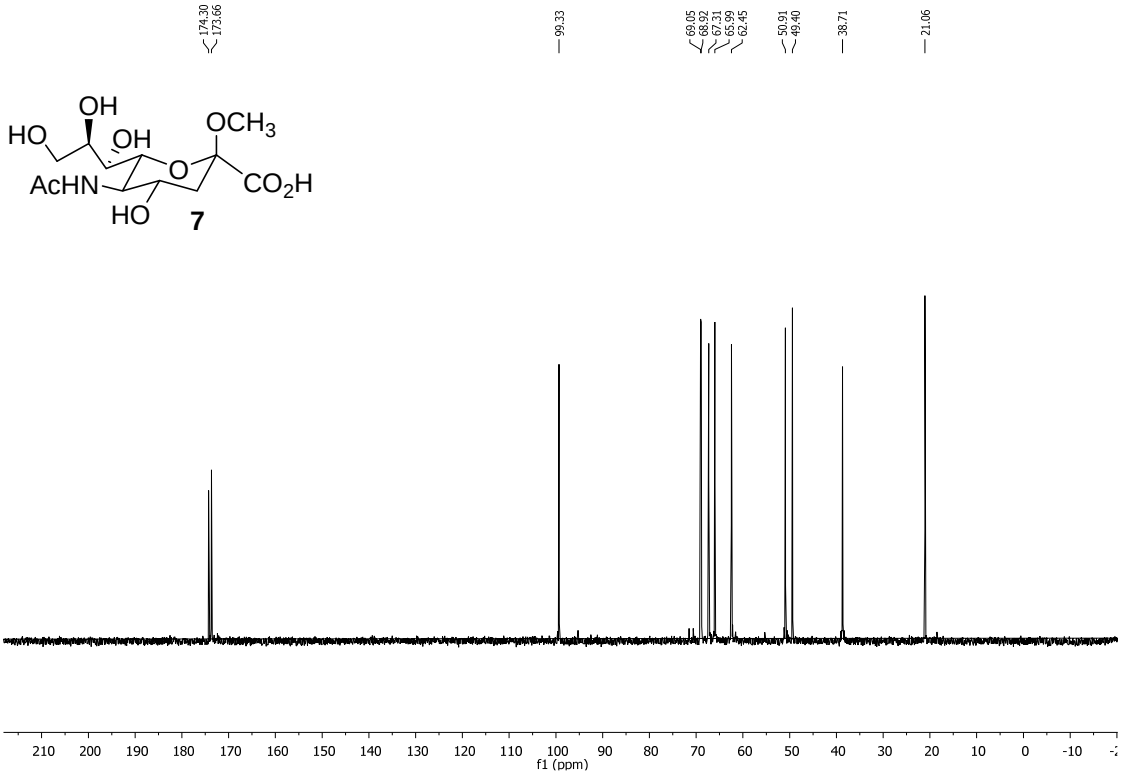

^{13}C HSQC-NMR spectrum of **7** in D_2O.

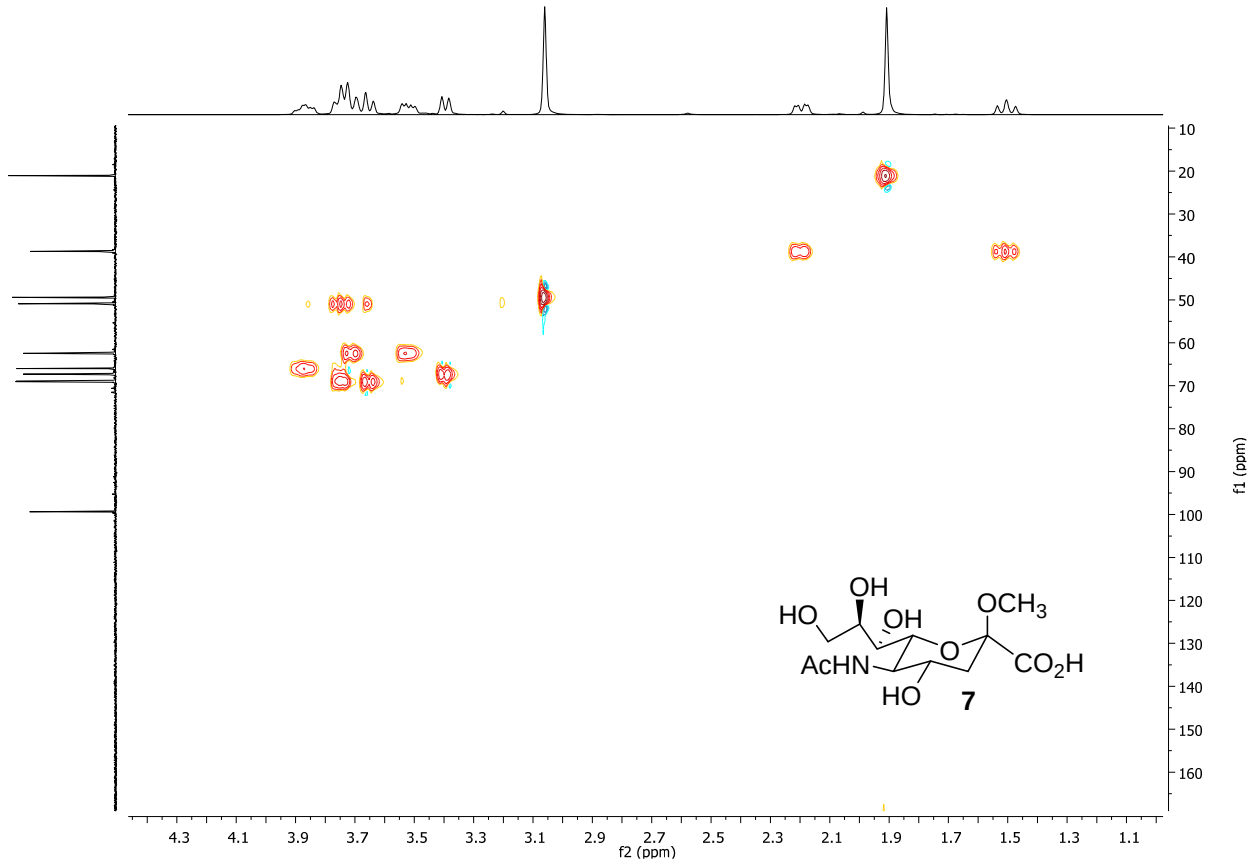

^{1}H-NMR spectrum of **8** in D_2O.

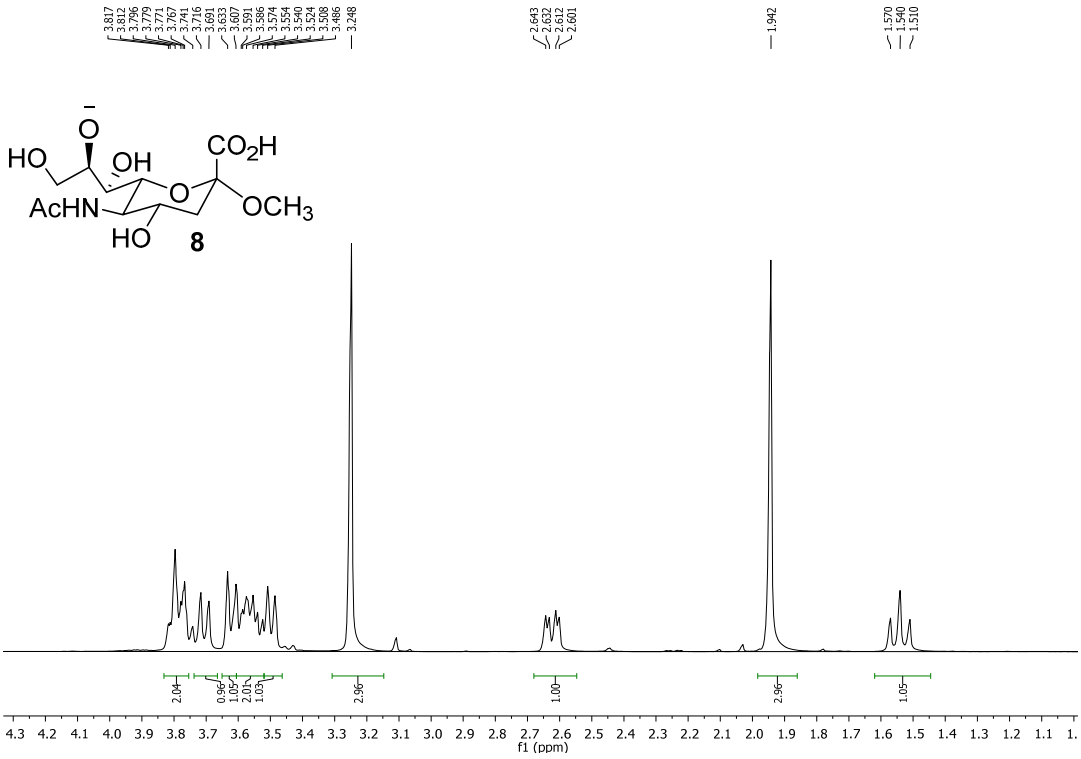

^{13}C-NMR spectrum of **8** in D_2O.

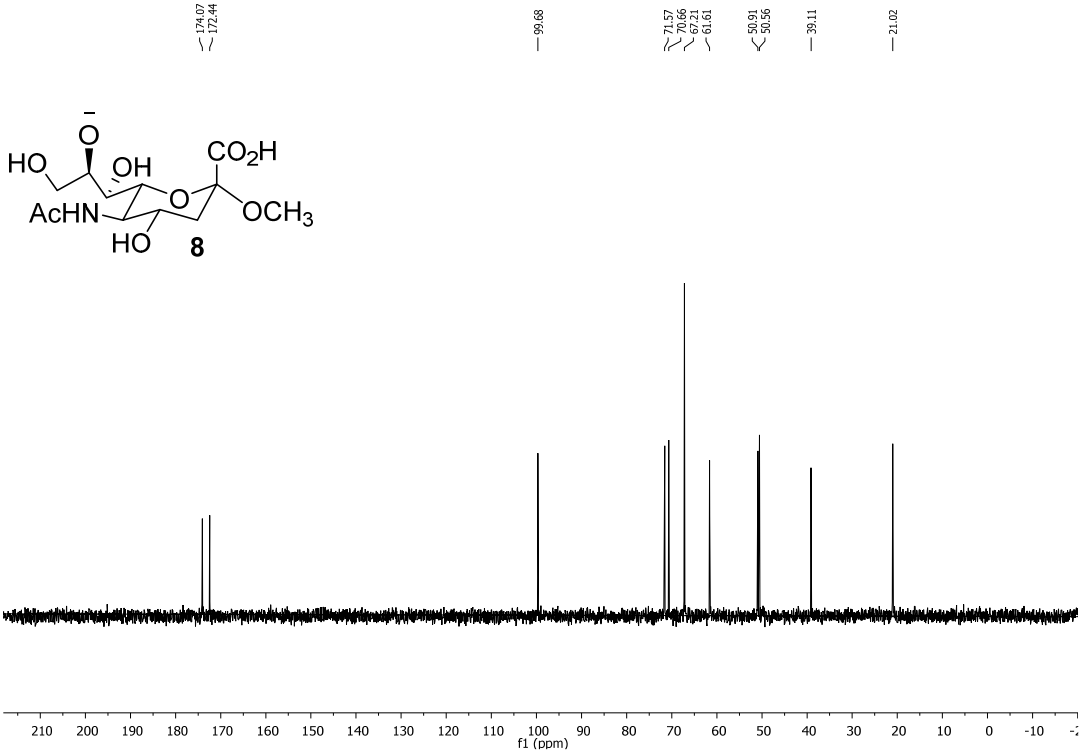

^{13}C HSQC-NMR spectrum of **8** in D_2O.

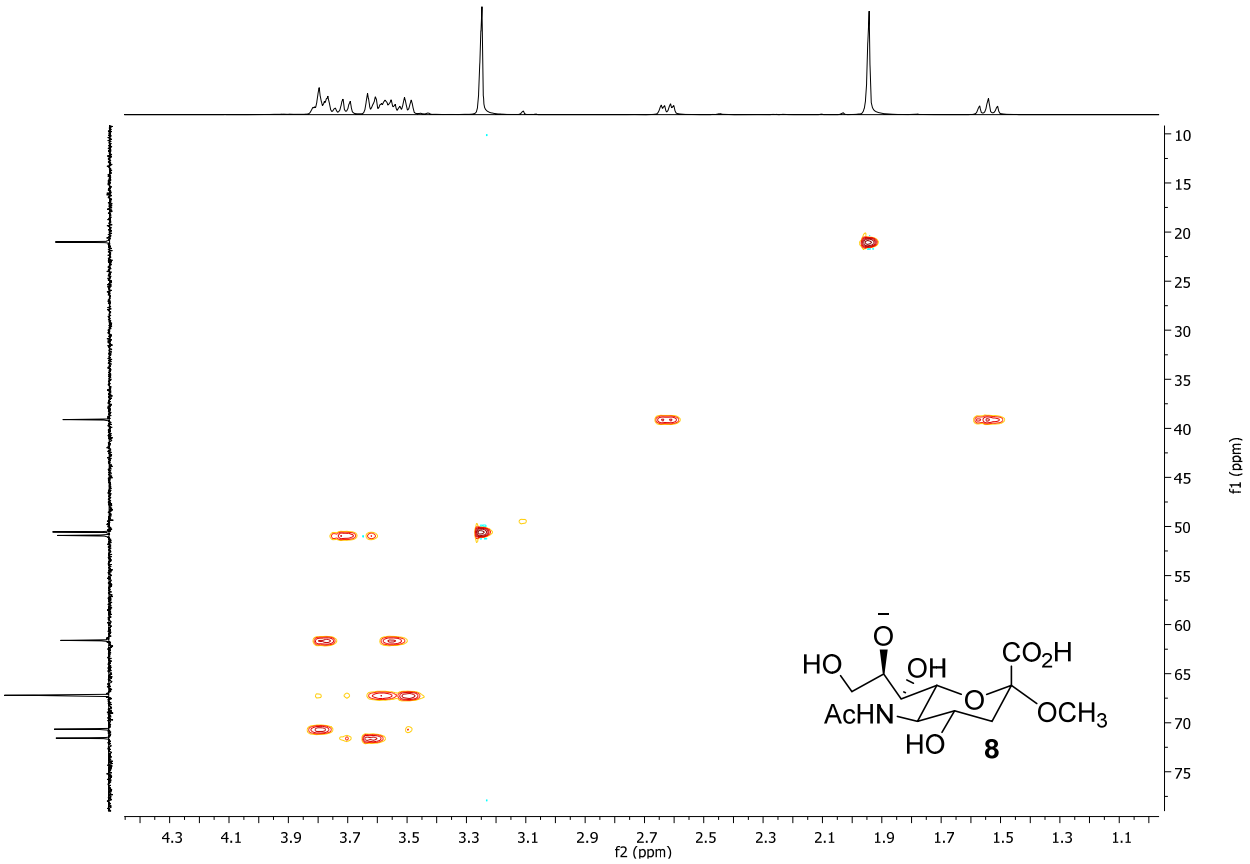

^{1}H-NMR spectrum of **9** in D_2O.

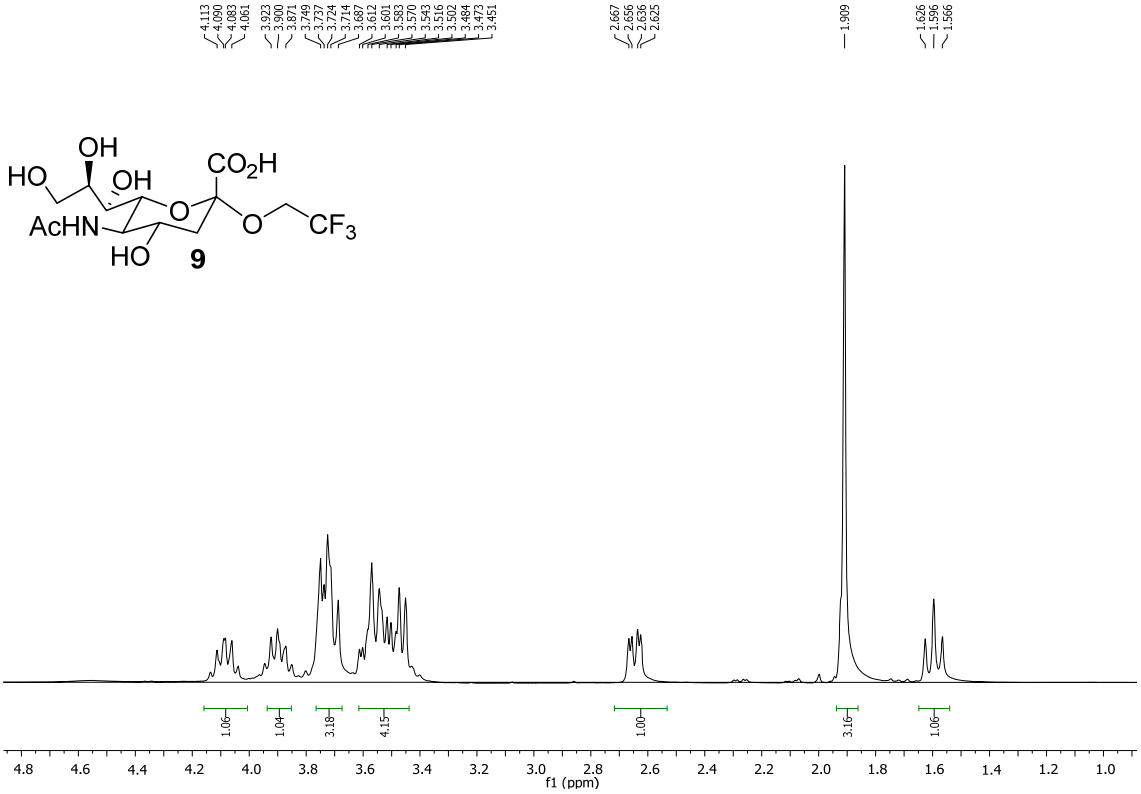

^{13}C-NMR spectrum of **9** in D_2O.

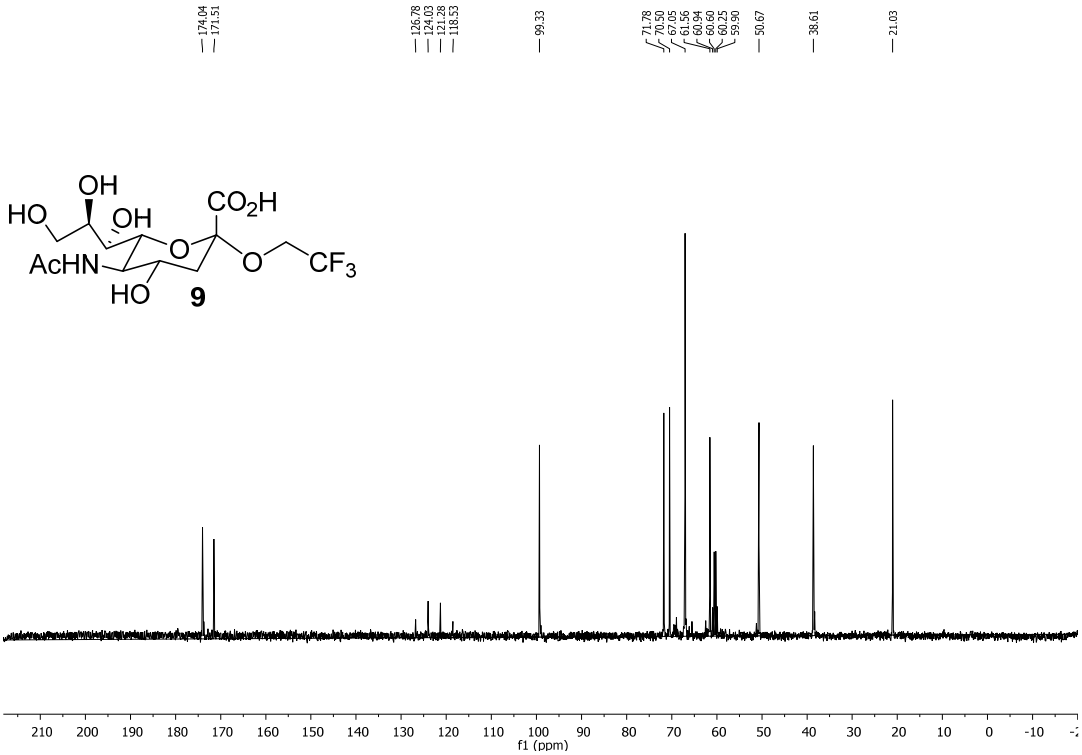

^{1}H-NMR spectrum of **10** in D_2O.

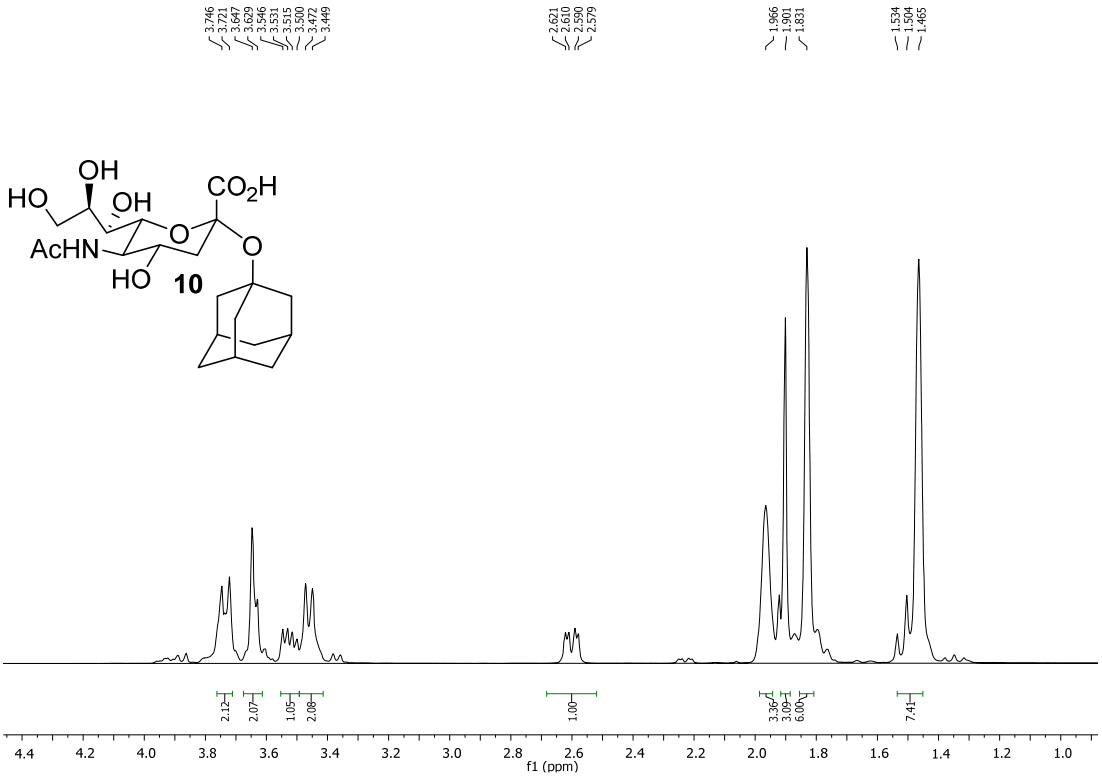

^{13}C-NMR spectrum of **10** in D_2O.

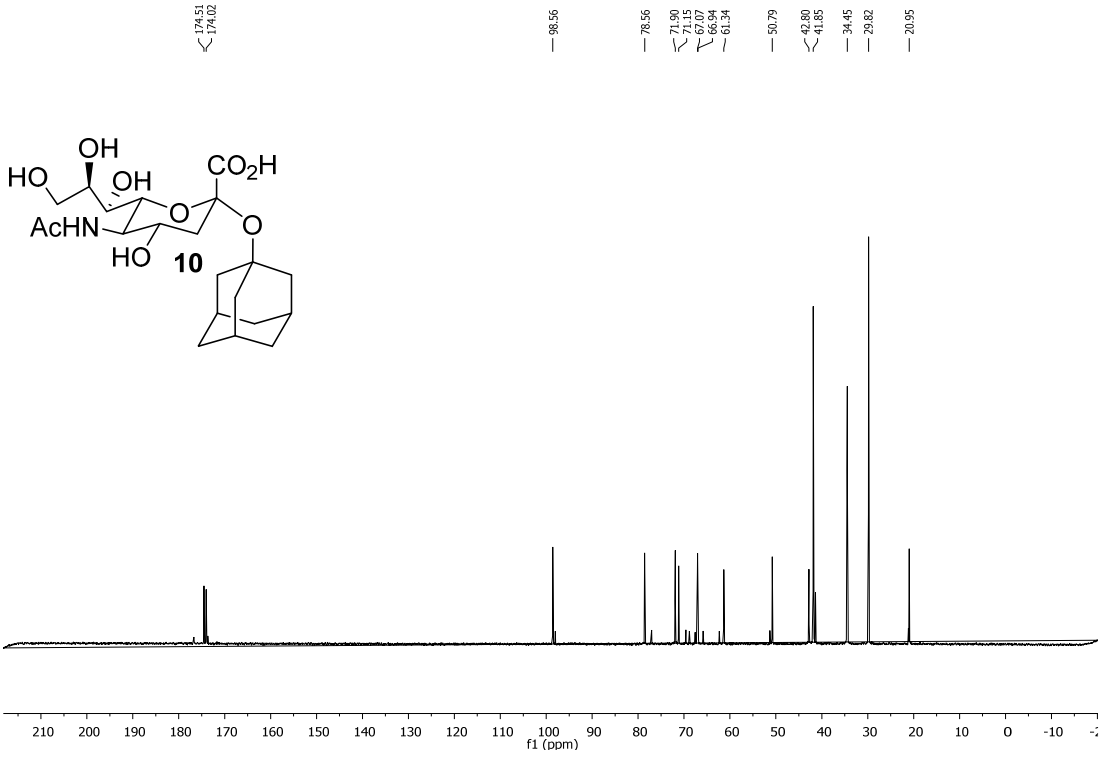

^{13}C HSQC-NMR spectrum of **10** in D_2O.

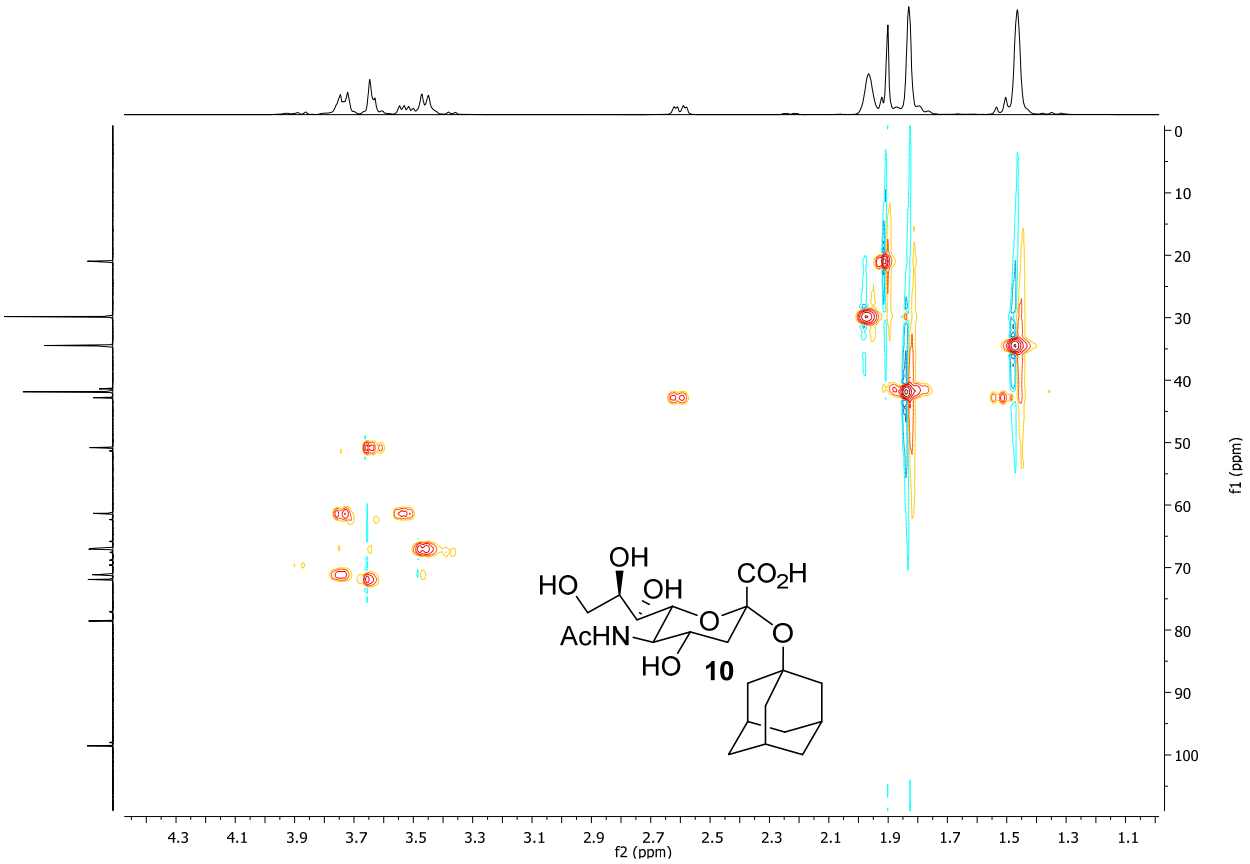

^{1}H-NMR spectrum of **12** in D_2O.

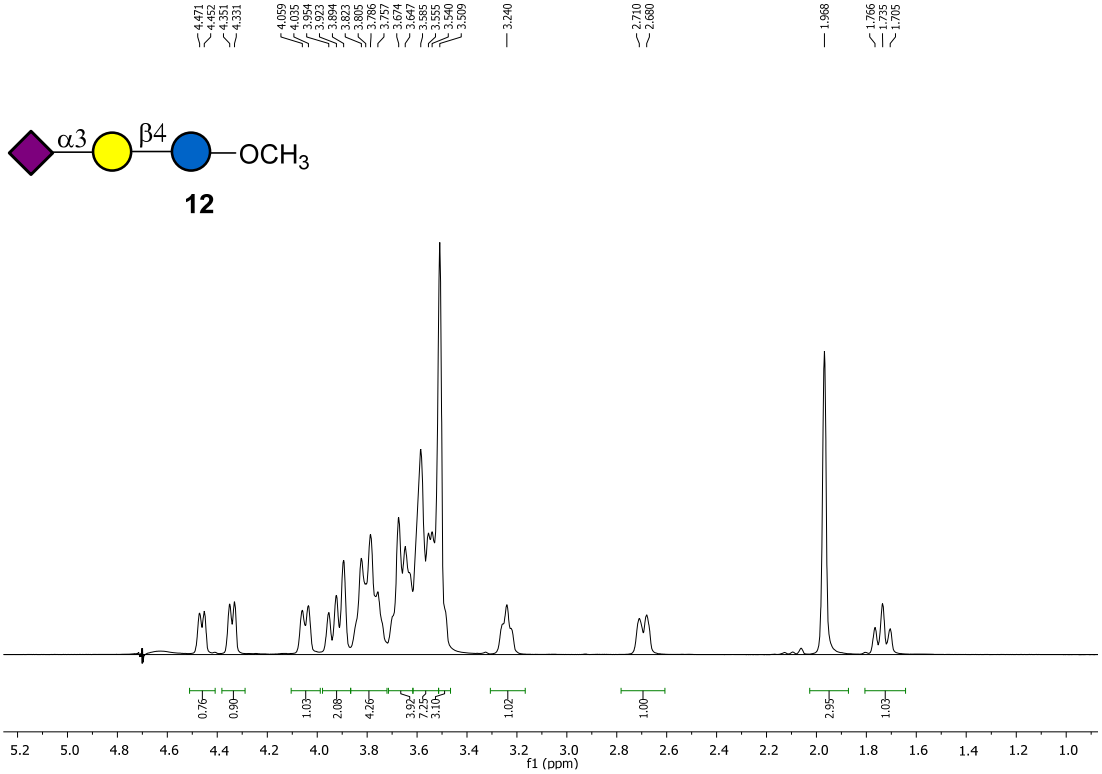

^{13}C-NMR spectrum of ADOA in D_2O.

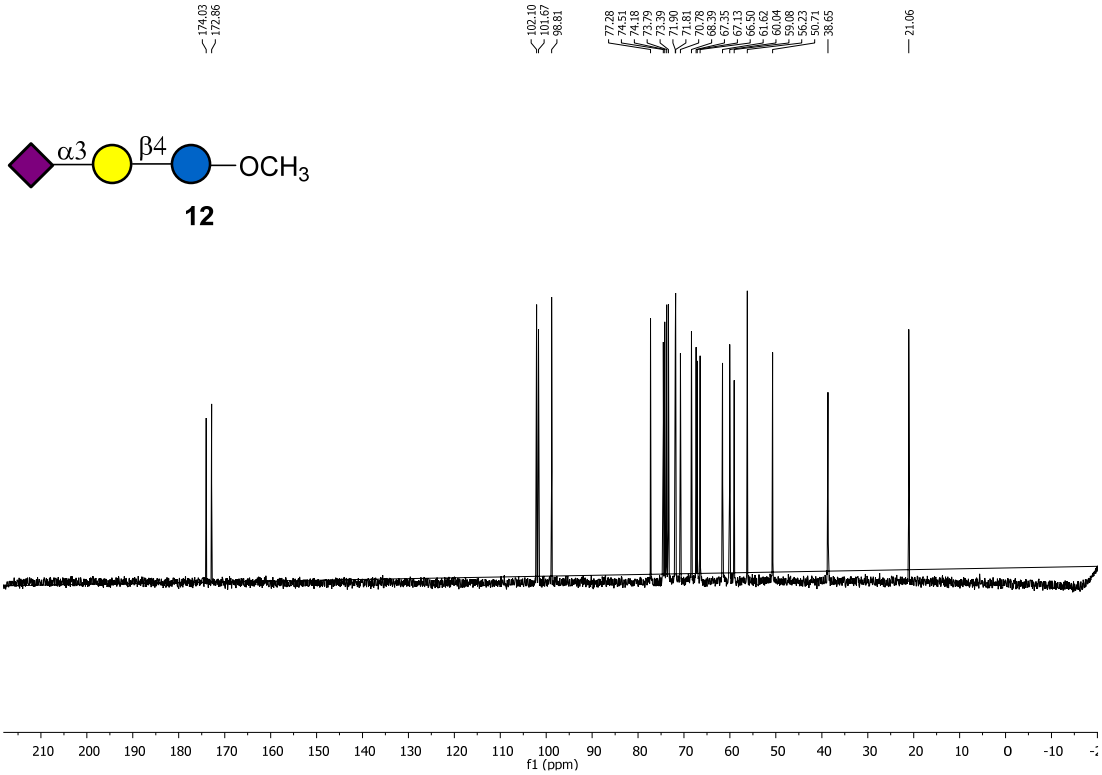

^{13}C HSQC-NMR spectrum of **12** in D_2O.

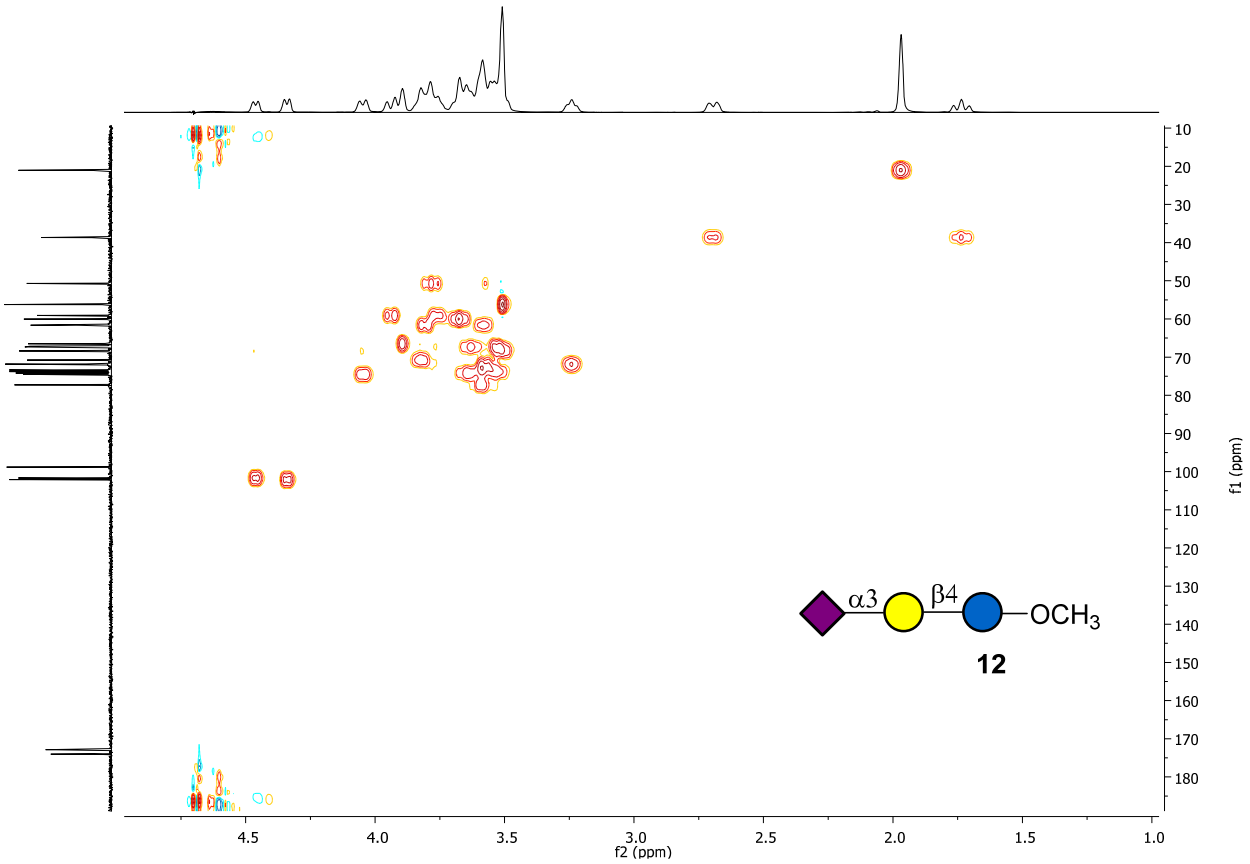

^{1}H-NMR spectrum of **13** in D_2O.

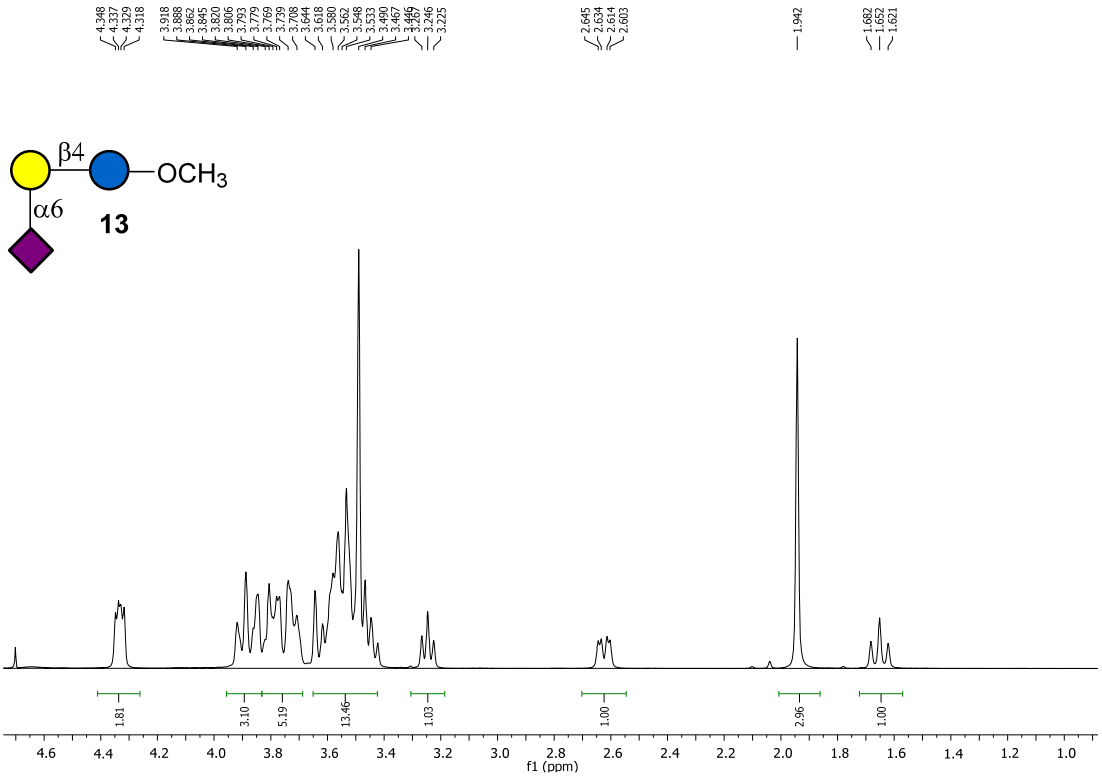

^{13}C-NMR spectrum of **13** in D_2O.

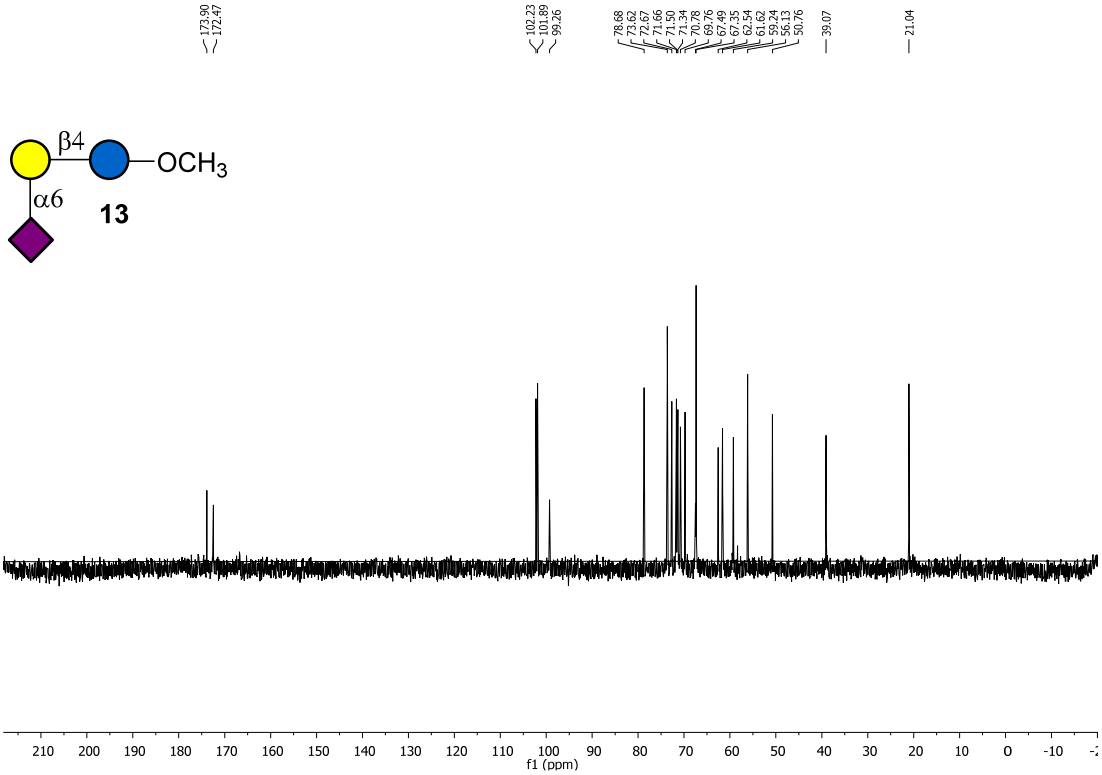

^{13}C HSQC-NMR spectrum of **13** in D_2O.

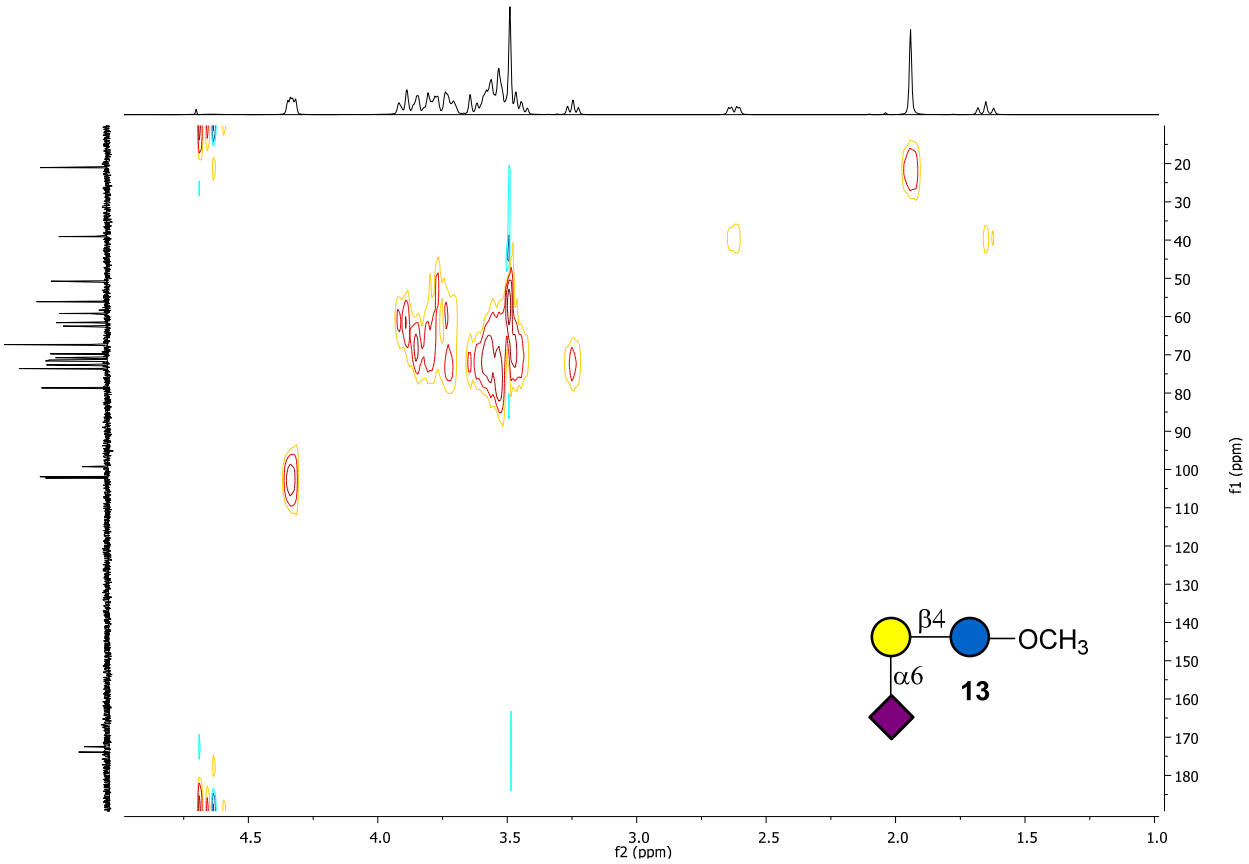

^{1}H-NMR spectrum of **14** in D_2O.

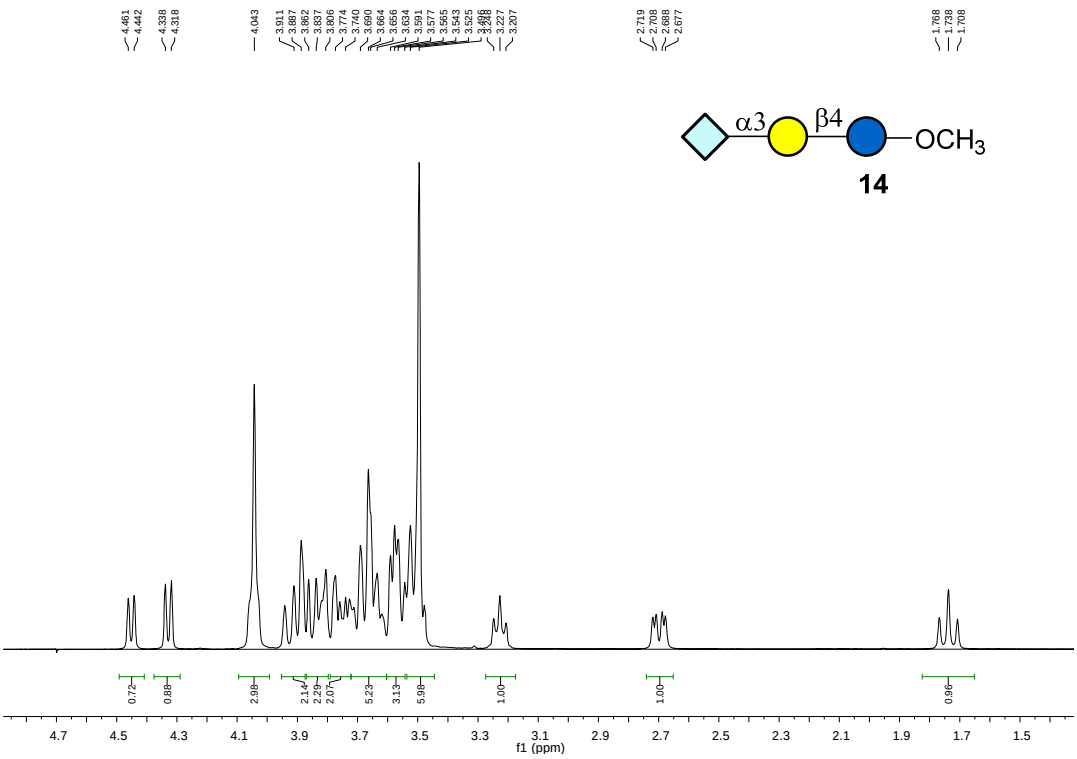

^{13}C-NMR spectrum of **14** in D_2O.

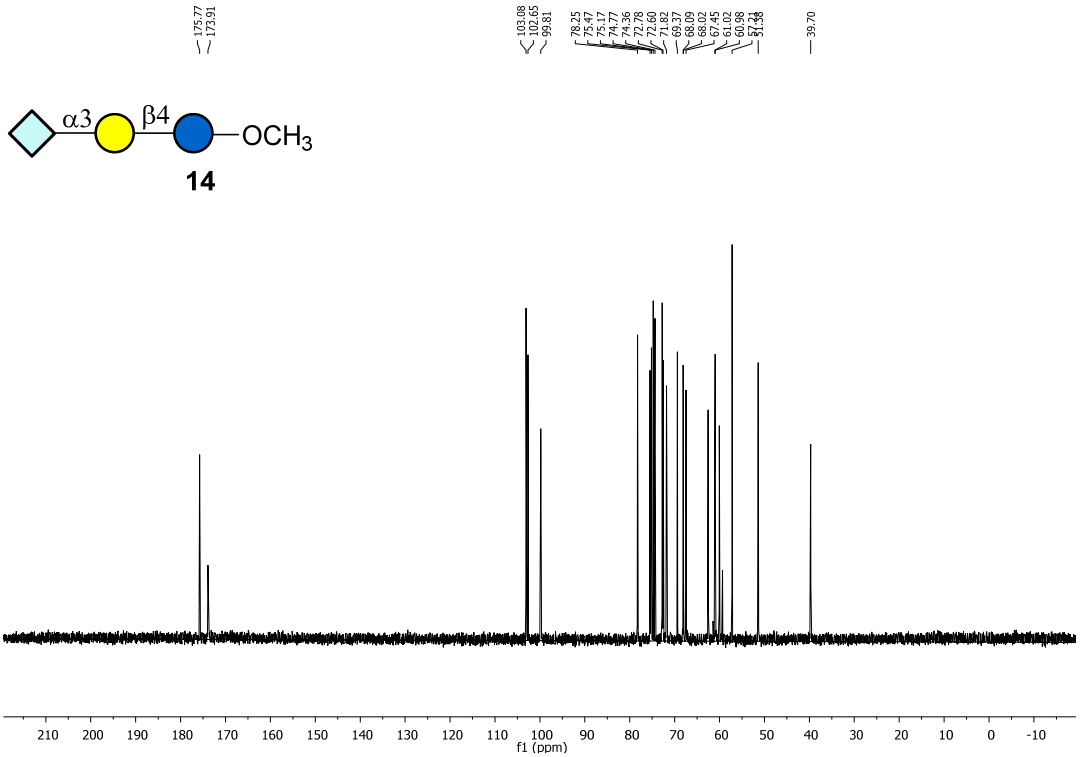

^{13}C HSQC-NMR spectrum of **14** in D_2O.

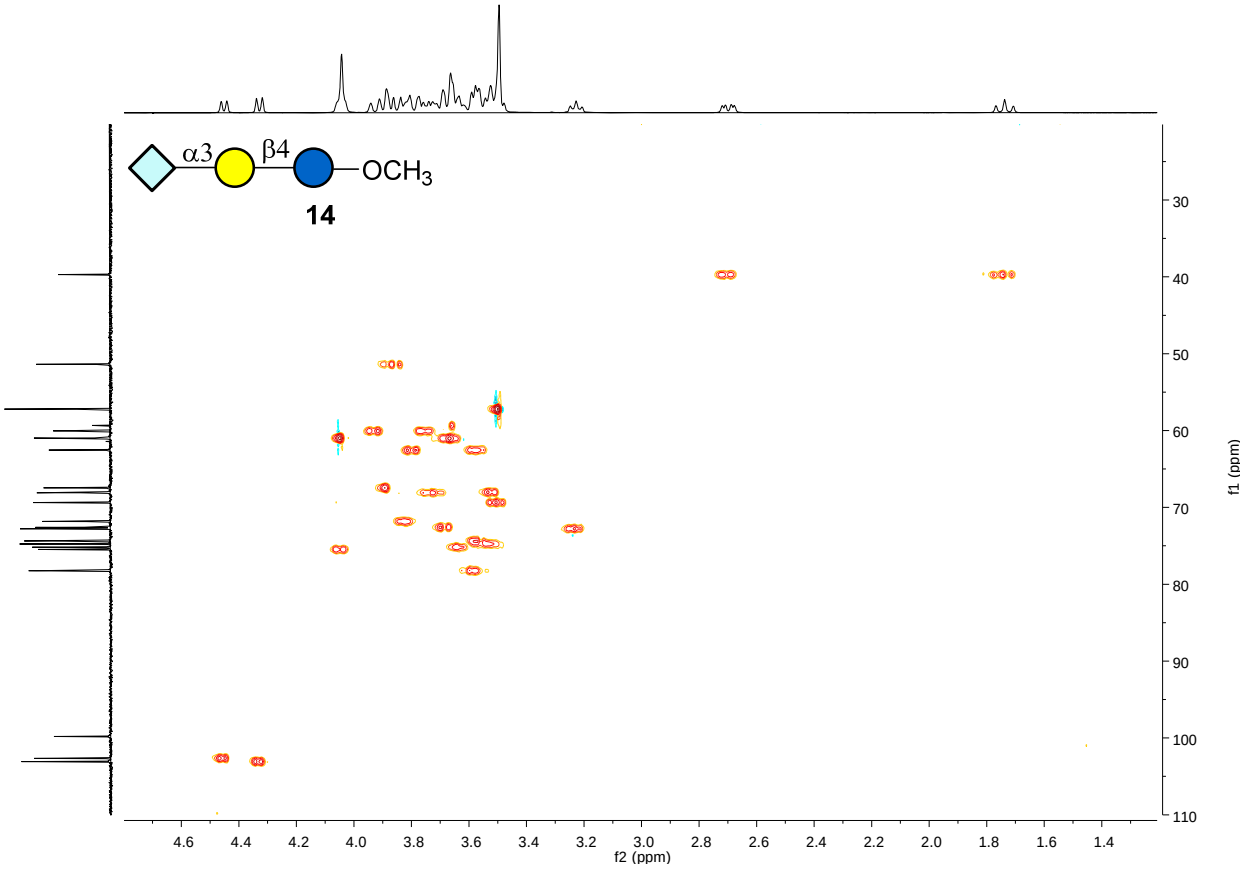

^{1}H-NMR spectrum of **15** in D_2O.

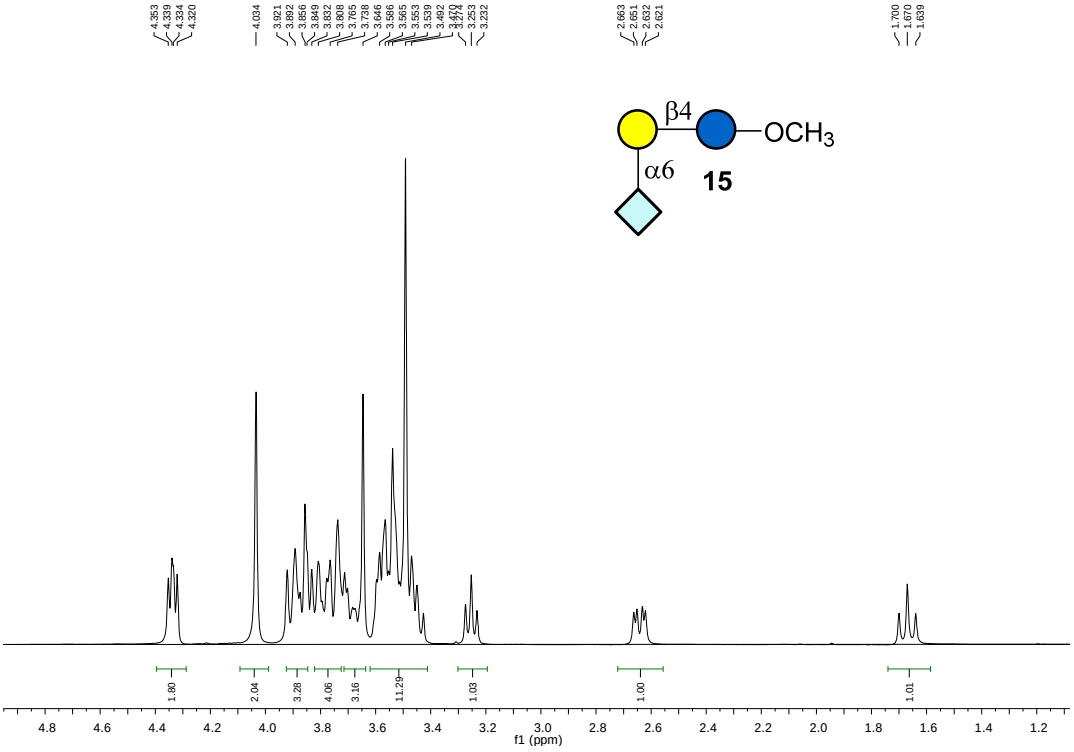

^{13}C-NMR spectrum of **15** in D_2O.

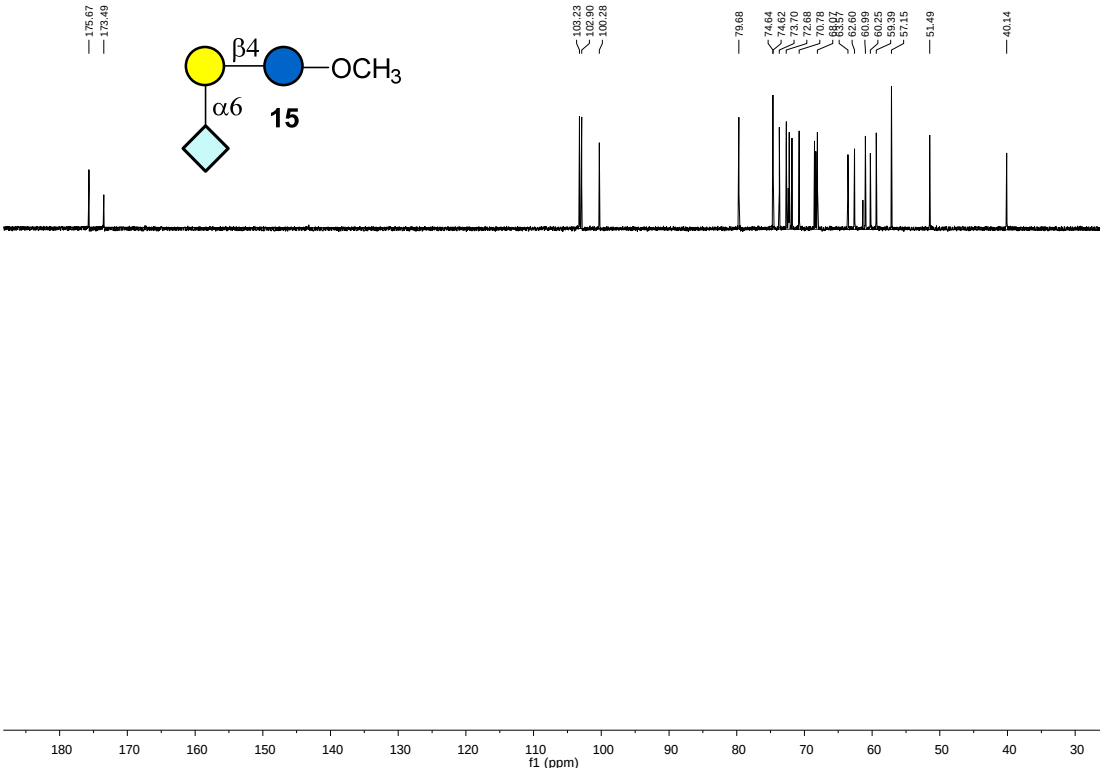

^{13}C HSQC-NMR spectrum of **15** in D_2O.

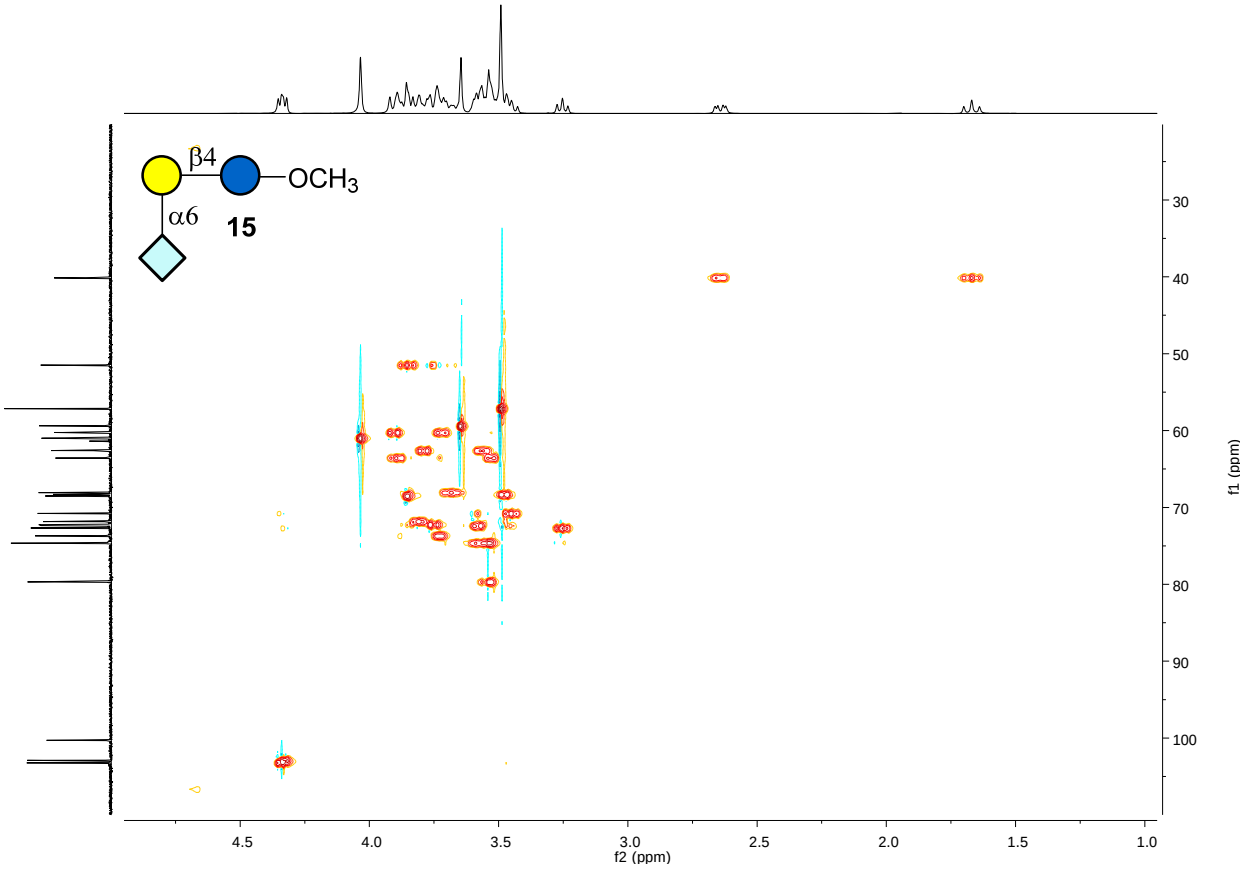

^{1}H-NMR spectrum of **16** in D_2O.

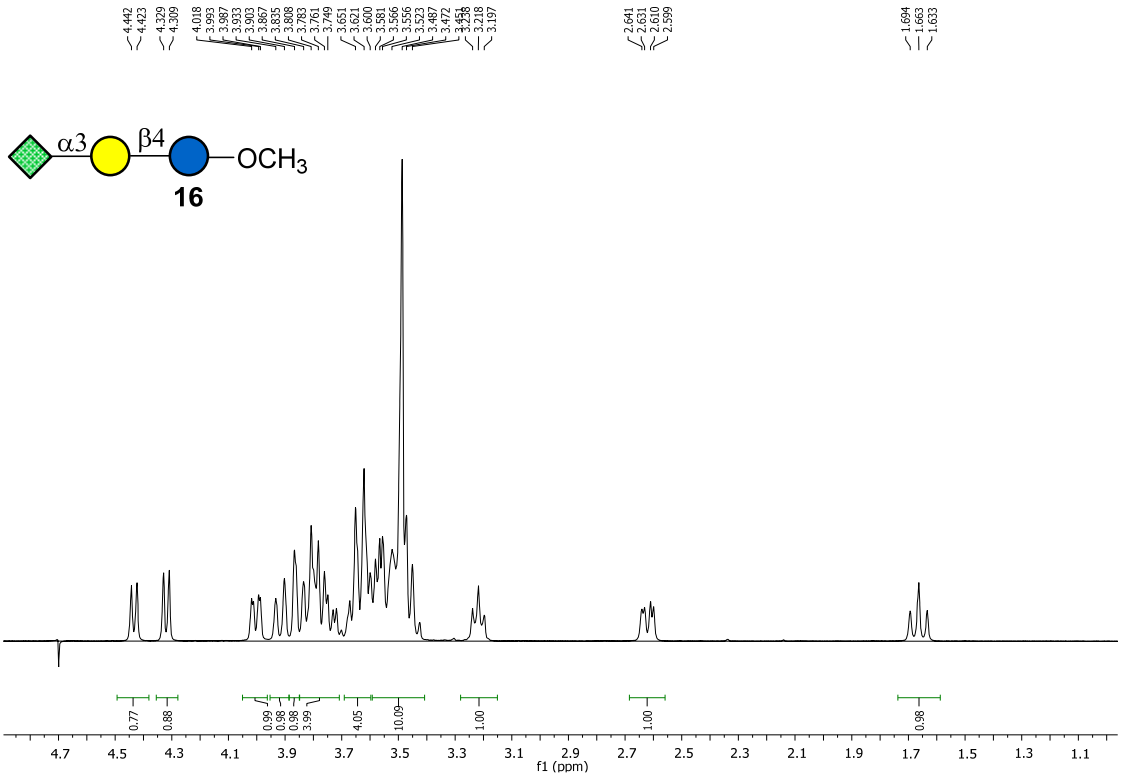

^{13}C-NMR spectrum of **16** in D_2O.

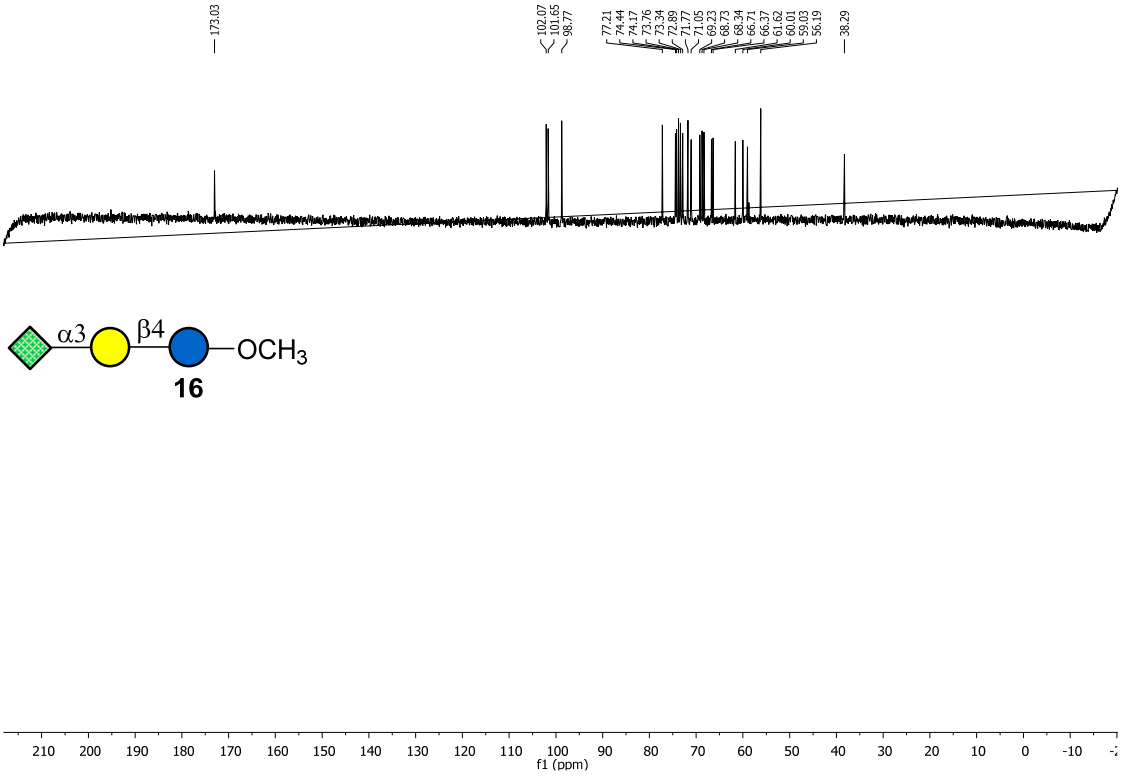

^{13}C HSQC-NMR spectrum of **16** in D_2O.

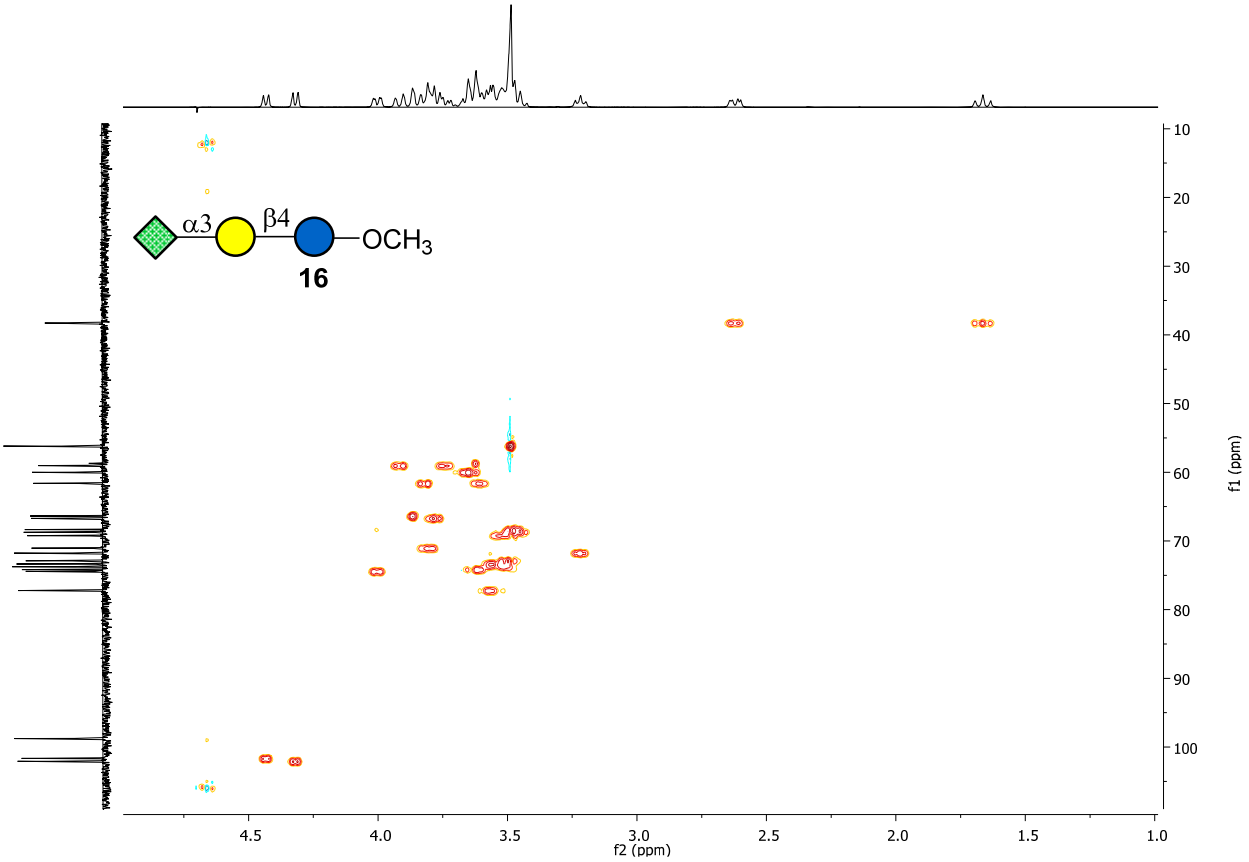

^{1}H-NMR spectrum of **17** in D_2O.

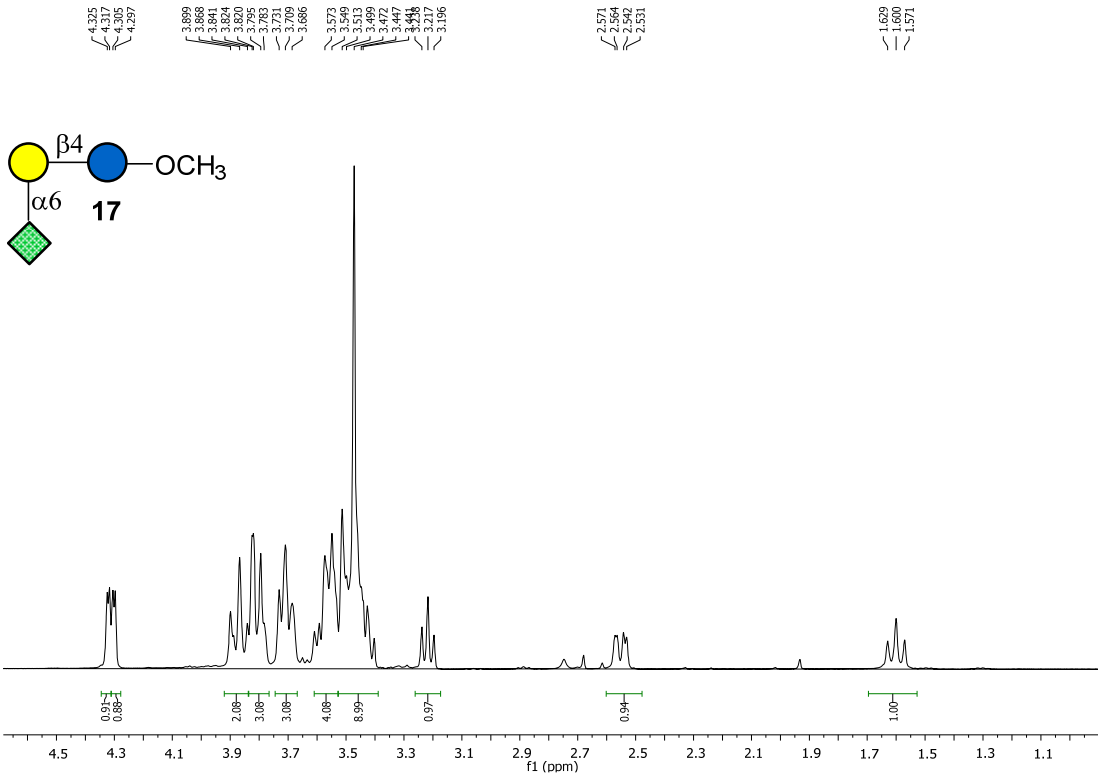

^{13}C-NMR spectrum of **17** in D_2O.

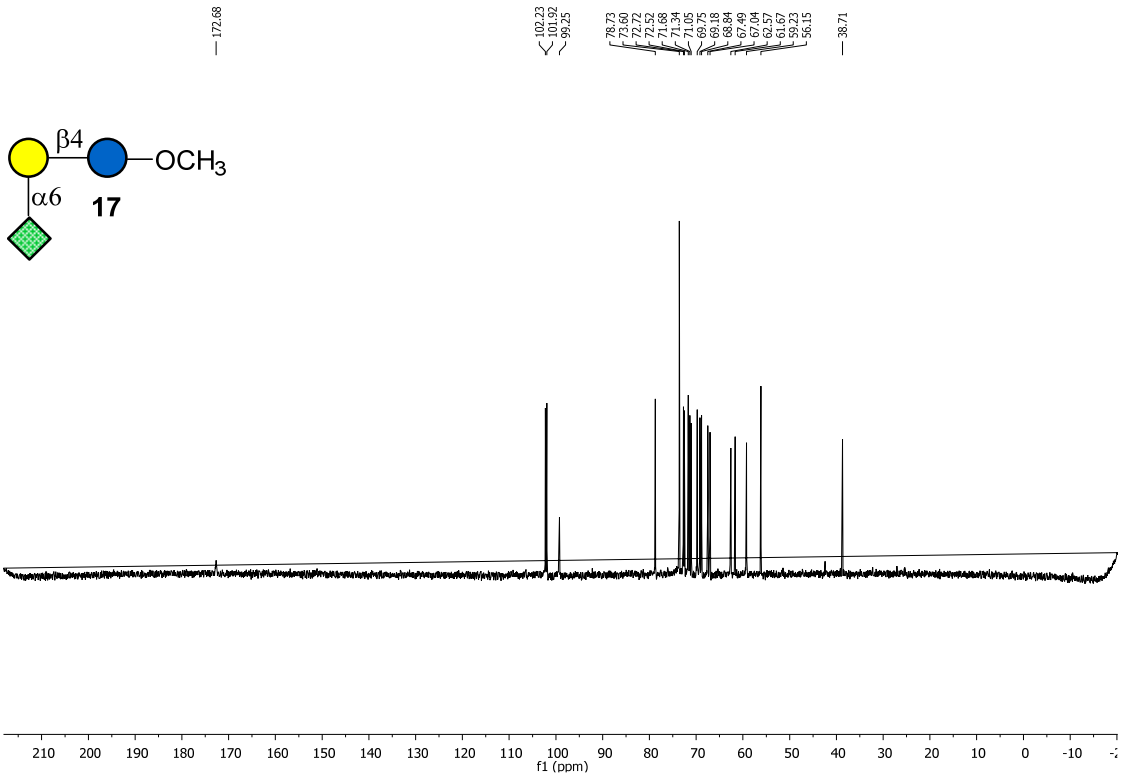

^{13}C HSQC-NMR spectrum of **17** in D_2O.

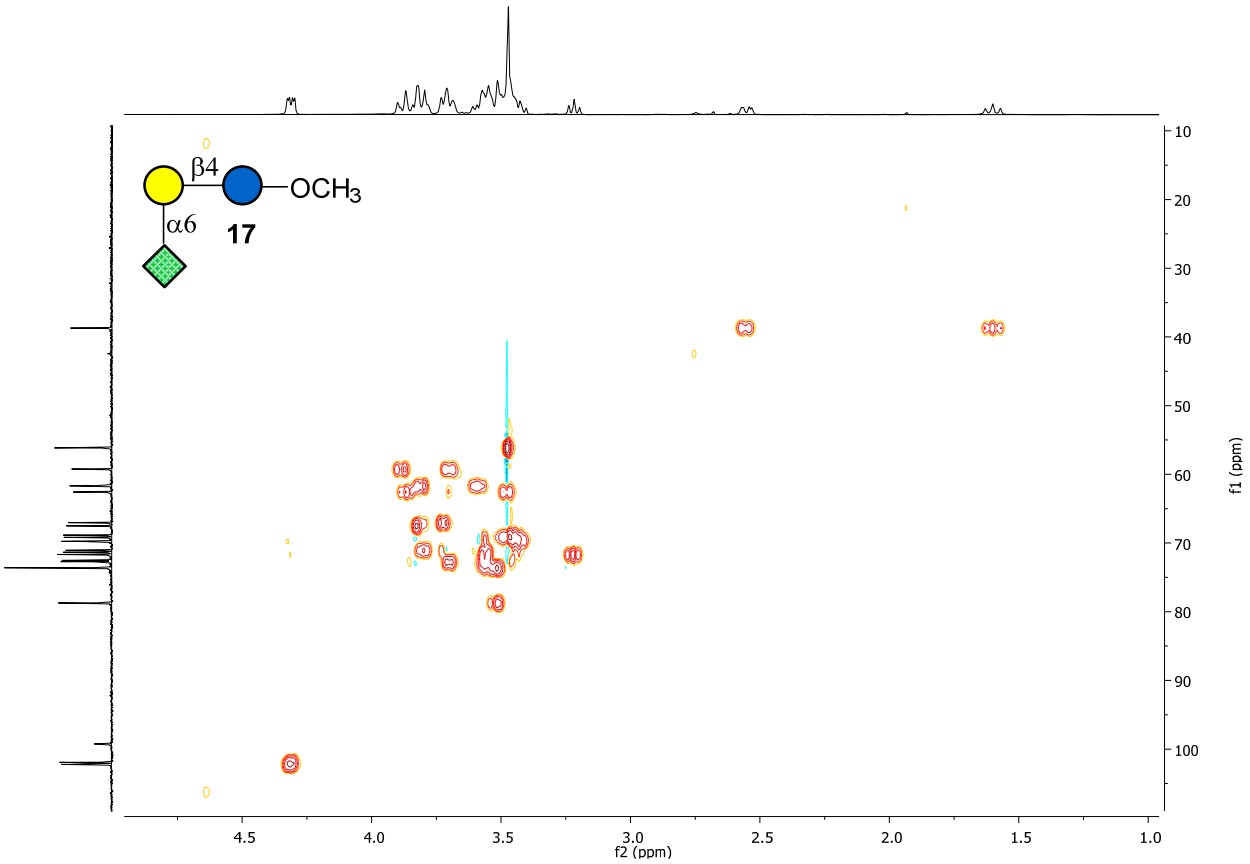

^{1}H-NMR spectrum of **18** in D_2O.

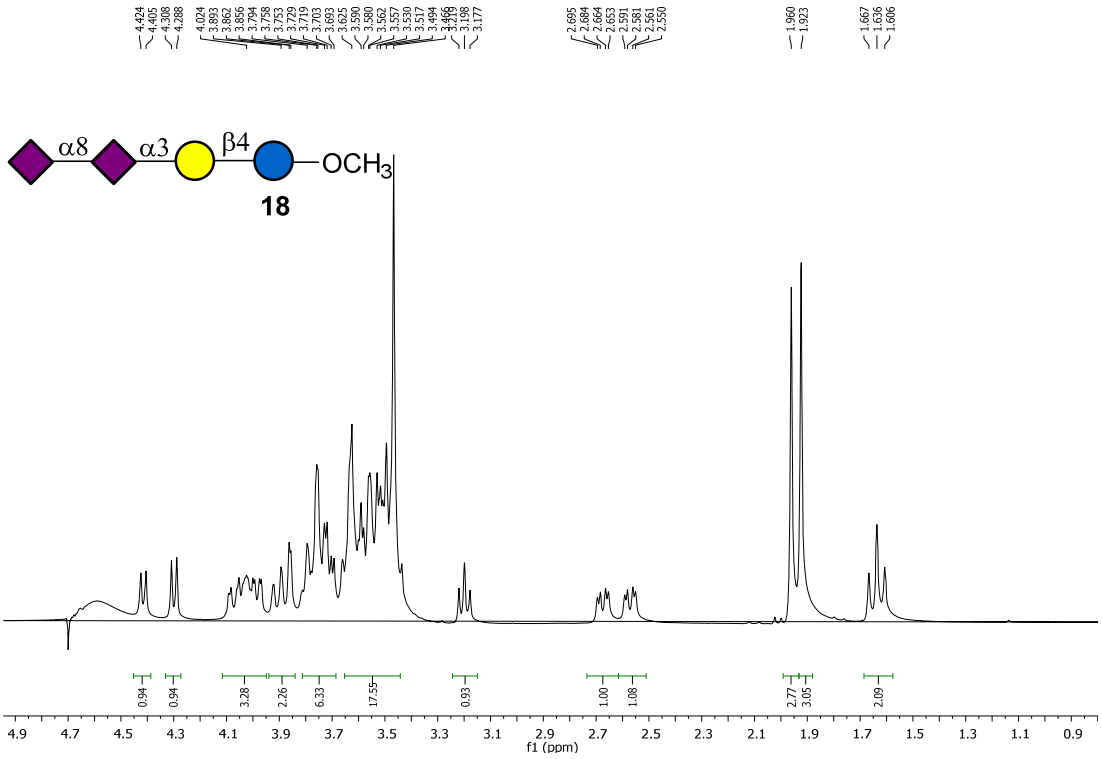

^{13}C-NMR spectrum of **18** in D_2O.

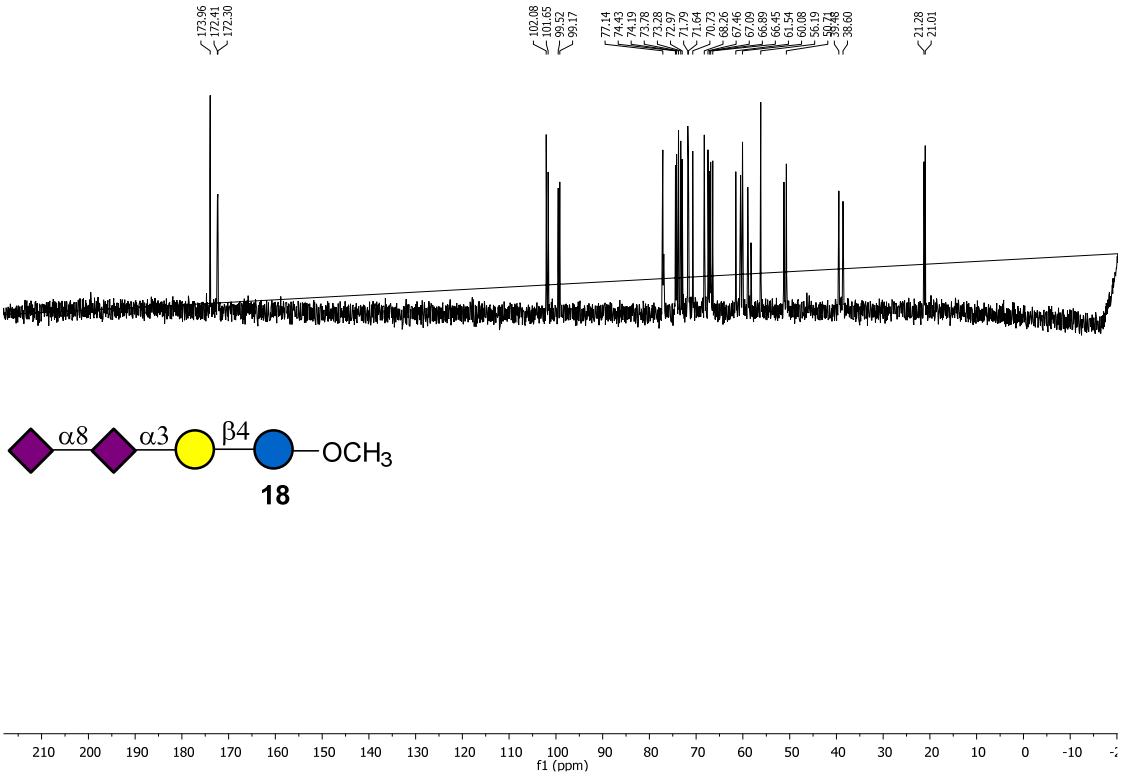

^{13}C HSQC-NMR spectrum of **18** in D_2O.

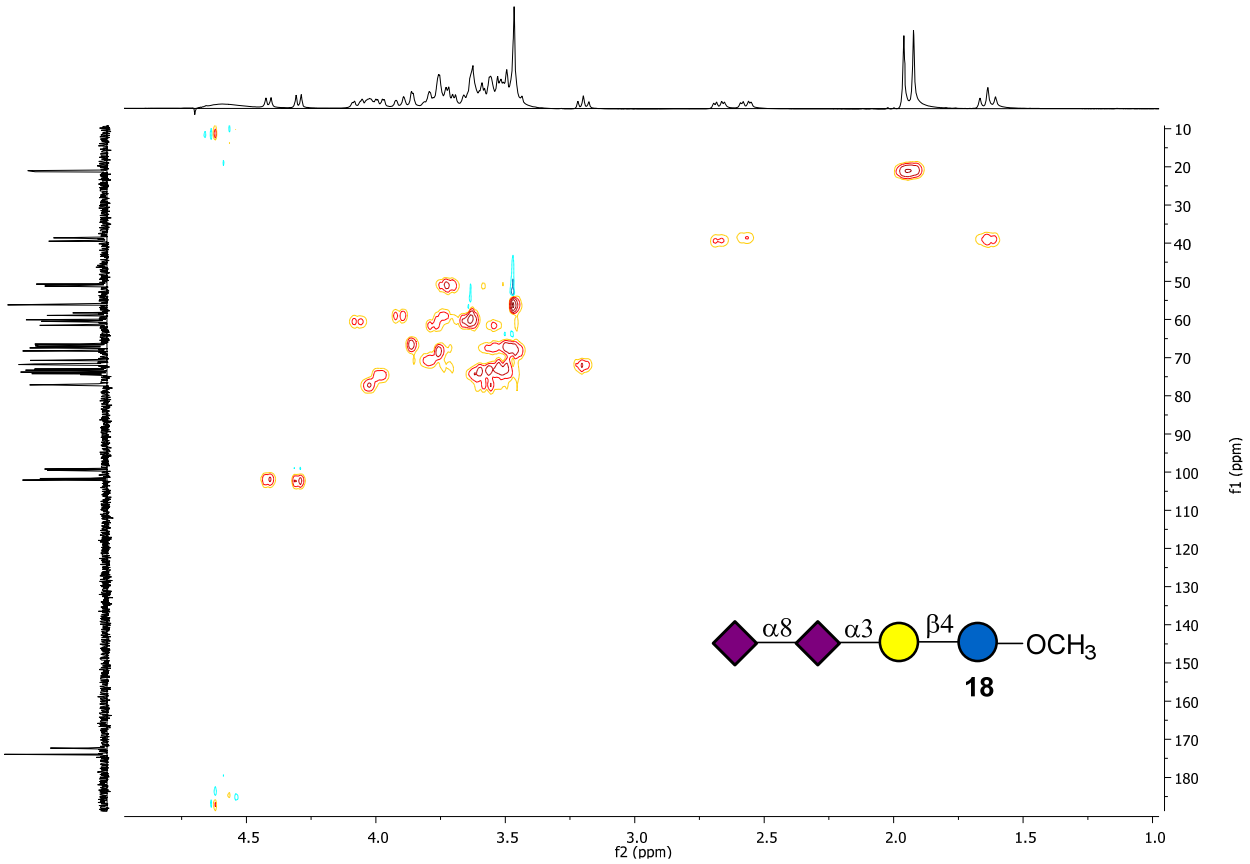

^{1}H-NMR spectrum of **19** in D_2O.

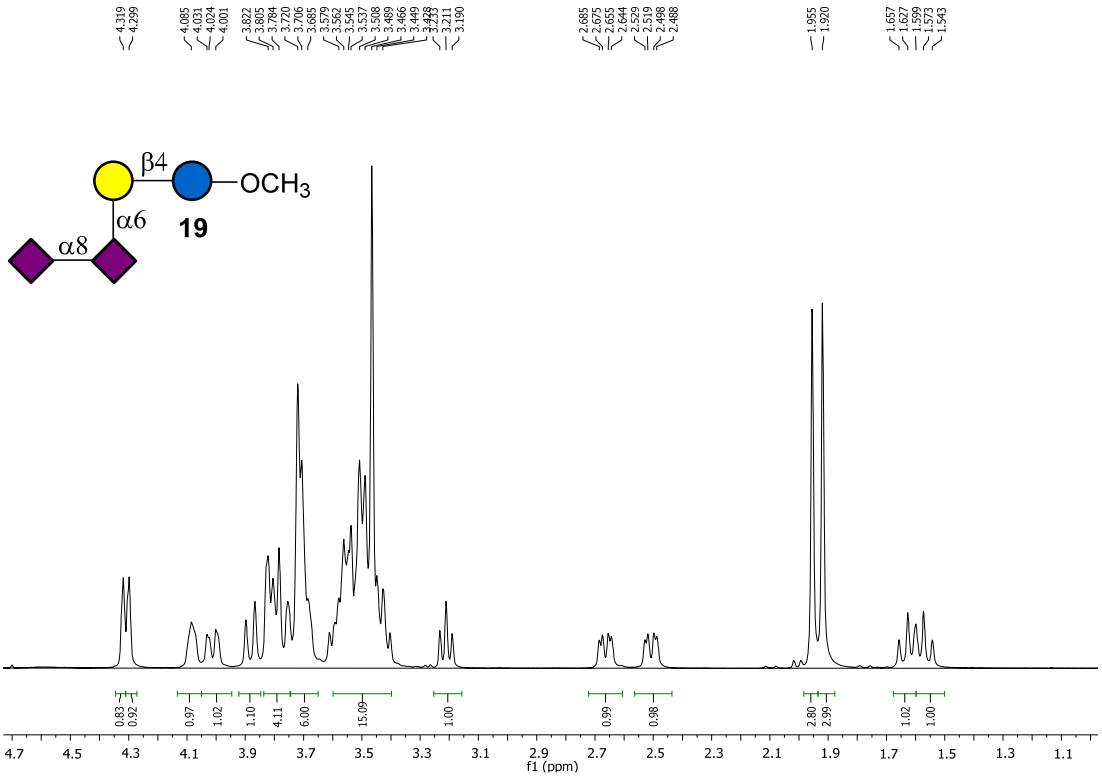

^{13}C-NMR spectrum of **19** in D_2O.

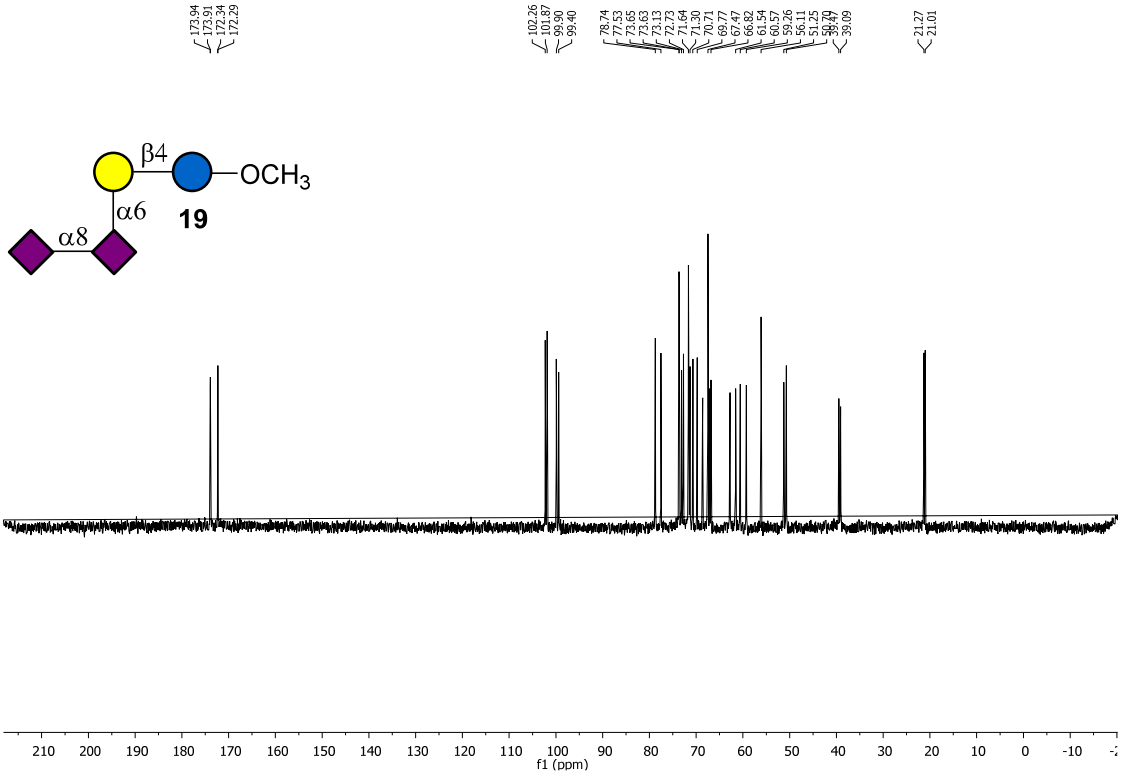

^{13}C HSQC-NMR spectrum of **19** in D_2O.

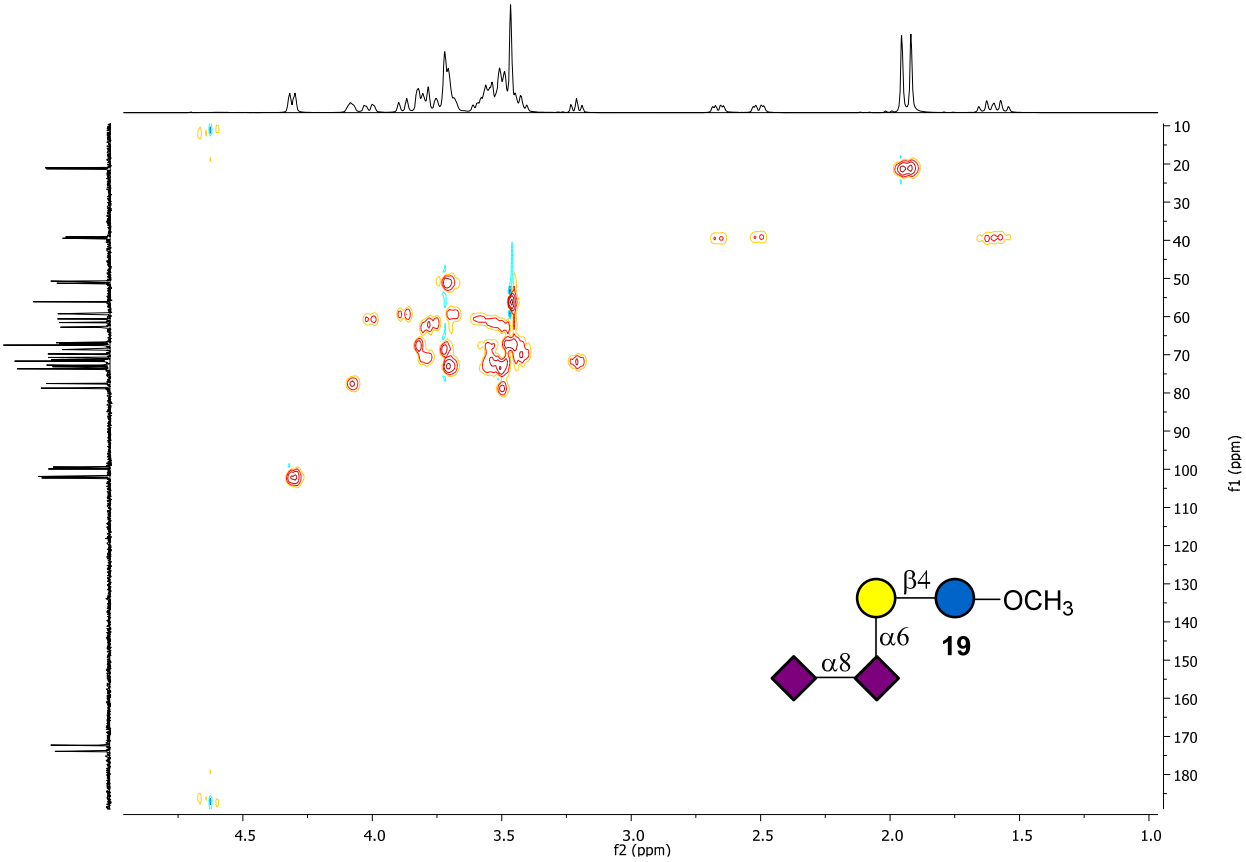

^{1}H-NMR spectrum of **20** in D_2O.

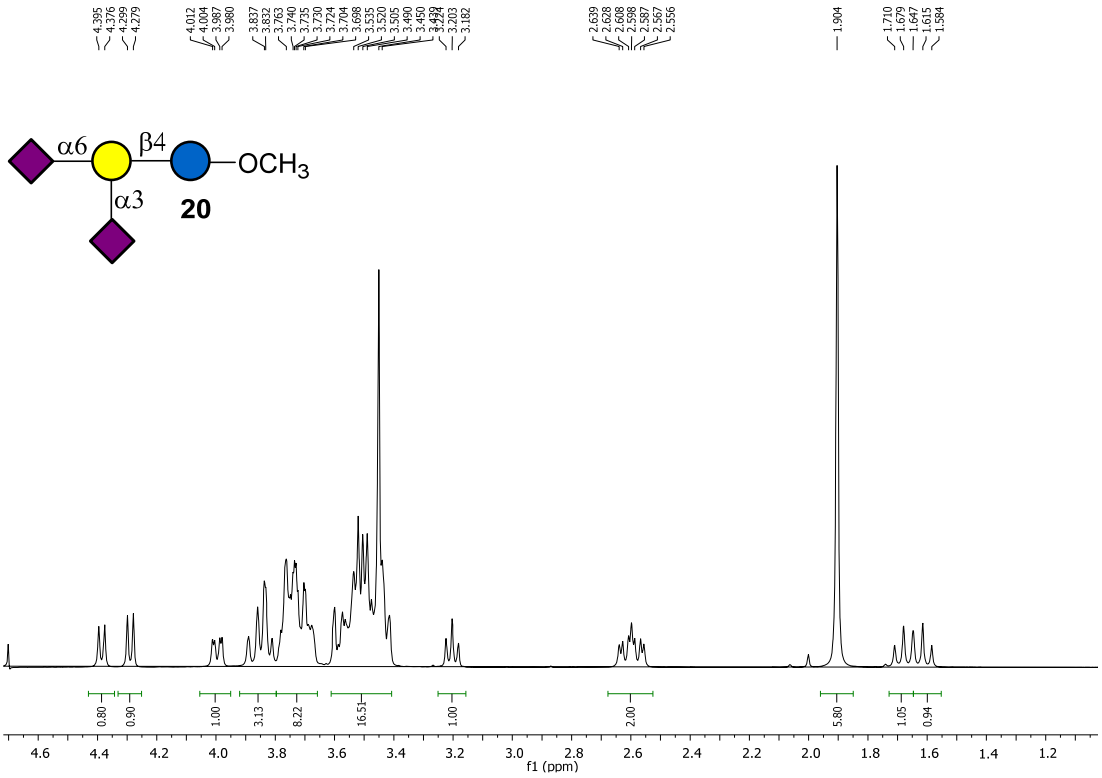

^{13}C-NMR spectrum of **20** in D_2O.

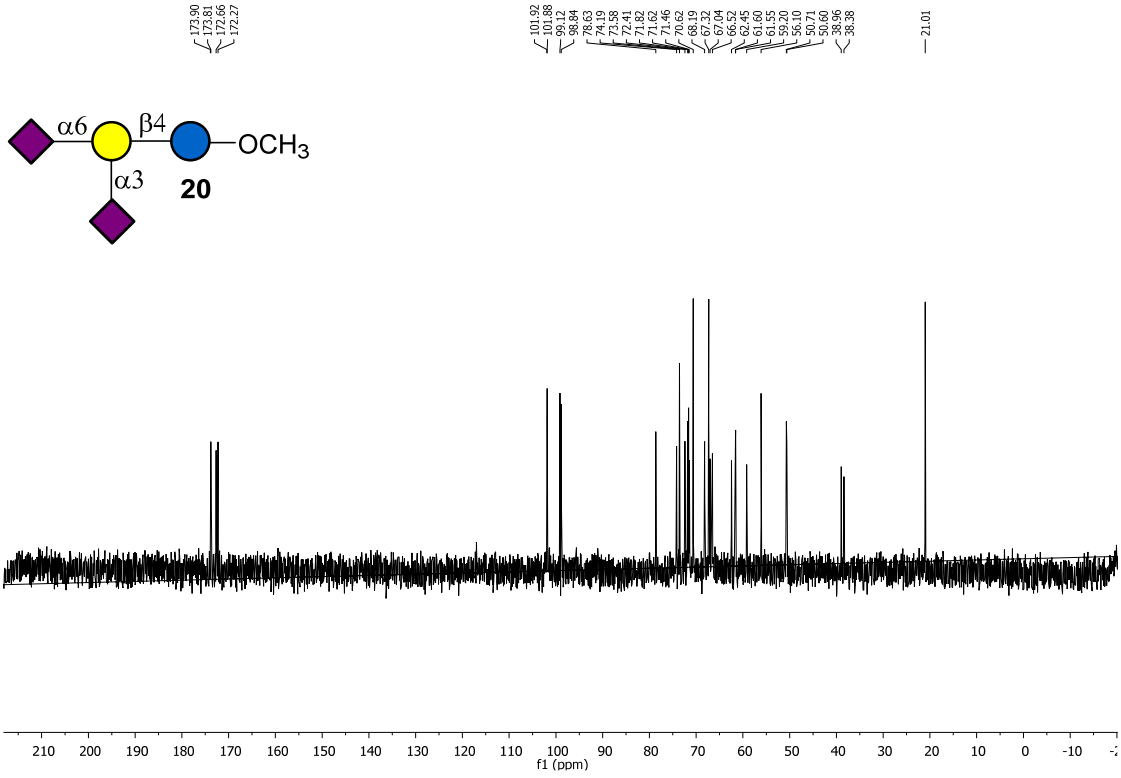

^{13}C HSQC-NMR spectrum of **20** in D_2O.